UNIVERSIDADE DA CORUÑA

DOCTORAL THESIS

CELLULAR AND MOLECULAR EFFECTS OF METAL OXIDE NANOPARTICLES ON HUMAN NEURONAL CELLS

Gözde KILIÇ

2015

UNIVERSIDADE DA CORUÑA

Cellular and molecular effects of metal oxide nanoparticles on human neuronal cells

Gözde Kılıç

Doctoral thesis

2015

Cellular and Molecular Biology

Thesis supervisors:

Blanca Laffon Lage

Vanessa Valdiglesias García

The experimental work presented in this thesis was performed at the:

- Toxicology laboratory, University of A Coruña, Spain.
- Genetics laboratory, University of A Coruña, Spain.
- EPIUnit Institute of Public Health, University of Porto, Porto, Portugal.
- Department of Environmental Health, Portuguese National Institute of Health, Porto, Portugal.
- REQUIMTE, Department of Chemistry and Biochemistry, University of Porto, Porto, Portugal.
- Nanotoxicology Group, Indian Institute of Toxicology Research, Uttar Pradesh, India.
- Laboratory for Health Protection Research, National Institute for Public Health and the Environment (RIVM), Bilthoven, The Netherlands.

This work was supported by Xunta de Galicia (EM 2012/079), MODENA COST Action; TD1204, Pre-doctoral researcher contract from University of A Coruña (May 2012- May 2014) and Inditex-UDC 2014 stay abroad grants for pre-doctoral students.

Publications

Scientific papers:

1. Comparative study on effects of two different types of titanium dioxide nanoparticles on human neuronal cells. Valdiglesias, V; Costa, C.; Sharma, V.; Kiliç, G.; Pásaro, E.; Teixeira, J.P.; Dhawan, A.; Laffon, B. Food and Chemical Toxicology vol. 57 (2013) p.352-361. DOI:10.1016/j.fct.2013.04.010.
2. Neuronal cytotoxicity and genotoxicity induced by zinc oxide nanoparticles. Valdiglesias, V.; Costa, C.; Kiliç, G.; Costa, S.; Pásaro, E.; Laffon, B.; Teixeira, J.P. Environment International vol. 55 (2013) p.92-100. DOI:10.1016/j.envint.2013.02.013.
3. Effects of iron oxide nanoparticles: Cytotoxicity, genotoxicity, developmental toxicity, and neurotoxicity. Valdiglesias, V.; Costa, C.; Kiliç, G.; Costa, S.; Pásaro, E.; Teixeira, J.P.; Laffon, B. Environmental and Molecular Mutagenesis vol. 56 (2015) p.125-148. DOI:10.1002/em.21909.
4. *In vitro* cytotoxicity of superparamagnetic iron oxide nanoparticles on neuronal and glial cells. Evaluation of nanoparticle interference with viability tests. Costa, C.; Brandão. F.; Bessa, M.J.; Costa, S.; Valdiglesias, V.; Kiliç, G.; Quaresma, P.; Pereira, E.; Pásaro, E.; Laffon, B.; Teixeira , J.P. Journal of Applied Toxicology (2015) (in press).
5. *In vitro* toxicity evaluation of silica-coated iron oxide nanoparticles in human SHSY5Y neuronal cells. Kiliç,G.; Costa,C.; Fernández-Bertólez, N.; Pásaro, E.; Teixeira, J.P.; Laffon,B.; Valdiglesias, V. (under revision)

Conference proceedings:

1. Neurotoxicity assessment of zinc oxide nanoparticles: Cytotoxic and genotoxic effects. Kiliç, G; Costa, C.; Teixeira, J.P.; Pásaro, E.; Valdiglesias, V.; Laffon, B. 49th Congress of the European Societies of Toxicology (EUROTOX). Interlaken, Switzerland, September 01-04, 2013. Toxicology Letters vol. 221 (2013) p.S243-S243. DOI:10.1016/j.toxlet.2013.05.600.

2. Cytotoxicity of iron oxide nanoparticles with different coatings on human neuronal cells. Costa, C.; Kiliç, G.; Brandao, F.; Bessa, M.J.; Costa, S.; Pásaro, E.; Valdiglesias, V.; Laffon, B.; Teixeira, J.P. 50th Congress of the European Societies of Toxicology (EUROTOX). Edinburgh, Scotland, September 07-10, 2014.Toxicology Letters vol. 229 (2014) p.S199-S199. DOI:10.1016/j.toxlet.2014.06.673.

Congress Communications:

1. 4th Croatian Congress of Toxicology (CROTOX 2012) October 02-05 2012, Primosten, Croatia. Oral Presentation. Kiliç, G.; Valdiglesias, V.; Sharma, V.; Teixeira, J.P.; Pásaro, E.; Dhawan, A.; Laffon, B. Cytotoxic and Genotoxic Effects of Titanium Dioxide Nanoparticles on Human Neuronal Cells.
2. European Society for Toxicology in vitro International Conference (ESTIV2012) October 16 - 19 2012, Lisbon, Portugal. Poster Presentation. Costa, C.; Valdiglesias, V.; Kiliç, G.; Laffon, B; Teixeira, J.P. The cellular response of human neuroblastoma cells to zinc oxide nanoparticles.
3. 3rd International Conference on Safe Production and Use of Nanomaterials (NANOSAFE 2012) November 13-15 2012, Grenoble, France. Poster Presentation. Costa, C.; Valdiglesias, V.; Kiliç, G.; Laffon, B; Teixeira, J.P. Cytotoxic and Genotoxic Effects of Zinc Oxide Nanoparticles on Human Neuroblastoma Cells.
4. 2nd Encontro Nacional de Nanotoxicologia (E2N 2013) April 02-03 2013, Lisbon, Portugal. Oral Presentation - in Portuguese. Costa, C.; Valdiglesias, V.; Kiliç, G.; Laffon, B.; Teixeira, J.P. Toxicidade celular de nanopartículas de óxidos metálicos em células de neuroblastoma humano.
5. 2nd Working Conditions International Congress (CICOT 2013) September 05-06 2013, Porto, Portugal. Oral presentation. Brandao, F.P.; Costa, C.; Valdiglesias, V.; Kiliç, G.; Pásaro, E.; Laffon, B.; Teixeira, J.P. In vitro cytotoxicity assessment of magnetite nanoparticles on neuronal cells.
6. 10th International Comet Assay Workshop (ICAW 2013) September 18-20 2013, Porto, Portugal. Invited Speaker. Kiliç G.; Costa C.; Teixeira J.P.; Pásaro E.; Laffon B.; Valdiglesias V. Neuronal genotoxicity assessment of iron oxide nanoparticles by comet assay.
7. 7th International Nanotoxicology Congress (NANOTOX 2014) April 23-26 2014, Antalya Turkey. Poster presentation. Costa, C.; Valdiglesias, V.; Kiliç, G.; Costa, S.; Pásaro E; Laffon, B.; Teixeira, J.P. Toxicity of zinc oxide nanoparticles on human neuronal cells.
8. 7th International Nanotoxicology Congress (NANOTOX 2014) April 23-26 2014, Antalya, Turkey. Poster presentation. Costa, C.; Kiliç, G.; Costa, S.; Pásaro E.; Valdiglesias, V.; Laffon B.; Teixeira, J.P. Cytotoxicity of silica coated iron oxide nanoparticles on human neuronal cells.
9. 7th International Nanotoxicology Congress (NANOTOX 2014) April 23-26 2014, Antalya, Turkey. Poster presentation. Kiliç, G.; Costa, C.; Pásaro E.; Laffon, B.; Teixeira, J.P.; Valdiglesias, V. Assessment of DNA Damage induced by Superparamagnetic iron Oxide Nanoparticles on Human Neuronal Cells.
10. International Conference on Environmental Health (ICEH2014) September 24-26 2014, Porto, Portugal. Invited speaker. Laffon, B.; Kiliç, G.; Castelo, A.; Costa, C.; Costa, S.;

Teixeira, J.P.; Pásaro, E. ; Laffon ,B. ; Valdiglesias, V. In vitro analysis of neuronal DNA damage induced by magnetite nanoparticles.

11. International Conference on Environmental Health (ICEH2014) September 24-26 2014, Porto, Portugal. Poster presentation. Costa, C.; Kiliç, G.; Costa, S.; Pásaro, E.; Valdiglesias, V.; Laffon, B. Teixeira, J.P. Neurotoxicity induced by silica coated iron oxide nanoparticles.
12. Nanosafety Forum for Young Scientists October 08-09 2014, Syracuse, Italy. Oral presentation. Kiliç, G.; Costa, C.; Teixeira, J.P.; Pásaro, E.; Valdiglesias, V.; Laffon, B.; Park, M. Analysis of reactive potential of iron oxide nanoparticles.
13. 6thInternational Conference on Nanomaterials - Research and Application (NANOCON2014) November 05-07 2014, Brno, Czech Republic. Oral presentation. Kiliç, G.; Fernández-Bertólez, N.; Costa, C.; Costa, S.; Teixeira, J.P.; Pásaro, E.; Laffon, B.; Valdiglesias, V. Toxicity of silica coated iron oxide nanoparticles on SH-SY5Y neuronal cells.

Acknowledgements

I would like to express my special appreciation and thanks to my advisors Dr. Blanca Laffon and Dr Vanessa Valdiglesias, you both have been not only tremendous mentors for my research, but also my translator, sometimes my lawyer, and most importantly you have been my family by helping me in a completely different country. I would like to thank you for encouraging my research, my life and supporting me at every step of this journey, and for allowing me to grow as a research scientist and a person.

I would also like to thank members of the Genetics Laboratory of University of A Coruña and their leader Prof. Josefina Mendez; members of Department of Environmental Health Department of Portuguese National Institute of Health, Porto, Portugal; especially Dr. João Paulo Teixeira and Dr. Carla Costa for their help and support on this research.

I also want to thank Dr. Margriet Park and her team for letting my stay in Netherlands be enjoyable and one of the most remarkable moments of my life, thanks for your brilliant comments and suggestions.

I would especially like to thank my fellow friends in Toxicology Laboratory; Maria, Natalia and Aida. All the new hearts that I touched during this PhD journey; friends that I had privilege to meet during scientific congresses and co-workers/friends in RIVM who have been there to support me whenever I needed, and incited me to strive towards my goal via Facebook or Skype.

Words cannot express how grateful I am to my Spanish sister Marga. Without her I would not be able to have the courage to follow my dreams and have the strength to tackle all the obstacles.

Lastly, special thanks to my family; my brother, my mother, and father for all of the sacrifices that you've made on my behalf. Your support for me was what sustained me thus far.

Determination in every way!!!

Annem Nevin ve babam Dr. Ismail KILIÇ´ a
Sizin için bütün zaferlerim…

I shall be telling this with a sigh
Somewhere ages and ages hence:
Two roads diverged in a wood, and I
I took the one less travelled by,
And that has made all the difference.

The Road Not Taken- by ROBERT FROST

Abstract

The wide scale use of metal oxide nanoparticles (NP) in the world consumer market has resulted in increase in likelihood of exposure to human beings. The potential toxic effects of these NP on mammal cells have been extensively studied. However, studies regarding neurotoxicity and specific effects on neuronal systems are very scarce. Therefore, the aim of this thesis was assessing the toxic potential of titanium dioxide NP (TiO_2-NP), zinc oxide NP (ZnO-NP) and silica-coated iron oxide NP (S-ION) on human SH-SY5Y neuronal cells, to elucidate the possible mechanism of their adverse effects at the cellular and molecular level on the nervous system. After NP characterization, a battery of assays was performed to evaluate the viability, cytotoxicity, genotoxicity and oxidative damage in NP-exposed SH-SY5Y cells. Obtained results showed that internalisation potential of each NP was different: TiO_2-NP and ION were effectively internalized in a concentration- and time-dependent manner; nevertheless, ZnO-NP were unable to be internalized by cells. The NP potential to induce toxic effects was material-dependent: TiO_2-NP did not reduce the viability; ION presented in general low cytotoxicity, whereas ZnO-NP affected the cells most at the cytotoxicity level. Similar to cytotoxicity, genotoxicity-inducing potential of metal oxide NP was found to be different for each NP. Furthermore, toxicity was found to be mediated by oxidative stress in ZnO-NP and S-ION exposed cells, but TiO_2-NP did not induce such oxidation-related changes. The results obtained in this work contributed to increase the knowledge on the genotoxic and cytotoxic potential of metal oxide NP in general, and specifically on human neuronal cells.

Resumen

El uso a gran escala de las nanopartículas (NP) de óxidos metálicos en el mercado de consumo mundial se ha extendido notablemente, dando lugar a un incremento en la probabilidad de exposición a las mismas en los seres humanos. Los potenciales efectos tóxicos de estas NP en las células de mamíferos han sido ampliamente estudiados. Sin embargo, los estudios sobre neurotoxicidad, y los efectos específicos en el tejido nervioso son muy escasos. Por tanto, el objetivo de esta tesis ha sido evaluar el potencial tóxico de NP de dióxido de titanio (TiO_2), (óxido de zinc) ZnO y óxido de hierro recubiertas de sílice (S-ION) en células neuronales humanas SH-SY5Y, para dilucidar el posible mecanismo de sus efectos adversos a nivel celular y molecular sobre el tejido nervioso humano. Tras la caracterización de las NP, se realizó una batería de ensayos para evaluar la viabilidad, citotoxicidad, genotoxicidad y daño oxidativo en las células SH-SY5Y expuestas a las NP. Los resultados obtenidos mostraron que el potencial de internalización de cada NP es diferente; así las NP de TiO_2 y las S-ION fueron eficazmente internalizadas, siendo esta captación dependiente de la concentración y del tiempo de exposición. Por otro lado, las NP de ZnO fueron incapaces de ser internalizadas por las células neuronales. El potencial de las NP analizadas para inducir efectos tóxicos fue dependiente del tipo de material. Las NP de TiO_2 no redujeron la viabilidad y las S-ION presentaron en general

baja citotoxicidad, mientras que las NP de ZnO mostraron un alto nivel de citotoxicidad. Al igual que en el caso de la citotoxicidad, el potencial genotóxico inducido por las NP de óxidos metálicos resultó diferente para cada una de ellas. Además, la toxicidad encontrada en células expuestas a NP de ZnO y a S-ION estuvo mediada por estrés oxidativo; sin embargo, para las NP de TiO_2 tales cambios no se relacionaron con la oxidación. Los resultados obtenidos en este trabajo contribuyen en general a incrementar el conocimiento sobre el potencial genotóxico y citotóxico de las NP de óxidos metálicos, específicamente sobre las células neuronales humanas.

Resumo

O uso a gran escala das nanopartículas de óxidos metálicos (NP) no mercado de consumo mundial estendeuse notablemente, dando lugar a un incremento na probabilidade de exposición ás mesmas nos seres humanos. Os potenciais efectos tóxicos destas NP nas células de mamíferos foron ampliamente estudados. Con todo, os estudos sobre neurotoxicidade, e os efectos específicos no tecido nervoso son moi escasos. Polo tanto, o obxectivo desta tese ten sido avaliar o potencial tóxico de NP de dióxido de titanio (TiO_2), óxido de zinc (ZnO) e óxido de ferro recubertas de sílice (S-ION) en células neuronais humanas SH-SY5Y, para dilucidar o posible mecanismo dos seus efectos adversos a nivel celular e molecular, no tecido nervioso humano. Logo da caracterización das NP, realizouse unha batería de ensaios para avaliar a viabilidade, citotoxicidade, xenotoxicidade e dano oxidativo nas células SH-SY5Y expostas ás NP. Os resultados obtidos mostraron que o potencial de internalización de todos os NP é diferente; así as NP de TiO_2 e as S-foron eficazmente internalizadas, sendo esta captación dependente da concentración e do tempo de exposición. Doutra banda, as NP de ZnO foron incapaces de ser internalizadas polas células neuronais. O potencial das NP analizadas para inducir efectos tóxicos foi dependente do tipo de material. As NP de TiO_2 non reduciron a viabilidade, e as S-ION presentaron en xeral baixa citotoxicidade, mentres que as NP de ZnO mostraron un alto nivel de citotoxicidade. Do mesmo xeito que no caso da citotoxicidade, o potencial xenotóxico inducido polas NP de óxidos metálicos resultou diferente para cada unha de elas. Ademais, a toxicidade atopada en células expostas a NP-ZnO e a S-ION estivo mediada por estrés oxidativo; sen embargo, para as NP-TiO_2 tales cambios non se realacionaron coa oxidación. Os resultados obtidos neste traballo contribúen en xeral, a aumentar o coñecemento sobre o potencial xenotóxico e citotóxico das NP de óxidos metálicos, específicamente sobre as células neuronais humanas.

Extended Summary in Spanish-Resumen Amplio

La nanotecnología se puede definir como la investigación científica y el desarrollo tecnológico que permiten entender, a nivel atómico y molecular, todos los fenómenos que ocurren a escala nanométrica, con el fin de utilizar este conocimiento para crear estructuras, materiales, dispositivos y sistemas de complejidad creciente que posean nuevas propiedades y realicen nuevas funciones debido al pequeño tamaño de sus componentes. La nanotecnología se está desarrollando en estos momentos a un ritmo frenético en un número creciente de laboratorios de entidades públicas y privadas de todo el mundo, y en los últimos años ha crecido considerablemente la producción y empleo de nuevos nanomateriales en la industria para muy diversas aplicaciones.

Los nanomateriales son, por definición, materiales cuyo tamaño oscila, en alguna de sus tres dimensiones, entre 1 y 100nm, confiriéndoles este pequeño tamaño propiedades únicas y diferentes de las del mismo material a mayor escala, debido fundamentalmente a la mayor área superficial, lo que les proporciona una reactividad muy superior. A medida que el tamaño de partícula desciende, su área superficial se incrementa, lo que causa que una mayor proporción de átomos o moléculas se encuentren en la superficie y no en el interior del material. Este aumento del área superficial determina por tanto muy probablemente a un incremento en la actividad biológica. Según el número de dimensiones que tengan en la nanoescala, estos materiales se clasifican en nanosuperficies (solo una dimensión), nanohilos o nanotubos (dos dimensiones) y nanopartículas (NP) (las tres dimensiones), siendo estas últimas las más frecuentemente utilizadas.

Los nanomateriales pueden ser orgánicos o inorgánicos, y su usos potenciales incluyen ahorro de energía para vehículos, desarrollo de energías renovables, disminución de la contaminación, filtración del agua, materiales de construcción, aplicaciones cosméticas (maquillajes, cremas de protección solar, etc.), textiles, electrónica, pinturas y tintas, entre otras. Asimismo, se han desarrollado aplicaciones biomédicas de las NP para liberación de medicamentos, terapias farmacológicas, prótesis, técnicas de imagen *in vivo*, diagnóstico *in vitro* e implantes activos. En concreto, en los últimos años se ha concentrado una gran atención en la utilización de NP para el tratamiento y diagnóstico de enfermedades neurológicas, tales como las enfermedades de Parkinson o Alzheimer, la esclerosis múltiple, neoplasias del sistema nervioso o enfermedades neurodegenerativas visuales. Actualmente hay más de 1.500 productos comercializados con usos muy diversos que contienen nanomateriales.

Junto con el rápido crecimiento de la industria de la nanotecnología se produce la expansión de la cantidad y tipos de nanomateriales manufacturados, lo que da lugar a exposiciones ocupacionales potencialmente elevadas, y a exposición de la población general a través de la utilización de los productos que las contienen y de sus productos de desecho. Es por

ello que, desde la primera década de este siglo, existe una creciente preocupación por los potenciales efectos adversos para la salud humana de la exposición a nanomateriales.

Numerosos autores muestran su acuerdo en que la progresiva presencia en el mercado de productos que contienen nanomateriales constituye un riesgo potencial emergente, principalmente debido a que los posibles efectos tóxicos de estos nanomateriales no han sido todavía caracterizados, y pueden diferir notablemente de los propios del material de que están compuestos cuando se encuentra en una escala mayor. La reducción en el tamaño proporciona una mayor biodisponibilidad, que se acompaña de un incremento en la capacidad de los nanomateriales para acceder a los sistemas biológicos. Además, las partículas y materiales en el rango nanométrico pueden causar daños debido a su elevada reactividad. Los organismos vivos están compuestos de células cuyo tamaño es habitualmente de 10-100μm. Sin embargo, los componentes celulares son mucho más pequeños, y las proteínas, el ADN y otras biomoléculas son incluso menores, encontrándose en un rango de tan solo 5-50nm. Esta sencilla comparación de tamaños da una idea de que los nanomateriales pueden resultar útiles para acceder a la maquinaria celular con objetivos diversos, pero también pueden interaccionar fácilmente con cualquier componente celular para causar efectos tóxicos.

En general, el comportamiento de los nanomateriales se podría resumir de la siguiente manera: las partículas en el rango nanométrico pueden introducirse en el cuerpo humano a través de las vías inhalatoria, transdérmica, oral o parenteral. Entonces los nanomateriales entran en contacto inmediato con un conjunto de proteínas y células característico de ese ambiente, y tratan de disminuir su energía superficial adsorbiendo sobre su superficie biomoléculas circundantes incluyendo proteínas, lípidos, sacáridos y ácidos nucleicos. Los nanomateriales absorbidos pueden ser transportados a órganos diversos incluyendo cerebro, corazón, hígado, riñones, bazo, médula ósea y el sistema nervioso. Finalmente, pueden atravesar las membranas celulares y penetrar en el citoplasma de las células que forman el órgano y residir allí por un período incierto de tiempo, antes de afectar a otros órganos o ser excretados fuera del organismo. Desde el citoplasma pueden también penetrar en los compartimentos subcelulares, tales como el núcleo y las mitocondrias. Esto hace a las NP singularmente adecuadas para usos terapéuticos y de diagnóstico, pero también motiva que órganos diana, como el sistema nervioso central, sean vulnerables a los potenciales efectos adversos.

Aunque la translocación de NP al cerebro es posible y ha sido ya estudiada bajo diferentes condiciones experimentales, la relevancia para la salud de estas situaciones todavía no está en absoluto clara. Por tanto, se hace necesaria la evaluación de los efectos tóxicos que las NP puedan ocasionar en las células neuronales, junto con una descripción detallada de sus posibles mecanismos de actuación.

El **objetivo general** de esta tesis consistió en evaluar el potencial tóxico de una serie de NP de óxidos metálicos (concretamente de dióxido de titanio, óxido de zinc y óxido de hierro)

sobre células neuronales humanas (SH-SY5Y). Para ello se aplicó un conjunto completo de metodologías celulares y moleculares *in vitro*, a fin de caracterizar los potenciales efectos adversos de las NP evaluadas e identificar sus mecanismos de acción subyacentes. Así, esta Tesis se divide en tres capítulos principales, cada uno de ellos dedicado un tipo diferente de NP evaluada.

Entre todos los nanomateriales manufacturados, las **NP de dióxido de titanio** (NP-TiO_2) son los que se produjeron industrialmente de forma más temprana y, de acuerdo con la *National Nanotechnology Initiative* de Estados Unidos, son los de mayor fabricación actualmente en el mundo. En la vida diaria estas NP se pueden encontrar en casi todas partes: en pinturas, revestimientos, plásticos, papeles, tintas, medicamentos, productos farmacéuticos, cosméticos y productos de higiene personal. Incluso se han utilizado como pigmento para blanquear la leche desnatada, y se han aprobado como aditivo alimentario colorante y para ser utilizados en envases alimentarios por la *Food and Drug Administration* de Estados Unidos (FDA).

El rápido incremento en el número de productos de uso cotidiano que contienen NP-TiO_2 en se acompaña de una creciente preocupación acerca de su seguridad para las personas y el medio ambiente. Está bien documentado el hecho de que las NP-TiO_2 pueden acceder al sistema nervioso, bien cruzando la barrera hematoencefálica o bien mediante transporte axonal directo a través del nervio olfatorio. Sin embargo, son todavía escasos los estudios sobre la potencial neurotoxicidad y efectos sobre el sistema nervioso de estas NP, y están esencialmente limitados a células u organismos animales.

Así, en el capítulo 3 de esta Tesis se investigó si las NP-TiO_2 podrían causar efectos adversos en las células neuronales, elucidando los posibles mecanismos moleculares. Además, mediante la comparación de dos tipos de NP-TiO_2 con dos estructuras cristalinas diferentes (anatasa pura y anatasa:rutilo 80:20), exploramos la posible influencia de esta característica sobre su interacción con las células neuronales bajo diversas condiciones *in vitro*.

Tras la caracterización físico-química de las NP, se realizó una batería de ensayos para evaluar viabilidad celular, citotoxicidad, genotoxicidad y daño oxidativo en células SH-SY5Y expuestas a NP-TiO_2. Aunque estas NP fueron internalizadas eficazmente por las células neuronales, no redujeron la viabilidad celular aunque sí causaron alteraciones del ciclo celular dependientes de la dosis y apoptosis por la vía intrínseca. Los ensayos de genotoxicidad mostraron resultados positivos en el ensayo del cometa y el test de micronúcleos (MN), pero resultados negativos en el ensayo γH2AX, sugiriendo que las NP-TiO_2 inducen genotoxicidad en las células neuronales no relacionada con la producción de roturas de cadena doble. Además, todos estos efectos no se asociaron con la producción de estrés oxidativo, ya que no se detectaron incrementos en el daño oxidativo en el ADN o descensos en la tasa glutatión reducido/glutatión oxidado. Los resultados obtenidos revelaron que el comportamiento de ambos tipos de NP resultó en gran medida comparable; los resultados de gentoxicidad fueron

similares, pero las NP de anatasa pura fueron internalizadas por las células con mayor efectividad y mostraron mayor potencial para inducir citotoxicidad, en concreto alteraciones del ciclo celular. Las observaciones realizadas en este estudio reiteran la preocupación acerca de la seguridad de las NP-TiO_2 que se utilizan en productos de consumo habitual.

Las **NP de óxido de zinc** (NP-ZnO) son también unas de las NP de óxidos metálicos más abundantemente utilizadas en bienes de consumo y aplicaciones biomédicas, debido a sus propiedades específicas como son la transparencia, su alto punto isoeléctrico, la biocompatibilidad y la eficiencia fotocatalítica. Estas NP se emplean ampliamente en una variedad de productos, incluyendo cosméticos, pasta de dientes, protectores solares, rellenos en materiales médicos, textiles, pinturas de pared, y otros materiales de construcción, y pueden ser también utilizadas en la remediación ambiental para la eliminación o degradación de los contaminantes en el agua o el aire. Como resultado de todos estos usos, la exposición humana a estas NP es altamente frecuente.

Aunque la toxicidad de las NP-ZnO se ha estudiado ampliamente y se ha demostrado que afectan a muchos tipos diferentes de células y sistemas animales, los datos toxicológicos acerca de las NP-ZnO en el sistema nervioso son significativamente escasos, especialmente en lo que se refiere a las células y tejidos nerviosos humanos. Por lo tanto, en el capítulo 4 de esta tesis, se investigaron los efectos citotóxicos y genotóxicos de las NP-ZnO en las células neuronales humanas SH-SY5Y, bajo diferentes condiciones de exposición.

Los resultados obtenidos por citometría de flujo mostraron que las NP-ZnO no entran en las células neuronales, pero su presencia en el medio indujo descensos significativos de la viabilidad celular dependientes de la dosis a partir de 25μg/ml, a todos los tiempos de tratamiento testados. La exposición a NP-ZnO causó importantes alteraciones en el ciclo celular, incluyendo detención mitótica, e inducción de apoptosis apenas relacionada con descenso en el potencial de membrana mitocondrial, indicando que este tipo de muerte celular se produjo principalmente por una ruta independiente de la mitocondria.

Los resultados también mostraron que las NP-ZnO causaron genotoxicidad en las células neuronales, esencialmente daño primario en el ADN, evaluado mediante el ensayo del cometa, y fosforilación de la histona H2AX desde las 3h de exposición, e inducción de MN tras 6h de exposición. Asimismo, estas NP produjeron incremento en el daño oxidativo en el ADN en todas las condiciones testadas. Sin embargo, no se observaron alteraciones en la integridad de la membrana citoplasmática en presencia de las ZnO-NP, aunque no se puede descartar la posibilidad de que las NP interaccionen con algún componente de la membrana sin alterar su integridad.

A fin de determinar si los iones de zinc pudiesen ser los responsables de los efectos tóxicos observados para las ZnO-NP, se evaluó la liberación de estos iones a partir de las NP.

Los resultados mostraron efectivamente la liberación de iones hasta niveles de 0.3mM. Sin embargo, estos niveles de iones no causaron descenso en la viabilidad celular, sugiriendo que no son los causantes de los efectos tóxicos descritos, al menos en lo que se refiere a la disminución en la viabilidad de las células neuronales. Sin embargo, no se puede descartar por completo que puedan jugar un papel relevante en otros tipos de daño celular.

Dado que en este estudio se han demostrado efectos neurotóxicos de la NP-ZnO a diferentes niveles, aunque su mecanismo de acción todavía requiere de mayor clarificación, se precisa realizar investigaciones adicionales para desarrollar las necesarias precauciones de seguridad y límites de exposición para las personas que trabajan en la producción y manufactura de materiales que contengan estas NP, y para aquellas que estén expuestas a ellas cuando se implementan en diferentes aplicaciones comerciales, industriales y médicas.

Las **NP de óxido de hierro** (ION) han ido ganando progresivo interés desde el nacimiento de la nanotecnología gracias a sus características únicas. Debido a sus propiedades magnéticas, las ION tienen un inmenso potencial en una amplia variedad de aplicaciones en diversos campos de la biotecnología y la biomedicina, tanto para diagnóstico como para terapia, tales como para agentes de contraste en imágenes por resonancia magnética, como vehículos para la administración de fármacos y genes, y como mediadores térmicos para terapia anticancerosa; de hecho algunas de ellas han sido ya aprobadas para su uso en clínica. Aparte de estas aplicaciones principales, las ION están siendo intensamente exploradas en neuromedicina dado que tienen la capacidad de atravesar la barrera hematoencefálica. Esta capacidad las hace muy adecuadas para ser utilizadas como herramientas terapéuticas y de diagnóstico prometedoras para tumores malignos del sistema nervioso.

Teniendo en cuenta que los óxidos de hierro se producen naturalmente en forma de cristales de tamaño nanométrico en la corteza terrestre, y que las ION ya se han utilizado en aplicaciones clínicas, podría parecer que no existe riesgo subyacente para la salud asociado con estas NP. Aunque algunos estudios en la literatura han demostrado que las ION son menos tóxicas que otros tipos de NP metálicas, son aún escasos los estudios sistemáticos acerca de sus efectos sobre el sistema nervioso humano, y sus resultados han sido hasta la fecha inconsistentes. Por lo tanto, teniendo en cuenta los usos relevantes y prometedoras aplicaciones de las ION en el campo de la neuromedicina, resulta necesario evaluar en profundidad sus potenciales efectos nocivos sobre las células neuronales.

Las ION desnudas (sin cubierta superficial) tienden a formar aglomerados que se vuelven inestables con el tiempo. Pueden ser fácilmente atrapadas por las células del sistema inmune como materiales extraños, lo que supone que no pueden llegar al objetivo deseado, y son además químicamente muy activas y fácilmente oxidadas, lo que resulta frecuentemente en la pérdida de magnetismo y dispensabilidad. Para resolver estos problemas, la superficie de las NP puede ser modificada mediante el recubrimiento con una serie de materiales con diferentes

propósitos, y la funcionalización de la superficie puede desempeñar un papel clave no sólo en la regulación de la penetración a través de la membrana celular, sino también interfiriendo con la actividad de las células. Sin embargo, la evaluación de los posibles efectos nocivos de ION recubiertas superficialmente con productos varios en diferentes líneas de células neuronales muestran hasta la fecha resultados contradictorios.

Entre todas las posibles modificaciones superficiales para las ION, la cubierta de sílice (SiO_2) tiene varias ventajas que la hacen especialmente adecuada para ser empleada con fines médicos. Por ejemplo, las ION recubiertas de sílice (S-ION) presentan carga negativa al pH de la sangre, lo que ayuda a evitar la formación de agregados en los fluidos corporales, y su matriz transparente permite el paso eficiente de la luz de excitación y emisión, lo que representa una propiedad relevante para el diagnóstico por imagen. Sin embargo, su potencial toxicidad sobre el sistema nervioso no se ha abordado en profundidad.

Por lo tanto, el objetivo del capítulo 5 de esta Tesis consistió en evaluar la toxicidad de las S-ION en las células neuronales humanas SH-SY5Y. Para ello se analizaron como parámetros de citotoxicidad las alteraciones en el ciclo celular, la muerte celular por apoptosis o necrosis y la integridad de la membrana plasmática. Se determinó también la genotoxicidad mediante la evaluación de los niveles de fosforilación de la histona H2AX (ensayo γH2AX), el test de MN, y el ensayo de cometa. Además, se analizó la producción de estrés oxidativo mediante la detección de la producción de especies reactivas de oxígeno (ROS), del nivel de glutatión y del daño oxidativo en el ADN. De forma complementaria, se evaluaron asimismo los posibles efectos de las S-ION sobre la reparación del daño en el ADN por medio de ensayo de competencia de reparación del ADN.

Los resultados de los experimentos mostraron que, a pesar de ser internalizadas eficazmente por las células neuronales, las S-ION presentan en general baja citotoxicidad; aunque se obtuvieron resultados positivos en algunas condiciones experimentales, la viabilidad celular se mantuvo por encima del 80% en todos los casos. Los ensayos de determinación de hierro en el medio de cultivo manifestaron que, a pesar de estar recubiertas por sílice, estas NP liberan iones de hierro de forma dependiente de la dosis y del tiempo.

En la evaluación de citotoxicidad se observó que las S-ION no producen cambios en la integridad de la membrana plasmática, y solamente inducen alteraciones del ciclo celular o muerte celular por apoptosis cuando se testan a las dosis más elevadas o el tiempo de exposición más prolongado.

Respecto a la genotoxicidad, el tratamiento de las células neuronales con S-ION indujo daño primario en el ADN dependiente de la dosis pero que, según los resultados negativos obtenidos en el test de MN y el ensayo γH2AX, no está relacionado con la producción de roturas de doble cadena del ADN o pérdidas cromosómicas. A pesar de que las S-ION no fueron

capaces de producir ROS en ausencia de contacto con células, se encontró incremento en la producción de estas especies reactivas en las células SH-SY5Y tras la exposición a las NP, resultando además en descenso del glutatión y aumento del daño oxidativo en el ADN.

Según los resultados obtenidos en el ensayo de competencia de reparación del ADN, en el que se induce un daño en el material genético utilizando peróxido de hidrógeno y luego se permite un cierto tiempo para su reparación, los mecanismos de reparación no resultaron afectados por las S-ION en las células cuando la exposición a las NP se realiza antes de la inducción del daño o durante el periodo de reparación. No obstante, cuando la exposición a las S-ION se produce simultáneamente con el peróxido de hidrógeno, el periodo de reparación de 30 minutos no resulta suficiente para reparar el daño provocado.

En suma, los resultados experimentales obtenidos en esta Tesis contribuyen a incrementar el conocimiento sobre el potencial citotóxico y genotóxico de las NP de óxidos metálicos en general, y específicamente en las células neuronales humanas. Los resultados obtenidos también destacan la necesidad evaluar las posibles interacciones de las NP con los sistemas vivos, con el fin de revelar sus efectos a diferentes niveles. En concreto, cuando los nanomateriales son diseñados para estar en contacto directo con el ser humano, o incluso para ser introducidos en el interior de su organismo (como es en el caso de las aplicaciones biomédicas o alimentarias), resulta de crucial importancia determinar si estos nuevos materiales son suficientemente seguros; en otras palabras, que para que la sociedad se beneficie plenamente de la nanotecnología la relación beneficio-riesgo ha de ser favorable, de forma que las enormes posibilidades de esta ciencia emergente puedan ser explotadas convenientemente sin riesgos para la salud, o con riesgos mínimos.

LIST OF ABBREVIATIONS **I**

LIST OF FIGURES **V**

LIST OF TABLES **XI**

1. GENERAL INTRODUCTION **1**

1.1. Nanotoxicology 3

1.1.1. A brief history of nanotechnology 3

1.1.2. Terminology 5

1.1.3. Physicochemical properties of nanomaterials 7

1.1.4. Exposure and biodistribution 10

1.1.5. Potential adverse effects 12

1.2. Methods for Understanding the Interaction between Nanoparticles and Cells 14

1.2.1. Characterization 14

1.2.1.1. Size and dispersion 15

1.2.1.2. Surface properties 17

1.2.2. Cellular interaction with nanoparticles 19

1.2.2.1. Cellular uptake of nanoparticles 19

1.2.2.2. In vitro cytotoxicity and cell death 20

1.2.2.3. In vitro genotoxicity 26

1.2.2.4. Generation of reactive oxygen species 30

2. OBJECTIVES AND OUTLINE OF THE THESIS **35**

3. EFFECTS OF TITANIUM DIOXIDE NANOPARTICLES WITH TWO DIFFERENT CRYSTALLINE STRUCTURE ON HUMAN NEURONAL CELLS **39**

3.1. Introduction 41

3.2. Materials and Methods 45

3.2.1. Nanoparticles: preparation and characterization 45

3.2.2. Cell culture and treatments 46

3.2.3. Cellular viability 46

3.2.4. Cellular uptake 47

3.2.5. Cell cycle 48

3.2.6. Apoptosis 48

3.2.6.1. Annexin V-FITC/PI staining 48

3.2.6.2. Mitochondrial membrane potential analysis 49

3.2.7. Genotoxicity 49

3.2.7.1. Micronucleus evaluation by flow cytometry 49

3.2.7.2. γH2AX assay 49

3.2.7.3. Comet assay 50

3.2.8. Oxidative damage 51

3.2.8.1. Oxidative DNA damage 51
3.2.8.2. Glutathione determination 51
3.2.9. Statistical analysis 52
3.3. Results and Discussion 52
3.3.1. Nanoparticle characterization 53
3.3.2. Cellular viability 55
3.3.3. Uptake 56
3.3.4. Cell cycle 57
3.3.5. Apoptosis 58
3.3.6. Genotoxicity 60
3.3.7. Oxidative damage 63
3.4. Conclusions 66

4. NEURONAL CYTOXICITY AND GENOTOXICITY INDUCED BY ZINC OXIDE NANOPARTICLES 67
4.1. Introduction 69
4.2. Materials and Methods 71
4.2.1. Nanoparticles: preparation and characterization 71
4.2.2. Cell culture and treatments 71
4.2.3. Cellular viability 72
4.2.4. Cellular uptake 72
4.2.5. Cell cycle 72
4.2.6. Apoptosis 72
4.2.6.1. Annexin V-PI staining 72
4.2.6.2. Mitochondrial membrane potential analysis 72
4.2.7. Genotoxicity 73
4.2.7.1. Micronucleus evaluation by flow cytometry 73
4.2.7.2. γH2AX assay 73
4.2.8. Comet assay 73
4.2.9. Oxidative DNA damage 73
4.2.10. Membrane integrity 73
4.2.11. Dissolved zinc concentrations in cell culture medium 74
4.2.12. Cytotoxic effects of Zinc(II)ions. 74
4.2.13. Statistical analysis 74
4.3. Results and Discussion 75
4.3.1. Nanoparticle characterization 75
4.3.2. Cellular viability 76
4.3.3. Cellular uptake 77
4.3.4. Cell cycle 78
4.3.5. Apoptosis 79
4.3.6. Genotoxicity 80
4.3.7. Oxidative DNA damage 83

4.3.8. Membrane integrity 84
4.3.9. Cytotoxic effects of Zinc(II)ions 85
4.4. Conclusions 88

5. NEURONAL CYTOTOXICITY AND GENOTOXICITY INDUCED BY IRON OXIDE NANOPARTICLES 91
5.1. Introduction 93
5.2. Materials and Methods 97
5.2.1. Nanoparticles: preparation and characterization 97
5.2.2. Dissolved iron concentrations in the cell culture medium 98
5.2.3. Cell culture and treatments 98
5.2.4. Cellular viability 98
5.2.5. Cellular uptake 98
5.2.6. Cell cycle 98
5.2.7. Apoptosis and necrosis 99
5.2.8. Membrane integrity 99
5.2.9. Genotoxicity 99
5.2.9.1. Micronuclei evaluation by flow cytometry 99
5.2.9.2. γH2AX assay 99
5.2.9.3. Comet assay 99
5.2.10. Oxidative stress 99
5.2.10.1. DCFH Assay 99
5.2.10.2. Glutathione determination 101
5.2.10.3. Oxidative DNA damage 101
5.2.11. DNA repair competence assay 101
5.2.12. Statistical analysis 101
5.3. Results and Discussion 102
5.3.1. Nanoparticle characterization 102
5.3.2. Cellular viability 104
5.3.3. Dissolved iron concentrations in the cell culture medium 105
5.3.4. Cellular uptake 106
5.3.5. Cell cycle 107
5.3.6. Apoptosis and necrosis 108
5.3.7. Membrane integrity 110
5.3.8. Genotoxicity 110
5.3.9. Oxidative stress 113
5.3.10. DNA repair competence assay 117
5.4. Conclusions 118

6. CONCLUDING REMARKS 121

7. REFERENCES 125

List of Abbreviations

8-oxoG	8-oxoguanine
%tDNA	percentage of DNA in the comet tail
α-Fe_2O_3	hematite
γ-Fe_2O_3	maghemite
$\Delta\psi m$	Changes in mitochondrial membrane potential
µm	micrometre
µM	micromolar
µl	microliter
AFM	atomic force microscopy
APTMS	(3-aminopropyl)trimethoxysilane
ATP	adenosine triphosphate
BBB	blood -brain barrier
BER	base excision repair
BET	Brunauer-Emmett-Teller
BLM	bleomycin
BSI	British Standards Institution
CAE	constant analyser energy
Campt	camptothecin
CM-H_2DCFDA	5-(and-6)-chloromethyl-2',7'-dichlorodihydrofluorescein diacetate, acetyl
CNS	central nervous system
DAPI	4,6-diamidino-2-fenilindol
DCF	2',7'-dichlorodihydrofluorescein
DCFH-DA	2',7'-dichlorodihydrofluorescein diacetate
DEM	diethyl maleate
DLS	dynamic light scattering
DMSA	dimercaptosuccinic acid
DMSO	dimethylsulfoxide
DNA	deoxyribonucleic acid
DSB	DNA double strand breaks
DTNB	5,5'-dithiobis-(2-nitrobenzoic acid)
EC	European Commission
ENDOIII	endonuclease III
ENM	engineered nanomaterials
EPA	Environmental Protection Agency
FAAS	flame atomic absorption spectroscopy
FBS	foetal bovine serum
FCM	flow cytometry
FDA	United States Food and Drug Administration
Fe^{2+}	ferrous ion
Fe^{3+}	ferric ion
Fe_3O_4	magnetite
FeO	wüstite
FPG	formamidopyrimidine DNA-glycosylase
FSC	forward scatter
GR	glutathione reductase enzyme
GSH	glutathione
GSSG	oxidized glutathione
h	hours

HRP	horseradish peroxidase
IARC	International Agency for Research on Cancer
ICP-MS	inductively coupled plasma mass spectrometry
INT	iodonitrotetrazolium
ION	iron oxide nanoparticles
ISO	International Standards Organization
JC-1	5,5′,6,6′-tetrachloro-1,1′,3,3′-tetraethylbenzimidazolylcarbocyanine iodide
LDH	lactate dehydrogenase
LMA	low-melting-point agarose
M3-PALS	mixed mode measurement phase analysis light scattering
mA	milliampere
MMC	mitomycin-C
MMP	mitochondrial membrane potential
MN	Micronucleus
MPTP	mitochondrial permeability transition pore
MRI	magnetic resonance imaging
MTT	3-(4,5-dimethylthiazol-2-yl)-2,5-diphenyltetrazolium bromide
mV	millivolt
NAD	nicotinamide adenine dinucleotide
NIOSH	National Institute for Occupational Safety and Health
nm	nanometre
NMA	normal melting point agarose
NP	nanoparticles
NRU	neutral red uptake
OECD	Organization for Economic Co-operation and Development
OGG1	8-oxoguanine DNA glycosylase
OH•	hydroxyl radicals
PBS	phosphate buffer solution
PI	propidium iodide
PS	phosphatidylserine
Rhod123	rhodamine 123
RNA	ribonucleic acid
ROS	reactive oxygen species
SCM	scanning capacitance microscope
SiO_2	silica
S-ION	silica-coated ION
siRNA	small interfering RNA
SSA	sulfosalicylic acid
SSB	DNA single strand breaks
SSC	side scatter
STM	scanning tunnelling microscope
TEM	transmission electron microscope
TEOS	tetraethyl-orthosilicate
TiO_2-D	TiO_2-NP in anatase:rutile (80:20) structure (purchased from Degussa)
TiO_2-NP	Titanium dioxide nanoparticles
TiO_2-S	TiO_2-NP in pure anatase structure (purchased from Sigma)
TMRM	tetramethylrhodamine methyl
TNB	5-thio-2-nitrobenzoic acid
UV	ultraviolet
W	watt

WHO	World Health Organization
XPS	Photoelectron spectroscopy
ZnO-NP	Zinc oxide nanoparticles

List of Figures

Figure 1.1. Number of publications from Thomson Reuters Web of Science™ database on 'nanotoxicity' or 'nanotoxicology' topics. Data for year 2015 is up to the end of May..... 5

Figure 1.2. Nanoscale showing nanomaterials compared to biological components, with indication of 'nano' and 'micro' sizes (from Wibke Busch, 2010). 6

Figure 1.3. Nanoparticles tend to agglomerate in physiological fluids but may also build stable aggregates. Agglomerates and aggregates are characterised by the hydrodynamic diameter that can differ significantly from the primary particle diameter (from Jiang et al., 2008). 7

Figure 1.4. For the same quantity of material, the decrease in particle size means a high increase in surface area (from www.uwgb.edu/dutchs/GRAPHIC0/GEOMORPH/SurfaceVol0.gif)..... 8

Figure 1.5. Summary of possible mechanisms of NP for entering cells and cellular compartments. NP may actively be taken up by cells via phagocytosis (A), macropinocytosis (B), clathrin-mediated endocytosis (C), clathrin- and caveolae-independent endocytosis (D), caveolae-mediated endocytosis (E) or by passive diffusion (F) (from Mühlfeld et al., 2008)..... 11

Figure 1.6. Schematic illustration of mechanisms of action of ENM (from Dusinska et al., 2011). 13

Figure 1.7. Principle of DLS technique. Smaller particles tend to diffuse more rapidly than larger particles at a given temperature and viscosity, and the hydrodynamic diameter is calculated by experimentally determining the fluctuations of the scattered light. 16

Figure 1.8. Analysing NP uptake in cells by flow cytometry. (A) Light scattering by a cell having no association with NP;(B) NP adhered to the cell surface leading to increase in both FSC and SSC; (C) NP internalization by the cell leading to increase only in SSC (from Sharma, 2011). 20

Figure 1.9. MTT reduction in live cells by mitochondrial reductase results in the formation of insoluble formazan (from http://www.intechopen.com/source/html/41784/media/image4_w.jpg) 21

Figure 1.10. LDH assay detection mechanism (from tools.lifetechnologies.com/content/sfs/gallery/high/88953-001-LDH-Cytotox.jpg). 22

Figure 1.11. The principle of apoptosis detection by annexin V/PI (from www.dojindo.com/store/p/847-Annexin-V-FITC-Apoptosis-Detection-Kit.html). 23

Figure 1.12. The principle of apoptosis detection with the fluorescent cationic dye JC-1 (from http://www.nexcelom.com/Applications/Apoptosis.html)..... 24

Figure 1.13. Phases of the cell cycle (from Mahmoudi et al., 2011)..... 25

Figure 1.14. Scheme of the standard comet assay (from Azqueta and Collins, 2006)..... 27

Figure 1.15. Images of cells subjected to comet assay. A) not damaged cell, B) moderately damaged cell, C) intensely damaged cell..... 28

Figure 1.16. Scheme of H2AX phosphorylation process and its consequences in DNA damage response (from http://www.amsbio.com/news/whitepaper/gamma_H2AX_white_paper.pdf)..... 29

Figure 1.17. Representation of MN formation in cells undergoing nuclear division (from Fenech et al., 2011)..... 30

Figure 3.1. TiO_2 rutile crystalline structure (from www.chemtube3d.com/solidstate/_rutile%28final%29.htm) 41

Figure 3.2. TiO_2 anatase crystalline structure (from http://www.chemtube3d.com/solidstate/_anatase%28final%29.htm). 42

Figure 3.3. Size distribution of TiO_2-S (a) and TiO_2-D (b) in water, and TiO_2-S (c) and TiO_2-D (d) in cell culture medium..... 54

Figure 3.4. MTT assay (a-b) and NRU assay (c-d) results on neuronal cells treated with TiO_2-S or TiO_2-D. The relative cell viability in the exposed cells was expressed as a percentage relative to the untreated control cells. 56

Figure 3.5. Flow cytometry analysis of TiO_2-S (a) or TiO_2-D (b) uptake by SH-SY5Y cells. **P*<0.05, significant difference with regard to the corresponding negative control. 56

Figure 3.6. Cell-cycle analysis after treatment of SH-SY5Y cells with TiO_2-S (a, b) or TiO_2-D (c, d) for 3h (a, c) or 6h (b, d). PC: positive control. **P*<0.05, ***P*<0.01, significant difference with regard to the negative control. 58

Figure 3.7.Genotoxicity in neuronal cells treated with TiO_2-S (a) or TiO_2-D (b) by MN evaluation. PC: positive control. **P*<0.05, ***P*<0.01, significant difference with regard to the corresponding negative control..... 61

Figure 3.8. Genotoxicity in neuronal cells treated with TiO_2-S (a) or TiO_2-D (b) by γH2AX assay. PC: positive control. ***P*<0.01, significant difference with regard to the corresponding negative control..... 61

Figure 3.9. Genotoxicity in neuronal cells treated with TiO_2-S (a) or TiO_2–D (b) by comet assay. PC: positive control. **P*<0.05, ***P*<0.01, significant difference with regard to the corresponding negative control..... 62

Figure 3.10. Results of OGG1-modified comet assay in neuronal cells treated with TiO_2–S for 3h (a) or for 24h (b), and with TiO_2–D for 3h (c), or for 24h (d). PC: positive control. **P*<0.05, significant difference with regard to the corresponding buffer. 64

Figure 3.11. Ratio of reduced to oxidised glutathione in neuronal cells treated with TiO_2-S (a) or TiO_2-D (b). PC: positive control. 64

Figure 4.1. The hexagonal wurtzite structure model of ZnO. The tetrahedral coordination of ZnO is shown; O atoms are the larger red spheres while the Zn atoms are the smaller yellow spheres (from http://pixshark.com/wurtzite-structure.htm). 70

Figure 4.2.Characterization of ZnO-NP: (a) hydrodynamic diameter and (b) zeta potential in water; (c) hydrodynamic diameter and (d) zeta potential in culture medium. 76

Figure 4.3. Results from MTT assay (a) and NRU assay (b) on viability of neuronal cells treated with ZnO-NP. Values inside the rectangle are statistically different from the corresponding controls. 77

Figure 4.4. Uptake of ZnO-NP by SH-SY5Y cells as analysed by FCM. PC: positive control. **P*<0.05, significant difference with regard to the corresponding negative control. 78

Figure 4.5. Results of cell cycle analysis in neuronal cells treated with ZnO-NP for 3h (a) or 6h (b) (percentage of cells in each phase). **P*<0.05; ***P*<0.01; significant difference with regard to the corresponding negative control. PC: positive control. 79

Figure 4.6. Results of MN evaluation in SH-SY5Y cells treated with ZnO-NP. **P*<0.05, ***P*<0.01, significant difference with regard to the corresponding negative control. PC: positive control..... 81

Figure 4.7. Results of γH2AX evaluation in SH-SY5Y cells treated with ZnO-NP. **P*<0.05, ***P*<0.01, significant difference with regard to the corresponding negative control. PC: positive control..... 82

Figure 4.8 Results of comet assay in SH-SY5Y cells treated with ZnO-NP. **P*<0.05, ***P*<0.01, significant difference with regard to the corresponding negative control. PC: positive control. 82

Figure 4.9. Results of OGG1-modified comet assay in neuronal cells treated with ZnO-NP for 3h (a) or 6h (b). **P*<0.05, ***P*<0.01, significant difference with regard to the corresponding buffer. PC: positive control. 84

Figure 4.10. Results of membrane integrity assessment (LDH assay) in SH-SY5Y cells exposed to ZnO-NP. PC: positive control. 85

Figure 4.11. Analysis of Zn (II) ions released from ZnO-NP in cell culture medium. 87

Figure 4.12. Cytotoxicity of Zinc (II) ions: MTT assay in SH-SY5Y cells treated with $ZnSO_4$. **P<0.01, significant difference with regard to the negative control. 88

Figure 5.1. Cellular toxicity induced by ION (from Singh et al., 2010). 95

Figure 5.2. Characterization of S-ION: (a) TEM microphotograph, (b) distribution of hydrodynamic diameter in cell culture medium. 103

Figure 5.3. Viability of SH-SY5Y cells after exposure to S-ION assessed by MTT assay (a) and NRU assay (b). Values were normalized considering negative control as 100%. PC: positive control. *P<0.05, significant difference with regard to the corresponding negative control. 104

Figure 5.4. Iron ion release from S-ION. 106

Figure 5.5. Cellular uptake of S-ION as analysed by FCM. **P<0.01, significant difference with regard to the corresponding control. 106

Figure 5.6. Cell cycle analysis of SHSY-5Y cells after exposure to S-ION: (a) 3h treatment; (b) 24h treatment. PC: positive control. **P<0.01, significant difference with regard to the corresponding negative control. 107

Figure 5.7. Apoptosis (subG_1 region) in neuronal cells treated with S-ION. PC: positive control. *P<0.05, significant difference with regard to the corresponding negative control. 109

Figure 5.8. Apoptosis and necrosis induction by S-ION for 3h (a) and 24h (b) evaluated by annexinV/PI staining. PC: positive control. *P<0.05, **P<0.01, significant difference with regard to the corresponding negative control. 109

Figure 5.9. LDH leakage analysis after S-ION exposure. PC: positive control. 110

Figure 5.10. Results of γH2AX analysis on neuronal cells treated with S-ION. PC: positive control. **P<0.01, significant difference with regard to the corresponding negative control. 111

Figure 5.11. Results of MN evaluation in SH-SY5Y cells treated with S-ION. PC: positive control. *P<0.05, significant difference with regard to the negative control. 111

Figure 5.12. Results of comet assay in neuronal cells treated with S-ION. PC: positive control. *P<0.05; **P<0.01, significant difference with regard to the corresponding negative control. 111

Figure 5.13. Results of the acellular DCFH assay with S-ION, expressed as %fluorescence fold increase. PC: positive control. 113

Figure 5.14. Results of the DCFH assay in neuronal cells treated with S-ION, expressed as % fold increase compared to control. PC: positive control. **P<0.01, significant difference with regard to the corresponding negative control. 115

Figure 5.15. Ratio of reduced to oxidised glutathione in neuronal cells treated with S-ION. PC: positive control. ***P*<0.01, significant difference with regard to the corresponding negative control..... 115

Figure 5.16. Results of OGG1-modified comet assay in neuronal cells treated with S-ION for 3h (a) and 24h (b). PC: positive control. **P*<0.05, ***P*<0.01, significant difference with regard to the corresponding buffer..... 115

Figure 5.17. Effects of S-ION on repair of H_2O_2-induced DNA damage in neuronal cells. Incubation with S-ION was carried out either before H_2O_2 treatment (phase A), simultaneously (phase B), or during the repair period (phase C). **P*<0.05, ***P*<0.01, significant difference with regard to the same treatment before repair; $^{\#}P$<0.05, significant difference with regard to the control..... 117

List of Tables

Table 1.1. Types of ENM classified by their structure and composition (adapted from (Dawidczyk et al., 2014; Tang et al., 2009). 9

Table 3.1. Characterization of TiO_2-NP. 54

Table 3.2. Apoptotic cell rates (%) after TiO_2-NP exposure 58

Table 4.1. Physicochemical characterization of ZnO-NP 76

Table 5.1. Physicochemical description of S-ION. 103

1. General Introduction

1.1. NANOTOXICOLOGY

1.1.1. *A brief history of nanotechnology*

Nanotechnology is the term given to those areas of science and engineering where nanometre scale (approximately 1-100nm) is utilized in the design, characterization, production and application of materials, structures, devices and systems (Blaunstein and Linkov, 2010).

Study of the nanoscale phenomena is not a new field since scientists have been working in nanoscience for many decades in several areas of technology and medicine (Pitkethly, 2004). For example Pasteur's work with spoilage bacteria, measurable on the micrometre (μm) scale (1μm = 1000nm), and Watson and Crick's discovery of the DNA structure (a molecule of DNA is about 2.5nm wide) can be considered nanoscience (Institute of Medicine (US) Food Forum, 2009). However, interest in nanomaterials, in particular in engineered nanomaterials (ENM), i.e., those not naturally produced but manmade, has increased significantly over the past several decades. ENM are intentionally developed materials that have at least one dimension of 1–100 nm and exhibit novel properties compared to the larger scale form of a material of the same composition (Majuru and Oyewumi, 2009).

The concept of nanotechnology was firstly introduced by the American physicist Richard Feynman in his lecture 'There's plenty of room at the bottom' at an American Physical Society meeting in Caltech on December 29, 1959 (Fitzpatrick et al., 2014). Dr. Feynman's talk has been viewed as the first academic talk where he issued an invitation to physicists of his generation to enter a new field of physics: the field of nanotechnology (Ando and Kumar, 2010). Although he did not use the term 'nanotechnology', he described a process by which the ability to manipulate individual atoms and molecules might be developed (Feynman, 1960).

A Japanese student called Norio Taniguchi was the first person in using the term 'nano-technology' in a 1974 conference, where he stated 'nano-technology mainly consists of the processing, separation, consolidation, and deformation of materials by one atom or one molecule' (Taniguchi, 1974). However, nanotechnology did not develop into a field until the 1980s, when Eric Drexler, scientist at the Massachusetts Institute of Technology, who was unaware of Taniguchi's prior use of the term, published his first paper on nanotechnology in 1981, entitled 'Molecular engineering: an approach to the development of general capabilities for molecular manipulation' in the journal Proceedings of the National Academy of Sciences. (Ranjit and Klabunde, 2007). In this article, Drexler discussed the possibility of molecular manufacturing as a process of fabricating objects with specific atomic specifications, using designed protein molecules (Drexler, 1981). Drexler took these concepts and expanded the

study of their potential in a book entitled 'Engines of creation: the coming era of nanotechnology' (Drexler, 1996). Later, due to the publicity generated by Drexler's work, scientists from all over the world began to have a vested interest in the field of nanotechnology.

Just as Watson and Crick's discovery of the structure of DNA led to a biotechnology revolution, Drexler created interest in the field but also outlined a nanotech revolution, and researchers around the world have brought nanotechnology to a more realistic and attainable level (Santamaria, 2012). Nanotechnology and nanoscience got a boost in the early 1980s with the availability of tools that allow scientists to see things that they were not able to see in the past, with the development of microscopic technologies such as scanning tunnelling microscope (STM) (Binnig and Rohrer, 1986) and atomic force microscopy (AFM).

While nanotechnology came into existence through Feynman's and then Drexler's vision of molecular manufacturing, the field has evolved into research in several fields, including chemistry, materials science, medicine, toxicology, ecology, and industrial hygiene by multidisciplinary attempts with combination of chemistry, materials science, molecular biology, and molecular engineering (Oberdörster et al., 2007). The past two decades have witnessed tremendous progress in nanotechnology. Not only nanomaterials became an important part of our everyday lives as components of cosmetics, polymers, sporting goods, sensors, gasoline additives, or materials for medical diagnostics, but also they moved into our research labs to narrow down the concerns about their possible toxicity and influence on organisms caused by long-term exposure.

Beginning in the early 2000s, concerns about the potential human and environmental health effects of nanomaterials were being expressed by many scientists, regulators, and non-governmental agencies, because particles and materials in the nanosize range may pose toxicological hazards due to their enhanced reactivity (Santamaria, 2012). It was not until very recently that this topic began to gain increased interest and, as seen in Figure 1.1, the number of scientific articles published on 'nanotoxicity' or 'nanotoxicology', progressively increased; before 2005 it was almost negligible.

An understanding of the toxicological profiles of ENM is necessary in order to ensure that these materials are safe for use and are developed responsibly, with optimization of benefits and minimization of risks. However, the development and production of ENM are increasing faster than their toxicological information is being acquired. The uncertainty and the lack of information on possible adverse effects of ENM have been taken into consideration by many organizations worldwide such as the US Environmental Protection Agency (EPA), the World Health Organization (WHO), the US National Institute for Occupational Safety and Health (NIOSH), the European Commission (EC) and the Organization for Economic Co-operation and Development (OECD). Many official documents have been published by these organizations

addressing the need of dedicated research on appropriate methodological assays for assessing ENM toxicity (Colognato et al., 2012).

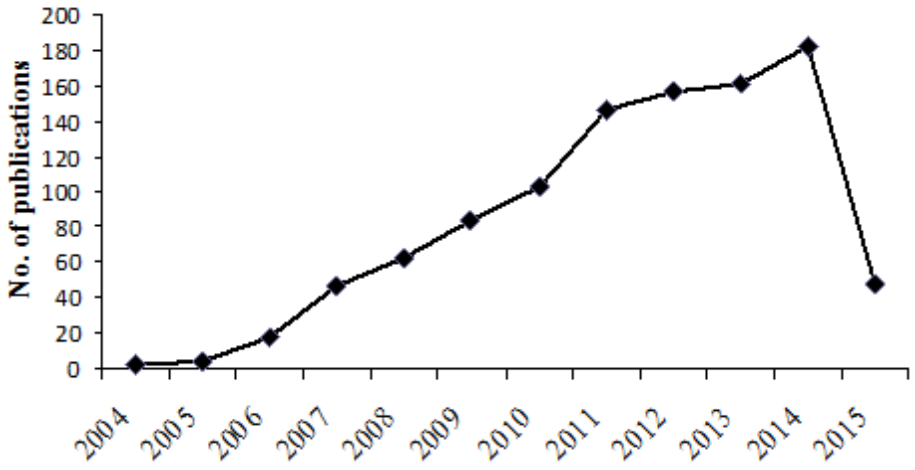

Figure 1.1. Number of publications from Thomson Reuters Web of Science™ database on 'nanotoxicity' or 'nanotoxicology' topics. Data for year 2015 is up to the end of May.

1.1.2. *Terminology*

Many committees and reports were set up worldwide by various institutions, to define terms in the context of nanotechnology [(Department for Environment, Food and Rural Affairs of the United Kingdom Government, 2007), (European Commission Joint Research Centre, 2011), US (National Institute for Occupational Safety and Health (NIOSH, 2006),US National Nanotechnology Initiative (NNI, 2007)] which might give a false impression of a not yet achieved consensus. Thus, this section will be devoted to define such important terms.

The prefix **'nano',** derived from the Greek **'**nanos**'** which means **'**dwarf**'**, is becoming increasingly common in scientific literature (Goncalves et al., 2011). Popularly, 'nano' is used as an adjective to describe objects, systems, or phenomena with characteristics arising from nanometre-scale structure (Buzea et al., 2007).

The term **'nanomaterial'** refers to a material, i.e., functionally specific matter, which, owing to its nanometric structure, has a modified chemical or physical property (or combination of properties) that is improved, adapted, or new compared with the bulk material of the same composition (Bréchignac et al., 2010). The British Standards Institution (BSI, 2011) makes the more precise definition of a nanomaterial as being either a nanoparticle (in the sense of a nano-object), or a nanostructured material whose dimensions exceed the nanometric scale (1nm to 100nm). The nanometre is a metric unit of length, and denotes one milliardth of a metre or 10^{-9}m.

The technical committee of the International Standards Organization (ISO) devoted to nanotechnologies defines nanoparticles (NP) as 'particles with a nominal diameter (such as geometric, aerodynamic, mobility, projected-area or otherwise) smaller than about 100 nm (ISO/TS 27687). For comparison purposes, the width of an average hair is 100,000 nm, human blood cells are 2,000 to 5,000nm long, and a strand of DNA has a diameter of 2.5nm (Naahidi et al., 2013) (Figure 1.2). These simple size comparisons give an idea of using NP as very small probes that would allow us to spy at the cellular machinery without introducing too much interference. Hence, NP possess the ability to imitate and interact with biological systems at the same scale of their parts; this is the explanation what has driven the burst of nanobiotechnology research recently. Materials engineered to such a small scale are often referred to as engineered nanomaterials (ENM), which can take on unique optical, magnetic, electrical, and other properties (NIH, 2014). In the context of this document, to avoid the confusion, the terms ENM and NP will be used interchangeably.

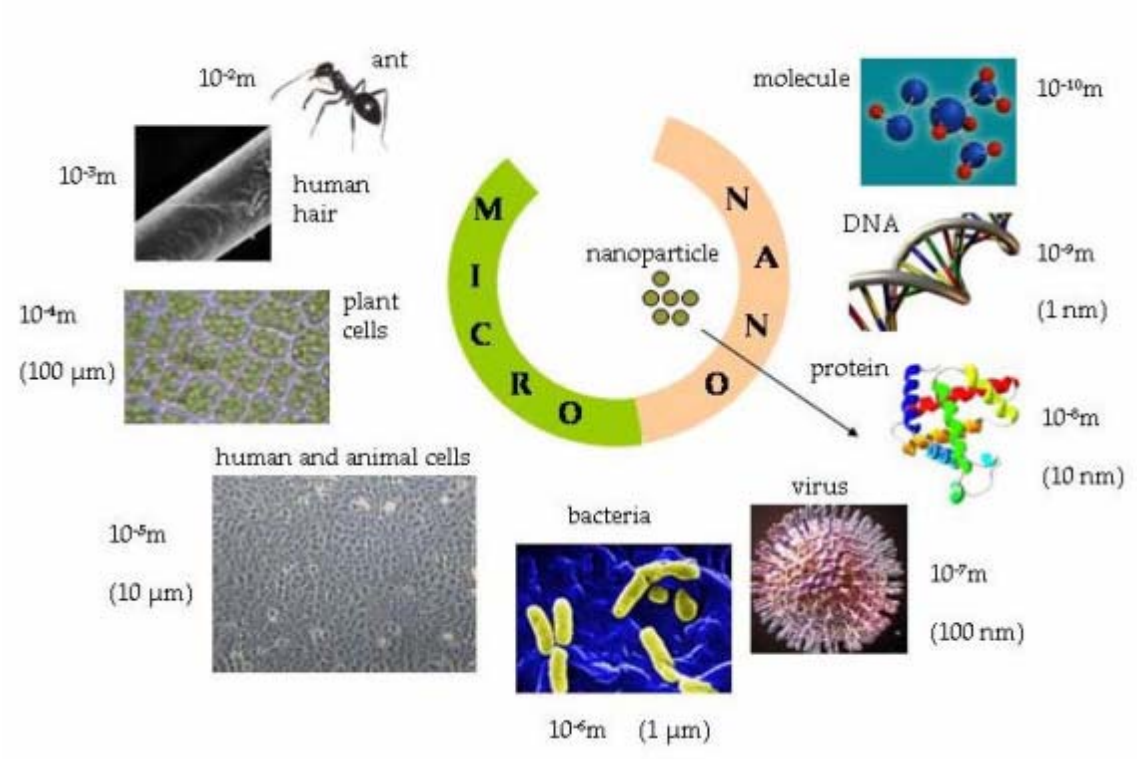

Figure 1.2. Nanoscale showing nanomaterials compared to biological components, with indication of 'nano' and 'micro' sizes (from Wibke Busch, 2010).

Nanotoxicology was proposed as a new branch of toxicology to address the adverse health effects caused by nanomaterials (Oberdörster et al., 2005). Toxicology, as it is defined by the Society of Toxicology, is the study of the adverse effects of chemical, physical or biological agents on living organisms and the ecosystem, including the prevention and improvement of such adverse effects (SOT, 2005). When this definition of toxicology is combined to nanomaterials, nanotoxicology could be described as the study of the adverse effects of ENM on

living organisms and the ecosystems, including the prevention and amelioration of such adverse effects (Oberdörster, 2010).

For many reasons related to their behaviour and environment, e.g., during their fabrication, nanomaterials rarely occur in free form, i.e., isolated from one another (Ju-Nam and Lead, 2008; S. Isfort and Rochnia, 2009). They tend to group together into more or less stable but disordered clusters, some dimensions of which may be significantly longer than 100 nm. The term 'primary particle' is also used to designate the elements making up a cluster. According to ISO/TR27628 document, there are two types of clusters: when primary particles adhere to one another by weak physical bonds, e.g., Van der Waals forces, it is called **agglomerate**. If the cluster consists of primary particles connected by strong chemical bonds (covalent bonds), or they have partially fused together, the cluster is referred to as an **aggregate** (Witschger, 2011) (Figure 1.3).

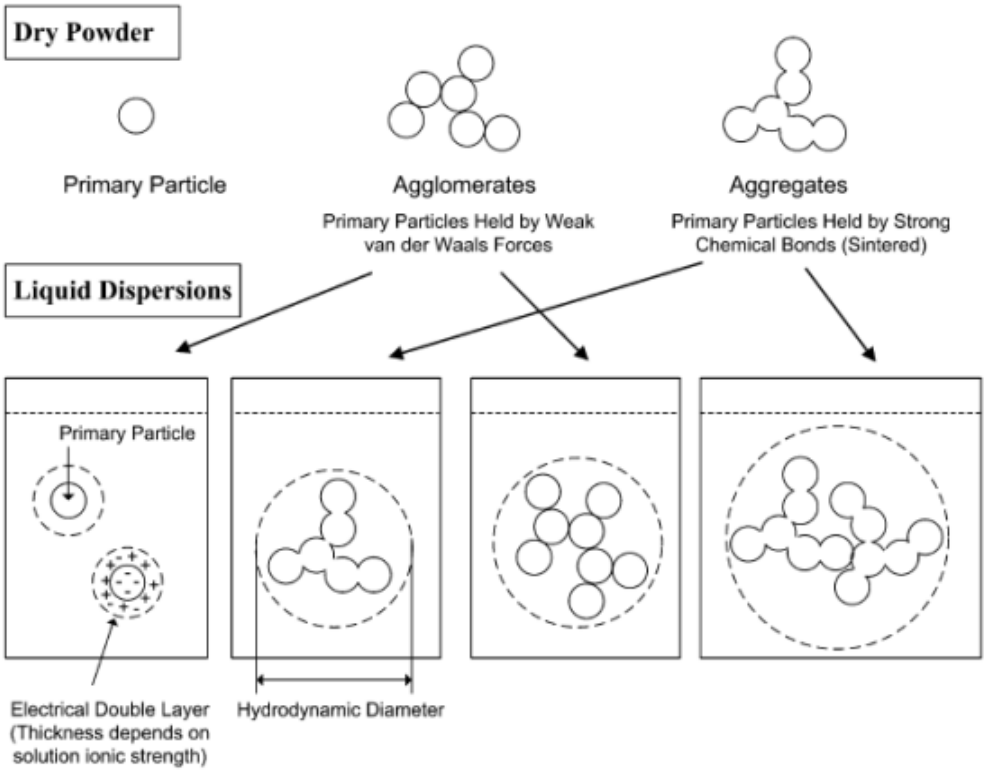

Figure 1.3. Nanoparticles tend to agglomerate in physiological fluids but may also build stable aggregates. Agglomerates and aggregates are characterised by the hydrodynamic diameter that can differ significantly from the primary particle diameter (from Jiang et al., 2008).

1.1.3. *Physicochemical properties of nanomaterials*

Advances in nanotechnology in both scientific research and application areas are likely to significantly benefit society and economy (Oberdörster et al., 2007). By some estimates, nanotechnology promises to far exceed the impact of the Industrial Revolution and is projected

to become a three billion dollars market by 2015. The reason for ENM to be that popular is mainly because of their unique physical and chemical properties, which give them a great potential for industrial and biomedical applications (Nel et al., 2006).

The unusual physicochemical properties of ENM, such as their small size, surface structure, solubility, shape, and aggregation (Sutariya and Pathak, 2015) are also the reason for requirement of an interdisciplinary approach to study these materials as potential toxic agents, involving multiple aspects ranging from physics and chemistry to biology and medicine (Fubini et al., 2007).

Nanosize is one of the main physicochemical features that make ENM different from their larger equivalents (De Jong and Borm, 2008). As size decreases, the mobility, potential transport, and availability of the particle in the environment increase. This mobility could translate to passive transport across cellular membranes. The NP that cross membranes will then be able to interact with macromolecules such as proteins, DNA, or RNA. Also, as a direct consequence of their small size, NP have a very large surface area with regard to the same mass of bigger particles. This may be one of the reasons why NP are generally considered more toxic than larger particles of the same material. In other words, while the size of a particle decreases, its surface area increases, which allows a greater proportion of its atoms or molecules to be exposed on the surface rather than the interior of the material (Figure 1.4). The increase in surface area determines the potential number of reactive groups on the particle surface and therefore it is strongly possible that biological activity might increase.

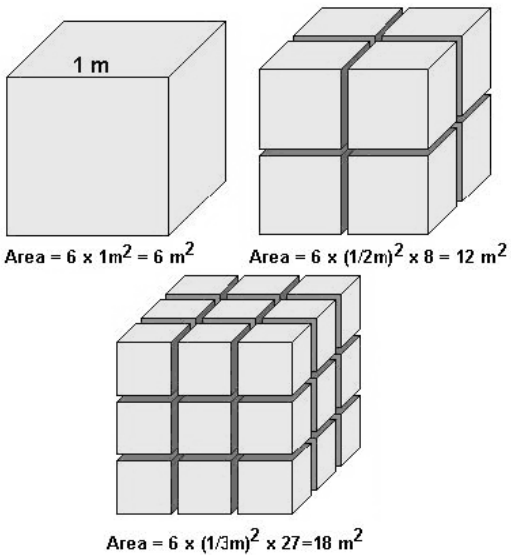

Figure 1.4. For the same quantity of material, the decrease in particle size means a high increase in surface area (from www.uwgb.edu/dutchs/GRAPHIC0/GEOMORPH/SurfaceVol0.gif)

Another very important factor that may contribute to the behaviour and biological responses of ENM is the state of dispersion in a particulate system, which refers to the relative

number of single particles in a suspending medium in comparison to agglomerates (Powers et al., 2006). Particles will tend to agglomerate in suspension unless the conditions are present for a stable dispersion. These agglomerates may be formed directly from attractive inter-particle forces (e.g., Van der Waals and hydrophobic interactions) or through the binding of molecules in the surroundings (e.g., polymers, proteins, polysaccharides) (Powers et al., 2009). Even though NP display a certain size after synthesis, the smaller the particle, the stronger the inter-particle forces that attract them. Thus, they might aggregate into vastly different shapes and sizes, which may also profoundly change the dynamics and properties of the resultant potential hazards (Fubini et al., 2007; Maynard et al., 2010).

As in the case of size, particles may also have a 'shape distribution'. Occasionally, ENM have readily definable shapes such as spherical, oval, cubic, prism, helical (Colognato et al., 2012). Different structural shapes and types of nanomaterials are summarised in Table 1.1. The effect of NP shape on their internalization was examined by Verma and Stellacci, (2010), who reported that spherical particles were taken up 500% more efficiently by cells than rod-shaped particles of similar size.

Table 1.1. Types of ENM classified by their structure and composition (adapted from Dawidczyk et al., 2014; Tang et al., 2009).

	Particle type	Description	Particle type	Description	
	Polymer	Colloidal particles of biodegredable polymer matrices.eg: PLGA ,Glycerol,chitosan, DNA monomers,hydrogels	Magnetic	Iron oxide or cobalt-based spheres ; display large moments in a magnetic field	
	Dendrimer	Highly branched macromolecules synthesized by polymerization growing from a central core. eg :PMAM	Metallic	Gold or silver nanoparticles	
	Lipid	Closed spherical assemblies of amphiphilic and phospolipid bilayers. eg: Liposomes,micelles	Metal oxides	Co3O4 ,Cu2O, MgO, SiO2,TiO2,ZnO,Zro2	
	Quantum dots	Semiconductor crystals with a cadmium core and metal shell . eg: CdSe,CdS,CulnSe,etc	Nanoshells	Dielectic silica core in a thin gold metal shell	
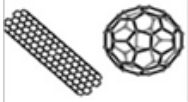	Carbon based	Carbon nanotubes,buckyballs,graphene	Ceramic	Inorganic,porous;containing bio-compatible materials eg:silica, titania,alumina	

Surface chemistry consists of a wide variety of properties that conduct the way in which particles interact with biomolecules and biological systems. Surface charge of ENM has great importance in the induction of biological effects, as it is a major factor in determining the particle dispersion characteristics and also influences the adsorption of ions and biomolecules, which may change how cells react to the particles (Powers et al., 2006). Classically, the surface charges of particulate systems are approximated through zeta potential measurements (Adamson, 1990). Zeta potential refers to the function of the surface charge of the particle and the nature and composition of the surrounding medium in which the particle is dispersed (Zuin et al., 2007).

Differences in physicochemical properties between NP and larger particles determine their behaviour and biodistribution in the body following translocation from the portal of entry, their cellular interactions, and their effects (Oberdörster, 2010). Whereas many of the effects at the organ of entry (primary target organ) usually the respiratory tract can be the same for both particle sizes, secondary organs can be affected differently. What distinguishes NP from their larger counterparts is a major influence of their toxic properties and unusual biokinetic behaviour, which will be discussed in the next sections.

1.1.4. *Exposure and biodistribution*

With the growing commercialization of ENM, chances for human exposure to these materials increase substantially. As their toxicity is generally related to their abundance and persistence, the effective dose, and the duration of the exposure, a systematic and thorough analysis is essential (Yoshioka et al., 2014). Hence, in this section, the current understanding regarding the exposure and biodistribution profile of NP will be represented.

In general, NP are considered to be able to enter into direct contact with the organism via four main routes: dermal penetration, ingestion, inhalation and systemic entrance (Martirosyan and Schneider, 2014). Because clothing, drugs, cosmetics, and various skin care products contain NP, their contact with the skin occurs intentionally as well as accidentally. Furthermore, as the use of ENM in food as food additive and in pharmaceuticals is increasing, people in developed countries ingest an estimated 10^{12}-10^{14} manufactured particles per person every day (Mahler et al., 2012).

One of the most important absorption pathways is the respiratory tract. Inhalation is probably the major route for NP in atmospheric pollutants, combustion-derived NP, and freely dispersible mineral or metal NP resulting from bulk manufacture and handing (Wang et al., 2009). Inhaled NP are deposited in all regions of the respiratory tract; however, larger particles may be filtered out in the upper airways, whereas smaller particles reach distal airways (Forbe et al., 2011). After absorption across the lung epithelium, they enter the blood and lymph to reach cells in the bone marrow, lymph nodes, spleen, heart, or any other organ. NP can even reach the central nervous system and ganglia following translocation (Oberdörster et al., 2005).

Regardless the absorption pathway, distribution of the particles in the body is strongly dependent on their surface characteristics (Hoet et al., 2004), and varies depending on their material, size, and charge. NP are small enough to penetrate very small capillaries throughout the body and to translocate across cell barriers. Therefore they might enter cells by various mechanisms and associate with subcellular structures and secondary organs (Kettiger et al., 2013). Thus, effects such as inflammation, oxidative stress and molecular cell activation are

likely to occur not only in the primary organ of entry, but also in secondary target organs (Oberdörster et al., 2009).

As it can be seen in Figure 1.5, NP may be actively incorporated via phagocytosis, pinocytosis, clathrin-dependent endocytosis, clathrin- and caveolae-independent endocytosis, or caveolae-mediated endocytosis (Sahay et al., 2010). Particles internalized via active uptake are commonly transported in vesicular structures that then fuse to phagolysosomes or endosomes (Barbara Rothen-Rutishauser et al., 2014). Sometimes, they might be exocytosed upon pinocytosis. Alternatively, they may also be carried to the cytosol, or transported via caveosomes to the endoplasmic reticulum, or cross the cell as part of transcytotic processes (Jud et al., 2013). Besides active transport, NP may also enter the cell passively via diffusion through the plasma membrane (Sahu and Casciano, 2009). From the cytoplasm they may then gain access to subcellular compartments such as the nucleus and mitochondria (Hart and West, 2009). This makes NP uniquely suitable for therapeutic and diagnostic uses, but it also leaves target organs, such as the central nervous system (CNS), vulnerable to potential adverse effects.

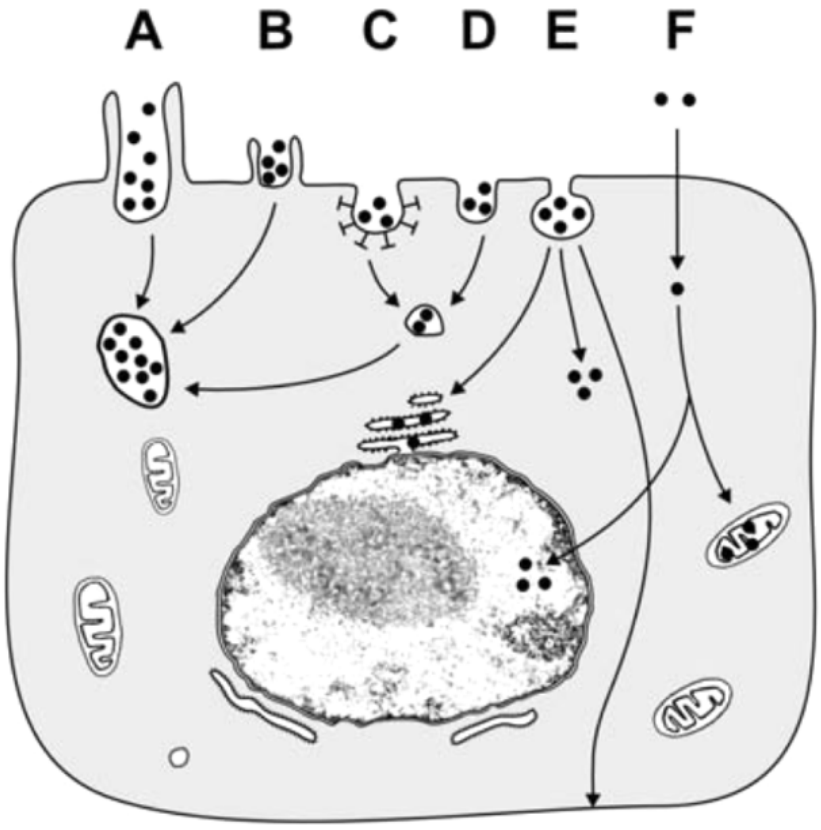

Figure 1.5. Summary of possible mechanisms of NP for entering cells and cellular compartments. NP may actively be taken up by cells via phagocytosis (A), macropinocytosis (B), clathrin-mediated endocytosis (C), clathrin- and caveolae-independent endocytosis (D), caveolae-mediated endocytosis (E) or by passive diffusion (F) (from Mühlfeld et al., 2008).

Although translocation of NP to the brain is possible and well-studied in the literature under different experimental conditions (Cheng et al., 2015; Mc Carthy et al., 2014; Pedram et al., 2014; Shim et al., 2014; Yemisci et al., 2014), the health relevance for real-life situations is far from clear. Therefore, the evaluation of the potential toxic effects of NP on neuronal cells is required, as specific mechanisms and pathways through which NP may exert their toxic effects remain largely unknown.

The brain is probably the best protected of the organs in the human body. Besides the protection against mechanical damage, it is also shielded from possibly damaging compounds (circulating pathogens, toxins, and also endogenous signalling substances) in the blood by means of structural barriers (M. Simkó and Mats-Olof Mattsson, 2014). The most important one is the blood-brain barrier (BBB). The BBB is a specialized protective barrier that separates blood from cerebrospinal fluid. It consists of endothelial cells connected by complex tight junctions, which restrict the access of large or hydrophilic compounds to the brain (Begley, 1996). However, NP made of different materials could cross the BBB and accumulate within the brain (Masserini, 2013). Due to their special physicochemical properties, such as large surface area, NP may cause neurotoxicity after entering the nervous system.

1.1.5. *Potential adverse effects*

Nanotechnology is a major source of innovation with important economic consequences. Nanotechnology-based products in general have already been catalogued and the global market size for these products is expected to grow to three billion dollars in the year 2015 (Kaur et al., 2014). However, safety concerns have arisen for such products because ENM, especially metal oxide NP, may catalyse generation of free radicals which could cause skin damage and even cancer (Manke et al., 2013).

As explained in the latter section, particles in the nano-size range can certainly enter the human body via inhalation, dermal contact, ingestion and parenteral routes (Hoet et al., 2004). Then the nanomaterials come into immediate contact with a collection of molecules and cells that is characteristic of the absorption site environment and attempt to lower its surface energy by adsorbing surrounding biomolecules including proteins, lipids, small molecules, saccharides, and nucleic acids (Walkey C., 2012). Later, the absorbed structures can be transported to various organs including the brain, heart, liver, kidneys, spleen, bone marrow and nervous system (Liu et al., 2007). Finally, they cross the cellular membranes and move into the cytoplasm of the cells that form the organ and reside there for an uncertain period of time before affecting other organs or to be excreted out of the host organism (Karagkiozaki et al., 2012).

The extremely small size of NP allows them to enter human cells; indeed, different studies showed a fast uptake of NP into cells *in vitro*. Their cellular uptake, subcellular

localization, and ability to catalyse oxidative products depend on NP chemistry, size, and shape, which are limited by the transport of the material to the cell (Figure 1.6). Unlike larger particles, NP may be transported within cells and be taken up by cell mitochondria and nucleus (Dar et al., 2014).

Nanostructures could enter the nucleus via transport through the nuclear pore complexes, diffusion through the nuclear membrane itself, or may be enclosed into the nucleus by chance as a result of the fact that the nuclear membrane is degraded during cell division procedure, and then reformed in each daughter nuclei (Karagkiozaki et al., 2012). This type of uptake and free movement within the cell makes NP very dangerous by having direct access to cytoplasm proteins and organelles.

Depending on their localization inside the cell, NP can damage organelles or DNA either directly or indirectly by interacting with DNA-related proteins, which causes physical damage to the genome. Indeed, *in vivo* and *in vitro* studies demonstrate the potential of nanomaterials to cause DNA damage (Chen and von Mikecz, 2005; Gassman et al., 2015; Al Gurabi et al., 2015; Paino and Zucolotto, 2014).

Indirect DNA damage may occur without a physical interaction between the DNA molecule and NP; yet their interaction with other cellular proteins, like the cell division process proteins, might be required. Additionally, they may induce other cellular responses that in turn lead to genotoxicity, such as causing oxidative stress, inflammation and aberrant signalling responses (Singh et al., 2009).

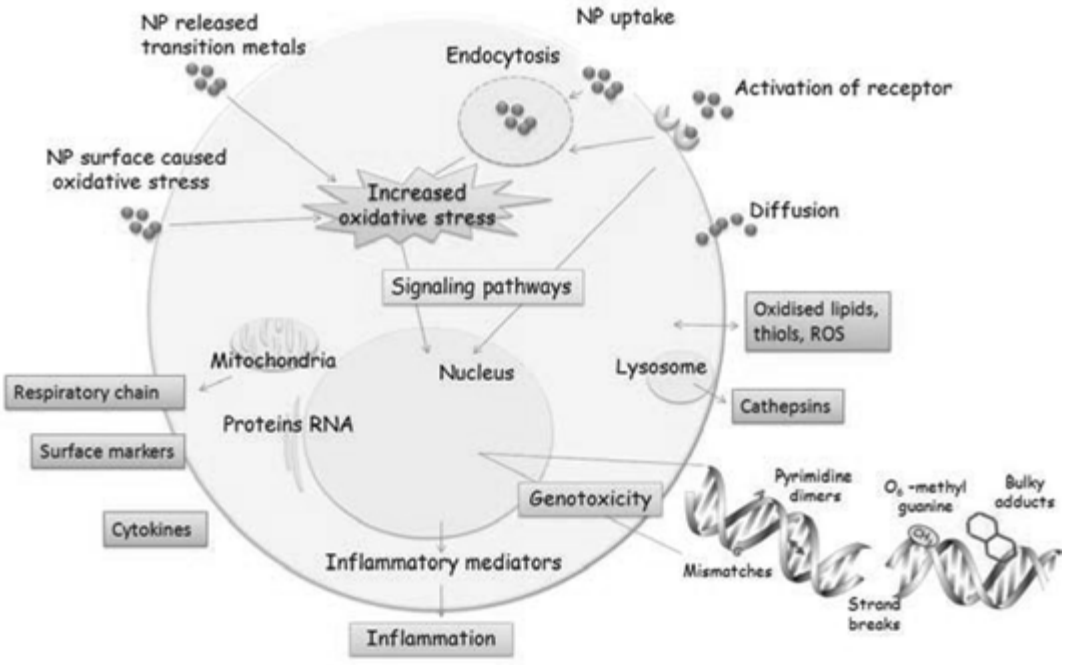

Figure 1.6. Schematic illustration of mechanisms of action of ENM (from Dusinska et al., 2011).

A number of studies have shown that NP can strongly interact with cell membranes and produce physical damage (Du et al., 2015; Landgraf et al., 2014; Sharma et al., 2010, 2014). This interaction is achieved either by adsorption of them onto the cell surface or by compromising the membrane integrity to result in the formation of holes, membrane thinning, and lipid peroxidation (Zupanc et al., 2009). Moreover, the result of sudden increase in the permeability of the inner mitochondrial membrane can cause loss of mitochondrial functionality and, finally, promote the cell necrosis procedure (Elmore, 2007).

As mentioned before, their size-dependent properties that influence NP reactivity are likely to affect their hazardous behaviour. Their greater chemical reactivity results in increased production of reactive oxygen species (ROS), including free radicals (Nel et al., 2006). Oxygen-derived ROS are a response to cell injury, and also can occur as an effect of normal cell functions such as cell respiration, endogenous metabolism, inflammation, and metabolism of foreign compounds (Uttara et al., 2009). ROS production has been found in a diverse range of nanomaterials including carbon fullerenes, carbon nanotubes and metal oxide NP. ROS and free radical production are among the primary mechanisms of nanomaterials toxicity; it may result in oxidative stress, inflammation, and consequent damage to proteins, lipid membranes and DNA (Nel et al., 2006).

Furthermore, NP can enter the human body and interact with components of the immune system by inducing inflammation, immune response, and allergic reactions, or even affect the immune cells (Salik Hussain, 2011). This interaction leads to an enhanced release of different immune signalling molecules, including cytokines.

Overall, how exactly NP behave in the cell and interact with its components is still a major question that needs to be resolved. An understanding of nanotoxicity is essential as it could also lead to the harnessing of ENM to be used for many approaches. Thus, in the next section the two key elements of toxicity screening strategy, physicochemical characterization of nanomaterials, and cellular assays to determine the potential interactions of NP with the cell and their mechanisms of action will be explained.

1.2. METHODS FOR UNDERSTANDING THE INTERACTION BETWEEN NANOPARTICLES AND CELLS

1.2.1. *Characterization*

Nanotechnology is a rapidly emerging field across disciplines in science and engineering. As the number of nanotechnology related products and devices in the market is advancing, it is essential to rigorously assess and understand their effects to both human health and environment (Maynard et al., 2006). The strategy of obtaining safety information on nanomaterials involves

conducting reliable and reproducible toxicity assessment. To properly assign mechanisms or causes for toxic effects of nanoscale materials, their properties and characteristics, both outside and within the biological environment, must be well understood.

Complete characterization of ENM for toxicological study is a complex task. It requires a variety of material attributes to be considered, including measurements of size and size distribution, shape and other morphological features, bulk chemistry of the material, solubility, surface, area, state of dispersion, surface chemistry and other physicochemical properties.

Conducting reproducible and reliable toxicological studies with ENM is further complicated by the behaviour of particulate matter in biological environments. In biological systems, the presence of multiple components, high ionic strength, limited temperature range, and potential toxic effects of dispersion can restrict the quantification and interpretation of properties such as size distribution, state of aggregation, surface charge, surface chemistry, translocation, and interaction with biological components (Powers et al., 2007).

There are many other properties that have been suggested for the complete characterization of ENM. Perhaps the most recent list has been compiled by an OECD report which most researchers agree with on the basic characterization parameters that predict toxicological behaviour of nanoscale materials (OECD, 2014). Although, this list includes a number of additional properties, the minimum set of characteristics that should be measured for test materials used in nanotoxicity studies are size and shape, state of dispersion, surface area, and surface chemistry.

1.2.1.1. *Size and dispersion*

The determination of particle size is far more challenging and complex than is generally assumed. The complexity in particle characterization is associated with two basic aspects. First, the small size particles exist in great quantity; hence a large number of particles must be sampled and measured in order to adequately represent the size distribution. The second aspect is that NP have a natural tendency to agglomerate in suspension. Unless stabilized by some form of repulsive surface forces, van der Waals forces will cause particles to stick together as they come into contact with each other. Therefore, it must be taken into account that the particle size changes as a function of time or with changes in the surrounding environment (Powers et al., 2007, 2009; Sayes and Warheit, 2009). Thus, the measured size distribution is highly dependent upon the state of dispersion of the system (Powers et al., 2009).

Most individual particle sizing techniques do not clearly differentiate between primary particles and particle agglomerates. When agglomeration causes particle shape or density to depart from a homogeneous state, the assessment of the particle size distribution becomes less reliable (Huynh and Chen, 2014). In order to develop a more complete picture of size

distribution and to obtain more stable dispersions, NP can be de-agglomerated by applying Shear techniques (mixing, sonication, grinding, and turbulence), but unless the conditions are present for a stable dispersion (by native surface charge at a given pH, surfactants, or steric stabilization), the system will be prone to re-agglomerate rapidly (Powers et al., 2007).

One of the most relevant techniques to conduct primary characterization of particle size and morphology for toxicological evaluations is observing and manually measuring particles from micrographs taken from either the transmission electron microscope (TEM) or the scanning capacitance microscope (Sayes and Warheit, 2009). But probably the most common sizing technique for ENM is dynamic light scattering (DLS), among others such as laser diffraction, centrifugal sedimentation, acoustic techniques, Brownian motion analysis, electrozone sensing, and dark field, fluorescent, or confocal microscopy.

DLS is based on the principle that particles in suspension diffuse under Brownian motion as a function of their hydrodynamic diameter (or size), fluid viscosity, and temperature. The sample is illuminated by a laser beam and the fluctuations of the scattered light are detected at a known scattering angle by a fast photon detector (Figure 1.7). From the NP point of view, the particles scatter the light and mark the information about their motion. Thus, analysis of the fluctuation of the scattered light yields information about the agglomeration and disagglomeration of the particles over time (Koppel, 1972; Sayes and Warheit, 2009).

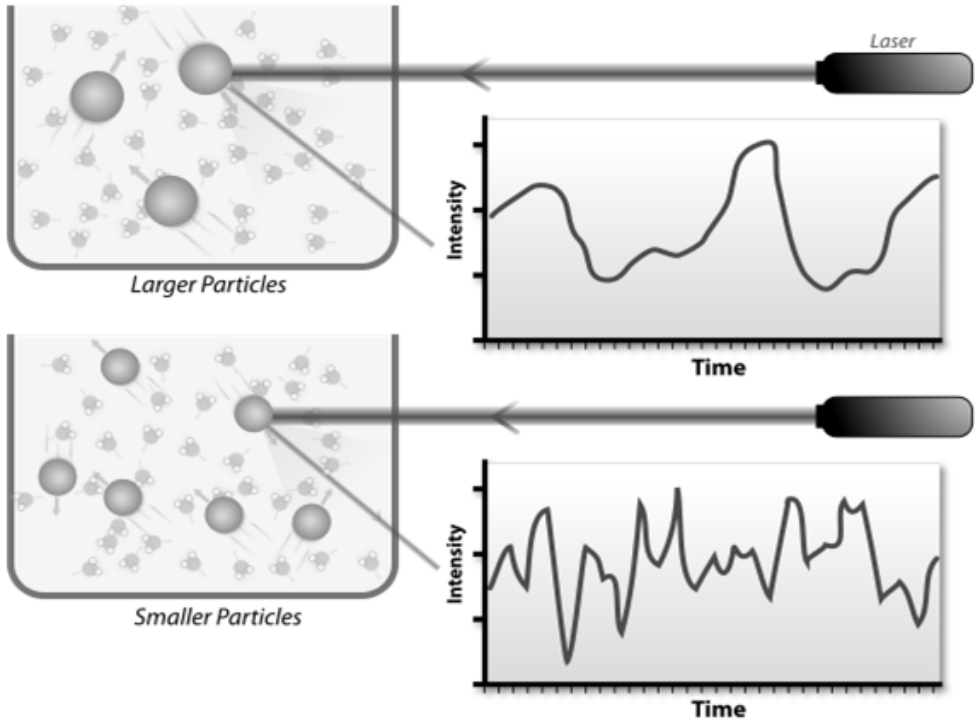

Figure 1.7. Principle of DLS technique. Smaller particles tend to diffuse more rapidly than larger particles at a given temperature and viscosity, and the hydrodynamic diameter is calculated by experimentally determining the fluctuations of the scattered light.

1.2.1.2. *Surface properties*

The ENM surface properties are expected to contribute substantially to the mode and extent of their biological interaction. Surface chemistry consists in the chemical structure of particle surfaces, surface charge, functional groups, and active sites. Surface adsorption and/or coating can completely change the nature of the particles and alter their cellular responses. Hence, NP can be even functionalized with different surface chemistries to target specific sites or organelles, enhance cellular uptake or improve retention without deleterious cell reactions (Rivet et al., 2012).

Surface properties clearly affect ENM interactions with biomolecules and biological systems. It is often unattainable to characterize the full spectrum of surface properties for each ENM system. Yet, it is recommended that an interactive approach to surface characterization is undertaken by using multiple techniques simultaneously (Powers et al., 2009).

The most obvious surface property for NP is the high surface area (Issa et al., 2013). The surface area plays an important role in the toxicity of ENM because it is the surface what interacts with the surroundings and best correlates with particle-induced adverse effects (Oberdörster, 2001, 2010).

Brunauer-Emmett-Teller (BET) analysis is a common method used to attain an surface area measurement that can then be converted to a primary particle size (Brunauer et al., 1938). However, the limitation of the BET measurement is that it can only be applied to the particle characterization whenever there is sufficient dry powder available. For wet systems, or when there is insufficient material available to conduct BET analysis, surface area is most often approximated by measuring particle size and calculating the surface area using a spherical assumption (Powers et al., 2012).

There is an inverse relationship between surface area and radius of the NP. For spheres, specific surface area increases inversely with particle diameter; thus for a given mass it increases dramatically as particle size approaches the nano range. The theoretical specific surface area is usually measured in squared meters per gram (Powers et al., 2012; Sayes and Warheit, 2009).

Although surface area is important, it is not surface area alone what defines interactions with the surroundings. Two principle measurements of surface chemistry are hydrophilicity (affinity for water) and surface charge, which will largely determine how the particles physically respond to dispersion in aqueous fluids. Since almost all exposures in toxicology studies eventually involve aqueous biological fluids, it is important to determine the surface charge that develops on particles when they are introduced into aqueous solutions (Powers et al., 2012).

Surface charge can aid in the determination of material dispersion characteristics. Since the charge at the particle surface is difficult to measure directly, zeta potential and isoelectric point of the particles are typically used to quantify particle charge. Zeta potential, in a colloidal system, is the difference in potential between the surface of a material dispersed in a suspension and the dispersion medium. Hence, when measuring zeta potential, the dispersion stability of the particles becomes more important and provides insight into the agglomeration behaviour of the materials; in some cases, if particle stability decreases, then surface charge may change (Powers et al., 2007, 2012; Sayes and Warheit, 2009).

A higher level of zeta potential (both positive and negative) results in greater electrostatic repulsion forces among the particles. This repulsion leads to greater separation distances among particles in the suspension, reducing agglomeration caused by Van der Waals interactions. A zeta potential of +/-30mV is often used as an approximate threshold for stability. Sample particles with measured zeta potentials in the range between -30mV and +30mV will have a tendency to agglomerate over time, while particles with a zeta potential magnitude just greater than 30mV (independent of sign) should be marginally stable (Fazio et al., 2008; Sharma et al., 2014; Singh et al., 2005).

The electrical charge properties control the interactions between particles; therefore they determine the overall behaviour of a sample suspension. Modifying the stability of a sample, for example to minimize agglomeration for drug delivery and pharmaceutical applications (high zeta potential required) or, on the contrary, to facilitate the removal of particles too small to filter out for water treatment applications (low zeta potential required), is of great importance in NP research. Zeta potential of a NP system can be measured with several techniques including electro acoustic, DLS, and electrophoretic methods (Alkilany and Murphy, 2010; Powers et al., 2009, 2012).

Clearly, there are many other reactions that take place at the surface of NP in the biological environment. There may be specific uptake of proteins, specific cell membrane interactions, and numerous other interactions, which might have effect on the toxicity profile of these materials. An understanding of these various processes controlling the behaviour of NP in suspension will be very useful in developing particles designed for therapeutic or imaging applications, which have particular surface properties specifically engineered to chemically target them to the desired location. When the properties of ENM are thoroughly understood, samples might be prepared appropriately for exposure with greater confidence and understanding.

1.2.2. *Cellular interaction with nanoparticles*

Due to the many different forms of NP being produced and used in a wide variety of consumer, industrial, and technological applications, exposure to these particles is often unavoidable. Depending on the way of exposure (inhalation, ingestion, injection, and permeation through skin), NP may distribute through the whole system and translocate to different organs/tissues and might induce adverse effects.

If NP are to translocate to secondary target organs (such as the liver or brain), then it is important for *in vitro* nanotoxicology studies to mimic the interaction between NP and those cell systems by applying them as suspended in cell culture medium. In order to correlate any toxic reaction with a NP type, it is necessary to investigate if the particles are adsorbed on the cell surface or if they enter cells.

1.2.2.1. *Cellular uptake of nanoparticles*

If NP are found inside cells, their localization in different compartments such as endosomes, lysosomes, mitochondria, the nucleus, or the cytosol may also provide some answers regarding their potential toxicity. In order to explain how NP accumulate in cells, without killing or altering cellular function, it is essential to quantitatively and qualitatively characterize their uptake and distribution within the cell (Rivera-Gil et al., 2012).

In general, NP taken up by cells have been identified by TEM or inductively coupled plasma mass spectrometry; however, these methods require an immense amount of time and effort. A rather faster method also employed frequently to measure NP uptake is flow cytometry (FCM).

FCM has been used to measure both light scattering and fluorescence from particles or cells as they flow in a liquid medium that passes an excitation light source (mainly 488nm laser) (Radcliff and Jaroszeski, 1998). When the laser beam strikes in various directions to the individual cells that flow as single file in the liquid stream, information about the cells is generated (Jaroszeski and Radcliff, 1999).

Light that is scattered in the direction of the laser path is called the forward-scatter (FSC) light. The FSC intensity is proportional to the cell and particle size. Light measured approximately at a 90° angle to the laser path is called side-scatter (SSC) light. The SSC intensity provides information on the inner structure and the granular content of the cell (Figure 1.8).

When NP are taken up by the cells, they can be differentiated by their unique FSC and SSC properties. Cells with NP would scatter more light than cells without nanoparticles primarily due to many NP located in the cytoplasm (Zucker and Daniel, 2012). SSC intensity

consequently increases without change of FSC intensity. This evaluation of NP uptake using FSC and SSC is suitable for initial screening of nanotoxicity because particular sample processing (staining, labelling, etc.), apart from preparation of single cell suspensions, are not required (Ibuki and Toyooka, 2012). In addition, statistically valid information about cell populations is quickly obtained since large numbers of cells are analysed in a short period of time (Zucker et al., 2013).

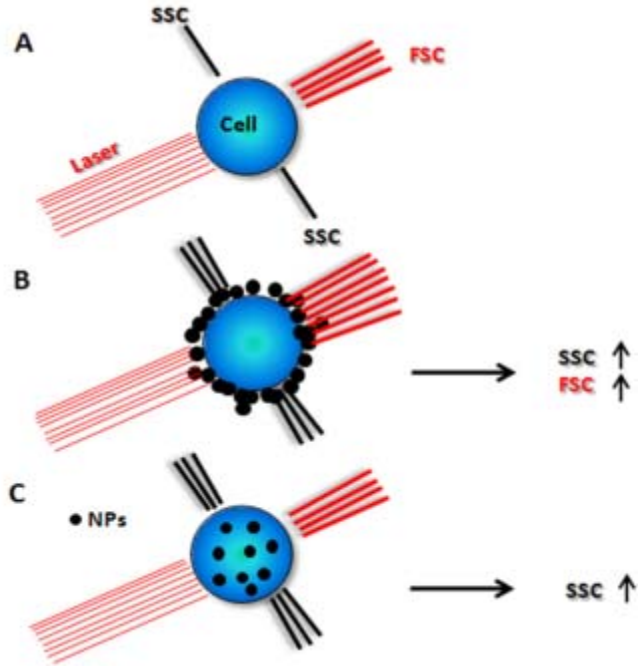

Figure 1.8. Analysing NP uptake in cells by flow cytometry. (A) Light scattering by a cell having no association with NP;(B) NP adhered to the cell surface leading to increase in both FSC and SSC; (C) NP internalization by the cell leading to increase only in SSC (from Sharma, 2011).

1.2.2.2. *In vitro cytotoxicity and cell death*

NP size, charge, surface chemistry, shape, and structure can affect the manner in which NP interact with biological environment and ultimately determine the potential for cytotoxicity. Numerous methods are used to evaluate cytotoxicity both *in vitro* and *in vivo*. Although most cytotoxicity studies for NP are conducted *in vitro*, they are limited in their ability to mimic the complexity of the *in vivo* environment. Thus, *in vitro* cytoxicity studies are often conducted to identify the "maximum tolerated dose" and "no observable effect level" of NP dosage (Adjei et al., 2014).

Colorimetric assays have widespread uses when studying the cytotoxic effects of NP in cell culture. These assays enable the determination of cell survival, proliferation, and activation within a wide variety of cells. In order to assess the number of **viable cells** in proliferation via mitochondrial integrity and functional capacity, the most commonly used cytotoxicity assay in

the literature is the **MTT [3-(4,5-dimethylthiazol-2-yl)-2,5-diphenyltetrazolium bromide] assay**. MTT, a yellow tetrazole, is reduced to purple formazan in the mitochondria of viable cells (Figure 1.9), process which can be detected spectrophotometrically by a microplate absorbance reader. The formation of formazan product has been found to correlate well with cell viability in terms of normal functioning of mitochondrial energy-requiring biochemical reactions. Hence, measurements of the intensity of the resulting coloured solution provide an accurate representation of the number of viable cells.

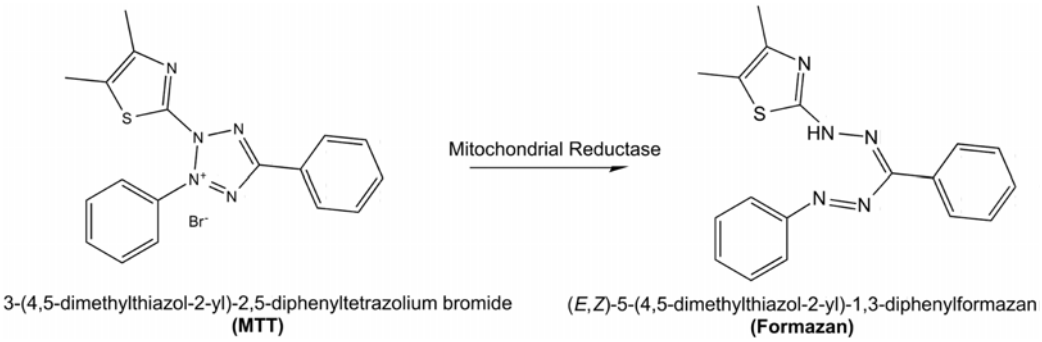

Figure 1.9. MTT reduction in live cells by mitochondrial reductase results in the formation of insoluble formazan (from http://www.intechopen.com/source/html/41784/media/image4_w.jpg)

Another efficient and often used technique for quantitative estimation of **cell viability** in a culture is the **neutral red uptake (NRU) assay**. This assay is based on the ability of viable cells to incorporate and bind the dye neutral red. This weakly cationic dye penetrates cell membrane by non-ionic passive diffusion and concentrates in the lysosomes, where it binds by hydrophobic bonds to anionic and/or phosphate groups of the lysosomal matrix (Nemes et al., 1979; Repetto et al., 2008; Winckler, 1976). The dye is then extracted from the viable cells and the absorbance of the solubilized dye is quantified using a spectrophotometer.

The uptake of neutral red depends on the cell capacity to maintain pH gradients, through the production of ATP (Koller et al., 2014). When the cell dies or the pH gradient is reduced, the dye cannot be maintained. Consequently, the amount of dye kept inside the cells is proportional to the number of viable cells, and the toxicity is expressed as percent inhibition of neutral red dye retention in the sample (Butler and Roesijadi, 2001).

The plasma membrane protects the cell from extracellular toxins and controls the transport of molecules in and out of the cell. It encloses the cell, defines its boundaries, and maintains the essential differences between the cytosol and the extracellular environment. If the plasma membrane is disturbed by materials such as NP, then cellular functions may be disrupted, causing toxicity. Binding of NP to the surface of the plasma membrane may also affect other essential cellular processes, such as ion transport and signal transduction. Bound NP may block or competitively bind signalling proteins or ion channels and isolate the cell from the extracellular space (Sahu and Casciano, 2009).

Alterations in membrane integrity can be investigated colourimetrically by the **lactate dehydrogenase (LDH) assay**. LDH is a stable cytosolic enzyme, present within all mammalian cells, that is only released when there is damage of the plasma membrane. The normal plasma membrane is impermeable to LDH, but damage to the cell membrane results in a change in its permeability and subsequently in the leakage of LDH into the extracellular fluid (Wang et al., 2005). Once in the extracellular space, LDH oxidizes lactate to pyruvate simultaneously reducing nicotinamide adenine dinucleotide (NAD) to NADH (reduced NAD). Finally, NADH reacts with iodonitrotetrazolium (INT, another tetrazolium salt) to form a formazan product (Martins et al., 2013). The resulting orange formazan product and can be measured quantitatively by spectrophotometry (Figure 1.10).

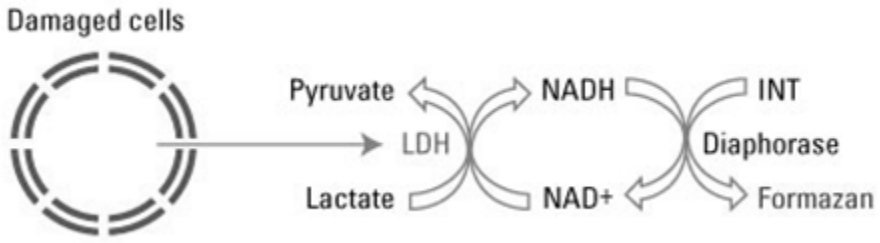

Figure 1.10. LDH assay detection mechanism (from tools.lifetechnologies.com/content/sfs/gallery/high/88953-001-LDH-Cytotox.jpg).

The release of LDH into culture supernatant correlates with the amount of cell death and membrane damage proving an accurate measure of the cellular toxicity induced by the test substance (Kendig and Tarloff, 2007). Because of this unique mechanism, the LDH assay provides a powerful tool to quantitatively measure cell membrane lysis in the presence of materials such as NP (Han et al., 2011).

Although the above-mentioned assays take into consideration the potential cytotoxicity of NP on the mitochondria and the cell membrane, in order to determine the absolute toxicity, an assessment of the substance ability to cause cell death is necessary (Rivera-Gil et al., 2012). There are, however, two specific forms of cell death, which have received increased attention in relation to NP exposure to cells (Clift and Stone, 2012).

The first of these processes is **apoptosis**, also known as programmed cell death, which is essential for the development and maintenance of multicellular organisms (Leist and Jäättelä, 2001). Apoptosis is an efficient defence mechanism to prevent damaged cells from undergoing a transition to malignancy (Brown and Attardi, 2005). The second process, **necrosis**, has been shown to occur in response to externally induced toxicity. Necrosis is characterized by the rapid loss of cellular homeostasis, early plasma membrane rupture, and disruption of cellular organelles, whereas apoptosis is characterized by shrinkage of the cell and the nucleus (Kerr et

al., 1972; Majno and Joris, 1995). Cell death is commonly assessed by the use of specific fluorescent staining solutions/antibodies for both apoptosis and necrosis.

Although there are many different tests available, annexin V-based tracers are the most frequently used agents for *in vitro* detection and quantification of apoptotic cells (AshaRani et al., 2009). When cells undergo apoptosis, the early response includes the transport of inner cell membrane lipids, such as phosphatidylserine (PS), to the outer surface of the membrane, serving as a marker for macrophages to eliminate these cells. **The annexin-V assay**, is based on the high affinity of annexin-V for PS (Yang et al., 2012). Upon exposure of cells to apoptotic stimuli PS is flipped to the outer leaflet of the plasma membrane, thereby allowing annexin V (which is labelled with a fluorescent dye: fluorescein) to bind it, thus marking the early apoptotic cells and making their identification possible by fluorescence detection. The necrotic/late apoptotic cells are also distinguished via the use of another fluorescent dye, propidium iodide (PI), which stains DNA in those cells with altered membrane permeability (necrotic/late apoptotic cells) (Wu et al., 2010a) (Figure 1.11).

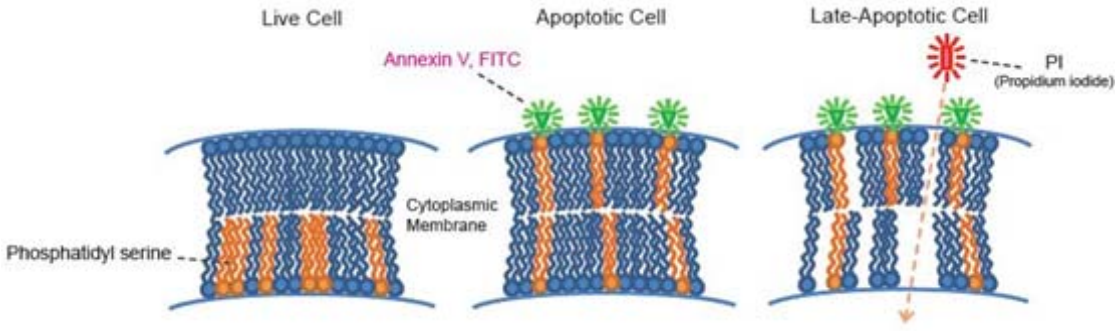

Figure 1.11. The principle of apoptosis detection by annexin V/PI (from www.dojindo.com/store/p/847-Annexin-V-FITC-Apoptosis-Detection-Kit.html).

Not only apoptosis is associated with a distinct set of biochemical and physical changes involving cytoplasm, nucleus, and plasma membrane, also mitochondria have been described to play a key role in the apoptotic process. In addition to being the source of energy that supports life under aerobic conditions, mitochondria can also be the source of signals that initiate apoptotic cell death (Gottlieb, 2000). Mitochondria contain key regulators of caspases; a family of proteases that are major factors in apoptotic processes (Hengartner, 2000).

As the energy power-plants of the cell, mitochondria generate adenosine triphosphate (ATP) by utilizing the proton electrochemical gradient potential generated by serial reduction of electrons through the respiratory electron transport chain (Perry et al., 2011). A distinctive feature of the early stages of programmed cell death is the disruption of active mitochondria. This mitochondrial disruption includes changes in their **membrane potential (MMP)** and alterations to the oxidation–reduction potential of the mitochondria (Kuznetsov et al., 2011).

Changes in MMP are presumed to be due to the opening of the mitochondrial permeability transition pore (MPTP), allowing passage of ions and small molecules. The resulting equilibration of ions leads in turn to the decoupling of the respiratory chain and the release of cytochrome *c* from the mitochondrial intermembrane space into the cytosol. This release induces the assembly of the apoptosome that is required for activating downstream caspases (Vander Heiden et al., 2001). Hence, cytochrome *c* release from mitochondria is a key event in initiating apoptosis.

As opening of the MPTP has been demonstrated to induce depolarization of the transmembrane potential, release of apoptogenic factors and loss of oxidative phosphorylation (Galluzzi et al., 2007), several fluorescent lipophilic cationic dyes [e.g., tetramethylrhodamine methyl (TMRM), rhodamine 123 (Rhod123) and 5,5′,6,6′-tetrachloro-1,1′,3,3′-tetraethylbenzimidazolylcarbocyanine iodide (JC-1)] have become important tools for directly measuring MMP. As positively charged molecules, these dyes will accumulate within mitochondria. More polarized mitochondria (where interior is more negative) will accumulate more cationic dye, and depolarized mitochondria (interior is less negative) will accumulate less dye. For instance, as it can be seen from Figure 1.12, in healthy cells JC-1 diffuses across the cellular membrane into the cytoplasm where it fluoresces green. Due to cationic properties of JC-1, it migrates into the mitochondria where the net negative charge is -180mV. As the concentration of JC-1 within the mitochondria increases, JC-1 begins to form aggregates that fluoresce red. However, in cells undergoing apoptosis or in those that have been treated with a drug (such as CCCP) the loss of MMP prevents JC-1 from forming aggregates within the mitochondria and therefore JC-1 fluoresces green in the cytoplasm.

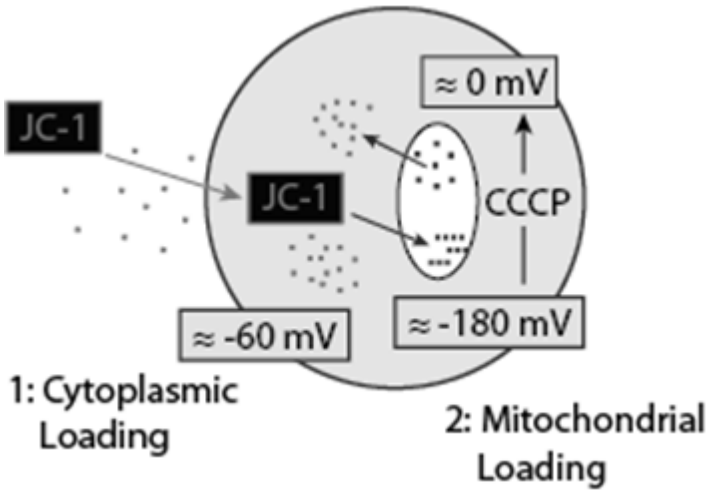

Figure 1.12. The principle of apoptosis detection with the fluorescent cationic dye JC-1 (from http://www.nexcelom.com/Applications/Apoptosis.html).

As nanotoxicological research continues to evolve, not only apoptotic and necrotic experimental end-points are usually applied but also more emphasis is directed toward the

mechanisms and pathways by which NP induce cell death. Mechanisms of cell death in various cell populations can also be elaborately linked with the cell cycle, as there are various check-points and controls in a cell life cycle to ensure that appropriate division process occur. Without control over the cell cycle, pathological processes can initiate; the most common example is cancer. Hence, it is important to study the effects that NP may have on the cell cycle and division for proper risk assessment.

Cell cycle is a vital process. Its most basic function is to duplicate accurately the vast amount of DNA in the chromosomes and then segregate the copies precisely into two genetically identical daughter cells (Alberts et al., 2002). In eukaryotes, cell cycle can be divided into two brief periods: (i) the interphase, during which the cell grows and accumulates nutrients needed for mitosis and DNA replication and (ii) chromosome segregation and cell division occur in the mitosis (M) phase, in which the cell splits itself into two distinct daughter cells. Although there are many stages in mitosis (prophase, metaphase, anaphase, and telophase) it typically occupies only a small fraction of the cell cycle (Alberts et al., 2002). The other, much longer, part of the cycle is spent in interphase, which is divided into three parts: G_1, S, and G_2 phases (Figure 1.13). In the first gap phase (G_1), the cell grows and produces enzymes that are necessary for cell division. In the synthesis phase (S), the DNA is replicated. Finally, in the second gap phase (G_2), the cell continues to grow and carries out processes necessary for mitosis. In both the G_1 and G_2 phases, there are checkpoints to ensure that the cell is prepared for crucial steps in its division.

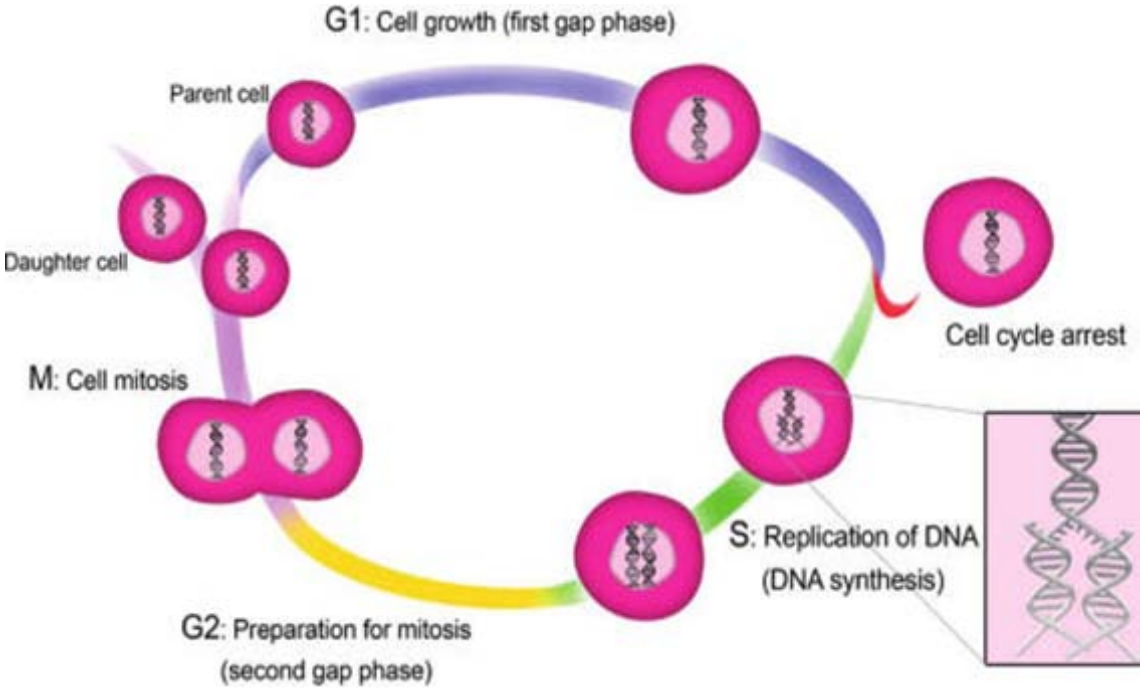

Figure 1.13. Phases of the cell cycle (from Mahmoudi et al., 2011).

The DNA content of cells is well correlated with the stage of the cells in the cell cycle. Cells in the G_0/G_1 step have half the DNA (2n) of a G_2/M phase cell (4n), while the DNA content is in between these two during the synthesis phase (Crosby, 2007). Cells with lower than 2n DNA are mostly cell garbage, or apoptotic cells which have lost different amounts of their DNA. Thus, techniques to perform cell cycle analysis are based on DNA content measurements. Probably the most commonly used is univariate (measurement of cellular DNA content alone) and bivariate (measurement of DNA versus RNA content) cell cycle analysis using flow cytometry, which is based on the use of fluorescent dyes (usually PI) which interact with DNA (Mahmoudi et al., 2011). These dyes bind in different ways to the double-stranded DNA, which is mainly in the cell nuclei. Nonspecific binding to the double-stranded RNA is easily resolved by adding RNase A in conjunction with PI stain. PI intensity in cells can be analysed by FCM and percentage of cells in G_0/G_1, S and G_2/M phases calculated (Chan et al., 2011; Darzynkiewicz et al., 2004).

1.2.2.3. *In vitro genotoxicity*

A vital area controlling most of the regulatory health risk assessment is genotoxicology, which can be defined as the study of damages on the genetic information within a cell, following exposure to test agent (Singh et al., 2009). Recently, considerable attention has been given to the genotoxicity of ENM. As DNA damage induced by ENM may initiate and promote carcinogenesis, the importance of their genotoxic potential on human health has been largely overlooked. Several reviews and research papers dealing with NP genotoxicity have been published in recent years (AshaRani et al., 2009; Karlsson, 2010; Kumar and Dhawan, 2013; Magdolenova et al., 2014; Stone et al., 2009; Xie et al., 2011). In this section the most frequently used methodologies for genotoxicity evaluation will be addressed.

NP-induced genotoxicity can be attributed to several factors, such as direct interaction with the genetic material, indirect damage due to ROS generation, and release of toxic ions from soluble ENM (Magdolenova et al., 2014). Due to the size of ENM, the probability of their internalization into the cells and interaction with cellular organelles and macromolecules (DNA, RNA, and proteins) is very high. Small sized NP that cross cellular membranes may be able to reach the nucleus through diffusion across the nuclear membrane or transportation through the nuclear pore complexes, and interact directly with DNA (Donaldson et al., 2010). These interactions can damage the genetic material by physical injury as well as by modulating biochemical pathways.

The genotoxic effects of many materials can be identified by a number of techniques that detect DNA damage. One of the most common DNA damage assays is the single cell gel electrophoresis assay, commonly known as the **comet assay**. The term “comet” describes the

pattern of electrophoretic migration of DNA from a single cell if there is DNA damage (Møller et al., 2014).

Depending on the pH used, the comet assay is able to detect a wide variety of DNA damage such as single and double strand breaks (DSB), incomplete excision repair sites, crosslinks, alkali-labile sites (e.g., abasic sites) and, by using lesion specific enzymes, oxidized DNA lesions (Catalán et al., 2014 ; Collins et al., 2014).

Several versions of the comet assay are currently in use although the most popular one is the alkaline version, which was firstly introduced by Singh et al. (1988). The general scheme of this assay represented at Figure 1.14. Briefly, under this method single-cell suspension in low melting point agarose is spread onto a normal melting agarose pre-coated microscope slide to make a monolayer of cells. Cells are then lysed in high salt concentration and detergent to unwind the super-coiled DNA and reveal the damage.

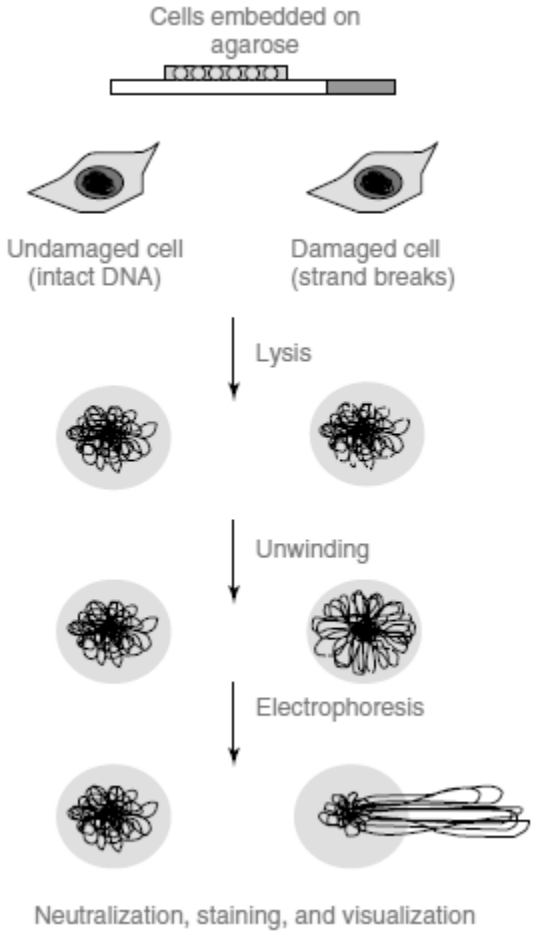

Figure 1.14. Scheme of the standard comet assay (from Azqueta and Collins, 2006).

During lysis, the aqueous salt disrupts proteins and their bonding patterns within the cell as well as RNA content of the cell. The detergent dissolves the cellular membranes, and cytoplasmic and nucleoplasmic constituents are disrupted and diffuse into the agarose matrix;

only the nuclear DNA remains. The extent of DNA damage is revealed via electrophoresis of the agarose embedded single cell samples; negatively charged damaged DNA migrates towards the anode away from the nucleus and form a comet shape (Rivera-Gil et al., 2012). The intact DNA, due to its large size and winding state migrates minimally.

The size and shape of the comet and the extent of DNA liberated from the head (to the tail) correlate with the extent of DNA damage (Fairbairn et al., 1995). The migrating DNA can be detected by different DNA specific fluorescent dyes and its intensity of fluorescence can be measured in the head and tail under the microscope either qualitatively by visual inspection, or quantitatively by using commercially available computer software (Figure 1.15).

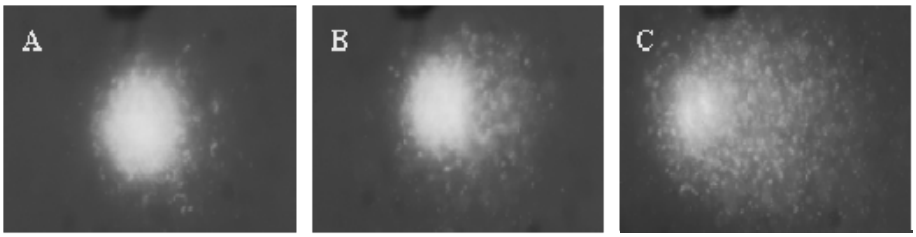

Figure 1.15. Images of cells subjected to comet assay. A) not damaged cell, B) moderately damaged cell, C) intensely damaged cell.

In the past few years, the comet assay has been extensively used to study genotoxic effects of NP; automated image analysis has been commercially available making the use of comet assay simple and effective (Tice et al., 2000). However, results published on genotoxicity of ENM show high variability even with the same type of material due the diversity of methods for preparing dispersions, variation in size distribution and dispersion stability, and different exposure conditions (Magdolenova et al., 2014).

Another specific and very sensitive test to detect DSB is the **γ-H2AX assay** (Valdiglesias et al., 2013). As response to the formation of DSB, the variant histones H2AX flanking the DSB sites are rapidly phosphorylated at the Serine 139 residue to become γH2AX (Redon et al., 2011), which is involved in recruiting repair factors (Bonner et al., 2008; Petrini and Stracker, 2003) (Figure 1.16).

Under normal conditions, γH2AX appear within few minutes after the lesion, reach maximum levels after about 30min and then decline and disappear after approximately 24h (Bourton et al., 2011; Rogakou and Sekeri-Pataryas, 1999). Therefore, H2AX phosphorylation represents an early event in the DNA damage response against DSB and plays a central role in sensing and repairing these lesions (Matsuzaki et al., 2010; Scarpato et al., 2013).

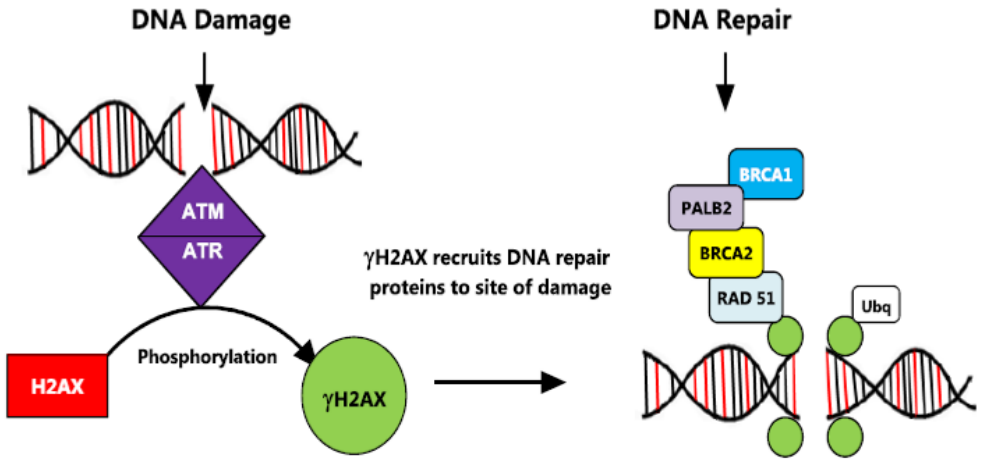

Figure 1.16. Scheme of H2AX phosphorylation process and its consequences in DNA damage response (from http://www.amsbio.com/news/whitepaper/gamma_H2AX_white_paper.pdf).

The presence of γH2AX is therefore a sensitive reporter of DNA damage and their presence can be detected by using fluorescently labelled antibodies specific to γH2AX (Singh et al., 2009). The alteration in the expression profile of γH2AX induced by ENM has been detected by different techniques such as immunohistochemistry, and Western blot. Alternatively, γH2AX can be measured by flow cytometry with a number of advantages (Sánchez-Flores et al., 2015). It provides an automated high-throughput platform that is fast, practical, reproducible, and may take into consideration variations due to cell-cycle effects (Watters et al., 2009). Besides, it increases considerably the number of cells evaluated, diminishing the variability and enhancing the statistical power of the results (Brzozowska et al., 2012).

A well-defined testing protocol for detection and evaluation of structural and numerical chromosome aberrations is the **micronucleus (MN) test**. The *in vitro* MN test is a simple cytogenetic assay based on the scoring of extra nuclear chromatin-containing structures in actively dividing cell populations. MN are formed during cell division and may arise from a whole lagging chromosome that have been lost during the anaphase (aneugenic event leading to chromosome loss) or from an acentric chromosome fragment which is not having a centromere to position itself at mitotic spindle, and eventually detaches from a chromosome after breakage (clastogenic event) (Botta and Benameur, 2011)(Figure 1.17). These displaced chromosomes or chromosome fragments are eventually enclosed by a nuclear membrane and, except for their smaller size, are morphologically similar to nuclei after conventional nuclear staining (Fenech et al., 2011).

Figure 1.17. Representation of MN formation in cells undergoing nuclear division (from Fenech et al., 2011).

MN are nuclear entities independent of the main nucleus, numbering anywhere between 1 and 6 per cell, with diameter between 1/3 and 1/16 of the diameter of the main nucleus (Botta and Benameur, 2011). Traditionally MN have been evaluated by visual scoring under the microscope but lately, as it adds the benefits of automated scoring, rapid frequency and low time-consuming measurements, flow cytometric method is also used to evaluate MN in genetic toxicology testing (Laingam et al., 2008).

Increased assay sensitivity can be obtained (in the *in vitro* and *ex vivo* assays) by incubating treated cells with cytochalasin B, which blocks cytoplasm division, but not mitosis (nuclear division), so that binucleated cells accumulate. However, this methodology is potentially a problem with regards to the study of ENM because cytochalasin B also inhibits endocytosis, which is an important cell uptake mechanism for some nanomaterials (Doak et al., 2009).

Another consideration about the *in vitro* MN assay when applied to the hazard assessment of ENM is that it is highly advisable to use fluorescent DNA dyes for staining the cells, in order to avoid falsely identifying NP agglomerates as MN (Magdolenova et al., 2014).

1.2.2.4. *Generation of reactive oxygen species*

If cell exposure to NP does not cause a lethal effect, then there are a variety of possible adverse sub-lethal effects that they can cause upon the cell. A key mechanism thought to be responsible for the genotoxic effects exerted by ENM involves oxidative stress (Singh et al., 2009). There are numerous assays to evaluate oxidative stress related endpoints. The most common are the ones associated with the assessment of ROS generation.

While oxygen is essential for life, the formation of ROS imposes a threat to cells. ROS are normal by-products of aerobic metabolism. All electron transport chains of metabolic processes possess the potential to “leak” electrons to oxygen resulting in superoxide formation (Cooke et al., 2003). Furthermore, inflammation may accelerate the production of ROS, as they

are released from phagocytic cells destined to destroy cells infected with viruses or bacteria (Williams et al., 2011).

Normal cellular homeostasis involves a delicate balance between the rate and amount of ROS production and oxidant elimination (Garza et al., 2008). To prevent oxidative damage, cellular antioxidants neutralize ROS and they are normally cleared from the cell by the action of enzymes (e.g., superoxide dismutase, glutathione peroxidase, and catalase) or antioxidants (e.g., ascorbic acid, cysteine, glutathione, carotenoids, and bilirubin) (Wu et al., 2014). But excess of free radicals not neutralized by the organism defence system can disturb the homeostasis of the intracellular surrounding (L'Azou and Marano, 2011). And when there is an imbalance between the generation of ROS and the level of antioxidants within a cell, then the result is oxidative stress (Rivera-Gil et al., 2012). This imbalance could be caused by enhanced generation of ROS after exposure to an agent or by deficiency of cellular antioxidants, the result of which can be the formation of oxidative DNA lesions that may be subsequently fixed as mutations (Doak et al., 2012).

ROS are defined as either 'primary' or 'secondary'. 'Primary' ROS can be generated through metabolic processes or through the activation of oxygen. That results in the formation of a reactive nucleophilic molecule of oxygen, so called superoxide anion radical ($O_2^{\cdot -}$), which does not react directly with DNA or polypeptides. However, it may interact with other molecules such as redox active transition metals (e.g., iron) or enzymes, resulting in the production of 'secondary' ROS (e.g., hydroxyl radical, $OH^{\cdot}$).

ENM of various kinds are reported to induce ROS and oxidative stress under *in vitro* and *in vivo* conditions (Geppert et al., 2012; Karlsson et al., 2008; Sharma et al., 2014; Toyooka et al., 2012). The transition metals ions (such as cadmium, chromium, cobalt, copper, iron, nickel, titanium and zinc) released from certain NP have the potential to cause the conversion of cellular oxygen metabolic products, such as H_2O_2 and superoxide anions, to hydroxyl radicals ($OH^{\cdot}$) via the Fenton-type reaction (Kruszewski et al., 2011), which is one of the primary DNA damaging species (Wu et al., 2014).

In addition to the presence of transition metal catalysts in their composition, the high surface area associated with ENM can promote the generation of ROS. Consequently, the smaller the NP, the higher the oxidative stress they induce (Brown et al., 2001; Buzea et al., 2007; Singh et al., 2009).

In regard to the determination of ROS production, a common parameter used is the fluorescent dye/probe **2',7'-dichlorodihydrofluorescein diacetate (DCFH-DA),** a reliable fluorogenic marker for ROS in living cells. This method assesses the production of ROS via the increase in fluorescence. Colourless and non-fluorescent DCFH-DA can passively diffuse into cells, and when the acetate groups are cleaved by intracellular esterases DCFH is generated

(Eruslanov and Kusmartsev, 2010). Oxidation of DCFH by ROS converts the molecule to highly fluorescent 2',7'-dichlorodihydrofluorescein (DCF). Accumulation of DCF in cells can be measured by an increase in fluorescence at 530nm when the sample is excited at 485nm. The fluorescence signal can be both quantified using flow cytometer analysis and spectrofluorimetry, and are assumed to be proportional to the concentration of hydrogen peroxide in the cells (Eruslanov and Kusmartsev, 2010).

To enhance retention of the fluorescent product, various analogues (improved versions of DCFH-DA) have been developed (Tiano et al., 2001). Yet, DCFH-DA can only detect cellular peroxides efficiently if they are decomposed to radicals, for example, by transition metal ions. The chemistry of the conversion is complex and neither H_2O_2 nor O_2- can oxidize DCFH, but $NO_2^{\cdot}$, carbonate ($CO_3^{\cdot -}$) and $OH^{\cdot}$ radicals can carry out the oxidation (Bilski et al., 2002; Eruslanov and Kusmartsev, 2010; Ohashi et al., 2002). This method is extremely advantageous, as it not only can be performed via multiple approaches, but can also be used in a cell-free environment. This is important, since it provides important information pertaining to the NP alone, and thus their ability to cause ROS independent on a cellular environment (Bhattacharya et al., 2009; Rivera-Gil et al., 2012).

Oxidative stress results from an imbalance between oxidant derivatives production and antioxidants defences (Le Lay et al., 2014). Therefore in order to obtain a thorough and clear understanding of the oxidant-related effects of NP, not only assessment of ROS production but also the antioxidant capacity should also be performed. This form of analysis has commonly been performed in regard to an assessment of **intracellular glutathione (GSH) levels** (Rivera-Gil et al., 2012).

GSH is a major free thiol in most living cells and is involved in many biological processes such as detoxification of xenobiotics, removal of hydroperoxides, and maintenance of the oxidation state of protein sulfhydryls. Usually present in cells as GSH (reduced form), it exists as oxidized glutathione (GSSG) in an oxidative environment, which can be rapidly converted to GSH via an enzymatic reaction using glutathione reductase (Hissin and Hilf, 1976). Reduced GSH is one of the most important antioxidant defences in the body, and the balance between GSH and GSSG provides a good indication of the level of oxidative stress (Rosemary M Gibson, 2007). The levels of both GSH and GSSG within cells can be determined via commercially available diagnostic kits by either absorbance or fluorescence.

ROS can directly attack the DNA and generate various modified DNA bases. Among these bases, 8-oxoguanine (8-oxoG) is one of the most common DNA lesions resulting from ROS and can result in a mismatched pairing with adenine due to G to T and C to A substitutions in the genome (Cheng et al., 1992; Cooke et al., 2003). It has been shown that the levels of 8-oxoG can be used as indicators of oxidative DNA damage after exposure to ENM using the

enzyme-modified comet assay (Jacobsen et al., 2008; Kim et al., 2011; Rinna et al., 2015; Rubio et al., 2015; Vesterdal et al., 2014).

In its standard form, the comet assay measures DNA strand breaks and (in the alkaline version) alkali-labile sites, i.e. apurinic/apyrimidinic sites (AP-sites) or baseless sugars (Collins, 2009a). This standard comet assay can be modified to detect oxidized purines or pyrimidines, by introducing an incubation of the nucleoids (just after lysis) with DNA repair enzymes. The most commonly used commercially available endonucleases in the modified comet assay are the bacterial enzymes formamidopyrimidine DNA-glycosylase (FPG) and endonuclease III (ENDOIII) which recognize different types of oxidative damage (Smith et al., 2006). FPG is specific for oxidized purines, including 8-oxoG, 2,6-diamino-4-hydroxy-5-formamidopyrimidine (FaPyGua) and 4,6–diamino–5-formamidopyrimidine (FaPyAde) and other ring-opened purines. ENDO III recognizes oxidized pyrimidines, including thymine glycol and uracil glycol (Collins, 2009b). However, when ENDO III and FPG enzymes were compared with the human analogue of FPG 8-oxoguanine DNA glycosylase (OGG1), it showed higher substrate specificity than the others (Smith et al., 2006). OGG1 participates in base excision repair (BER), the major repair pathway for removal of 8-oxoG from DNA. This enzyme catalyses the hydrolysis of 8-oxoG from the DNA backbone, leaving an abasic site in the DNA (Singh et al., 2011).

When using these enzymes to measure oxidative DNA damage with comet assay, the usual practice is to incubate microgels with enzyme, in parallel with incubation with the enzyme buffer alone (as a control). An increase in DNA damage after incubation with the enzyme, compared with the incubation with buffer alone, indicates the presence of oxidized bases (Collins, 2014).

2. OBJECTIVES AND OUTLINE OF THE THESIS

The rapid development of nanotechnology industries and increased use of nanomaterials have arisen concerns associated with uncertainties regarding risks posed by these new materials to health and environment; it is therefore necessary to study their possible hazards on human health. Especially, considering their unique physicochemical properties, they might reach the brain and induce neurotoxicological effects. On this basis, the overall aim of this Thesis was to elucidate the toxicological impacts of a set of engineered metal oxide nanoparticles (namely titanium dioxide, zinc oxide and iron oxide NP) on human neuronal cells (SH-SY5Y). To this aim, a complete set of *in vitro* cellular and molecular methodologies were applied in order to characterize the potential adverse effects of the studied NP and to identify their underlying modes of action.

This main goal will be achieved by the following specific objectives:

- To characterize the candidate NP by defining different physicochemical properties including size, morphology, agglomeration state, zeta potential, metal ion release, etc. that may influence their toxicity pattern.

- To investigate the internalisation behaviour of the different metal oxide NP by human neuronal cells.

- To evaluate the cellular toxicity profile of the metal oxide NP on human neuronal cells in terms of analysing viability, cell cycle, apoptosis/necrosis death, and membrane integrity.

- To assess direct and indirect genotoxicity outcomes induced by the metal oxide NP on SH-SY5Y cells, namely primary DNA damage and MN production, H2AX histone phosphorylation, generation of oxidative stress and DNA repair alterations.

This thesis will be divided into three sections. In the first section (Chapter 3), details on the toxicity investigation of two types of titanium dioxide NP (TiO_2-NP) with different crystalline structure on human neuronal cells will be discussed. The second section (Chapter 4) is dedicated to the potential toxicity of zinc oxide NP (ZnO-NP) and, finally, the third section (Chapter 5) illustrates reactivity of silica-coated iron oxide NP (S-ION) on the same cultured cell line.

3. Effects of titanium dioxide nanoparticles with two different crystalline structure on human neuronal cells

3.1. INTRODUCTION

Nanotechnology has been showing a significant impact on almost all industries and areas of society (Karmakar et al., 2014). Metal and metal oxide NP are often used as industrial catalysts or to improve product functional properties (Sarkar et al., 2014a). Among the manufactured metal oxide NP, titanium dioxide NP (TiO_2-NP) are the earliest industrially produced nanomaterials (Baan et al., 2006) and, according to the U.S. National Nanotechnology Initiative, these NP are one of the most highly manufactured ENM in the world (Khan et al., 2015).

Titanium, the ninth most abundant element in the earth crust (Fang et al., 2013), is found in a wide variety of minerals, rocks, water bodies and soils. Because it reacts easily with oxygen and carbon at high temperatures, titanium metal is relatively uncommon and it naturally occurs as titanium dioxide [also known as titanium (IV) oxide, titanic acid anhydride, titania, titanic anhydride, or titanium white], with chemical formula TiO_2.

TiO_2 is a white non-combustible and odourless powder which resists fading in sunlight, and due to its properties of absorption and reflection of ultraviolet (UV) light is very opaque (Winkler, 2003). Hence, this naturally occurring mineral is widely used as a bright white pigment for paints, in the food industry as a colouring, and in sunscreens and cosmetics. Approximately four million tons of this pigment are consumed annually worldwide (Ortlieb, 2010).

TiO_2 exists in nature in three different crystalline phases (anatase, rutile, and brookite); yet, only anatase and rutile are of industrial interest. Stable phase rutile structure contains titanium atoms occupying the centre of a surrounding core composed of six oxygen atoms, placed approximately at the corners of a quasi-regular octahedron (Diebold, 2003), as shown in the Figure 3.1.

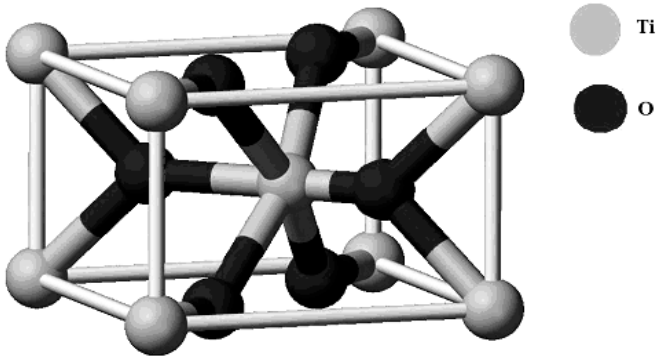

Figure 3.1. TiO_2 rutile crystalline structure (from www.chemtube3d.com/solidstate/_rutile%28final%29.htm)

Anatase structure is tetragonal, with two TiO_2 formula units (six atoms) per primitive cell as shown in Figure 3.2 (Diebold, 2003). TiO_2 anatase converts to rutile generally at temperatures above 700°C (Lin et al., 2008a). Thus, anatase and rutile phases strongly depend on thermal treatment conditions.

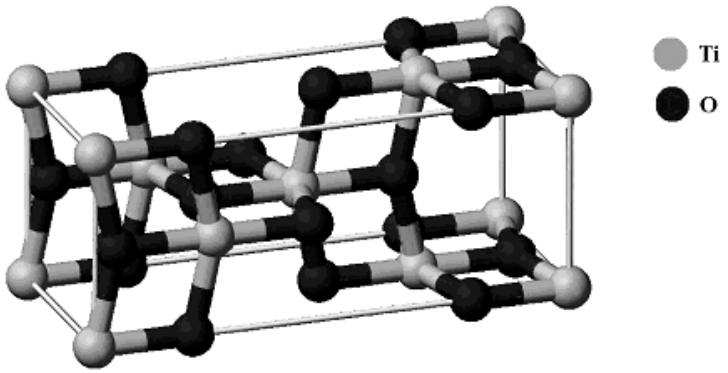

Figure 3.2. TiO_2 anatase crystalline structure (from http://www.chemtube3d.com/solidstate/_anatase%28final%29.htm).

The photocatalyst TiO_2 captures UV light and forms activated oxygen from water or oxygen in the air. This process is similar to photosynthesis, in which chlorophyll captures sunlight to transform water and carbon dioxide into oxygen and glucose. The activated oxygen formed is strong enough to oxidize and decompose organic materials and is even strong enough to kill bacteria (Ortlieb M, 2010). Thus, TiO_2-NP show antibacterial effect against *Escherichia coli, Staphylococcus epidermidis, Streptococcus pyogenes, Streptococcus mutans* and *Enterococcus faecali* up to two hours post UV (Cai et al., 2013). Industrial utilization of the photocatalytic effect of TiO_2-NP has also found its way into other applications, especially for self-cleaning and anti-fogging purposes such as self-cleaning tiles, self-cleaning windows, self-cleaning textiles, and anti-fogging car mirrors (Montazer and Seifollahzadeh, 2011).

TiO_2-NP are among the top five NP used in consumer products, paints and pharmaceutical preparations (Shukla et al., 2011). In daily use, it can be found nearly everywhere - in paints, coatings, plastics, papers, inks, medicines, pharmaceuticals, cosmetics, and personal hygiene products such as toothpaste (Kaida et al., 2004; Wolf et al., 2003). It has even been used as a pigment to whiten skim milk (CCOHS, 2009), and approved as a food colour additive and food contact substance in food packaging by the United States Food and Drug Administration (FDA, 2014).

Human exposure to TiO_2-NP may occur during both manufacturing and use of products containing these NP. They can be encountered as aerosols, suspensions, or emulsions. The major exposure routes to TiO_2-NP that have toxicological relevance in the workplace are inhalation and dermal exposure (Shi et al., 2013). Exposure may also result from intentional use of certain manufactured NP. In the field of nanomedicine, TiO_2 has long been used as a component for articulating prosthetic implants, especially for the hip and knee because of its

high stability and anticorrosive properties (Diebold, 2003). The use of TiO_2-NP in sunscreen creams to improve the spreading quality of the cream on the skin and protect against the sun UV radiation leads to the dispersal of these NP in water when people bathe (Baeza-Squiban and Lanone, 2011). TiO_2-NP are also widely used for toothpaste, food colorants, and nutritional supplements; thus oral exposure may occur during use of such products (Weir et al., 2012).

With the rapid increase in the number of nano-related products and common use of TiO_2-NP in everyday life, comes an increasing concern about their safety to humans and the environment. The rapid growth in the number of published studies confirms that there is a high level of interest concerning the safety of TiO_2-NP. Many *in vitro* studies showed that TiO_2-NP were cytotoxic (Hamzeh and Sunahara, 2013; Setyawati et al., 2013) and genotoxic (Jugan et al., 2012; Prasad et al., 2013a; Toyooka et al., 2012), led to apoptosis (Botelho et al., 2014; Ghosh et al., 2013; Lagopati et al., 2014; Vamanu et al., 2008; Wang et al., 2014b), induced ROS (Gao et al., 2015; Magdolenova et al., 2012a; Niska et al., 2015) and DNA damage (Demir et al., 2015; Kansara et al., 2014; Magdolenova et al., 2012a; Petersen et al., 2014; Setyawati et al., 2015; Ursini et al., 2014), and changed enzyme activities (Armand et al., 2013; Becker et al., 2014; Takaki et al., 2014; Wan et al., 2008) and gene expression (Chen et al., 2014b; Orazizadeh et al., 2014; Periasamy et al., 2015; Prasad et al., 2013a; Tuomela et al., 2013) in different cell lines.

However, there are also studies showing lack of TiO_2-NP toxicity. Du et al. (2012) reported that there were no significant changes in ROS, GSH, 8-hydroxy-2'-deoxyguanosine (8-OHG), or OGG1 levels when human embryo hepatocytes L02 cells were treated with TiO_2-NP. Similarly, Woodruff et al. (2012) found that TiO_2-NP were not genotoxic under the conditions of the Ames test and comet assay in TK6 cell line; there was no significant primary or oxidative DNA damage observed. Similarly, a chronic (60 days) study with Chinese hamster ovary , CHO cells showed no cytotoxic or genotoxic effects by TiO_2-NP (Wang et al., 2011a).

Furthermore, *in vivo* studies showed that once TiO_2-NP enter the body at the initial site of exposure, they are absorbed through the gastrointestinal tract, the skin and the pulmonary system. Once they reach the systemic circulation, they potentially interact with plasma proteins, coagulation factors, platelets, and red or white blood cells. The systemic circulation can distribute these NP to all organs and tissues in the body (Shi et al., 2013). More recently, it was even shown that the NP (8nm) are transferred from mother to pups through breastfeeding, after four intravenous administrations of TiO_2-NP (anatase) of different sizes (8nm, 50nm) to lactating female CD-1 mice (Zhang et al., 2015).

In concordance with *in vitro* experiments, Numano et al. (2014) compared the *in vivo* toxic effects induced by anatase and rutile TiO_2-NP by treating rats with NP suspensions by intra-pulmonary spraying. As a result, treatments increased alveolar macrophage numbers and levels of 8-oxoG in the lungs; yet these increases were lower in the anatase-treated group

compared to the rutile-treated group. Likewise, TiO_2-NP (99.7% anatase) induced oxidative stress and DNA damage in mice liver cells after oral exposure (Shukla et al., 2013). Similarly, Sang et al. (2014) reported decrease in the levels of protein expression involved in immune responses, lymphocyte healing and apoptosis in the spleen of mice following intragastric exposure to pure anatase TiO_2-NP. When Trouiller et al. (2009) treated C57Bl/6J wild-type mice with TiO_2-NP (75% anatase and 25% rutile) in drinking water, they found out that TiO_2-NP induced 8-OxoG, γ-H2AX foci, MN, and DNA deletions in peripheral blood of mice.

However, there are also *in vivo* studies showing lack of TiO_2-NP toxicity. For instance, Naya et al. (2012) did not find significant apoptosis induction in rat lung cells following intratracheal instillation of TiO_2-NP. Negative responses were also shown in reticulocytes (MN test) and in leukocytes (comet assay) of bone marrow cells of rats following intravenous injection of TiO_2-NP (Dobrzyńska et al., 2014). More recently, Elgrabli et al. (2015) showed absence of toxicological effects on lungs, blood, liver, spleen and kidneys of male Sprague-Dawley rats after TiO_2-NP (anatase) intravenous injection at concentrations of 7.7 to 9.4mg/kg.

It is also well documented that TiO_2-NP could easily cross the blood-brain barrier (BBB), reside in the central nervous system (CNS) and produce damage to the barrier integrity (De Jong and Borm, 2008; Shrivastava et al., 2014; Xue et al., 2012; Ze et al., 2014a; Zhang et al., 2011). For example, TiO_2-NP could be observed in the brain following 60 days dermal exposure to hairless mice, i.e., they could penetrate the skin and were found in the brain (Wu et al., 2009). Also, Ze et al. (2014a, 2014b) showed titanium accumulation in the hippocampus and neuroinflammation in mice following daily intranasal exposure to TiO_2-NP for 90 days. Likewise, a significant increase in the bioaccumulation of TiO_2-NP in brain and ROS production was observed following intravenous injection to Wistar rats (Meena et al., 2015) and intraperitoneal injection to ICR mice (Ma et al., 2010), which caused in both studies oxidative stress and injury of the brain, and in turn inhibition of the normal metabolism of neurochemicals.

Furthermore, several *in vitro* studies performed in neuronal cell lines reported that TiO_2-NP induced some levels of neurotoxicity in rat brain microglia (Long et al., 2006, 2007; Sheng et al., 2014,2015) human U87 astrocytoma cells (Lai et al., 2008), and rat PC12 cells (Hernández et al., 2015; Liu et al., 2010; Wu et al., 2010a).

Even though studies have illustrated that TiO_2-NP, could settle in the brain tissue of rodents, and induce adverse effects, to our knowledge there are limited data indicating the possible effects of TiO_2-NP on human neuronal cells. Let alone, there are no studies examining effects of particle variations from the same crystal structure or different crystal structures with the same particle size on the neurotoxicity of TiO_2-NP.

Neurons are the core components of CNS, which are crucial for the maintenance of CNS function, and the irreversible degeneration of neurons plays an essential role in some neurodegenerative diseases including Hallervorden–Spatz syndrome, Parkinson's disease and Alzheimer's disease (Pettmann and Henderson, 1998). The possibility that neurons in CNS might be targeted by TiO_2-NP has increased the potential risks in developing neurodegenerative diseases (Migliore et al., 2015). Therefore, it is immensely needed to carry out new investigations dealing with the adverse effect of TiO_2-NP on human neuronal cells. Furthermore, although the principal parameters determining toxicity of NP are their physicochemical properties, including shape, size, surface characteristics and inner structure, Sayes et al. (2006) reported that surface characteristics may be a less important factor than phase composition in the toxicological responses of TiO_2. It has been suggested that anatase has a greater toxic potential than rutile (Petković et al., 2011; Xue et al., 2010) due to its higher catalytic activity, which would determine its potential to dissociate water to hydroxyl radicals (Monteiro-Riviere et al., 2007). Based on this fact, it is important to characterize carefully the physicochemical properties of TiO_2-NP and to consider the influence of their crystalline structure on their bioactivity when evaluating adverse health effects and environmental biosafety.

In the present study, we investigated whether TiO_2-NP could cause adverse cytotoxic and genotoxic effects on human neuronal cells, interpreted the routes of biological impacts, and elucidated the possible molecular mechanisms. Furthermore, by comparing TiO_2-NP with two different crystalline structures, we explored how this feature may influence their interaction with the neuronal cells under diverse *in vitro* conditions.

3.2. MATERIALS AND METHODS

3.2.1. *Nanoparticles: preparation and characterization*

The NP used in this study were TiO_2-NP with two different crystalline structures: NP in pure anatase structure were purchased from Sigma–Aldrich Co. (TiO_2-S) and anatase:rutile (80:20) were obtained from Degussa-Evonik (TiO_2-D). The manufacturers' specifications by transmission electronic microscopy (TEM) indicated the average primary particle size of both types of NP as 25nm. They were obtained as white powders and suspended in either deionized water or complete cell culture medium at a final concentration of 150µg/ml. Before their physicochemical characterization and each toxicity test, the NP suspension was dispersed by probe ultra-sonication (Branson Sonifier, USA) at 30W for 5min (1.5min on and 1min off twice, and 2min on) in a plastic test tube surrounded by ice.

Average hydrodynamic size, size distribution and zeta potential of the TiO_2-NP in deionized water and cell culture medium were determined using dynamic light scattering (DLS) and mixed mode measurement phase analysis light scattering (M3-PALS) in a Zetasizer Nano-ZS, Model ZEN3600 equipped with 4.0mW, 633nm laser (Malvern instruments Ltd.).

3.2.2. *Cell culture and treatments*

Human neuroblastoma SH-SY5Y cell line was purchased from the European Collection of Cell Cultures. Cells were cultured in nutrient mixture EMEM/F12 (1:1) medium supplemented with 10% heat-inactivated foetal bovine serum (FBS), 1% antibiotic and antimycotic solution, with 1% non-essential amino acids. All ingredients were obtained from Invitrogen. Cells were incubated in a humidified atmosphere with 5% CO_2 and 37^{o}C.

Particle exposure experiments were performed using flat bottom 96-well plates. Cells were seeded in the plates at 2-5x10^4 cells/well, and allowed to adhere at 37ºC for 24h. Upon reaching near confluency, cell culture medium was removed and cells were exposed to fresh culture medium containing different concentrations of TiO_2-NP, a positive control and a negative control for each experiment. Complete medium was used as negative control in all cases, whereas camptothecin (Campt, 10µM), mitomycin-C (MMC, 1.5µM), bleomycin (BLM, 1µg/ml), diethyl maleate (DEM, 2µl/ml) or H_2O_2 (2µM for 3h treatments, and 1µM for 6h treatments) were used as positive controls in cytotoxicity, genotoxicity or oxidative damage assays.

3.2.3. *Cellular viability*

Cell viability was assessed by means of 3-(4,5-dimethyldiazol-2-yl)-25diphenyl-tetrazolium bromide (MTT) assay, based on the mitochondrial conversion of MTT, following the protocol of Mosmann,(1983). Briefly, cells were seeded in 96-well plates. After 24h, cell culture medium was removed and cells were exposed to 100µl of TiO_2-NP at a total of seven concentrations (20–150µg/ml) and three exposure times (3, 6 and 24h) in cell culture medium. Then the supernatant was removed and cells were incubated with 100µl fresh medium and 10µl MTT solution (5mg/ml) for 3h at 37°C. The formazan (dark purple) was then solubilized with 200µl of dimethylsulfoxide (DMSO), and the absorbance was measured at 595nm using a Cambrex ELx808 microplate reader equipped with a kinetic analysis software (Biotek, KC4). The untreated sets and positive controls were also run in parallel under identical conditions.

Neutral red uptake (NRU) assay was carried out following the protocol described by Borenfreund and Puerner,(1985) to determine cell viability. Cells were seeded in 96 well plates and are allowed to adhere for 24h. Next, the medium was aspirated and cells were incubated at 37ºC with seven concentrations of TiO_2-NP range in the range 20-150µg/ml for three exposure

times (3, 6 and 24h) in cell culture medium. After the incubation medium was aspirated, cells were washed twice with phosphate buffer solution (PBS); then they were incubated for 3h in culture medium supplemented with neutral red (50µg/ml). Cells were subjected to further incubation for 20min at 37ºC in a mixture of acetic acid (1%), ethanol (50%) and water (49%) to extract the dye, and the absorbance at 540nm was measured using a Cambrex ELx808 microplate reader equipped with a kinetic analysis software (Biotek, KC4). The untreated sets and positive controls were also run parallel under identical conditions.

The percentage of cellular viability proportional to mitochondrial function and uptake of neutral red were calculated relative to untreated cells. The possible interference of TiO_2-NP with the dyes used in MTT and NRU assays was tested by measuring their reactivity with TiO_2-NP in the absence of cultured cells. There are various ways in which the TiO_2-NP may interfere with the MTT and NRU based cytotoxicity assays. Therefore, the interference test was designed to assess whether TiO_2-NP scatter or absorb light or interfere with the dyes used in those assays. In a 96-well plate either 100µl of cell culture medium or cell culture medium containing TiO_2-NP were added to the wells (without cells) and MTT and NRU experiments were conducted as described above. Data obtained demonstrated no interference between the TiO_2-NP tested and the dyes used for cytotoxicity assessment.

From the results obtained in the viability experiments, two periods of exposure (3 and 6h) and three different concentrations of each TiO_2-NP (80, 120 and 150µg/ml) were selected to perform the following experiments.

3.2.4. *Cellular uptake*

The potential of the TiO_2-NP to enter the cells was evaluated by following the protocol described by Suzuki et al. (2007). Cells were seeded in 96-well cell culture plates. After 24h of seeding, the cells were exposed to TiO_2-NP (80, 120 and 150µg/ml) for 3 and 6h. After exposure, the culture medium containing NP was removed and cells were harvested using 0.025% trypsin. They were then centrifuged at 250xg for 5min. The supernatant was discarded and the pellet was re-suspended in 0.5ml PBS. The amount of NP taken up by the cells was analysed using a FACSCalibur flow cytometer (Becton Dickinson).

In flow cytometry (FCM), the laser beam (488nm) illuminates cells in the sample stream, which go through the sensing area. As mentioned previously in Chapter 1, the laser light scattered at narrow angles to the axis of laser beam is called forward-scatter(ed) (FSC) light. The laser light scattered at about a 90º angle to the axis of the laser beam is called side-scatter(ed) (SSC) light. The analysis was carried out based on the size and the intracellular complexity of the cells by measuring the FSC and the SSC, respectively. Data were acquired from a minimum of 10^4events per sample using Cell Quest Pro software (Becton Dickinson).

3.2.5. *Cell cycle*

In order to examine the cell distribution along the different phases of the cell cycle, the relative cellular DNA content was evaluated by means of FCM as previously described Valdiglesias et al. (2011a). Specifically, after treatments with each TiO_2-NP or positive control (MMC, final concentration 1.5μM), cells were trypsinized and suspended in PBS. Then cells were centrifuged, washed with PBS and fixed with cold (-20^{o}C) 70% (V/V) ethanol. Then, fixed cells were stored overnight at 4^{o}C. Next, for analysis, cells were centrifuged, and re-suspended in PBS containing 0.1mg/ml RNase A and 50mg/ml propidium iodide (PI) and incubated at 37^{o}C in the dark for 30min.

Samples were kept in ice prior to analysis. The analysis was performed using a FACSCalibur flow cytometer (Becton Dickinson). A minimum of 10^4 events were acquired, and the DNA content was assessed from the PI signal detected by the FL2 detector. In order to obtain information on the percentage of cells at G_0/G_1, S and G_2/M regions, cell cycle histograms were evaluated using Cell Quest Pro software (Becton Dickinson).

3.2.6. *Apoptosis*

3.2.6.1. *Annexin V-FITC/PI staining*

Annexin V-fluorescein isothiocyanate (FITC)/PI double staining was carried out with BD Pharmingen™ Annexin V-FITC apoptosis detection kit I (Becton Dickinson), following the manufacturer's protocol using FCM. Contents of the kit are as follows: (i) annexin V-FITC conjugate: 50μg/ml in 50mM Tris-HCl, pH 7.5, containing 100mM NaCl; (ii) PI solution: 100μg/ml in 10mM potassium phosphate buffer, pH 7.4, containing 150mM NaCl; (iii) 10X binding buffer: 100mM HEPES/NaOH, pH 7.5, containing 1.4M NaCl.

After treatments with TiO_2-NP or Campt 10μM as positive control, cells were harvested with 0.025% trypsin, suspended in PBS and centrifuged at 300xg for 5min at room temperature. After centrifugation, supernatant was removed and pellet was re-suspended in 200μl of 1X binding buffer, and 5μl of annexin V-FITC and 5μl of PI were added to each sample; then the samples were incubated at room temperature in the dark for 15min. Analysis was done immediately using a FASCalibur flow cytometer (Becton Dickinson). Events for annexin V-FITC were recorded from FL1, and events for PI were taken from FL2. Data were acquired from a minimum of 10^4 events per sample using Cell Quest Pro software (Becton Dickinson). Early apoptosis was expressed as percentage of annexin V+/PI– cells.

3.2.6.2. *Mitochondrial membrane potential analysis*

Mitochondrial membrane potential (MMP) was detected with the fluorescent probe 5,5′,6,6′-tetrachloro-1,1′,3,3′-tetraethylbenzimidazolcarbocyanine iodide (JC-1; Molecular probes). using FCM following the protocol described by Sharma et al. (2012). JC-1 exists predominantly in green fluorescent monomeric form in cells with depolarized mitochondria and in reddish orange aggregate form in cells with polarized mitochondria.

Cells exposed to TiO_2-NP or Campt 10µg/ml as positive control, were harvested with 0.025% trypsin and centrifuged at 300xg for 5min at room temperature. Supernatant was discarded, and the pellet was re-suspended in cold PBS and centrifuged again at 300xg for 5min. Cells were incubated with 10µM JC-1 dye for 15min at 37ºC, washed with PBS and re-suspended in 500µl PBS. Lastly, a minimum of 10^4 events were acquired with a FACSCalibur flow cytometer (Becton Dickinson), fluorescence exhibited from JC-1 monomers was measured in the FL1 channel, and from JC-1 aggregates was measured in the FL2 channel; data were analysed using Cell Quest Pro software (Becton Dickinson).

3.2.7. *Genotoxicity*

3.2.7.1. *Micronucleus evaluation by flow cytometry*

Micronucleus (MN) frequency was evaluated by FCM following the protocols reported by Nüsse et al. (1994); Roman et al. (1998) with some modifications (Valdiglesias et al., 2011b). After the predetermined exposure of cells to each type of TiO_2-NP and positive control MMC (1.5µM), cell culture medium was removed and cells were cultured for an additional period of 24h in fresh medium. Then, cells were trypsinized at 0.025% and suspended in PBS. After centrifugation, the supernatant was removed and 0.25ml cold solution (4ºC) containing NaCl (10mM), trisodium citrate (1g/l), and nonidet P40 (0.3mg/l) was added to each tube alongside 5µl of 50mg/ml PI and 1.25µl of 0.1mg/ml RNase A. After the incubation of samples in the dark at room temperature for 15 min, a second solution consisting of citric acid (1.5mg/l) and sucrose (0.25M) was added and incubated for 30min. The final suspension of nuclei and MN was analysed with a FACSCalibur flow cytometer (Becton Dickinson). PI-associated fluorescence emission was collected in the FL2 channel. The incidence of FCM-scored MN was expressed as frequency percent and was based on the acquisition of at least $5x10^4$ events.

3.2.7.2. *γH2AX assay*

The evaluation of H2AX histone phosphorylation was performed following the general protocol proposed by Tanaka et al. (2009). After the exposure to each type of TiO_2-NP and

positive control (Campt 10µM), cells were trypsinized at 0.025% and suspended in PBS. After centrifugation and removal of supernatant, cells were incubated with 1% *p*-formaldehyde for 15min at 4ºC. Then, the samples were centrifuged and the supernatant was removed. Next, samples were incubated overnight at 4ºC with 1ml of cold (-20ºC) ethanol 70%. The following day, samples were washed with PBS and 100µl anti-γH2AX antibody labelled with Alexa Fluor® 488 [1:20, 1% bovine serum albumin (BSA) in PBS] was added and incubated for 15min at room temperature. Next, samples were washed in PBS, supernatant was removed, and 500µl PBS containing PI (40µg/ml) and RNase A (0.1mg/ml) were added and incubated for 30min at room temperature. Finally, a minimum of 10^4 events were acquired with a FACSCalibur flow cytometer (Becton Dickinson). Data obtained from Alexa Fluor 488 (FL1) and PI (FL2) were analyzed using Cell Quest Pro software (Becton Dickinson).

3.2.7.3. *Comet assay*

After treatments with both TiO_2-NP and the positive control (BLM 1µg/ml) the alkaline comet assay was performed following the general protocol proposed by Singh et al. (1988). Briefly, after collecting cells by trypsinization at 0.025%, they were suspended in 100µl of 0.7% low-melting-point agarose (LMA) in PBS (pH 7.4). Then cells were dropped as two drops onto a slide that was previously pre-coated with a 1% layer of normal melting point agarose (NMA), and covered with coverslips. Slides were placed on ice for 4 min and, after the second layer of agarose solidified, coverslips were removed and slides were immersed in freshly prepared lysis solution (2.5M NaCl, 100mM Na_2EDTA, 10mM Tris-HCl, 250mM NaOH, pH 10, and 1% triton X-100 added just before use) for 1h at 4°C in the dark.

After the lysis step, slides were placed on a horizontal electrophoresis tank (420x300x90mm) in an ice bath. Then, the tank was filled with freshly made alkaline electrophoresis solution (1mM Na_2EDTA, 300mM NaOH, pH 13) and left in the dark for 20min to allow DNA unwinding. Later, electrophoresis was carried out for 20min at 30V and 300mA (0.83V/cm). Slides were then washed three times for 5min with neutralizing solution (0.4M Tris–HCl, pH 7.5). Following neutralization, slides were left to air-dry in the dark, and stained with 60µl of 4,6-diamidino-2-fenilindol (DAPI), The preparations were kept in a humidified sealed box to prevent drying of the gel and analysed within 48h.

Image capture and analysis were performed using the comet IV software (Perceptive Instruments). In all cases, 50 cells were scored from each replicate drop (i.e. 100 cells in total), and percentage of DNA in the comet tail (%tDNA) was used as DNA damage parameter.

3.2.8. *Oxidative damage*

3.2.8.1. *Oxidative DNA damage*

By following the protocol described by Smith et al. (2006), a modified version of the alkaline comet assay was performed in order to evaluate the oxidative DNA damage, specifically the presence of 8-oxoG, by incubating with the human 8-oxoG DNA glycosylase (OGG1) repair enzyme. For each experimental condition, two slides were prepared. After the lysis step, slides were washed with buffer (pH 8) composed of EDTA (0.5mM), BSA (0.2mg/ml), KCl (0.1M) and Hepes (40mM). Then, the slides were separated into two groups and treated with either 50µl of OGG1 (0.0016U/µl buffer) or 50µl of buffer, covered with coverslips and incubated at 37ºC for 10min. After this incubation, coverslips were removed and slides were processed as in the standard alkaline comet assay, described in the precedent section, and 100 cells per condition were scored to determine %tDNA. For each experimental situation, slides incubated with enzyme were compared with slides incubated with just buffer to measure the quantity of oxidative DNA damage.

3.2.8.2. *Glutathione determination*

Determination of reduced (GSH) and oxidized (GSSG) forms of glutathione was based on the glutathione recycling method described before (Shaik and Mehvar, 2006). In this reaction, GSH reacts with 5,5'-dithiobis-(2-nitrobenzoic acid) (DTNB) to form the disulfide GSTNB and the yellow-coloured compound 5-thio-2-nitrobenzoic acid (TNB). The disulfide product (GSTNB) is then reduced by glutathione reductase (GR) in the presence of NADPH, recycling GSH back into the reaction. The rate of formation of TNB, measured at 405 nm, is proportional to the concentration of GSH in the sample. This method also quantitates GSSG because GSSG is reduced by GR, present in the reaction mixture, to two molecules of GSH. The method was used for determination of total (GSH plus GSSG) and oxidized (GSSG) glutathione by subjecting to the recycling reaction the samples either untreated or treated with the thiol masking agent 1-methyl-2-vinyl-pyridinium (M2VP, which completely masks GSH), respectively.

After treatment with TiO_2-NP or the positive control (DEM 2µl/ml, suspended in medium), cells were scraped and homogenized in ice-cold 5% sulfosalicylic acid (SSA). Resulting supernatant after centrifugation (8000xg for 5min) was separated and stored at -20ºC for further analysis. For determination of total glutathione, the supernatant was consecutively diluted using SSA 5% (1:2), sodium carbonate 400mM (1:4) and sodium phosphate-EDTA (100mM Na_3PO_4; 1mM EDTA) buffer (1:32) before analysis. For GSSG measurement, samples were treated with M2VP (0.3mM) and further diluted (1:4) in sodium carbonate (400mM).

Standards (0.5-5ng/µl as GSH equivalent) were prepared daily by diluting a GSH stock solution (10ng/µl) in 200mM sodium carbonate-2.5% SSA buffer. Standards and diluted supernatants (20µl), prepared as described above, were transferred to a 96-well microplate. Subsequently, 170µl of the recycling reagent [NADPH 0.40mM and GR 1.9U/ml in a sodium phosphate-EDTA buffer (100mM Na_3PO_4; 1mM EDTA)] were added. After 10min of incubation, 10µl of DTNB (4.5mM) were added and colour development was immediately recorded at 405nm for 20min (readings were carried out every two minutes) using a Cambrex ELx808 microplate reader equipped with kinetic analysis software (Biotek, KC4).

The rate of TNB formation, which is proportional to the concentrations of GSH or GSSG in the sample, was determined by linear regression analysis of the change in absorbance of the sample at 405nm versus time (ΔA/min). The ΔA/min values for individual standards were then plotted against the standard concentrations, and the parameters of the standard curve were determined using linear regression analysis. Total and reduced glutathione concentrations were determined from their respective standard curves following linear regression analysis and then normalized to total protein. The GSH:GSSG ratio was calculated by dividing the difference between the total glutathione and GSSG concentrations by the concentration of GSSG.

For protein determination, 5µl of sample pellet diluted in NaOH 0.05N was added to 250µl of Bradford reagent and absorbance was read at 595nm after 5min of incubation. Protein concentration was determined using a BSA standard curve (0.125-1.0mg/ml).

3.2.9. *Statistical analysis*

A minimum of three independent experiments were performed for each experimental condition tested, always in duplicate and under blind conditions. Statistical analyses were carried out by using SPSS for Windows statistical package (version 21.0). Experimental data were expressed as mean ± standard error. Distribution of the response variables departed significantly from normality (Kolmogorov–Smirnov goodness of fit test) and therefore non-parametric tests were considered adequate for the statistical analysis of these data. Differences between groups were tested with Kruskal–Wallis test and Mann–Whitney *U*-test. The associations between two variables were analysed by Spearman´s correlation. *P* value lower than 0.05 was considered significant in all cases.

3.3. RESULTS AND DISCUSSION

Titanium dioxide nanoparticles (TiO_2-NP) are one of the most frequently used NP in industrial applications, ranging from paints to ceramics and from food to cosmetics. Therefore, investigation of risks associated with occupational exposure to TiO_2-NP is of vital interest. The International Agency for Research on Cancer (IARC) has classified TiO_2 as possibly

carcinogenic to humans (group 2B), based on sufficient evidence in experimental animals and inadequate evidence from epidemiological studies (IARC, 2010). Besides, even though the accumulation of two crystalline phases of TiO_2-NP (80nm rutile, and 155nm anatase; purity >99%) in female mice brain after intranasal instillation was reported Wang et al. (2008), the neurotoxic potential of these NP has only recently been examined.

Despite studies regarding neurotoxicity of TiO_2-NP are very limited, these NP were already shown to induce important neurotoxic effects at the cell and tissue levels in *in vitro* studies with cultured human and rodent cells (Huerta-García et al., 2014; Lai et al., 2008; Long et al., 2006; Márquez-Ramírez et al., 2012; Wu et al., 2010; Xue et al., 2012), as well as in *in vivo* studies (Mohammadipour et al., 2014; Shrivastava et al., 2014; Zhang et al., 2011). Furthermore, several neurophysiological symptoms, including passive behaviour, loss of appetite, tremor, and lethargy have been described in mice after TiO_2-NP administration (Chen et al., 2009). However, to our knowledge, this was the first study dealing with the potential toxic effects of TiO_2-NP on human neuronal cells, and also the first one in evaluating the toxicity of these NP at genetic level in any neuronal system.

TiO_2-NP were selected to perform this study because of two main reasons: (i) exposure to these NP by different routes, mainly dermal and inhalatory, is very frequent and extremely easy since they are highly employed as nanomaterials in common consumer products; and (ii) the techniques used for their synthesis have recently matured to the stage that we can produce differently sized and shaped NP on demand, so evaluation of their toxicological properties is imperative. Moreover, two different types of TiO_2-NP were chosen to carry out the toxicity testing in order to determine the influence of crystalline structure on the cellular effects of these NP.

The SH-SY5Y neuroblastoma cell line was selected as neurotoxicological cell model since they are human derived and express a number of human-specific proteins and protein isoforms that would not be inherently present in rodent primary cultures, which has afforded them numerous benefits in the field of neuroscience research and neurotoxicological studies (Kovalevich and Langford, 2013). Both, undifferentiated and differentiated SH-SY5Y neuroblastoma cells have been previously utilized for *in vitro* experiments requiring neuronal-like cells (Asci et al., 2013; Coccini et al., 2014; Li et al., 2014; Maddirala et al., 2015; Martins et al., 2013; Olivieri et al., 2001).

3.3.1. *Nanoparticle characterization*

Physicochemical characterization of NP is regarded as important for their *in vitro* toxicity. Table 3.1 shows the description and characterization data of the TiO_2-NP used in this study. Information on NP size evaluated by TEM (25nm for both NP) and specific surface area

were both provided by the commercial suppliers while behaviour of TiO_2-NP in water and cell culture medium was evaluated by DLS in order to understand the extent of agglomeration and hydrodynamic size of these NP before cellular exposure.

Table 3.1. Characterization of TiO_2-NP.

NP	Crystalline phase	Particle size[a] (nm)	Specific surface area[a] (m^2/g)	Hydrodynamic diameter (nm) (DLS)		Zeta potential (mV) (DLS)	
				Water	Medium	Water	Medium
TiO_2-S	100% anatase	25 (TEM)	200-220	447.9	504.5	-9.96	-10.7
TiO_2-D	80% anatase 20% rutile	25 (TEM)	35-45	160.5	228.3	-27.8	-10.7

TEM: Transmission Electronic Microscopy, DLS: Dynamic Light Scattering

[a] Provided by the commercial supplier

DLS is widely used to determine the size of brownian NP in colloidal suspensions in the nano and submicron ranges (Saquib et al., 2012). The average hydrodynamic particle diameters in medium were slightly higher both for TiO_2-S (504.5nm) and TiO_2-D (228nm) as compared to deionized water (447.9 and 160.5nm, respectively), which indicates relatively higher NP aggregation in medium as compared to water due to limited colloidal stability. The presence of variable sized TiO_2-NP aggregates in cell culture medium corroborates well with earlier reports (Janer et al., 2014; Saquib et al., 2012; Singh et al., 2007).The size distribution graphs obtained by DLS showed a good dispersion of both NP in water and in medium (Figure 3.3).

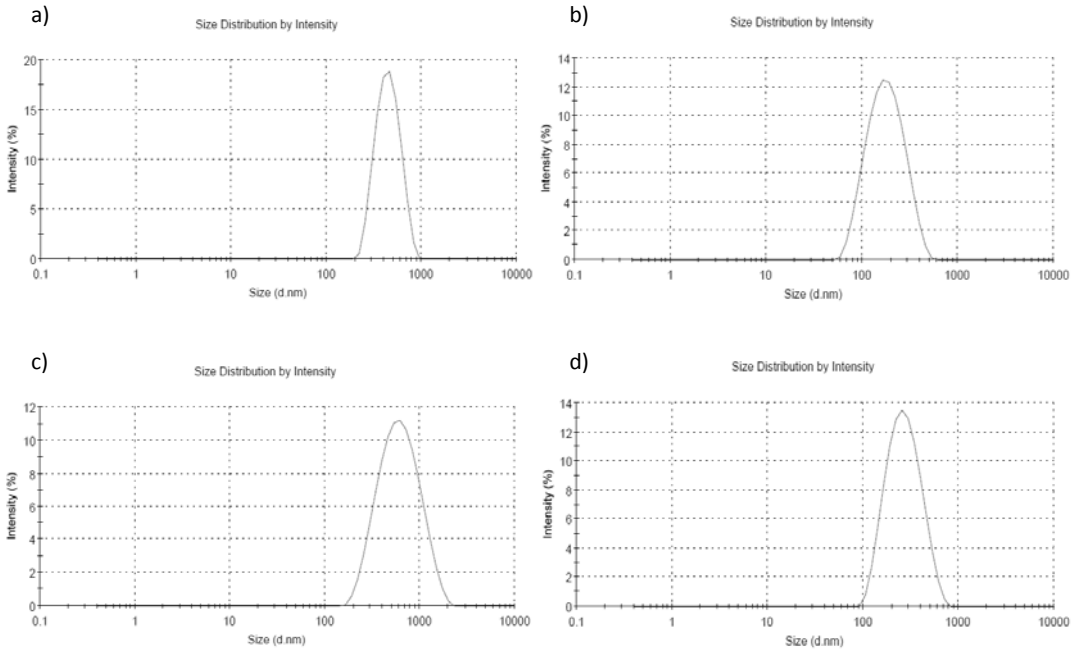

Figure 3.3. Size distribution of TiO_2-S (a) and TiO_2-D (b) in water, and TiO_2-S (c) and TiO_2-D (d) in cell culture medium.

Despite having small differences in the water suspension, zeta potential obtained was the same (-10.7mV) for both TiO_2-NP suspended in medium. Since zeta potential measured was lower than the generally accepted approximate threshold for stability (+/-30mV), TiO_2-NP used would be expected to have tendency to agglomerate over time due to instability in aqueous medium. Yet, those findings are in line with other studies in literature; Shukla et al. (2011) reported zeta potential of TiO_2-NP in anatase structure as -11.5mV in DMEM supplemented with 10% FBS, and Long et al. (2006) also found TiO_2-D zeta potential as -11.6mV in the same medium.

3.3.2. *Cellular viability*

The behaviour of nanomaterials when in contact with cells is an important factor for evaluation of their biocompatibility. Cell adhesion, spreading, and growth on substrates are the first sequential reactions when coming into contact with a material surface, which is extremely important for cell survival. It is well documented that, due to their unique physical and chemical properties, insoluble NP might cause problems in the *in vitro* assay systems; cells adhering to the bottom of a culture plate may not be exposed to the majority of NP in suspension or these might interfere with the dyes used in this assays (Guadagnini et al., 2013; Kansara et al., 2014). Based on this fact, before performing cellular viability assays, potential interference of NP with MTT and NRU assays was excluded by a parallel set of experiments conducted without cells. These assays are based on two different mechanisms; MTT represents mitochondrial activity whereas NRU provides information on lysosomal activity of the cells.

A wide dose range (eight concentrations between 20 and 150µg/ml) and three incubation times (3, 6, and 24h) were tested for the viability assays. As it can be seen in Figure 3.4, MTT and NRU results showed that TiO_2-NP, regardless of the NP crystalline structure, did not impair the viability of SH-SY5Y cells at any treatment time. These results were in line with the microscopic evaluation of the cells (phase contrast), since morphological alterations were not observed in any case (data not shown).

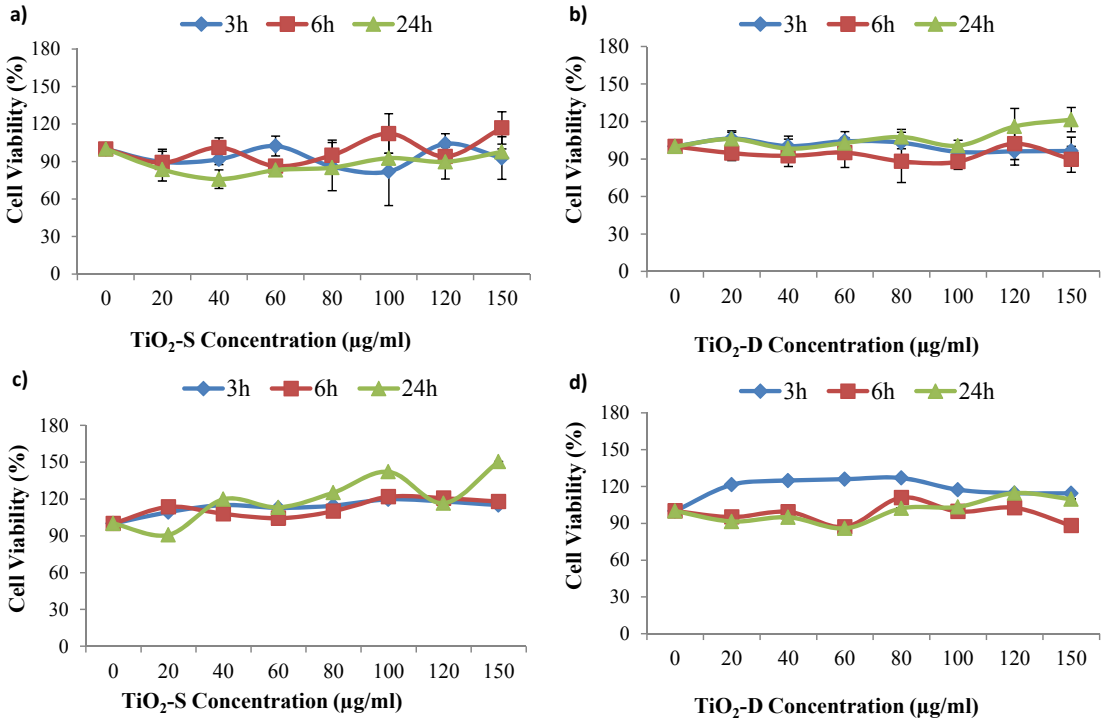

Figure 3.4. MTT assay (a-b) and NRU assay (c-d) results on neuronal cells treated with TiO_2-S or TiO_2-D. The relative cell viability in the exposed cells was expressed as a percentage relative to the untreated control cells.

Since it was observed that TiO_2-NP cause no significant decrease in viability at concentrations ranging from 20 to 150µg/ml after 3, 6 and 24h of exposure in SH-SY5Y cells, three different concentrations (80, 120 and 150µg/ml) and two time points (3 and 6h) were selected to carry out all subsequent assays.

3.3.3. *Uptake*

To quantify the amount of TiO_2-NP taken up by cells, the SSC parameter was measured by FCM. Results obtained are shown in Fig. 3.5. Uptake of both types of TiO_2-NP by human neuronal cells increased with time of treatment, regardless of the crystalline structure.

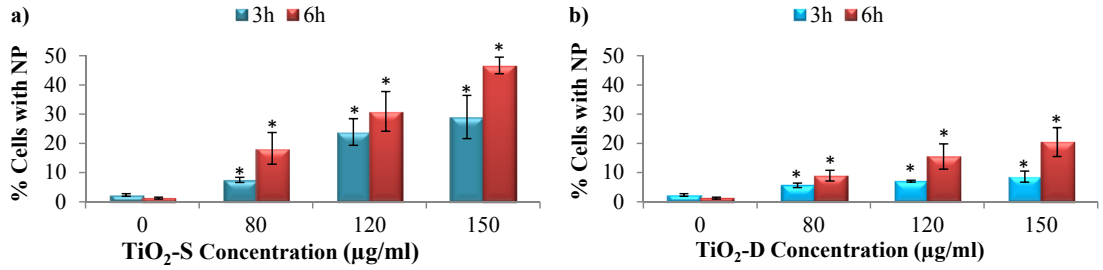

Figure 3.5. Flow cytometry analysis of TiO_2-S (a) or TiO_2-D (b) uptake by SH-SY5Y cells. *P<0.05, significant difference with regard to the corresponding negative control.

The uptake followed a concentration-dependent pattern after 3h (r=0.873, $P<0.01$ for TiO_2-S; r=0.703, $P<0.01$ for TiO_2-D) and 6h exposure (r=0.897, $P<0.01$ for TiO_2-S and r=0.825, $P<0.01$ for TiO_2-D), and was always higher for TiO_2-S than for TiO_2-D.

These results are supported by previous studies that used the same kind of NP in different human cell lines. For instance, the uptake of different crystal structures of TiO_2-NP was observed using Caco-2 human intestinal cells by Gitrowski et al. (2014); Caco-2 monolayers exhibited time-dependent uptake of TiO_2-NP in anatase, anatase:rutile, and rutile forms, with the nano rutile form being taken up the least. Similar results were also obtained in human epidermal cells (Shukla et al., 2011), human bronchial epithelial cells (Janer et al., 2014; Tedja et al., 2012), human osteoblast cells (Niska et al., 2015), and human epithelial cells from amnion (Saquib et al., 2012).

3.3.4. *Cell cycle*

The relative cellular DNA content in cells treated with TiO_2-NP was examined by FCM in order to determine the cell distribution in the different phases of the cell cycle (G_0/G_1, S, and G_2/M). Figure 3.6 exhibits the effect of TiO_2-NP on cell cycle progression. Results obtained showed that TiO_2-S exposure altered cell cycle of neuronal cells, especially after 6h exposure when an arrest in S-phase was observed (Figure 3.6 a and b).

Under these conditions, positive dose-response for S-phase (r=0.436, $P<0.05$) and inverse dose-response for G_2/M-phase (r=-0.617, $P<0.01$) were observed. Slighter effects were induced by TiO_2-D, according to their lower cellular uptake (Figure 3.6 c and d). They were not found to alter the SH-SY5Y cell cycle after 3h exposure, although concentration-dependent cell cycle alterations were found after 6h treatment; effects on G_0/G_1 (r=0.522, $P<0.01$) and G_2/M (r=-0.420, $P<0.05$) phases were also observed in this case.

These findings agree with some previous studies in other different cells in which anatase TiO_2-NP were more potent than rutile TiO_2-NP in activating apoptosis and cell cycle checkpoint proteins (Lagopati et al., 2014; Wu et al., 2010a), and anatase TiO_2-NP were more biologically active than rutile TiO_2-NP in terms of cytotoxicity (Jin et al., 2010).

Furthermore, these results are consistent with others which have demonstrated the effect of TiO_2-NP on cell cycle in different cell lines and *in vivo*. For instance, TiO_2-NP with mixed crystalline structure resulted in a statistically significant increase in the proportion of human lung fibroblast WI-38 cells in the G_2/M phase, and a significant decrease in the proportion of cells in the G_0/G_1 phase (Periasamy et al., 2014). Also, Medina-Reyes et al. (2015) found that TiO_2-NP exposure induces higher percentage of lung epithelial A549 cells in the G_2/M phase.

Likewise, the same cells treated with TiO_2-NP showed arrest in G_2/M phase, suggesting DNA damage and consequent activation of DNA repair processes (Wang et al., 2014b).

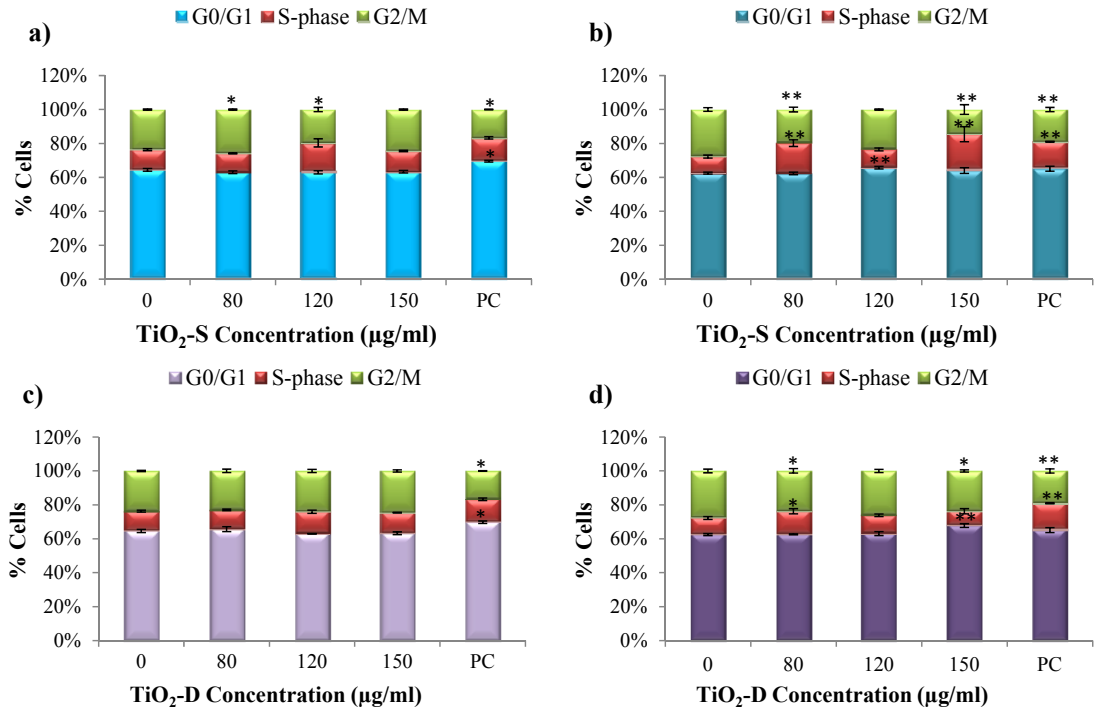

Figure 3.6. Cell-cycle analysis after treatment of SH-SY5Y cells with TiO_2-S (a, b) or TiO_2-D (c, d) for 3h (a, c) or 6h (b, d). PC: positive control. **P*<0.05, ***P*<0.01, significant difference with regard to the negative control.

Most research about the effect of TiO_2-NP on cell cycle has focused on their pulmonary impact via inhalation or skin damage after dermal exposure. However analyses on neuronal cells after TiO_2-NP exposure are quite scarce. There is only one another study with neuronal cells present in the literature in which it was demonstrated that both crystalline forms were able to arrest the cell cycle in G_2/M phase of rat neuronal PC12 cells (Wu et al., 2010a).

3.3.5. *Apoptosis*

To assess the extent and mode of cell death, the rate of early apoptotic cells was evaluated by means of FCM analysis of annexin/PI staining, based on analysis of the percentage of cells stained with annexin V but not with PI (early apoptotic cells). Experimental results indicate a dose-dependent increase in the apoptosis rate after treatment with both types of TiO_2-NP at the two times tested (r=0.790, *P*<0.01 and r=0.398, *P*<0.01 for TiO_2-S 3 and 6h, respectively; r=0.449, *P*<0.01 for TiO_2-D 3h) (Table 3.2).

Dose-dependent apoptosis induced by TiO_2-NP was previously demonstrated in other different cell types: human endothelial cells (Hou et al., 2014), human erythrocytes and lymphocytes (Ghosh et al., 2013), human liver HepG2 cells (Shukla et al., 2011), human neural

U87 astrocytoma cells (Lai et al., 2008), murine C6 and human U373 glial cells (Márquez-Ramírez et al., 2012), and rodent neuronal P12 cells (Liu et al., 2010; Wu et al., 2010a).

Table 3.2. Apoptotic cell rates (%) after TiO_2-NP exposure.

		3h		6h	
		Annexin-V	MMP	Annexin-V	MMP
Control		4.71±0.27	4.93±0.33	6.94±0.34	5.03±0.52
TiO_2-S	80µg/ml	6.67±0.40**	5.87±0.45	8.03±0.57	7.26±0.64*
	120µg/ml	7.13±0.32**	6.07±0.25*	8.60±0.24**	11.93±0.73**
	150µg/ml	8.74±0.40**	7.87±0.47**	8.62±0.35**	10.01±0.84**
TiO_2-D	80µg/ml	7.57±0.20**	9.92±0.79**	9.30±0.47**	11.88±0.60**
	120µg/ml	7.67±0.22**	13.75±0.39**	8.92±0.43**	15.16±0.71**
	150µg/ml	7.03±0.14**	17.11±1.31**	8.90±0.56*	12.91±0.86**
PC		8.28±0.14**	6.69±1.09	10.27±0.41**	9.07±0.70**

We further analysed the crucial step of apoptosis by intrinsic pathway, i.e., mitochondrial membrane depolarization, in TiO_2-NP treated cells by means of comparing differences in fluorescence intensity of JC-1 fluorescent staining. JC-1 dye exhibits potential-dependent accumulation in mitochondria, indicated by a fluorescence emission shift from green (~529nm, measured in the FL1 channel) to red (~590nm, measured in FL2 channel). In healthy cells fluorescence is seen in both FL1 and FL2 channels of the FCM. Since JC-1 does not accumulate in mitochondria with depolarized membrane and remains in the cytoplasm as monomers, these monomers do not have the red spectral shift, and therefore have low fluorescence in the FL2 channel. On the other hand, in mitochondria undergoing a transition from polarized to depolarized membrane (due to apoptosis or other physiological events), JC-1 leaks out of the mitochondria into the cytoplasm as monomers resulting in a decrease of red fluorescence, measured by FL2 channel.

We found a dose-dependent collapse of MMP following treatment with both types of TiO_2-NP, at the two times tested (Table 3.2) ($r=0.754$, $P<0.01$ and $r=0.727$, $P<0.01$ for TiO_2-S 3 and 6h, respectively; $r=0.959$, $P<0.01$ and $r=0.619$, $P<0.01$ for TiO_2-D 3 and 6h, respectively). Furthermore, these losses observed in MMP suggest that these NP induce apoptotic death by intrinsic (mitochondrial) pathway. Accordingly, other authors recorded apoptosis induction by TiO_2-NP through mitochondrial pathway in neuronal rat PC12 cells (Wu et al., 2010a), human skin HaCat cells (Xue et al., 2010), rat C6 and human U373 glial cells (Huerta-García et al., 2014), human lung fibroblast WI-38 cells (Periasamy et al., 2014, 2015), murine macrophage RAW264.7 cells and human bronchial epithelial BEAS-2B cells (Xiong et al., 2013). Besides,

alterations in the expression pattern of genes related to cell death and cell cycle were found in rodent neuronal cells exposed to TiO_2-NP (Long et al., 2007). Specifically, TiO_2-D exposure induced up-regulation of inflammatory, apoptotic and cell cycling pathways and down-regulation of energy metabolism in mouse BV2 microglia cells.

Data obtained from apoptosis assessment contrast with the absence of decrease in cell viability observed. Nevertheless, the significant differences observed in the percentage of apoptotic cells in the NP exposed cells with regard to the controls were over 2% (12% maximum). Thus it is probable that these low magnitude differences, observed by FCM due to the high sensitivity of the technique, and could not be detected by MTT and NRU spectrophotometrical assays.

3.3.6. *Genotoxicity*

Due to the size of NP, the probability of their internalization into the cells and interaction with cellular organelles and macromolecules (DNA, RNA, and proteins) is very high. These interactions can be the origin of damage in the genetic material, so genotoxicity data are important for nanotechnology regulation and risk assessment. As Petković et al. (2011) suggested that the different genotoxicity responses of TiO_2-NP could depend not only on size but also on their crystalline structure, in this study the potential genotoxic effects of two different TiO_2-NP (pure anatase and 20% rutile) were evaluated by means of three different genotoxicity tests, namely MN test, γH2AX assay and comet assay. In general, results regarding genotoxicity obtained from both types of NP were quite similar to each other.

MN test measures damage to the chromosomes and mitotic apparatus of cells. Thus, an increase in the frequency of micronucleated cells is an indication of induced chromosome damage (Chen et al., 2014a). Here we evaluated MN formation by means of FCM. No increase in MN formation was observed after 3h treatments, but dose-dependent MN induction was detected after 6h exposure to both types of TiO_2-NP ($r=0.662$, $P<0.01$ for TiO_2-S and $r=0.684$, $P<0.01$ for TiO_2-D) (Figure 3.7).

These positive results of MN assay show the ability of TiO_2-NP to produce structural and/or numerical chromosome damage, and agree with those studies reporting positive induction of MN in Chinese hamster ovary (CHO-K1) cells by using 80% anatase-20% rutile TiO_2-NP (Di Virgilio et al., 2010), in human lymphocytes by using pure anatase and 86% anatase-14% rutile TiO_2-NP (Tavares et al., 2014), in human epidermal A431 lung cancer A549 and liver carcinoma HepG2 cells treated with 99.7% pure anatase TiO_2-NP (Shukla et al., 2011, 2013; Srivastava et al., 2011, 2013), in human bronchial epithelium BEAS-2B and HepG2 cells exposed to anatase:rutile (86:14) TiO_2-NP (Prasad et al., 2014), and in human embryonic kidney

HEK293 cells and mouse embryonic fibroblast NIH/3T3 cells by treatment with anatase TiO_2-NP (Demir et al., 2015).

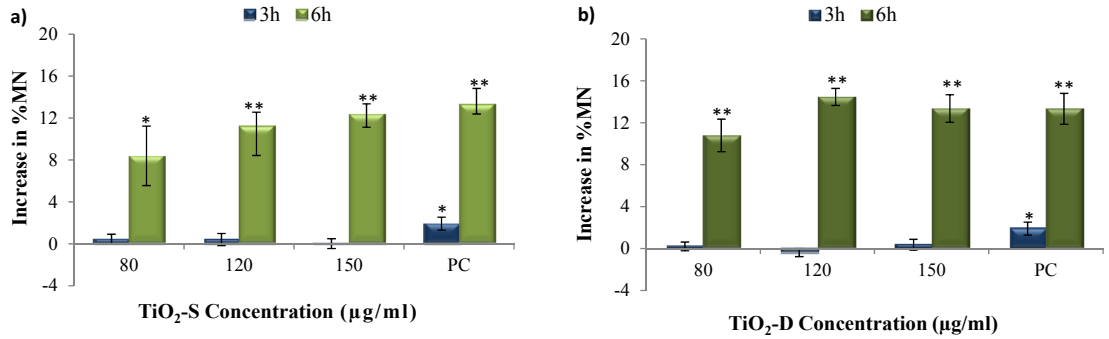

Figure 3.7.Genotoxicity in neuronal cells treated with TiO_2-S (a) or TiO_2-D (b) by MN evaluation. PC: positive control. **P*<0.05, ***P*<0.01, significant difference with regard to the corresponding negative control.

One of the earliest responses to DNA double strand breaks (DSB) involves phosphorylation of the C-terminal tails of H2AX histones located near the break (Rogakou et al., 1998). The DNA repair machinery will recognize this phosphorylated histone, called γH2AX, and repair will start at that point. On this basis, the level of γH2AX has been used as a precise marker of DSB but is also indicative of replication stress (Tu et al., 2013).

In our study, the effect of TiO_2-NP on γH2AX levels was measured by FCM, using an anti-γH2AX antibody. Results of this assay revealed no increase in H2AX phosphorylation after exposure to both types of TiO_2 under every experimental condition (Figure 3.8).

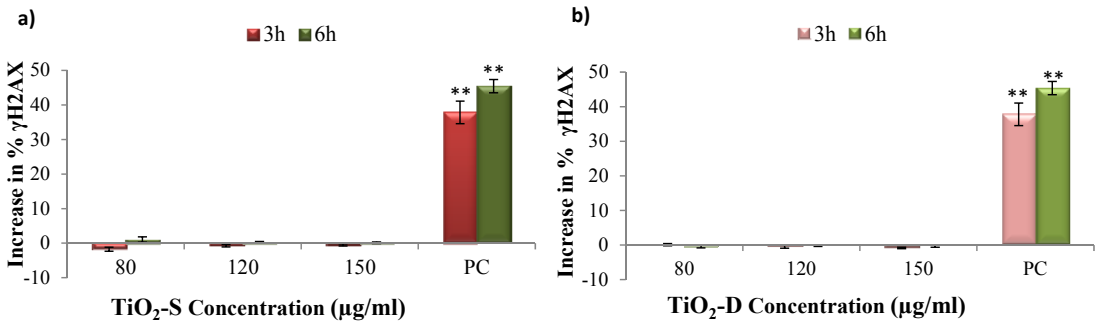

Figure 3.8. Genotoxicity in neuronal cells treated with TiO_2-S (a) or TiO_2-D (b) by γH2AX assay. PC: positive control. ***P*<0.01, significant difference with regard to the corresponding negative control.

These results disagree with a previous study employing γH2AX assay after treating human lung epithelial A549 cells with TiO_2-NP, which found significantly elevated levels of histone phosphorylation (Toyooka et al., 2012; Wan et al., 2012). Moreover, these authors observed that increased γH2AX levels were attenuated by coating the surface of TiO_2-NP with

bovine serum albumin. According to this, the negative results obtained in our study and in the ones previously stated by Jugan et al. (2012) and Wan et al. (2012) in A549 cells, might be in part explained by the use of complete medium, supplemented with FBS, for the NP treatment. Yet there is not enough evidence to prove the effect of FBS on protein corona formation around the TiO_2-NP or the disparate effects of a given protein corona on particle-cell interactions.

TiO_2-NP induced DNA strand breaks and alkali labile sites were assessed through the alkaline version of comet assay, which reveals both DNA single strand breaks (SSB) and DSB. In contrast to γH2AX assay, comet assay results showed that treatment with both types of TiO_2-NP induced a significant increase of DNA damage at both time points (Figure 3.9). This increase was dose-dependent for TiO_2-D (r=0.478, $P<0.01$ at 3h treatment, and r=0.454, $P<0.01$ at 6h treatment).

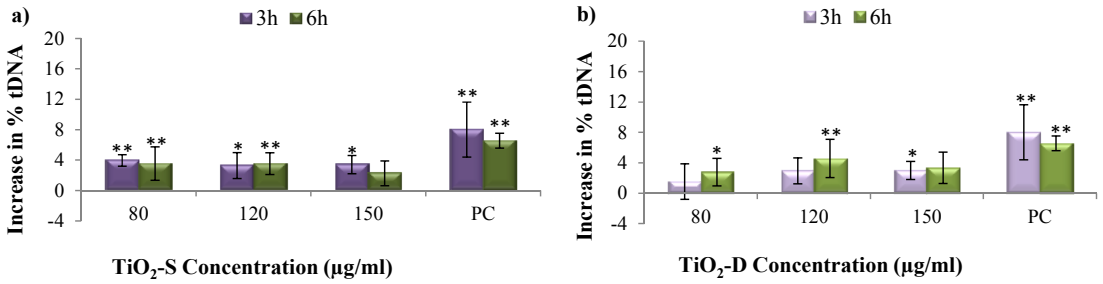

Figure 3.9. Genotoxicity in neuronal cells treated with TiO_2-S (a) or TiO_2–D (b) by comet assay. PC: positive control. *$P<0.05$, **$P<0.01$, significant difference with regard to the corresponding negative control.

To our knowledge, this is the first study assessing DNA strand breaks induced by TiO_2-NP on neuronal cells. Our findings agree with previous studies that showed effect of different types of TiO_2-NP on DNA damage evaluated by comet assay. Few examples can be given as Syrian hamster embryo (SHE) cells treated with anatase and anatase:rutile (80:20) TiO_2-NP (Guichard et al., 2012), Chinese hamster lung fibroblast cells using rutile and anatase:rutile 83:17 TiO_2-NP (Hamzeh and Sunahara, 2013), human embryonic kidney cells (HEK293) and mouse embryonic fibroblasts (NIH/3T3) exposed to pure anatase TiO_2-NP (Demir et al., 2015), human bronchial epithelial BEAS-2B cells and human liver HepG2 cells using anatase:rutile (86:14) TiO_2-NP (Prasad et al., 2013b, 2014), A549 cells treated with pure anatase TiO_2-NP (Wang et al., 2014b), human gastric epithelial AGS cells exposed to anatase:rutile (80:20) TiO_2-NP (Botelho et al., 2014), and mouse NIH/3T3 fibroblasts, human SVK14 keratynocytes and human BJ fibroblasts exposed to TiO_2-NP anatase or rutile, being more efficient the former one (Tomankova et al., 2015).

As mentioned previously, γH2AX assay and comet assay usually provide similar results since both of them evaluate DNA breaks. However, the alkaline version of the comet assay not

only detects DSB, but also SSB, alkaline-labile sites and incomplete excision-repair sites, which are not related to phosphorylation of H2AX. From all the results of genotoxicity assays it seems that TiO_2-NP induce DNA damage on human neuronal cells but different from DSB which, if any, would increase the γH2AX levels. Perhaps this DNA damage induced by TiO_2-NP exposure could not be properly repaired and became fixed as structural chromosomal alterations, detected by the MN test. Still, the involvement of aneugenic processes in the generation of MN by exposure to these NP cannot be ruled out.

3.3.7. *Oxidative damage*

Oxidative stress has been suggested to play an important role in the mechanism of NP toxicity. A number of studies suggest that TiO_2-NP induce toxicity via oxidative stress due to their relatively larger surface area and greater reactive activity than bulk TiO_2 particles (reviewed in Chen et al., 2014). Nonetheless, in this study even the highest TiO_2-NP concentration did not produce DNA oxidative damage, according to OGG-modified comet assay, or decrease in GSH:GSSG ratio after 3 or 6h treatments (Figures 3.10 and 3.11, respectively).

As ROS are known to react with DNA molecules causing damage to both purine and pyrimidine bases as well as to the DNA backbone (Shukla et al., 2011), we investigated the link between oxidative stress and DNA damage in SH-SY5Y cells via the OGG1 modified comet assay. One of the most frequently used repair enzymes for detecting specific types of damage in the comet assay is OGG1, which recognizes specifically the most common marker for DNA oxidation: 8-oxo-7,8-dihydroguanine (8-oxoG), and nicks the DNA at these oxidized sites (Collins, 2009b). The difference in tail intensity between cells treated with this enzyme and those not treated (treated only with the enzyme buffer) gives a measure of the amount of oxidatively damaged DNA.

In the present study, levels of enzyme sensitive sites (8-oxoG) have not changed significantly after treatment with both types of TiO_2-NP as compared to buffer (Figure 3.10). Despite the majority of studies stated positive response results with different types of TiO_2-NP for enzyme-modified comet assay (Magdolenova et al., 2012a; Petković et al., 2011; Sekar et al., 2014; Shukla et al., 2011, 2013, 2014; Ursini et al., 2014), these findings are supported by several other studies in the literature. Recently, Demir et al. (2015) did not observe oxidative DNA damage induction using the OGG1-modified comet assay when human embryonic kidney HEK293 cells and mouse embryonic NIH/3T3 fibroblasts were exposed to TiO_2-NP in pure anatase form. Similarly, oxidative DNA damage was not observed in Caco-2 cells exposed to mixed anatase/rutile TiO_2-NP (Gerloff et al., 2009), or in TK6 cells (Woodruff et al., 2012) and BEAS-2B cells (Vales et al., 2014) treated with pure anatase TiO_2-NP.

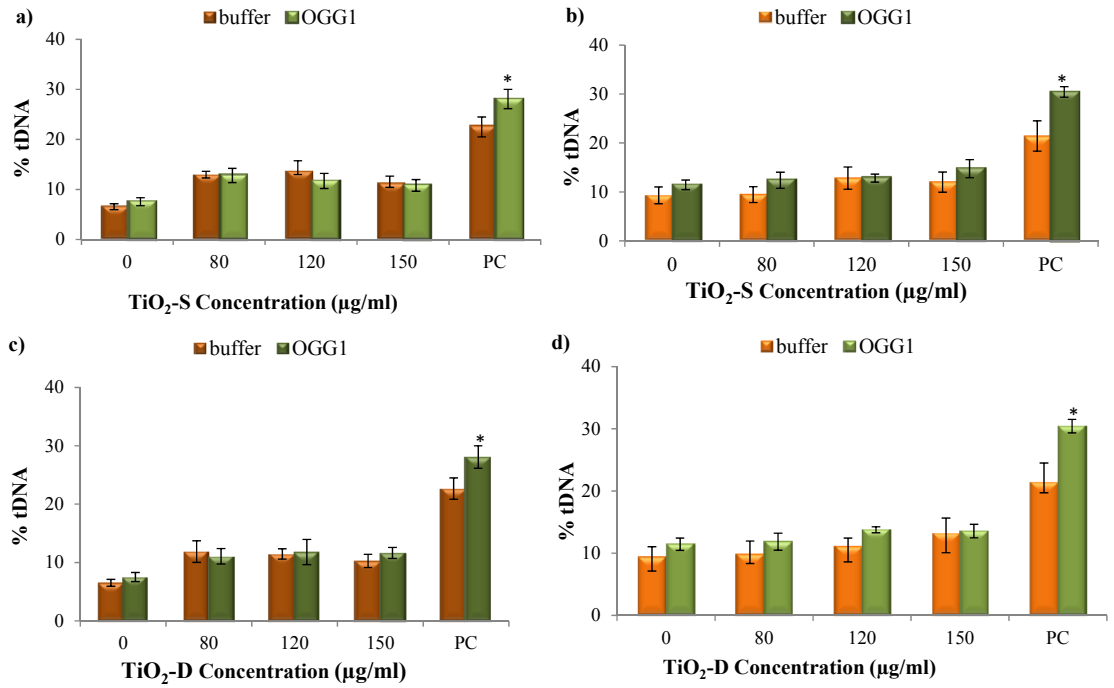

Figure 3.10. Results of OGG1-modified comet assay in neuronal cells treated with TiO_2–S for 3h (a) or for 24h (b), and with TiO_2–D for 3h (c), or for 24h (d). PC: positive control. **P*<0.05, significant difference with regard to the corresponding buffer.

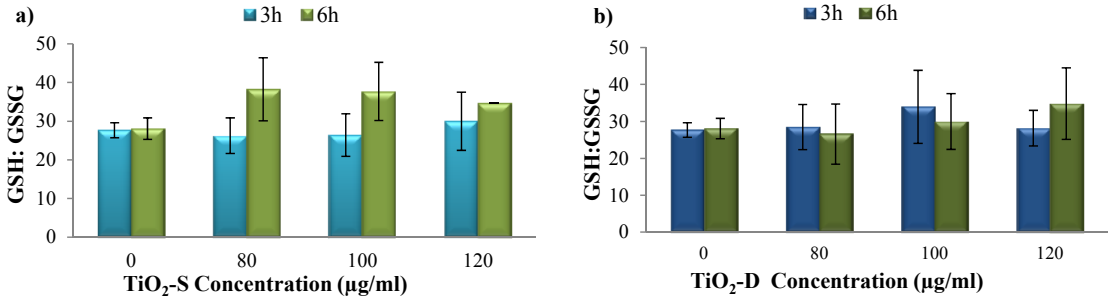

Figure 3.11. Ratio of reduced to oxidised glutathione in neuronal cells treated with TiO_2-S (a) or TiO_2-D (b). PC: positive control.

In this study all comet assay steps after cell lysis were performed as usual in the dark. Although the relevance of the photosensitizing action of TiO_2-NP and their potential to cause inconsistency with this assay are still ongoing discussion, Gerloff et al. (2009) could demonstrate enhanced strand breaks and by using the comet assay after handling of the already lysed slides by normal interior light. Likewise, both Jugan et al. (2012) and Woodruff et al. (2012) reported that if experiments were processed in the dark to avoid any photocatalytic effects of TiO_2-NP, ROS accumulation decreased, suggesting that TiO_2-NP generated ROS in cells via photocatalysis. This reveals the necessity of careful handling when performing the

comet assay to avoid false positive results, especially when photocatalytic compounds such as TiO_2 are used.

The GSH redox cycle is a recycling process that maintains GSH homeostasis during intracellular detoxification of ROS. The intracellular GSH redox status is described by the GSH:GSSG ratio (Kung et al., 2015). A decrease in the ratio of reduced to oxidised glutathione (GSH:GSSG) is indicative of oxidative stress. Figure 3.11 shows the results obtained in the determination of GSH and GSSG in cells exposed to TiO_2-NP; treated neurons expressed levels of GSH:GSSG ratio similar to basal levels.

The GSH redox cycle is present both in the cytosol and in mitochondria. Reports have shown that TiO_2-NP exposure can attenuate antioxidant enzyme activity such as catalase and glutathione reductase, and increase glutathione peroxidase activity and GSSG/total GSH ratio in different cells, such as human lung WI-38 fibroblasts (Periasamy et al., 2014), human hepatocarcinoma cells (El-Said et al., 2014), or human alveolar type-I-like epithelial cells (Sweeney et al., 2014). This fact suggests that TiO_2-NP enhanced ROS generation and blocked cellular antioxidant defences. These reported results are inconsistent with our observations of stable GSH:GSSG ratio in SH-SY5Y cells treated with pure anatase and mixed anatase/rutile which, in turn, were parallel to the observations in OGG1-modified comet assay.

It is generally accepted that most NP induce oxidative stress leading to the generation of free radicals that could disrupt the BBB and cause certain dysfunctions in the brain (Simkó and Mattsson, 2014). Particularly, TiO_2-NP were reported to induce oxidative stress in many cell types including several neural cells such as rat PC12 neuronal cells (Wu et al., 2010a), mouse brain microglia (Long et al., 2006, 2007), human neuronal cells (Nalika and Parvez, 2015), murine C6 glial and human U373 glial cells (Huerta-García et al., 2014), and in *in vivo* studies with mice (Cui et al., 2014; Ma et al., 2010; Shrivastava et al., 2014; Ze et al., 2013). Nevertheless, in this current study TiO_2-NP did not significantly affect the level of GSH:GSSG ratio suggesting that there was no need of antioxidants for detoxifying ROS overproduced by TiO_2-NP. The evidence for the induction of oxidative damage to DNA was not gained either from the measurement of the level of OGG1 sensitive sites. Therefore, the cytotoxic and genotoxic effects observed in this work as produced by TiO_2-NP were induced by mechanisms other than oxidative stress generation. Thus, Gheshlaghi et al. (2008) proposed the interaction with different cellular components as an alternative mechanism for TiO_2-NP toxicity, after observing that these NP disrupted microtubules by inhibiting tubulin polymerization in sheep brain cells.

3.4. CONCLUSIONS

In the present study we investigated the effects of TiO_2-NP with two types of crystalline structure on the human SH-SY5Y neuroblastoma cell line exploring the different mechanisms underlying their cytotoxic and genotoxic potential. From the results obtained in this study we may draw the following conclusions:

1. TiO_2-NP did not reduce the viability of neuronal cells but were effectively internalized by them in a concentration and time-dependent manner.
2. Both crystalline structures induced dose-dependent cell cycle alterations and apoptosis by intrinsic pathway.
3. Genotoxicity assays showed positive results in the comet assay and MN test, but negative results in γH2AX assay. These data indicate that TiO_2-NP induce genotoxicity in neuronal cells not related to the production of DSB.
4. TiO_2-NP did not induce oxidative DNA damage or decrease in the GSH:GSSG ratio, suggesting that their genotoxic effects are not associated with oxidative stress generation.
5. Behaviour of both types of TiO_2-NP, TiO_2-S and TiO_2-D, resulted quite comparable. Genotoxicity results were similar, but TiO_2-S were more effectively taken up by the neuronal cells and showed a higher potential in inducing cytotoxicity, particularly cell cycle alterations.

These results provide valuable insights into the mechanism of TiO_2-NP induced toxicity in human neuronal cells. These observations once again reiterate concern about the safety of TiO_2-NP in consumer products.

4. Neuronal cytoxicity and genotoxicity induced by zinc oxide nanoparticles

4.1. INTRODUCTION

Zinc oxide (ZnO) is an attractive material due to its unique physical and chemical properties, such as high chemical stability, high electrochemical coupling coefficient, broad range of radiation absorption and high photostability (Kołodziejczak-Radzimska and Jesionowski, 2014). Also, at nanoscale, ZnO-NP have interesting characteristics, e.g. transparency, high isoelectric point, biocompatibility, and photocatalytic efficiency that makes them very suitable for a number of different applications.

Hence, ZnO-NP are one of the most abundantly used nanomaterials in consumer products and biomedical applications due to their specific properties, e.g. transparency, high isoelectric point, biocompatibility, and photocatalytic efficiency. They are widely employed in a variety of devices including cosmetics, toothpaste, sunscreens, fillings in medical materials, textiles, wall paints, and other building materials, and they can be also utilized in environmental remediation for elimination or degradation of pollutants in water or air (Jing et al., 2001). Furthermore, ZnO-NP have promising applications in medicine field since they have been proposed as a possible treatment for cancer and/or autoimmune diseases after being found to be selectively toxic towards potential disease-causing cells (Akhtar et al., 2012; Hanley et al., 2009; Premanathan et al., 2011), and they have been considered to be used in fabrication of nerve guidance channels for treatment of nerve injury (Seil and Webster, 2008). As a result of all these uses, human exposure to these NP is highly frequent. They can enter the organism through different pathways (respiratory tract, digestive system, transdermic and parenteral routes) and have shown a systemic distribution in *in vivo* studies (Vandebriel and De Jong, 2012), so they can potentially reach any organ or tissue involving a risk for human health.

ZnO-NP have been considered as one of the most toxic NP due to their lower cation charges (Hu et al., 2009). Accumulating evidence from *in vitro* studies has revealed that ZnO-NP are toxic to mammalian cells such as: human keratinocyte HaCaT and human lung epithelial A549 cells (Horie et al., 2009), L-132 cells (Sahu et al., 2013), human hepatocyte and embryonic kidney cells (Guan et al., 2012), human liver HepG2 cells (Sharma et al., 2011), and human peripheral blood lymphocytes (Sliwinska et al., 2015).

In general, toxicity of NP vary significantly with their size, as it has been found that smaller size usually involves more toxicity (Kang et al., 2013; Lin et al., 2014; Shang et al., 2014); indeed, toxicity of ZnO-NP has been reported to be greater than for bulk ZnO (Hanley et al., 2009; Hsiao and Huang, 2011). As far as the effect of shape is concerned, it was found that rod shapes are more toxic than the spherical ones, which means different shapes with fixed size and surface area have different effects on cell toxicity (Kwon et al., 2014a; Roy et al., 2015).

Additionally, in a study on the effect of surface charge, Jiang et al. (2009) found that ZnO-NP preferentially attached to a negatively charged bacterial surface. According to these studies, the toxicity of these NP was significantly influenced by their physicochemical properties. Therefore, it is important to understand relationships between biological toxicity and physicochemical properties of ZnO-NP to develop an unbiased assessment of the potential risks associated with their exposure.

Crystalline ZnO has a wurtzite (B4) hexagonal crystal structure at ambient conditions. Figure 4.1 clearly shows that the structure of ZnO can be simply described as a number of alternating planes composed of tetrahedrally coordinated O^{-2} and Zn^{+2}, stacked alternately along the c-axis. The tetrahedral coordination of ZnO gives rise to the non-centrosymmetric structure, and each anion is surrounded by four cations at the corners of the tetrahedron, resulting in a spontaneous polarization as well as a divergence in surface energy (Morkoç and Özgür, 2009; Wang, 2004).

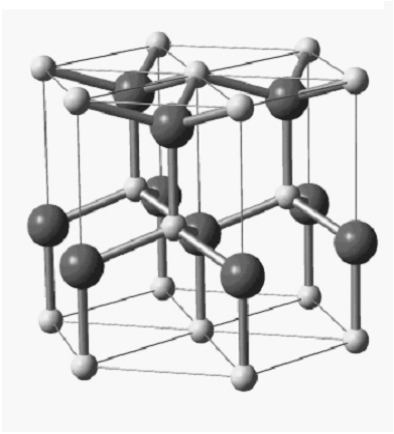

Figure 4.1. The hexagonal wurtzite structure model of ZnO. The tetrahedral coordination of ZnO is shown; O atoms are the larger red spheres while the Zn atoms are the smaller yellow spheres (from http://pixshark.com/wurtzite-structure.htm).

According to recent reports, inhaled NP could travel to brain either systemically via lung or through olfactory nerves on the upper section of the nasal cavity by axonal transport (Elder et al., 2006; Lanone and Boczkowski, 2006; Oszlánczi et al., 2011), resulting in inflammatory changes and brain edema formation in rats (Sharma et al., 2010). Kao et al. (2012) showed by electron microscopy that when ZnO-NP were intranasally administered to Sprague Dawley rats (6h exposure) they translocated into the olfactory bulb. The translocation of ZnO-NP across the blood-brain barrier and into the central nervous system was also confirmed by Cho et al. (2013) after 13 weeks of repeated oral administration; enhanced ZnO-NP levels were measured in rat brains compared with the untreated group. Additionally, ZnO-NP were reported by Xie et al. (2012) to disrupt memory of Swiss male mice with induced depressive-like behaviour.

In *in vitro* studies, ZnO-NP caused toxicity of mouse C17.2 neural stem cells (Deng et al., 2009), mouse neuroblastoma Neuro-2A cells (Jeng and Swanson, 2006), primary rat neuronal cells (Chiang et al., 2012), human glioma cells (Ostrovsky et al., 2009), and they also interfered with the ion channel current in primary hippocampal neurons from rat brain (Zhao et al., 2009). Nevertheless, there is still lack of information on the toxic effects of these NP on neurons and on the nervous system, particularly those from humans.

Therefore, in the present study human SH-SY5Y neuronal cells were used as an *in vitro* model to understand the mechanism of neurotoxicity of ZnO-NP. To achieve this aim a systematic study, which involved assessment of cell viability, cytotoxicity, genotoxicity, and oxidative stress, was undertaken. We also investigated whether the toxicity found was mediated by Zinc (II) ions released from ZnO-NP.

4.2. MATERIALS AND METHODS

4.2.1. *Nanoparticles: preparation and characterization*

ZnO-NP in powder form were purchased from Sigma-Aldrich Co. A stock suspension of NP was prepared in either deionized water or cell culture medium supplemented with foetal bovine serum (FBS) (final concentration 80μg/ml).

Prior to each treatment, this suspension was ultrasonicated (Branson Sonifier, USA) at 30W for 5min (1.5min on and 1min off twice, and 2min on), and diluted to prepare the different ZnO-NP concentrations tested.

Average hydrodynamic size, size distribution, and zeta potential were characterized by DLS as described in section 3.2.1.

4.2.2. *Cell culture and treatments*

Human neuroblastoma SH-SY5Y cell line was obtained from the European Collection of Cell Cultures and cultured in nutrient mixture EMEM/F12 (1:1) medium with 1% non-essential amino acids, 1% antibiotic and antimycotic solution, and supplemented with 10% heat inactivated FBS, all from Invitrogen™. Cells were incubated in a humidified atmosphere with 5% CO_2 at 37°C.

As it was explained previously in section 3.2.2, to carry out the experiments cells were seeded in 96-well plates (flat bottom) and allowed to adhere for 24h at 37°C. Cell densities were approximately in the range of 2-5x10^4 cells/well. Cells were then exposed to different concentrations of ZnO-NP for diverse times as per the experimental design. Cell culture medium was used as negative control in all experiments.

The following chemicals were used as positive controls: Campt (10μM) in apoptosis assessment, cell cycle and γH2AX analysis; MMC (1.5μM) in MN test; BLM (1μg/ml) in comet assay, and H_2O_2 (2μM for 3h treatments, and 1μM for 6h treatments) for oxidative DNA damage experiments. Besides, TiO_2-NP (120μg/ml) and triton X-100 (1%) were used as positive controls in cellular uptake and lactate dehydrogenase (LDH) assays, respectively.

4.2.3. *Cellular viability*

Cellular viability after exposure to ZnO-NP, and possible interference of these NP with the assay methodologies, were analysed by MTT and NRU assays, as described in section 3.2.3.

From the results of cell viability experiments, two exposure times (3 and 6h) and three different concentrations of ZnO-NP (20, 30 and 40μg/ml) were selected to perform the further experiments.

4.2.4. *Cellular uptake*

The uptake of ZnO-NP by the neuronal cells was determined by FCM as described in section 3.2.4. TiO_2-D NP (150μg/ml) were used as positive control.

4.2.5. *Cell cycle*

The cell distribution along the different phases of the cell cycle was examined in cells treated with ZnO-NP or the controls by FCM as described in section 3.2.5.

4.2.6. *Apoptosis*

4.2.6.1. *Annexin V-PI staining*

Apoptosis rate after exposure to ZnO-NP was determined by means of annexin V/PI double staining, using the BD Pharmingen Annexin V–FITC apoptosis detection kit I (Becton Dickinson), as previously explained in section 3.2.6.1.

4.2.6.2. *Mitochondrial membrane potential analysis*

Mitochondrial membrane potential (MMP) of neuronal cells exposed to ZnO-NP was detected with fluorescent probe JC-1 (Molecular probes) using FCM as described in section 3.2.6.2.

4.2.7. *Genotoxicity*

4.2.7.1. *Micronucleus evaluation by flow cytometry*

MN induction after incubation of cells in the presence of ZnO-NP was measured by a FCM methodology as described previously in section 3.2.7.1.

4.2.7.2. *γH2AX assay*

The effect of ZnO-NP treatments on H2AX histone phosphorylation was analysed by FCM as described in section 3.2.7.2.

4.2.8. *Comet assay*

After treatments with ZnO-NP, comet assay was performed as stated previously in section 3.2.7.3.

4.2.9. *Oxidative DNA damage*

The levels of oxidative DNA damage caused by ZnO-NP in neuronal cells were analysed by OGG1 enzyme-modified comet assay as described in section 3.2.8.1.

4.2.10. *Membrane integrity*

Lactate dehydrogenase (LDH) activity in extracellular medium due to membrane damage was assessed by a commercial kit (Roche Diagnostics Corp.) using manufacturer's protocol. The LDH assay measures metabolic conversion of lactate to pyruvate by LDH enzyme and resulting coloured compound is measured spectrophotometrically. Therefore, an increase in LDH activity measured in the cell culture supernatant alone is representative for cell membrane damage due to leakage of the enzyme to extracellular fluid.

Cells were seeded in 96-well plates and allowed to adhere for 24h. Medium was aspirated and cells were incubated at 37ºC for different time periods with ZnO-NP suspensions. After completion of exposure periods, the culture plates were centrifuged at 250xg for 4min. The supernatant of each well was transferred to a new flat bottom 96-well plate. LDH assay mixture was prepared by mixing equal amounts of LDH assay substrate, cofactor and dye solutions. This assay mixture was added in an amount equal to 2X the volume of supernatant present in each well. The plate was incubated in the dark at room temperature for 20min, and the reaction was terminated by the addition of 1/10 volume of 1N HCl. The untreated cells and cells treated with

1% triton X-100 were also run in parallel under identical conditions and served as negative and positive controls, respectively. The resulting coloured compound was measured spectrophotometrically at 490nm with a reference wavelength of 655nm using a Cambrex ELx808 microplate reader (Biotek, KC4). LDH release was calculated as follows:

$$LDH(\%) = \frac{[A]_{sample} - [A]_{negativecontrol}}{[A]_{positivecontrol} - [A]_{negativecontrol}} \times 100$$

$[A]_{sample}$ is the value of absorbance measured from the sample, $[A]_{negative\ control}$ refers to the absorbance of cell culture medium, and $[A]_{positive\ control}$ refers to the absorbance of triton X-100, which was set as 100% cytotoxicity.

4.2.11. *Dissolved zinc concentrations in cell culture medium*

To quantify the Zinc (II) ions concentrations released from the ZnO-NP, cell culture medium containing ZnO-NP at different concentrations (2, 4, 6, 8, 10, 15, 20, 25, 30, 35, 40, 45, 50 and 55µg/ml) were incubated at 37ºC for 3, 6, 12 and 24h in a humidified 5% CO_2 environment. Cell culture medium without NP but subjected to the same conditions was used as the blank control. A solid phase ZnO was removed from the liquid medium by centrifugation at 14,000rpm for 30min. The Zn content in the supernatant was analysed by flame atomic absorption spectroscopy (FAAS) (Thermoelemental Solaar S4 v.10.02).

4.2.12. *Cytotoxic effects of Zinc (II) ions.*

In order to test whether cytotoxicity of ZnO-NP was due to Zinc (II) ions released from NP, cells were treated for 3h with $ZnSO_4.7H_2O$, at 0.05, 0.1, 0.2, 0.4, 0.6, and 0.8mM. These concentrations were set according to the results obtained in FAAS. Cell viability was evaluated using the MTT assay as described in section 3.2.3.

4.2.13. *Statistical analysis*

Distribution of the response variables departed significantly from normality (Kolmogorov-Smirnov test) and therefore non-parametric tests were considered adequate for the statistical analysis of these data. Differences among groups were tested with Kruskal-Wallis test and Mann-Whitney *U*-test. The associations between two variables were analysed by Spearman's correlation. Statistical analyses were performed using SPSS for Windows statistical package (version 21.0). Experimental data were expressed as mean ± standard error. A minimum of three independent experiments were performed for each experimental condition tested, and each condition was always run in duplicate and under blind conditions. In all cases, $P<0.05$ was considered significant.

4.3. RESULTS AND DISCUSSION

Zinc is an essential trace element which plays an important role in regulating cellular metabolism. The increasing use of the ZnO-NP in a number of worldwide industries and in the medicine field has brought attention to their potential toxicity and health risks. It is well established that, under specific conditions, ZnO-NP may result toxic to a variety of mammalian and human cells (De Berardis et al., 2010; Kim et al., 2010a; Osman et al., 2010; Sharma et al., 2009, 2011; Wahab et al., 2011) and to animals after intratracheal instillation (Fukui et al., 2015) or after oral (Pasupuleti et al., 2012; Yang et al., 2011a) or inhalatory (Adamcakova-Dodd et al., 2014; Wang et al., 2010) administration. Furthermore, it has been well documented that ZnO-NP can also reach rodent brain after inhalation (Kao et al., 2012) or oral administration (Lee et al., 2012). However, although it has been reported that ZnO-NP affect spatial learning and memory ability of young rats (Yang et al., 2011a), their effects at the cellular and molecular level, especially on human neuronal cells, are not clear yet.

The present study explores the effects of ZnO-NP on human neuroblastoma cells and provides significant insight into the possible mechanism through which ZnO-NP exert their toxic effects on these cells. Several concentrations and exposure times were tested and a battery of methodologies were employed with the aim of characterizing in depth the genotoxic and cytotoxic effects of ZnO-NP on human neuronal cells as well as attempting to understand the underlying action mechanisms.

4.3.1. *Nanoparticle characterization*

To understand the extent of aggregation of these NP before cellular exposure, the average hydrodynamic size, size distribution and zeta potential of ZnO-NP in water and in cell culture medium suspensions were assessed by DLS.

Table 4.1 summarizes the description and characterization data of the ZnO-NP employed in this study. BET evaluation of NP size, as provided by the commercial supplier, was 100nm. The average particle hydrodynamic diameter in medium was determined to be slightly higher (273.4nm) as compared to deionized water (243.7nm). The size distribution graphs showed a good dispersion of NP in medium (Figure 4.2c), despite having small differences in the water suspension (Figure 4.2a). The zeta potential was measured as -8.23mV in water (Figure 4.2b), and -11.7mV in medium (Figure 4.2d), which are lower than the generally accepted approximate threshold for stability; thus they would be expected to have a tendency to aggregate over time due to instability in aqueous medium.

Table 4.1. Physicochemical characterization of ZnO-NP

Particle size [a] (nm) (BET)	**Specific surface area [a] (m^2/g) (BET)**	**Hydrodynamic diameter (nm) (DLS)**		**Zeta potential (mV) (DLS)**	
		Water	Medium	Water	Medium
100	15–25	243.7	273.4	− 8.23	− 11.7

BET : Brunauer Emmett Teller, DLS: Dynamic Light Scattering

[a] Provided by the commercial supplier

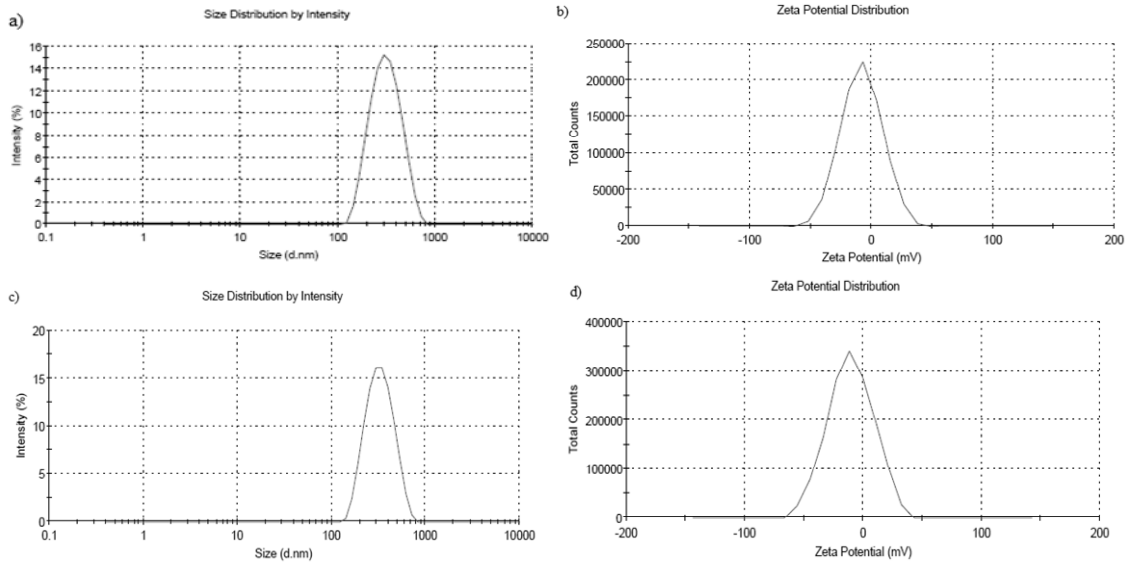

Figure 4.2.Characterization of ZnO-NP: (a) hydrodynamic diameter and (b) zeta potential in water; (c) hydrodynamic diameter and (d) zeta potential in culture medium.

4.3.2. *Cellular viability*

For evaluating the cytotoxic potential of ZnO-NP in SH-SY5Y cells, more than one cytotoxicity assay was used to get more reliability. After demonstrating with acellular experiments that there was no interference between the ZnO-NP and the spectrophotometry methodologies (data not shown), SH-SY5Y cells were exposed to ZnO-NP (10-80µg/ml) for 3, 6, 24 and 48h and their effect on cellular viability was determined with MTT and NRU assays.

Dose-dependent decrease in the percentage of viability (relative to control) was observed in MTT assay after exposure to ZnO-NP from 10µg/ml on at treatment periods longer than 6h (Figure 4.3a). The cytotoxicity was evident at 25µg/ml even after 3h. The results of NRU assay showed a similar concentration dependent response with loss in cell viability at 25µg/ml at all the treatment times tested (Figure 4.3b).

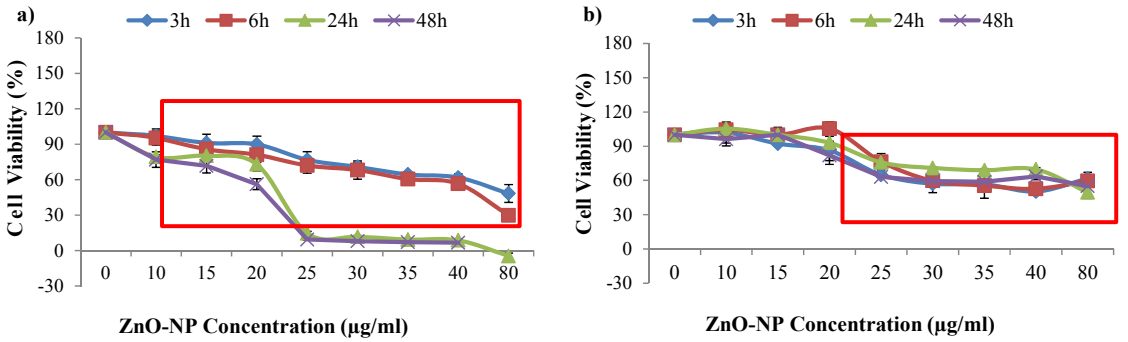

Figure 4.3. Results from MTT assay (a) and NRU assay (b) on viability of neuronal cells treated with ZnO-NP. Values inside the rectangle are statistically different from the corresponding controls.

Results obtained from MTT and NRU assays showed that ZnO-NP diminished the viability of the neuronal cells in a dose dependent manner at all the treatment times. In accordance with these results, concentration-dependent decrease in cellular viability after ZnO-NP exposure was previously described for several human cell types, including HepG2 and MCF-7 cancer cells (Wahab et al., 2014), THP-1 monocytes (Sahu et al., 2014), lymphocyte cells (Sarkar et al., 2014b) and adipose tissue-derived mesenchymal stem cells (Hackenberg et al., 2014).

Moreover, grantees of a US National Institute of Health Sciences (NIEHS)-funded consortium program performed two phases of *in vitro* testing with selected ENM, including ZnO-NP, using three mammalian cell lines (human bronchial epithelial BEAS-2B, rat alveolar epithelial RLE-6TN, and human monocytic THP-1), which were selected in order to cover two different species (rat and human), two different lung epithelial cells (alveolar type II and bronchial epithelial cells), and two different cell types (epithelial cells and macrophages). From this study ZnO-NP were found to be cytotoxic to all cell types at concentrations ≥ 50 µg/ml (Xia et al., 2013). There is also evidence that ZnO-NP are particularly cytotoxic to rapidly dividing cancer cells relative to quiescent cells of the same lineage, suggesting that ZnO-NP toxicity is related to the proliferative potential of the cell (Hanley et al., 2009). Our results also support that ZnO-NP present an anti-proliferative effect; this capacity led different authors to propose ZnO-NP as a promising antibacterial and anticancer agent (Salem et al., 2015).

4.3.3. *Cellular uptake*

The internalization of ZnO-NP in neuronal cells was assessed using FCM. Surprisingly, no significant increase in the SSC parameter was observed for cells treated with ZnO-NP (20-40µg/ml) for either 3 or 6h as compared to the control cells (Figure 4.4).

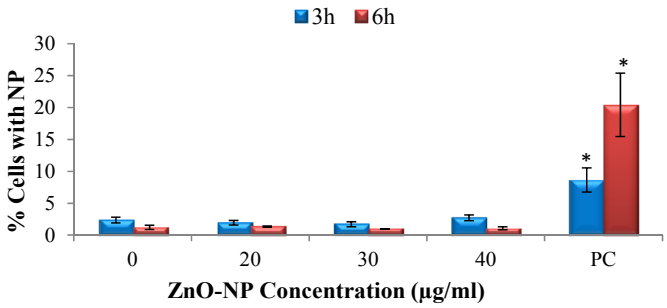

Figure 4.4. Uptake of ZnO-NP by SH-SY5Y cells as analysed by FCM. PC: positive control. **P*<0.05, significant difference with regard to the corresponding negative control.

NP in general elicit a wide range of intracellular responses depending on their physicochemical properties, intracellular concentrations, duration of contact, subcellular distributions and interactions with biological molecules (Dobrovolskaia and McNeil, 2007). Although cell types and their states of differentiation can determine the choice of internalization pathway, the physicochemical properties and surface reactivity of NP are also important for their biological fate (Nel et al., 2009). For particle uptake to occur, specific (ligand–receptor) and non-specific (hydrophobic, Coulombic) binding interactions must decrease the free energy at the contact site to overcome resistive forces. Several proteins are known to form transient complexes with NP; large variations in their dissociation rates establish preferential binding interactions between specific particle types and the biological fluids in which they are suspended. The kinetics of NP–protein association and dissociation, and concurrent exchange with free proteins in the media, has important roles in determining the NP interactions with biological surfaces and receptors. Although the presence and composition of the protein corona was not determined in the current study, the protein corona formation around ZnO-NP in DMEM medium including 10% FBS is well documented in literature (Kwon et al., 2014a). The nature of the NP surface controls which biomolecules interact with the particles, and hence might mediate or limit their access to cells (Nel et al., 2009). Thus, it seems that the specific conditions employed in our experiments, especially regarding the use of medium supplemented with FBS, are limiting in some way the entry of ZnO-NP into the neuronal cells.

4.3.4. *Cell cycle*

Cell percentages in the different phases of the cell cycle (G_0/G_1, S, and G_2/M) were assessed by FCM after ZnO-NP treatment. SH-SY5Y cells were exposed to 20, 30 and 40µg/ml ZnO-NP for 3 and 6h; data obtained are collected in Figure 4.5.

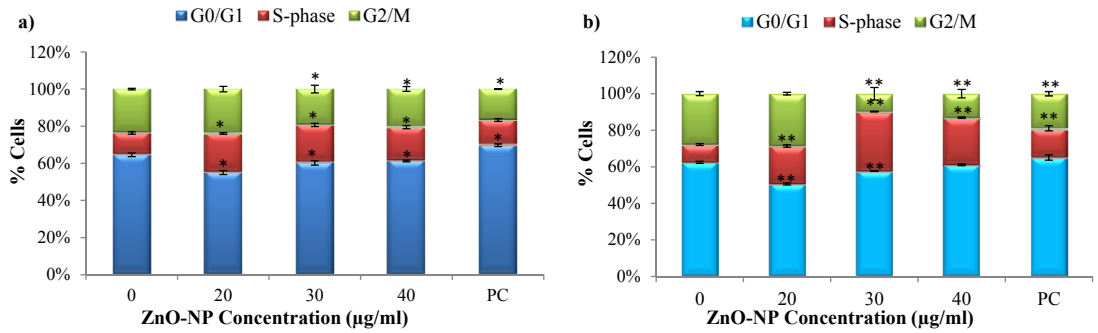

Figure 4.5. Results of cell cycle analysis in neuronal cells treated with ZnO-NP for 3h (a) or 6h (b) (percentage of cells in each phase). **P*<0.05; ***P*<0.01; significant difference with regard to the corresponding negative control. PC: positive control.

Results from the cell cycle analysis showed that the ZnO-NP induce important cell cycle alterations, including mitotic arrest, in SH-SY5Y cells after both 3 and 6h treatments. Specifically, ZnO-NP induced decreases in the percentage of cells in G_0/G_1 and G_2/M phases, and an increase in the percentage of cells in S-phase. Besides, significant dose-response relationships were found in phase G_2/M (r = -0.631, *P*<0.01) at 3h, and in phase S (r = 0.759, *P*<0.01) and G_2/M (r = -0.743, *P*<0.01) at 6h.

Similar to these results, ZnO-NP were also recently found to induce cell cycle arrest at S/G_2 phase in human breast adenocarcinoma MCF-7 and mouth epidermal carcinoma KB cells exposed for 24h (100-300µM) leading to apoptosis (Sasidharan et al., 2011), and G_2/M cell cycle arrest in neural Schwann RSC96 cells treated for 12h (8-80µg/ml) (Yin et al., 2012).

4.3.5. *Apoptosis*

In order to figure out whether ZnO-NP are able to induce apoptosis cell death, SH-SY5Y cells were treated with these NP and annexinV/PI staining was carried out and analysed by FCM. Results obtained can be seen from Table 4.3. ZnO-NP exposure for both 3 and 6h resulted in increases in apoptotic rates as compared to the control.

ZnO-NP were previously reported to induce cell death in a variety of cell lines under experimental conditions similar to this study, such as head and neck squamous carcinoma derived cells (HNSCC) (Hackenberg et al., 2014), human umbilical vein endothelial cells (Paszek et al., 2012), or mouse neural stem cells (Deng et al., 2009).

Apoptosis can be mediated by different routes; the best characterized and the most prominent ones are called the extrinsic and intrinsic pathways. In the extrinsic pathway (also known as “death receptor pathway”), apoptosis is triggered by the ligand-induced activation of death receptors at the cell surface. Key event in the intrinsic pathway is disruption of the mitochondrial trans-membrane potential. This leads to osmotic mitochondrial swelling with

subsequent rupture of the outer mitochondrial membrane, resulting in the release of pro-apoptotic elements (e.g. cytochrome c, apoptosis inducing factor) from the mitochondrial intermembrane space into the cytoplasm. Cytochrome c induces the formation of apoptosome which binds to downstream caspases, such as caspase-9, and processes them into proteolytically active forms. Active caspase-9 further mediates activation of effector caspases resulting in apoptosis (Galluzzi et al., 2007; Henry-Mowatt et al., 2004; Kroemer et al., 2007).

Table 4.3. Apoptotic rates (%) in neuronal cells after ZnO-NP exposure.

		3h		6h	
		Annexin-V	MMP	Annexin-V	MMP
Control		4.71±0.27	4.93±0.33	6.94±0.34	5.03±0.52
ZnO-NP	20µg/ml	6.63±0.15**	7.57±0.24**	9.80±0.98**	3.52±0.48
	30µg/ml	6.38±0.31**	6.91±0.72	8.17±0.37	7.68±1.74
	40µg/ml	6.33±0.21**	5.62±0.49	8.98±0.74	5.62±0.69
PC		8.28±0.14**	6.69±1.09	10.27±0.41**	9.57±0.70**

**P<0.01; significant difference with regard to the corresponding negative control. PC: positive control.

When this crucial step of mitochondrial membrane depolarization was analysed in ZnO-NP treated SH-SY5Y cells, only slight increases in MMP with just a statistically significant result at 20µg/ml after 3h of exposure was observed (Table 4.3). Hence, our results suggest that ZnO-NP induce cell death mainly by a mitochondria-independent pathway. Some previous studies reported mitochondrial alterations after ZnO-NP treatments in other different experimental systems (De Berardis et al., 2010; Li et al., 2012a; Sharma et al., 2012; Wang et al., 2014a). Nonetheless, in the studies by Sharma et al. (2012) and Wang et al. (2014) NP were efficiently taken up by HepG2 cells and primary astrocytes, respectively. Moreover, penetration of NP in LoVo cells was not evaluated in the work by De Berardis et al. (2010), and Li et al. (2012a) exposed rat mitochondrion directly to the ZnO-NP. Thus there are substantial differences between these studies and the current one, which may justify our different results regarding involvement of mitochondria in the ZnO-NP induced apoptotic cell death.

4.3.6. *Genotoxicity*

ZnO-NP were previously reported to induce genotoxicity in other different human cell types including HepG2 cells (Sharma et al. 2012), lymphocytes (Sliwinska et al., 2015), and hepatocyte and embryonic kidney cells (Guan et al., 2012). However, studies evaluating the effects of these NP on genetic material of neuronal cells are still limited. Therefore, the potential of ZnO-NP to induce genotoxic damage in SH-SY5Y neuroblastoma cells was evaluated in this

study by combination of three different genotoxicity biomarkers, i.e., MN test, comet assay and γH2AX analysis.

In vitro MN scoring by FCM with measurement of two parameters, fluorescence from PI and light scattering, was used to estimate the frequency of MN in SH-SY5Y cells after treatment with 20, 30 and 40µg/ml ZnO-NP for 3 and 6h (Figure 4.6). Exposure did not induce MN production after 3h. However, important dose-dependent MN induction was observed after 6h treatment (r=0.635, $P<0.01$).

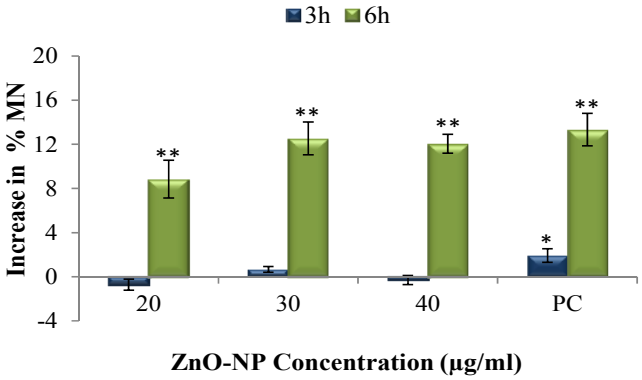

Figure 4.6. Results of MN evaluation in SH-SY5Y cells treated with ZnO-NP. *$P<0.05$, **$P<0.01$, significant difference with regard to the corresponding negative control. PC: positive control.

Despite increasing population exposure to ZnO-NP, studies about their potential genotoxicity using MN test still remain controversial. Corradi et al. (2012) reported that there was no significant increase in MN rate for ZnO-NP on A549 human lung carcinoma cells, except at the highest dose tested (50µg/ml) in the presence of 10% serum. But our results are very parallel to the findings of Wahab et al. (2011), who reported positive induction of MN in human U87 glioma cells treated with ZnO-NP at concentrations similar to ours (15.6µg/ml and 31.2µg/ml) for 24h.

Furthermore, although increases in the levels of H2AX phosphorylation were observed in all cases, statistically significant values were obtained only at the 30µg/ml treatments (Figure 4.7), similar to γH2AX activation that was observed in a time-dependent manner after ZnO-NP application to macrophages of Balb/c mice (Roy et al., 2014). As mentioned earlier, it has been reported that γH2AX is required for G_2/M arrest, hence there is connection between γH2AX level and normal G_2/M progression (Fernandez-Capetillo et al., 2002). Observed γH2AX after 30µg/ml ZnO-NP exposure would explain the G_2/M arrest induced by ZnO-NP at the same concentration.

The DNA damaging potential of the ZnO-NP was assessed by the comet assay, which detects SSB as well as DSB, alkali labile sites, and incomplete excision repair places. DNA

damage was measured as %DNA in the comet tail in control cells and in cells exposed to ZnO-NP. Cells exposed to different concentrations of NP showed significantly more DNA damage than control cells at all concentrations and times tested, excepting for the highest concentration after the 6h exposure (Figure 4.8).

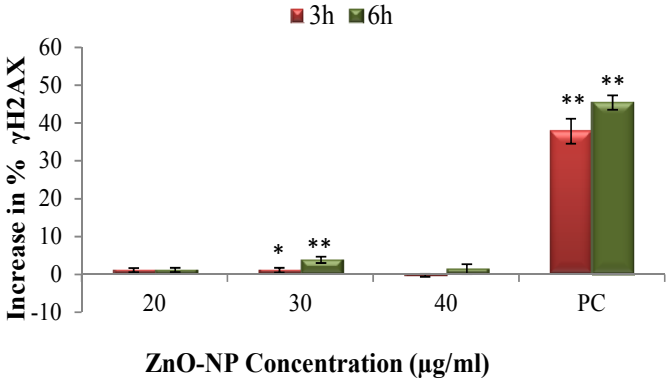

Figure 4.7. Results of γH2AX evaluation in SH-SY5Y cells treated with ZnO-NP. **P*<0.05, ***P*<0.01, significant difference with regard to the corresponding negative control. PC: positive control.

These results are in accordance with previous studies in which positive genotoxic effects of ZnO-NP from the comet assay were observed in CaCo-2 cells (Gerloff et al., 2009), human lymphocytes and sperm cells (Gopalan et al., 2009), human lymphoblastoid TK6 cells (Demir et al., 2014a), human hepatoblastoma C3A cells (Kermanizadeh et al., 2012), human embryonic kidney HEK293 cells and mouse embryonic NIH/3T3 fibroblasts (Demir et al., 2014a), and human skin melanoma A375 cells (Alarifi et al., 2013).

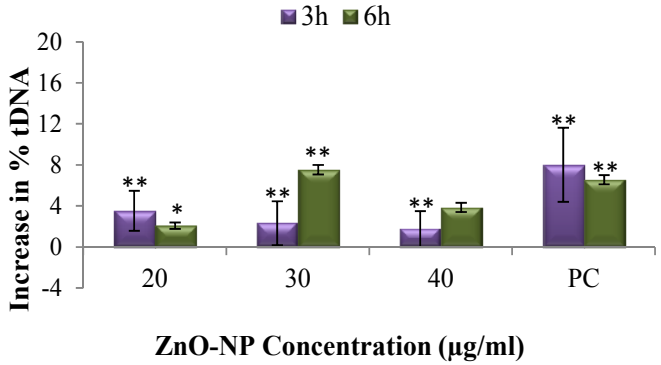

Figure 4.8 Results of comet assay in SH-SY5Y cells treated with ZnO-NP. **P*<0.05, ***P*<0.01, significant difference with regard to the corresponding negative control. PC: positive control.

Among all 21 comet assay publications about these NP in the literature (reviewed by Golbamaki et al., 2015), only two studies reported no positive results with *in vivo* mice bone

marrow cells (Kwon et al., 2014b) and human lymphocyte cells (Sarkar et al., 2014b). In both of those studies the size of agglomerates was about 200nm; therefore, large size due to agglomeration is one possible explanation for the negative results that we obtained for the highest concentration after 6h exposure.

When we look at the of ZnO-NP induced genotoxic damage evaluated in this study by several genotoxicity biomarkers, comet assay results revealed that significant primary DNA damage was already induced at 3h exposure. But statistically important MN induction could be only observed after 6h exposure, accompanied by an increase in phosphorylation of the histone H2AX at both exposure times. It should be taken into account that the highest concentration of ZnO-NP used (40μg/ml) induced around 40% of cytotoxicity at 3 and 6h, so this fact can be influencing the non-significant results obtained with this concentration for histone phosphorylation (at both treatment times) and comet assay (at 6h).

ZnO-NP were previously reported to induce genotoxicity in other different cells types including primary keratinocytes (Sharma et al., 2011), fibroblasts (Chiang et al., 2012), epidermal A431 cells (Sharma et al., 2009), lung A549 cells (Fukui et al., 2015), cervix HEp-2 carcinoma cells (Osman et al., 2010), liver HepG2 cells (Sharma et al., 2012), and embryonic kidney HEK293 cells and NIH/3T3 fibroblasts (Demir et al., 2014a). However, studies evaluating the effects of these NP on genetic material of neuronal cells are highly scarce. Particularly, Chiang et al. (2012) observed DNA damage after exposing rat primary neuronal cells to ZnO-NP, and Wahab et al. (2011) found results very parallel to ours in MN induction on human U87 glioma cells treated with different Zn nanostructures, at similar concentrations to those employed in the current study.

4.3.7. *Oxidative DNA damage*

The OGG1-modified comet assay was used to investigate the ability of ZnO-NP to induce oxidative DNA damage in SH-SY5Y cells. Treatment of cells with NP showed that slides incubated with OGG1 accumulated significantly more DNA damage than those incubated only with buffer, indicating that this damage corresponds to oxidative damage (particularly, presence of 8-oxoG) (Figure 4.9). These results revealed the induction of oxidative DNA damage by ZnO-NP at all concentrations and treatment times tested, as evident by an increase in enzyme sensitive sites.

The data agree with previous studies reporting increased values of oxidative stress and ROS production in cells treated by ZnO-NP, such as human lymphoblastoid TK6 cells (Demir et al., 2014b), human epithelial colorectal adenocarcinoma Caco-2 cells (Song et al., 2014), human skin melanoma A375 cells (Alarifi et al., 2013), human dermal neonatal fibroblasts (Ramasamy et al., 2014), human lung epithelial L-132 cells (Sahu et al., 2013), murine

macrophage RAW 264.7 cells (Wilhelmi et al., 2013), liver tissues of mice and rat (Yang et al., 2015; Yousef and Mohamed, 2015), mouse bone marrow mesenchymal stem cells (Syama et al., 2014), rat primary neuronal cells (Chiang et al., 2012), and rat retinal ganglion RGC-5 cells (Guo et al., 2013a, 2013b).

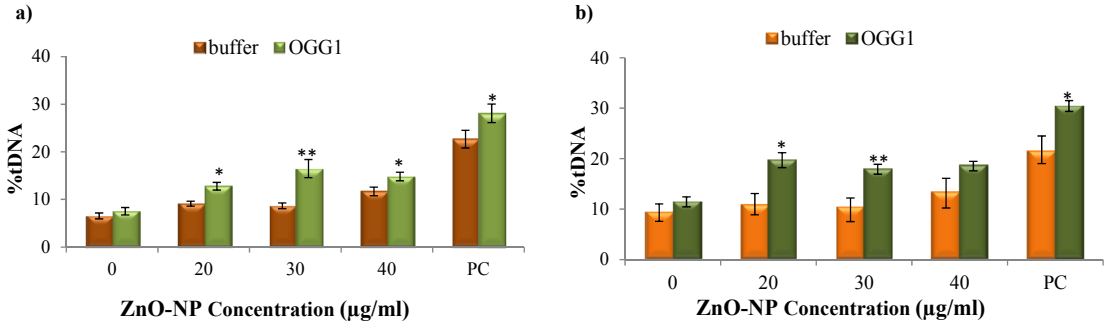

Figure 4.9. Results of OGG1-modified comet assay in neuronal cells treated with ZnO-NP for 3h (a) or 6h (b). **P*<0.05, ***P*<0.01, significant difference with regard to the corresponding buffer. PC: positive control.

Besides, positive results in oxidative stress induced by ZnO-NP were also obtained in animal studies (Fukui et al., 2015; Hao and Chen, 2012; Sharma et al., 2012). Indeed, a very recent study on C3A hepatocytes reported a dramatic increase in both gluconeogenesis and glycogenolysis induced by ZnO-NP, and proposed the intracellular increase of ROS production as responsible for these effects (Filippi et al., 2015).

4.3.8. *Membrane integrity*

As expounded so far, although no cellular uptake of ZnO-NP was obtained in this study, these results showed induction of cytotoxic and genotoxic effects by these NP on neuronal cells. One possible reason to explain these effects is that ZnO-NP could potentially interact with the cell membrane to cause the observed toxicity. Thus, the potential alterations in the membrane integrity caused by ZnO-NP exposure were assessed by LDH assay.

The colorimetric LDH release assay is a simple and robust method to assess effects of agents on cell membrane integrity by measuring the activity of LDH enzyme in the cell culture supernatant. Figure 4.10 shows that after a 3 or 6h incubation, ZnO-NP did not significantly increase LDH release in comparison with the controls, thus cell membrane was intact at all treatment concentrations.

Similar to these results, Osmond-McLeod et al. (2013) reported that only after 24h exposure, but not after 2 or 6h, of human olfactory neurosphere-derived cells from healthy adult donors to ZnO-NP, cell membrane disruption was observed as measured by an increase in LDH activity in culture medium.

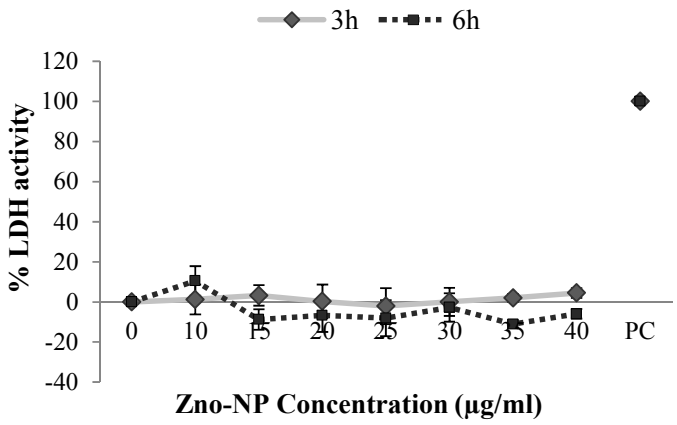

Figure 4.10. Results of membrane integrity assessment (LDH assay) in SH-SY5Y cells exposed to ZnO-NP. PC: positive control.

In spite of these results, we cannot rule out the possible interaction of ZnO-NP with some component of the cellular membrane without altering its integrity. The contact with ion channels may disturb ionic homeostasis and consequently neuron physiological functions. This hypothesis can be supported with the study of Zhao et al. (2009) in which ZnO-NP were reported to enhance the excitability of rat neurons by increasing the opening number of sodium channels and delaying rectifier potassium channels.

4.3.9. *Cytotoxic effects of Zinc (II) ions*

In a very recent review Pandurangan and Kim,(2015) proposed three different mechanisms of ZnO-NP toxicity, depending on the cell type: (i) ZnO-NP dissolve in the extracellular region and increase the intracellular Zinc(II)ions level, which in turn reduces the activity of Zn-dependent enzymes and transcription factors; (ii) ZnO-NP enter the cells and dissolve in the intracellular region, which leads to the disruption of Zn-dependent enzymes and transcription factors; and (iii) ZnO-NP dissolve in the lysosomes that lead to the reduction of pH level and lysosomal destabilization.

Hence, according to the first mechanism proposed, other possible reason to explain these positive results in cytotoxicity and genotoxicity assays in neuronal cells treated with ZnO-NP in the absence of NP uptake, is that toxicity might result from the zinc ions dissolved from the NP outside the cells and present either in the cell culture medium or intracellularly. This hypothesis was supported also by Deng et al. (2009) based on the fact that ZnO-NP induced cytotoxicity at different levels (cell viability, apoptosis and necrosis) in mouse neuronal stem cells, but they were not detectable inside the cells by electron microscopy. Moreover, extracellular dissolution of ZnO-NP and release of Zinc(II)ions have been reported to induce cell death in human T-cell

leukaemia Jurkat cells (Buerki-Thurnherr et al., 2012), mouse macrophage Ana-1 cells (Song et al., 2010), or apically-exposed rat alveolar epithelial cell monolayers (Kim et al., 2010a).

Furthermore, it was previously demonstrated that increases in intracellular levels of Zinc (II) ions released from ZnO-NP were correlated with high levels of ROS and, consequently, with cell death in ZnO-NP exposed human immune cells (Shen et al., 2013), human monocyte-derived macrophages, monocyte-derived dendritic cells, and Jurkat T cells (Tuomela et al., 2013), agreeing with the positive results obtained in our study from apoptosis and oxidative DNA damage assessments. Contrarily, Lin et al. (2008) concluded that neither free Zinc(II)ions nor metal impurity in the ZnO-NP samples was the cause of the observed cytotoxicity and oxidative stress in A549 cells treated with these NP.

Regarding the brain, zinc is an essential nutrient for normal neurological functions and may play an important role in the processing of memory formation (Daniels et al., 2004). To understand the possible effects of this ion in brain cells is particularly relevant as transition metals (such as Zn) may contribute to the aetiology of neurodegenerative diseases, such as Alzheimer‘s disease, Parkinson‘s disease, amyotrophic lateral sclerosis, stroke or epilepsy (Pavlica et al., 2009).

The tendency of ZnO-NP to dissolve in aqueous solutions, especially biological fluids, has been well documented, but the relative contributions of nanoparticulated and dissolved zinc to the mechanism(s) of toxicity remain very challenging to assess directly. The failure of conventional imaging techniques or FCM to detect cellular uptake of ZnO-NP has been suggested to be likely a consequence of complete or partial ZnO dissolution (Gilbert et al., 2012).

To determine the amount of Zinc (II) ions released from ZnO-NP, we incubated them (2-55µg/ml) in complete cell culture medium for 3, 6 or 24h, and measured the Zinc (II) ions concentrations by FAAS in the liquid supernatant fraction. Results obtained were very similar at all the treatment times tested (Figure 4.11). A dose-dependent linear increase in Zinc (II) ions was observed in the medium up to approximately 30µg/ml ZnO-NP; then a plateau was reached at around 0.3mM Zinc (II) ions.

Other studies reporting experiments of Zinc(II)ions release from ZnO-NP showed similar Zinc(II)ions concentrations in DMEM (Reed et al., 2012), but lower in seawater (Wong et al., 2010) or in complete minimal essential medium (Sharma et al., 2012). But Reed et al. (2012) demonstrated, using nanopure water and different cell culture media, that solubility of ZnO-NP may be highly variable and dependent on the matrix they are suspended in.

In the study of Gilbert et al. (2012) X-ray microprobe data showed that BEAS-2B cells exposed to ZnO-NP accumulate zinc from solution and that only organic-complexed ionic Zinc(II)ions is present intracellularly one hour following exposure. This finding strongly

indicates that ZnO-NP toxicity is caused by free or complexed Zinc(II)ions within cells, and not by reactions occurring on the surfaces of internalized solid phase ZnO-NP (Nel et al., 2009). However, these studies do not reveal whether the uptake of Zinc (II) ions or ZnO-NP is the dominant pathway for internalizing Zn. This question was addressed by combined scanning transmission X-ray microscopy (STXM) and atomic force microscopy (AFM) studies of BEAS-2B cells exposed to less-soluble iron-doped and undoped ZnO-NP, which provided evidence that less soluble NP were more readily internalized than the soluble ZnO-NP (Gilbert et al., 2012). As dissolution is affected by several physicochemical factors and the bio-reactivity of NP may be greatly influenced by their biological environment, dissolution characteristics of ZnO-NP might be associated with their possible toxic behaviour.

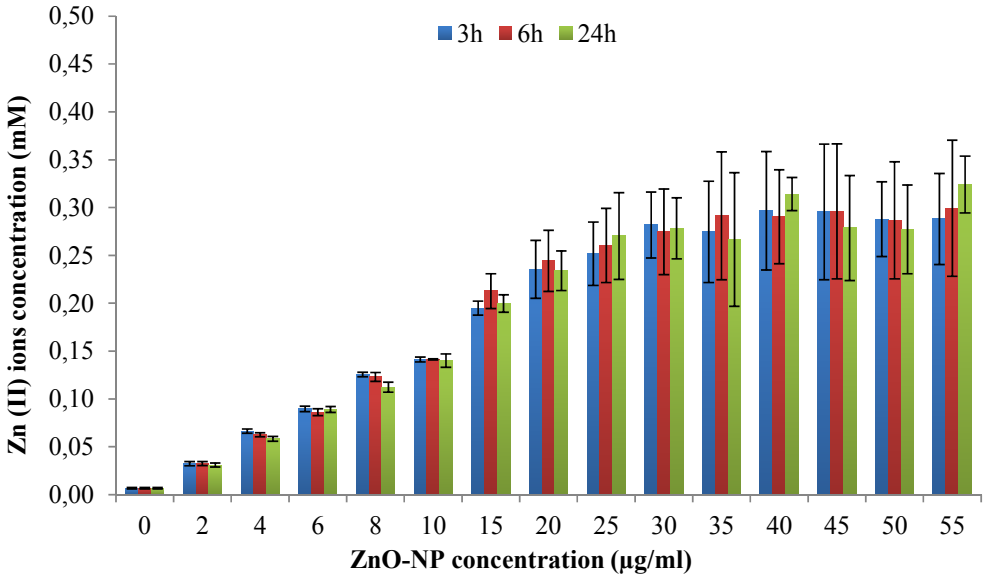

Figure 4.11. Analysis of Zn (II) ions released from ZnO-NP in cell culture medium.

We further examined the toxicity of released Zinc (II) ions on SH-SY5Y cells in order to test whether cytotoxicity and genotoxicity previously observed for ZnO-NP were due to these ions. Cells were treated with a soluble Zn salt ($ZnSO_4$) to obtain Zinc(II)ions at a range of concentrations including the ones obtained as released from ZnO-NP (0.05-0.8mM) (Figure 4.11). As it can be seen from the Figure 4.12, Zinc (II) ions exerted cytotoxicity (MTT assay), only at doses higher than 0.4mM (0.6 and 0.8mM).

Previous analysis by FAAS had shown that ZnO-NP released Zinc (II) ions to the medium at levels up to 0.3mM, but results of these last experiments suggested that this amount was insufficient to cause toxicity. Therefore, the observed decrease in neuronal cell viability by exposure to ZnO-NP was due to the NP themselves rather than to the Zinc (II) ions released from them. These results are in agreement with those of Lin et al. (2008) and Xu et al. (2013), who demonstrated that cytotoxicity associated with ZnO-NP is not a function of Zinc(II)ions

concentration, although these studies used different cellular systems and exposure conditions; they also suggested that other factors may play an important role in the toxic effect of ZnO-NP.

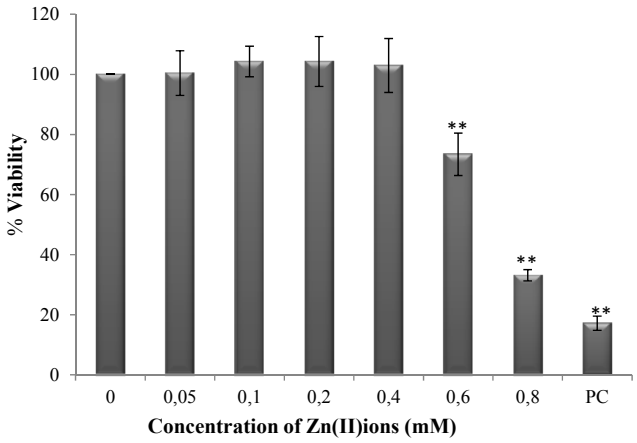

Figure 4.12. Cytotoxicity of Zinc (II) ions: MTT assay in SH-SY5Y cells treated with $ZnSO_4$. $^{**}P<0.01$, significant difference with regard to the negative control.

Still, as Zinc(II)ions were released from the ZnO-NP even at the lowest concentrations, the possibility that these ions are involved in the genotoxic and cytotoxic effects observed in this study cannot be excluded, since experiments aimed at testing the toxic potential of Zinc(II)ions on SH-SY5Y cells were only focused on cell viability decrease.

Recently, it was proposed that ZnO-NP cytotoxicity requires direct particle-cell contact and uptake, resulting in the release of high intracellular concentrations of Zinc(II)ions from ZnO-NP dissolution within lysosomes and late endosomes (Saptarshi et al., 2015; Shen et al., 2013; Turney et al., 2012). Nevertheless, these results prove that scenario wrong in the current experimental conditions: ZnO-NP do not have to enter the cells to induce harmful effects at the cytogenetic and molecular level. However, the question of whether toxic effects, different from decrease in cell viability, are caused by increase of intracellular Zinc(II)ions due to NP dissolution in medium still remains to be resolved.

4.4. CONCLUSIONS

In the present study we investigated the effects ZnO-NP on the human SH-SY5Y neuroblastoma cell line, exploring the different mechanisms underlying their cytotoxic and genotoxic potential. Taken all results of this study together we can draw the following conclusions:

1. MTT and NRU assays revealed that ZnO-NP exposure induced significant concentration-dependent decreases in neuronal cell viability from 25µg/ml on at all treatment times tested.

2. According to FCM analyses, ZnO-NP were not taken up by the neuronal cells at any experimental condition assayed.

3. Exposure of neuronal cells to ZnO-NP caused important cell cycle alterations, including mitotic arrest, and apoptosis induction scarcely associated with losses of the mitochondrial membrane potential, indicating that it was mainly mediated by a mitochondria independent pathway.

4. ZnO-NP produced genotoxicity in neuronal cells: primary DNA damage and H2AX phosphorylation since 3h exposure and MN induction after 6h exposure.

5. ZnO-NP caused increases in oxidative DNA damage at all concentrations and times tested.

6. ZnO-NP did not alter neuronal cell membrane integrity, although the possible interaction of these NP with some component of the cell membrane without altering its integrity cannot be ruled out.

7. ZnO-NP released Zinc (II) ions to the cell culture medium at levels up to 0.3mM, but this amount was insufficient to cause decrease in neuronal cell viability. Therefore, the observed decrease in viability by exposure to ZnO-NP was due to the NP rather than to the Zinc (II) ions dissolved from them.

The results obtained in this work contribute to increase the knowledge on the cytotoxic and genotoxic potential of ZnO-NP in general, and specifically on human neuronal cells. Since neurotoxic effects of these NP at different levels were demonstrated in this study, although their mechanism of action still needs clarification, further investigations are needed to develop the necessary safety precautions and exposure limits for people working with materials containing ZnO-NP and those who might be exposed to them when they are implemented in commercial, industrial, and medical applications

5. Neuronal cytotoxicity and genotoxicity induced by iron oxide nanoparticles

5.1. INTRODUCTION

Iron is one of the most abundant of all metals, comprising nearly 5.6% of the earth crust and nearly all of the earth core (McDonald et al., 2010; Morgan and Anders, 1980). Metallic iron is rarely found on the surface of the earth because it tends to oxidize. Iron forms compounds mainly in the +2 and +3 oxidation states. Traditionally, iron (II) compounds are called ferrous and iron (III) compounds ferric. There are also iron oxides with six different crystal structures composed of ferrous or ferric iron centres and oxygen: hematite (α-Fe_2O_3), magnetite (Fe_3O_4), maghemite (γ-Fe_2O_3), β-Fe_2O_3, ε-Fe_2O_3 and wüstite (FeO) (Martinez, 2009).

Iron is essential for the functioning of many biochemical processes, including electron transfer reactions, gene regulation, binding and transport of oxygen, and regulation of cell growth and differentiation (Beard, 2001). Thus, iron plays an important role in biology, forming complexes with molecular oxygen in haemoglobin and myoglobin; iron compounds are common oxygen transport proteins in vertebrates (Oliveira, 2012).

Iron is both an essential nutrient and a potential toxicant to cells; it requires a highly sophisticated and complex set of regulatory approaches to meet the demands of cells as well as prevent excess accumulation (Beard, 2001). Iron is also the metal at the active site of many important redox enzymes dealing with cellular respiration and oxidation, and reduction in plants and animals (Tamás and Martinoia, 2006)., its ability to both donate and accept electrons thus means that it can be harmful when present in high concentrations. When not bound to functional proteins, free iron can participate in the Fenton reaction that leads to the production of 'free radicals' unwanted by-products of the reaction between free iron and hydrogen peroxide (Tomasi et al., 2003). This, in turn, can lead to the detrimental oxidation of molecules including DNA, lipids and carbohydrates, which causes damage to cells and tissues (Vaziri, 2013).

As clinically approved metal oxide NP, iron oxide nanoparticles (ION) hold immense potential in a vast variety of applications in various fields of biomedicine and biotechnology (Singh et al., 2010). Owing to their small size, they are an ideal platform for use as nanocarriers in drug delivery. A further advantage of ION is that due to their magnetic properties, mainly superparamagnetism, they can be used as contrast agents for nuclear magnetic resonance imaging (MRI). In fact, currently there are six FDA approved ION contrast enhancement agents: Feridex®, Endorem™, GastroMARK®, Lumirem®, Sinerem®, and Resovist® (FDA 2015). Their magnetic response to external magnetic fields can be even used for local overheating of cancer tissues, known as hyperthermia therapy. Among these biomedical applications, magnetic properties of ION can be also fully explored in separation techniques of various (bio) substances or pollutants.

However, only magnetite and maghemite have been found to be functional and promising candidates in biomedical and biotechnological applications due to their favourable magnetic properties (Gupta and Gupta, 2005; Pankhurst et al., 2003; Tuček et al., 2014). Since the

unpaired electrons make a material magnetic, iron oxide is less magnetic than iron due to having only two unpaired electrons. Iron oxide is therefore called a paramagnetic material (Boysen and Muir, 2011). More importantly, if the size of γ-Fe_2O_3 or Fe_3O_4 NP falls below a certain threshold (usually below ~15nm), they display superparamagnetism (Hola et al., 2015). This means that each individual particle has a large constant magnetic moment and behaves like a giant paramagnetic atom with a fast response to applied magnetic fields. Upon application of a magnetic field, the ION align in the direction of the field and this gives rise to be manipulated by an external magnetic field gradient (Hola et al., 2015; Issa et al., 2013). In contrast to multiple-domain ferromagnetic materials that retain their magnetism even after the removal of the magnetic field, superparamagnetic NP lose their magnetization when the magnetic field is switched off. This feature makes superparamagnetic NP very attractive for a broad range of biomedical applications (Huber, 2005).

For biomedical and biotechnological applications, the surface of commercially available maghemite and magnetite NP may be modified by coating with different materials such as: polymeric coatings (dextran, citrate, polyethylene glycol, polyacrylic acid, etc.), inorganic molecules (silica, gold, silver, platinum, palladium, iron, carbon) and numerous biological molecules (polypeptides, proteins, antibodies, biotin, etc.) (reviewed in Singh et al., 2010). Surface modification not only stabilizes ION in an environment of slightly alkaline pH or high salt concentrations, but also allows biomolecule binding favouring surface attachments between ION and antibodies, peptides, hormones or drugs then magnetically targeted to a particular tissue/organ in order to benefit a therapeutic or diagnostic application (Sadeghiani et al., 2005).

Furthermore, naked metallic NP are chemically highly active, and are easily oxidized in air, resulting generally in loss of magnetism and dispersibility (Lu et al., 2007). For example, in MRI a better image can be obtained if paramagnetic NP are attached to the object of interest. Thus, functionalizing ION by coating them with molecules that are attracted to cancer tumours contributes to MRI image improvement (Boysen and Muir, 2011). Moreover, naked NP can be easily trapped by the immune system as foreign materials, which means that they cannot reach the target (Santhosh and Ulrih, 2013). Surface modification adds functions including prolonging the recognition time by the immune system or treating unhealthy cells and tissues (Hola et al., 2015).

Given that iron oxides occur naturally in the earth crust or are engineered for specific purposes, the major concern is the increased exposure level to humans and the ecosystem as more and more ION are being manufactured to meet the demands of the rapidly proliferating field of nanomedicine (Borm et al., 2006). The dramatic growth and the therapeutic benefits that ION have to offer, accompanies the concerns associated with the risks of their exposure (Maynard et al., 2006, 2010). Efforts to achieve the maximum therapeutic effect can lead to iron overload at the target site and the disruption of iron homeostasis, promoting ROS generation (Soenen et al., 2011).

Therefore, there is a considerable need to address biocompatibility and biosafety concerns associated with their usage in a variety of applications. So far there are some inconsistencies in the literature about toxicological assessment of ION in different cell systems and interpretation of the results. Despite those contradictory results, ION are generally considered as biocompatible (Kunzmann et al., 2011) and associated with low toxicity to the human body (Jeng and Swanson, 2006;Karlsson et al., 2009). Nonetheless, exposure to ION has been associated with significant toxic effects such as inflammation, formation of apoptotic bodies, impaired mitochondrial function (MTT assay), alterations in membrane integrity (LDH assay), generation of reactive oxygen species (ROS), increase in MN, and chromosome condensation (Singh et al., 2010) (Figure 5.1). These effects of ION seem to be affected by dose, exposure time, surface coating, and cell type.

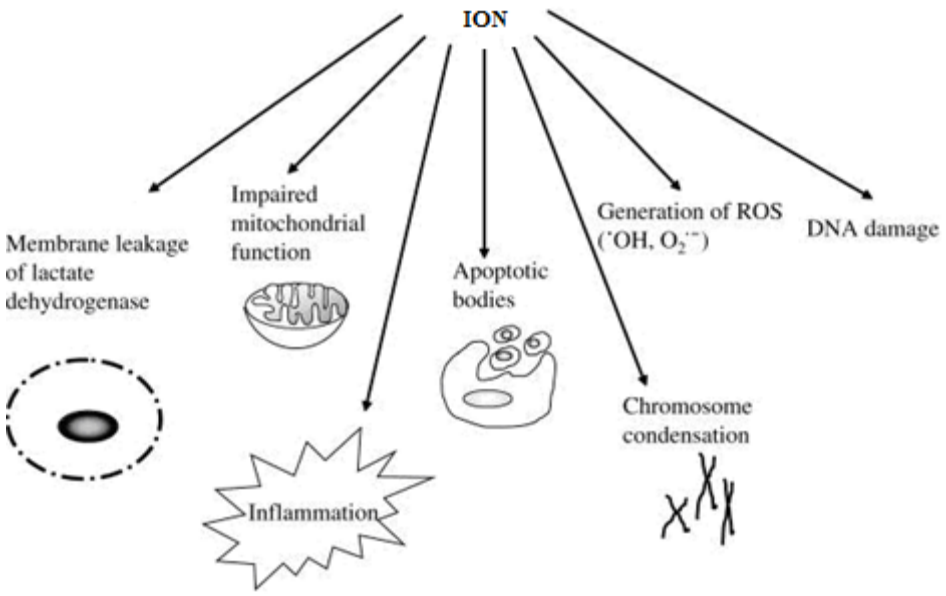

Figure 5.1. Cellular toxicity induced by ION (from Singh et al., 2010).

Some *in vitro* studies comparing several types of ION showed them to be very low toxic or nontoxic at all. For instance, low cytotoxicity and no genotoxicity of Fe_2O_3 and Fe_3O_4 was reported in human alveolar epithelial cells A549 (Karlsson et al., 2009). L-929 fibroblast cells also revealed no toxicity from either Fe_3O_4 and mesoporous silica composites (Huang et al., 2012), or from meso-2,3-dimercaptosuccinic acid (DMSA) coated maghemite NP (Auffan et al., 2009). Likewise, human lymphoblastoid cells treated with uncoated ION (Fe_2O_3) (Singh et al., 2012), or Chinese hamster lung cells treated with glutamic acid coated ION (Fe_2O_3) (Zhang et al., 2012) did not show genotoxic response.

On the contrary, several reports have stated that these particles can in fact exert drastic effects on the cell wellbeing. ION modified with different functional groups induced a dose-dependent reduction in viability of L-929 fibroblast cells (Hong et al., 2011). Similarly, Li et al.

(2012b) indicated that uncoated magnetite NP were toxic to human cervical cancer cells (HeLa) and immortalized normal human retinal pigment epithelial cells.

Furthermore, *in vivo* studies comparing several types of ION also showed controversial results. Negative toxicity results were reported from mouse embryonic stem cells (Au et al., 2009), human mesenchymal stem cells (Yang et al., 2011b), and leukocytes of Wistar rats (Singh et al., 2013). On the other hand, mice after intraperitoneal injection to Fe_3O_4 ION (Ma et al., 2012; Freitas, 2002; Wu et al., 2010b) and γ-Fe_2O_3 ION encapsulated within albumin based nanospheres (Estevanato et al., 2011) or intravenous administration of polyaspartic acid-coated magnetite ION (Sadeghiani et al., 2005), showed some levels of toxicity.

With diameters in the range of a few tens of nanometres, it has been demonstrated *in vivo* that ION could pass across the blood-brain barrier (Qiao et al., 2012) and distribute along mice brain after intranasal installation (Wang et al., 2007). This ability makes them very eligible for medical applications on nervous system, especially drug delivery and imaging diagnostics purposes.

In order to improve the delivery of contrast agents to the brain, ION were administered intravenously to individuals with neurological disorders. These ION have been used with this aim in multiple sclerosis in the central nervous system of humans (Dousset et al., 2006; Manninger et al., 2005) and in rodent models (Dousset et al., 1999a, 1999b; Floris et al., 2004; Rausch et al., 2003, 2004), in stroke in human (Nighoghossian et al., 2007; Saleh et al., 2004) and in animal brains (Kleinschnitz et al., 2005; Schroeter et al., 2004), and in human or murine brain tumours (Neuwelt et al., 2004; Zimmer et al., 1995).

Although the number of *in vivo* studies on ION neurotoxicity is restricted, Kumari et al. (2012) reported that Wistar rats exposed orally to ION (Fe_2O_3) for 28 days showed distribution of these NP to various organs, including brain, and toxic signs and symptoms, such as dullness, irritation and moribund conditions, but no mortality. Besides, intranasal ION (Fe_2O_3) exposure caused neuronal fatty degeneration and microglial proliferation in mice (Kim et al., 2013; Wang et al., 2011b).

When ION functionalized with various surface chemicals were tested in different neuronal cell lines they also showed conflicting results. Exposure to DMSA-coated ION or naked ION (Fe_3O_4) caused a dose-dependent reduction of viability in PC12 rat cells (Pisanic et al., 2007). Also Soenen et al. (2011) reported that citrate-coated ION were the most toxic NP among the dextran-coated, carboxydextran-coated, and lipid-coated ION on PC12 cells. Furthermore, DMSA-coated Fe_3O_4 and Fe_2O_3 showed toxic effects on human glioma U251 cells (Chen et al., 2012b), whereas poly-L-lysine-modified ION did not show any effect on the same cells (Xiang et al., 2003).

Among all the possible surface modifications for ION, silica (SiO_2) cover has several advantages that make it especially suitable to be employed for medical purposes. For instance,

silica-coated ION (S-ION) are negatively charged at blood pH, helping to avoid aggregate formation in body fluids (Arruebo et al., 2007), and its transparent matrix allows the efficient passage of excitation and emission light, which is a relevant property for imaging diagnosis (Alwi et al., 2012). However, their potential toxicity on the nervous system has not been deeply addressed. Thus, further and more detailed studies, particularly those employing human neural cells, are required to identify any potential toxicity associated with the use of ION with particular surface coatings.

Therefore, the objective of this study was to evaluate the toxicity of S-ION on human neuronal SH-SY5Y cells. To that aim, alterations in the cell cycle, cell death by apoptosis or necrosis, and membrane integrity were assessed as cytotoxicity parameters. Besides, genotoxicity was determined by γH2AX assay, MN test and comet assay. Complementarily, generation of oxidative stress and effects on DNA damage repair were also analysed.

5.2. MATERIALS AND METHODS

5.2.1. *Nanoparticles: preparation and characterization*

Silica-coated magnetite nanoparticles (S-ION) were synthesized and prepared as stable water suspensions (5mg/ml) as described by Yi et al. (2006). Prior to each treatment, a stock suspension (1mg/ml) was prepared in SH-SY5Y culture medium and sonicated in a water bath for 5min. Serial dilutions were carried out to obtain the different test concentrations, and sonicated in water bath for an additional 5min period.

Particle size and particle morphology were characterized by monolayer TEM using a HITACHI H-8100 microscope equipped with EDS (ThermoNoran, Thermo Scientific) operated at 200kV. Images were analysed using ImageJ public domain software. Average hydrodynamic size and zeta potential of particles in suspension were determined by DLS as described in section 3.2.1.

X-ray photoelectron spectroscopy (XPS) was used to determine particle surface chemistry. The XPS analysis was performed using an ESCALAB 200A, VG Scientific (UK) with PISCES software for data acquisition and analysis. For analysis, an achromatic Al (Kα) X-ray source (1486.6eV) operating at 15kV (300W) was used, and the spectrometer, calibrated with reference to Ag 3d5/2 (368.27eV), was operated in Constant Analyser Energy (CAE) mode with a pass energy of 20eV (ROI) and 50eV (survey). Data acquisition was performed with a pressure lower than $1x10^{-6}$P. Surface charging effect was corrected using the carbon peak as reference (285eV). The deconvolution of spectra was performed using the XPSPEAK41 program, in which an adjustment of the peaks was performed using peak fitting with Gaussian-Lorentzian peak shape and Shirley type background subtraction.

5.2.2. *Dissolved iron concentrations in the cell culture medium*

To analyse the release of iron ions from the S-ION, suspensions (10, 50, 100 and 200µg/ml) were incubated in cell culture medium for 3, 6 and 24h at 37ºC. The iron content in the supernatant medium after removing the S-ION solid phase by centrifugation was analysed by FAAS as described previously in section 4.3.9.

5.2.3. *Cell culture and treatments*

Human neuroblastoma SH-SY5Y cells (European Collection of Cell Cultures) were grown in nutrient mixture EMEM/F12 (1:1) with 1% non-essential amino acids, 1% antibiotic and antimycotic solution, supplemented with 10% heat inactivated FBS (all from Invitrogen^{TM}) in a humidified incubator at 37°C with 5% CO_2.

To carry out the experiments, cells were seeded in 96-well plates (5–6 x10^4 cells/well), and allowed to adhere for 24h at 37°C prior to the experiments. For each experiment, these cells were incubated with S-ION and controls. Cell culture medium was used as negative control in all experiments. The following chemicals were used as positive controls: Campt (10µM) for apoptosis, triton X-100 (1%) for membrane integrity and viability; MMC (1.5µM) for cell cycle and MN test; BLM (1µg/ml) for comet assay and γH2AX analysis, H_2O_2 (1µM for 15min) for comet assay and DCFH assay, and DEM (2µl/ml) for glutathione determination.

5.2.4. *Cellular viability*

The effect of S-ION (5-300µg/ml for 3, 6 or 24h) on viability of SH-SY5Y cells by the MTT and NRU assays, and acellular experiments to check possible interferences between NP and assay procedures were performed as described in section 3.2.3.

From the results of cell viability assays, four treatment doses (10, 50, 100 and 200µg/ml) and two exposure times (3 and 24h) were selected to perform further experiments.

5.2.5. *Cellular uptake*

The potential of the S-ION to be uptaken by the cells was evaluated by FCM as reported in section 3.2.4.

5.2.6. *Cell cycle*

The cell distribution along the different phases of the cell cycle was examined in cells treated with S-ION or the controls by measuring the relative cellular DNA content with FCM as

described in section 3.2.5. Complementarily, subG$_1$ region of the cell cycle distribution was also evaluated, as indicative of the late stages of apoptosis.

5.2.7. *Apoptosis and necrosis*

BD Pharmingen™ Annexin V-FITC apoptosis detection kit was used to measure apoptosis cell death that may be potentially induced by S-ION treatment, by means of FCM as already described in section 3.2.6.1. Additionally, late apoptosis/necrosis was determined as the percentage of annexin V+/PI+ cells.

5.2.8. *Membrane integrity*

Effect of S-ION treatment on neuronal cell membrane integrity was measured by LDH assay as described in section 4.2.10.

5.2.9. *Genotoxicity*

5.2.9.1. *Micronuclei evaluation by flow cytometry*

MN induction after incubation of SH-SY5Y cells with S-ION was measured by FCM as described previously in section 3.2.7.1.

5.2.9.2. *γH2AX assay*

The effect of S-ION on H2AX histone phosphorylation was analysed by FCM as reported in section 3.2.7.2.

5.2.9.3. *Comet assay*

To evaluate primary DNA damage induction after treating neuronal cells with S-ION, the alkaline comet assay was performed as described in section 3.2.7.3.

5.2.10. *Oxidative stress*

5.2.10.1. *DCFH Assay*

As mentioned earlier, researchers have already reported the interference of different types of NP with the fluorescence emission of DCFH-DA fluorimetric dye frequently used for oxidative stress measurements, in both cell-free systems and cellular models (Aranda et al., 2013; Doak et al., 2009; Kroll et al., 2012). Hence, in order to check ROS generation potential

of S-ION and rule out their potential interference with fluorimetric probe, an acellular DCFH assay was performed as described in previous publications (Foucaud et al., 2007; Pal et al., 2011; Rota et al., 1999), with some modifications for dye preparation as well as for ROS measurements.

Firstly, as there are no cells present, DCFH-DA must be hydrolysed to DCFH. Briefly, 11.62µl of 0.89mM DCFH-DA chloromethyl derivative dye [5-(and-6)-chloromethyl-2',7'-dichlorodihydrofluorescein diacetate, acetyl ester] (CM-H_2DCFDA) (molecular probes ®C-6827)], were chemically hydrolysed in 20µl of 0.01N NaOH in the dark for 30min at room temperature, followed by neutralizing with 988.38µl of 0.1M PBS (pH 7.4). Following hydrolysis, 25µl of the 10µM DCFH obtained were added to the 96-well plate containing ION alongside a blank and a positive control (1µl of 50mM H_2O_2), in triplicate. Only to the wells containing H_2O_2, horseradish peroxidase (HRP) enzyme (1µl) was added. After 60min incubation on ice in the dark, fluorescence generated from the oxidation of DCFH to DCF was measured using a microplate multimode reader (TriStar LB 941, Berthold technologies) at 485nm excitation and 520nm emission wavelengths.

Next, intracellular ROS generation was estimated by using a commercial kit (Cellular ROS Detection Assay Kit, Abcam/Mitosciences) in a 96-well microplate, generally following the manufacturer's instructions. Different protocols were followed for measurement of ROS generation for 3 and 24h of S-ION incubation due to instability of DCFH-DA for treatments longer than 6h.

For 3h treatments cells were seeded in 96 well plates and allowed to adhere for 24h. Medium was aspirated and cells were washed twice with PBS and incubated with DCFH-DA dye at a concentration of 10µM in 100µl/well. Plates were kept in a 37°C, 5% CO_2 atmosphere for 45min. Following incubation, the dye solution was removed; cells were washed twice with PBS and incubated with S-ION (10, 50, 100, 200 µg/ml) at 37ºC. Afterwards, the fluorescence of oxidized DCF dye was immediately measured at the respective excitation and emission wavelengths of 490nm and 545nm in a TECAN GENios plate reader. The results were calculated and presented as percentage of ROS generation in comparison with the negative control.

For intracellular ROS measurements with 24h exposure to S-ION, after exposing cell to S-ION for 24h, NP suspensions were removed and 100µg/ml DCFH-DA dilutions were over laid on top of the treated cells and they were incubated for additional 45min. Following the incubation, the fluorescence of oxidized DCF dye was immediately measured in a TECAN GENios plate reader using the conditions described above.

5.2.10.2. *Glutathione determination*

Glutathione content and GSH:GSSG ratio after S-ION exposure was measured by a colorimetric method described previously in section 3.2.8.2.

5.2.10.3. *Oxidative DNA damage*

The level of oxidative DNA damage induced by S-ION was analysed by OGG1 enzyme modified comet assay, as described in section 3.2.8.1.

5.2.11. *DNA repair competence assay*

The experimental design described by Laffon et al. (2010) was followed to evaluate the effects of S-ION on DNA damage repair. It consisted of three consecutive phases: (i) in phase A (pre-treatment) cells were incubated for 3 or 24h in the presence or absence of S-ION (50µg/ml) at 37°C; (ii) in phase B (DNA damage induction) cells were challenged with H_2O_2 (100µM) for 5min at 37°C in the presence or absence of S-ION (50µg/ml); and (iii) in phase C (repair) cells were washed in fresh medium to remove treatment, and incubated with or without S-ION (50 µg/ml) for 30min at 37°C to allow DNA repair. Alkaline comet assay was then performed after phase B (data labelled as "before repair") and phase C (data labelled as "after repair") as described previously in section 3.2.7.3.

Additionally, cells were treated with S-ION (50µg/ml) for 30min and the comet assay was performed immediately after. This was done to test whether 30min incubation with S-ION (as occurs in phase C) might induce significant damage to DNA.

5.2.12. *Statistical analysis*

Statistical analyses were performed using SPSS for Windows statistical package (version 21.0). A minimum of three independent experiments were performed for each experimental condition tested, and each condition was always run in duplicate and under blind conditions. Experimental data were expressed as mean ± standard error. Distribution of the response variables departed significantly from normality (Kolmogorov-Smirnov test) and therefore non-parametric tests were considered adequate for the statistical analysis of these data. Differences among groups were tested with Kruskal–Wallis test and Mann–Whitney *U*-test. The associations between two variables were analysed by Spearman's correlation. A *P*-value of less than 0.05 was considered significant.

5.3. RESULTS AND DISCUSSION

Magnetic nanoparticles were one of the first nanomaterials to be approved for clinical use (Gould, 2006). In general, knowledge about ION toxic effects indicates that they mainly depend on NP size and surface coating (Rivet et al., 2012). Together with ROS production and iron ion release, other forms of cytotoxicity reported after ION exposure which may be or may be not related to these mechanisms include cell cycle alterations (Wu and Sun, 2011), decreases in cell viability (Wang et al., 2010), cytoskeleton alterations (Wu et al., 2010), and disruption of the mitochondrial membrane potential (Zhu et al., 2010). Besides, because of their ability to overcome the restraints of the BBB (Thomsen et al., 2013), they have been used as carriers for the transport of drugs, siRNA, or DNA into the brain. Still, little is known on the effects of ION on the human nervous system. Few studies were published regarding the *in vitro* neurotoxicity of ION on human neural cell lines, and results obtained were not consistent (Chen et al., 2012b; Kenzaoui et al., 2012; Xiang et al., 2003).

Due to its chemical stability, coating with silica can transform ION by increasing their biocompatibility and offering the capacity to functionalize their surface without affecting magnetic properties (Kolhatkar et al., 2013; Larumbe et al., 2012; Rittikulsittichai et al., 2013). Moreover, silica-coating helps to convert hydrophobic NP into hydrophilic water-soluble particles (Wu et al., 2008). Nevertheless, despite the numerous advantages and potential applications in neuromedicine, the possible neurotoxicity of S-ION has not been completely discarded yet. In this part, the possible toxicity of S-ION on human neuroblastoma cells at different levels was evaluated using a range of concentrations and treatment times.

5.3.1. *Nanoparticle characterization*

Characterization of NP is the most essential part of nanotoxicological studies. The behaviour and activity of NP is largely dependent on a number of physical and chemical properties such as particle number, mass concentration, surface area, charge, chemistry and reactivity, size distribution, aggregation, elemental composition, as well as structure and shape. Therefore, a complete characterization is essential for better understanding and interpretation of results. In this study, characterization of S-ION was done in deionized water and complete cell culture medium (DMEM-F12) using TEM, DLS and XPS. Table 5.1 describes physicochemical features of S-ION used in this study.

Surface chemistry analysis revealed that only a small fraction of the S-ION surface presents iron (less than 2%). S-ION also presented carbon and nitrogen on their surface, possibly resultant from the synthesis process (reverse microemulsion using cyclohexane, ammonium hydroxide, and tetraethyl orthosilicate).

TEM measurements showed that they are spherical particles with a mean diameter of 20.2nm (Figure 5.2a), hydrodynamic size measurements by DLS showed that S-ION maintain their nanoparticulated size when dispersed in water and culture medium (Figure 5.2b). All dispersions showed negative values for zeta potential, but values indicating stable colloidal dispersions were only observed in water (-31.8mV), which decreased in cell culture medium (-10.3mV).

Table 5.1. Physicochemical description of S-ION.

Primary particle size	(nm) TEM	10.0 ± 2.1 (core) 20.2 ± 2.9 (core and coating)
Particle morphology	TEM	Spherical
Surface chemistry (%)	XPS	9.07 (C 1s) 0.27 (N 1s) 60.02 (O 1s) 29.22 (Si 2p) 1.41 (Fe 2p3)
Dispersed in water	Size (nm) DLS	93.3 ± 0.5
	Zeta potential (mV)	-31.8 ± 2.1 (pH=7.73)
Dispersed in cell culture medium	Size (nm) DLS	111.1 ± 1.1
	Zeta potential (mV)	-10.3 ± 1.1 (pH=8.14)

TEM: Transmission Electronic Microscopy,XPS: X-ray photoelectron spectroscopy , DLS: Dynamic Light Scattering

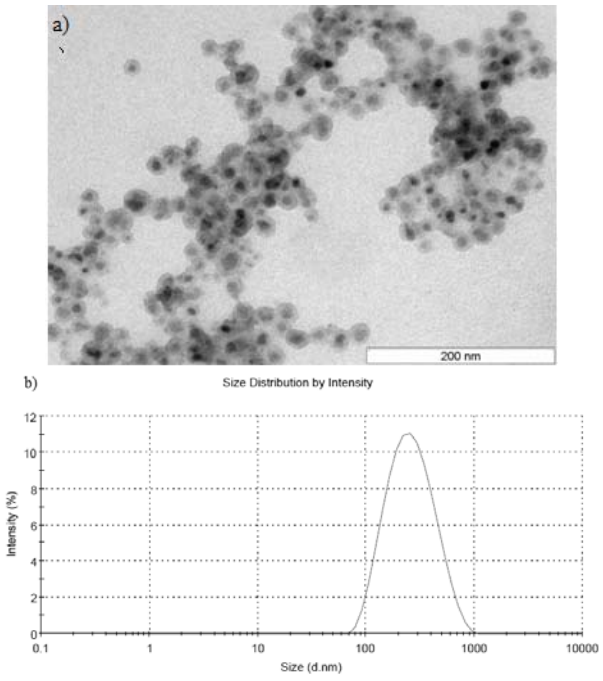

Figure 5.2. Characterization of S-ION: (a) TEM microphotograph, (b) distribution of hydrodynamic diameter in cell culture medium.

5.3.2. *Cellular viability*

As it has been well documented in the literature, NP may interfere with assay components and alter the reliability of *in vitro* cell viability assay results (Kroll et al., 2012; Monteiro-Riviere et al., 2007; Stone et al., 2009). Possible causes include NP interference with light absorption, chemical reactions between NP and reactants and dye adsorption on NP surface.

To analyse the reactivity of S-ION and to study the possible ION interference with cytotoxicity assays either with dyes or with the spectrophotometric read-out, the whole assay protocols were carried out with the ION in the absence of cells. No interferences of S-ION with MTT or NRU assay methodologies were observed.

Thus, cellular viability after exposure of SH-SY5Y cells to different concentrations of S-ION was assessed by employing MTT and NRU assays. Results obtained are presented in Figure 5.3. S-ION exposure was responsible for some slight but significant decreases in viability at 6h (MTT and NRU assays), or at 24h exposure (MTT assay). Nevertheless, cell viability was higher than 80% in all cases.

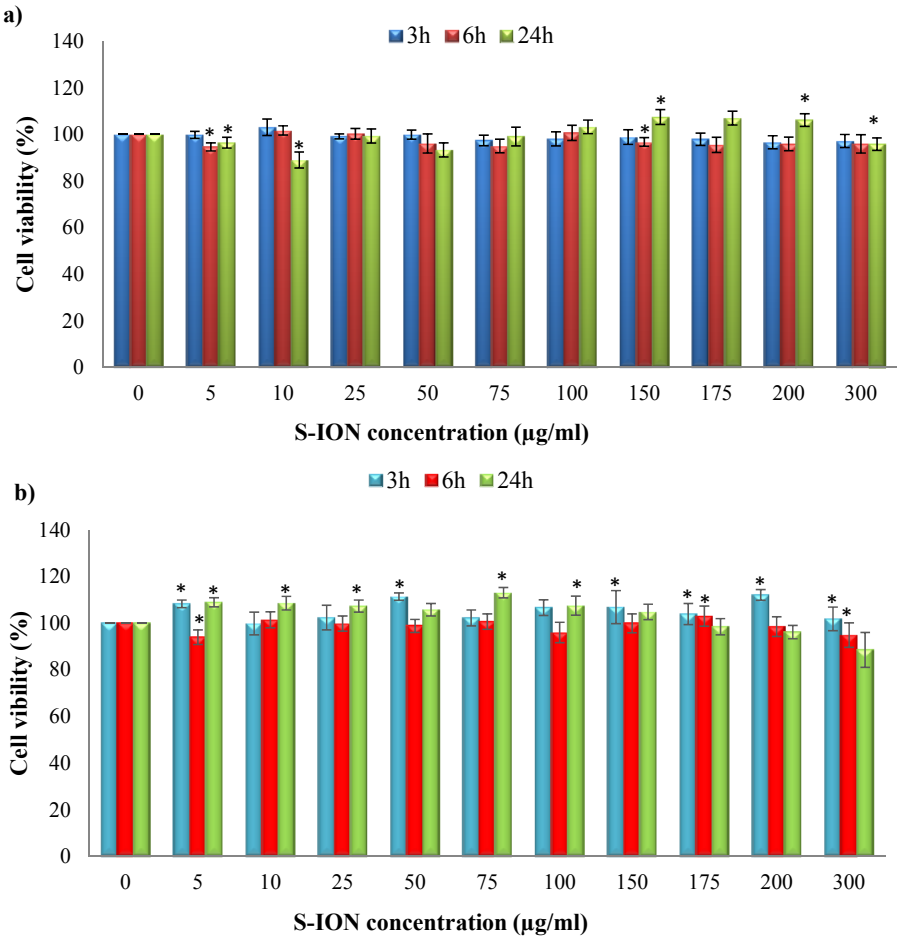

Figure 5.3. Viability of SH-SY5Y cells after exposure to S-ION assessed by MTT assay (a) and NRU assay (b). Values were normalized considering negative control as 100%. PC: positive control. *P<0.05, significant difference with regard to the corresponding negative control.

There are several *in vitro* studies that have demonstrated little or no toxicity of ION. For instance, Malvindi et al. (2014) reported that S-ION had no effect on cellular viability of A549 and HeLa cells, which led to the suggestion that these are biocompatible nanomaterials (Boyer et al., 2010). However, earlier studies on neurotoxicity of ION revealed a decrease in viability of mouse neuroblastoma cells (Jeng and Swanson, 2006), astrocytes (Au et al., 2007), brain glioma cells (Xiao et al., 2014) and pheochromocytoma neuronal cell lines (Pisanic et al., 2007) after exposure to ION.

Previous studies stated that ION are stored in lysosomes where they degraded to free iron by lysosomal enzymatic activity (Laskar et al., 2012). Free iron ions can affect mitochondrial membrane and/or increase radical concentration. In addition, ION can also directly damage mitochondria by causing morphological alterations or decrease in mitochondrial membrane potential (Fröhlich, 2013; Sioutas et al., 2005).

It is well known that MTT assay provides information on mitochondrial activity (Hillegass et al., 2010), whereas NRU assay evaluates lysosomal integrity (Repetto et al., 2008). These results showing lower viability detected by MTT assay than NRU assay suggest that mitochondria is particularly sensitive to the ION tested in the current study, which is in accordance with prior works (Jeng and Swanson, 2006). From the results of cell viability assays the doses and exposure periods of S-ION for further toxicity assays were determined: 10, 50, 100 and 200µg/ml for 3 and 24h.

5.3.3. *Dissolved iron concentrations in the cell culture medium*

Upon metabolisation of ION, free iron can be transferred out of the endocytic compartment into the normal cellular iron pool (Soenen et al., 2010). Iron is an innate metal that is essential for life, mainly because of its ability to accept and donate electrons readily by switching between ferrous (Fe^{2+}) and ferric (Fe^{3+}) ions (Kim et al., 2012). This reduction-oxidation reaction plays a critical role in energy production and in many other metabolic pathways such as DNA synthesis, mitochondrial oxidative phosphorylation, oxygen transport, and cytochrome P450 function (Shander et al., 2009). The total quantity of iron in the body is tightly regulated, because excess iron can be extremely toxic (Kunzmann et al., 2011). It can affect cellular functionality (e.g., by altering the level of transferrin receptor expression) (Schäfer et al., 2007), as well as cellular proliferation capacity (Huang et al., 2009), among other effects. As it can be seen from Figure 5.4, the release of iron ions from the S-ION was found to be generally increasing with exposure time and NP dose at the 3 times tested.

Relevantly increased intracellular iron levels were found in different cells after ION exposure (reviewed in Soenen and De Cuyper, 2009), though usually not initially associated with cytotoxicity (Geppert et al., 2009; Hohnholt et al., 2013; Rosenberg et al., 2012). However this release can vary depending on the suspension conditions (e.g., pH) and the NP surface

coating (Malvindi et al., 2014). NP chemical synthesis, their physico-chemical properties and the surface coating which surrounds and isolates the magnetic material from the environment, may influence the degradation rate of the particles and so the release of iron ions (Lévy et al., 2010; Mahon et al., 2012). This would explain the iron release observed into cell culture medium, since ION might be externally interacting with serum proteins present in the medium thus enabling their ability to release ions.

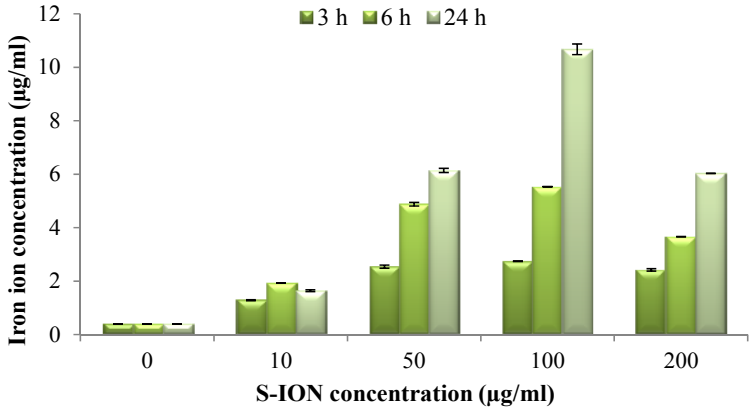

Figure 5.4. Iron ion release from S-ION.

5.3.4. *Cellular uptake*

The evaluation of cellular uptake of NP by FCM using side scatter parameter (indicative of cell granularity/complexity) is suitable for initial screening of nanotoxicity (Ibuki and Toyooka, 2012). Results obtained from testing the ability of S-ION to enter the human neuroblastoma cells are shown in Figure 5.5. NP were effectively internalized by the cells at all conditions tested in a dose-dependent manner (r=0.737, $P<0.01$ for 3h treatment, and r=0.692, $P<0.01$ for 24h treatment).

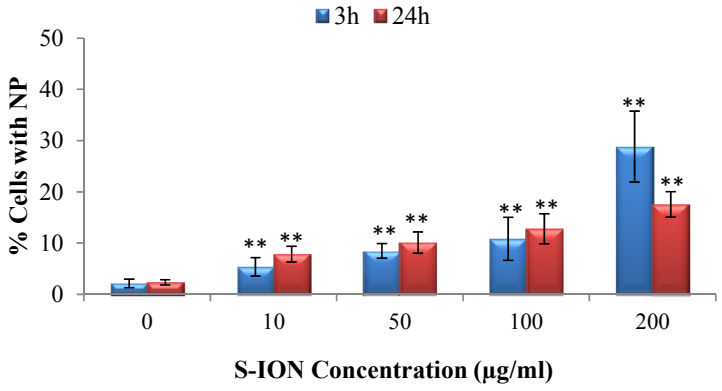

Figure 5.5. Cellular uptake of S-ION as analysed by FCM. $^{**}P<0.01$, significant difference with regard to the corresponding control.

These findings agree with previous studies in other cell types showing that S-ION are quickly internalized by macrophages (Kunzmann et al., 2011), and by A549 and HeLa cells (Malvindi et al., 2014). In which regards to neural cells, exposure of cultured rat microglial cells to ION caused a time-, concentration- and temperature-dependent uptake of the particles, predominantly mediated by macropinocytosis and clathrin-mediated endocytosis (Luther et al., 2013).

Besides, this *in vitro* study revealed a remarkable lower degree of internalization for the highest S-ION concentration at 24h when compared to the one obtained at 3h. This is likely due to the progressive S-ION agglomeration at this high concentration, which causes a more noticeable interference with the uptake process at the longest exposure period.

5.3.5. *Cell cycle*

Cell cycle machinery corresponds to series of events which lead the cell to its division and duplication (Morgan, 2007). Figure 5.6 shows the cell distribution along the various phases of the cell cycle after exposing the neuronal cells to S-ION. The 3h treatments did not modify the cell cycle, and significant alterations at 24h treatments were only observed for the highest concentration tested (decrease in G_2/M phase and increase in S phase).

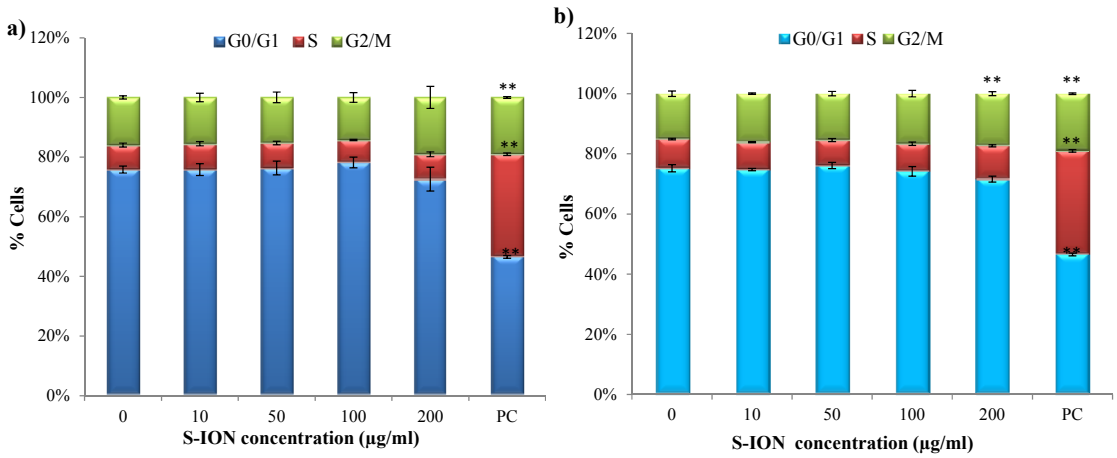

Figure 5.6. Cell cycle analysis of SHSY-5Y cells after exposure to S-ION: (a) 3h treatment; (b) 24h treatment. PC: positive control. ***P*<0.01, significant difference with regard to the corresponding negative control.

Negative results obtained for 3h exposure to S-ION agree with previous findings from some other studies using bare or differently coated ION (Mahmoudi et al., 2011). Besides, alterations in the cell cycle similar to the ones observed at 24h treatment were obtained by Namvar et al. (2014) after exposing Jurkat cells to bare magnetite NP prepared by green biosynthesis (using a brown seaweed), but the dose used was much lower (6.4µg/ml, corresponding to the inhibitory concentration 50 [IC_{50}], calculated by MTT assay). In the cell viability experiments with S-ION, viabilities obtained for treatments up to 200µg/ml were

always higher than 85% as calculated by MTT and NRU; therefore cytotoxicity of the current S-ION, at least to SH-SY5Y cells, was much lower than cytotoxicity of the ION used by Namvar et al. (2014) in Jurkat cells. These observations agree with the general assumption that ION coated with silica are indeed less toxic that bare ION. Besides, in a very recently published study, Couto et al. (2015) did not find any alteration on cell cycle when testing polyacrylic acid (PAA)-coated and non-coated ION on human T lymphocytes (48h treatments).

5.3.6. *Apoptosis and necrosis*

The two principal modes of cell death are apoptosis and necrosis, which can be distinguished by morphological and biochemical features. While necrosis is usually induced by pathological and accidental damage to cells, apoptosis accounts for most of the physiological cell death and is a tightly regulated process controlled by a complex set of molecules (Elmore, 2007).

To further investigate whether treatments with S-ION were able to induce cell death by apoptosis or necrosis, we used two alternative strategies: analysis of the $subG_1$ region of the cell cycle distribution, indicative of DNA fragmentation at the late stages of apoptosis, and double staining with annexin V and PI for sensitive detection of early stage apoptosis and late stage apoptosis/necrosis.

The $subG_1$ region of the cell cycle distribution was evaluated since DNA fragmentation, which occurs late in the apoptosis process, results in the appearance of PI-stained events containing $subG_1$ levels of genetic material (Fraker et al., 1995). Data obtained are gathered in Figure 5.7; no significant increase in the $subG_1$ fraction was observed after either 3 or 24h treatments.

Similarly, results obtained from the annexin V/PI staining analyses showed that S-ION did not induce early apoptosis (events positive for annexin V but negative for PI) at any concentration after 3h of exposure (Figure 5.8). After 24h of treatment significant increases in apoptosis rate could only be observed for the highest doses assayed (100 and 200µg/ml). No significant induction of necrosis/late apoptosis (events positive for both annexin V and PI) was obtained at any experimental condition tested.

The different results observed in the 24h treatment between the two techniques used may be explained by their methodological differences. Annexin V/PI measurement is carried out right after the treatments and reflects early stage apoptosis, whereas $subG_1$ region analysis is performed after an additional 24h incubation period following the treatments, and is indicative of late stage apoptosis. Hence, probably the cells undergoing early apoptosis detected by annexin V/PI staining have already been mostly removed when $subG_1$ region was analysed.

Similar apoptosis results were reported by Jeng and Swanson, (2006), who found that ION only induce apoptosis in mouse Neuro-2A neuroblastoma cells after exposure to

concentrations higher than 100µg/ml. Contrarily, Namvar et al. (2014) described time-dependent (from 12 to 48h) increases in the apoptosis rates in Jurkat cells treated with bare magnetite NP (6.4µg/ml), evaluated by the two same methodologies used in the current work, but, in their study, toxicity of these ION (in terms of cell viability decrease) was much higher. Malvindi et al. (2014) also found significant apoptosis induction (evaluated by means of mitochondrial membrane potential, JC-1 assay) in cervical and lung cells exposed to 2.5nM S-ION (magnetite) for 48h. This concentration is equivalent to approximately 30µg/ml of our S-ION, dose which produced negative results in all conditions tested in this study.

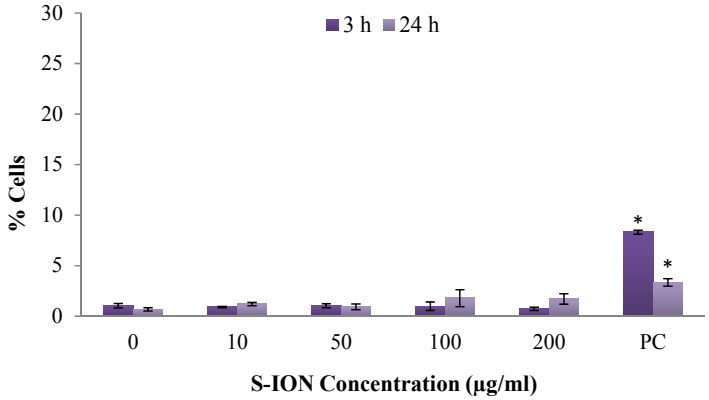

Figure 5.7. Apoptosis (subG$_1$ region) in neuronal cells treated with S-ION. PC: positive control. **P*<0.05, significant difference with regard to the corresponding negative control.

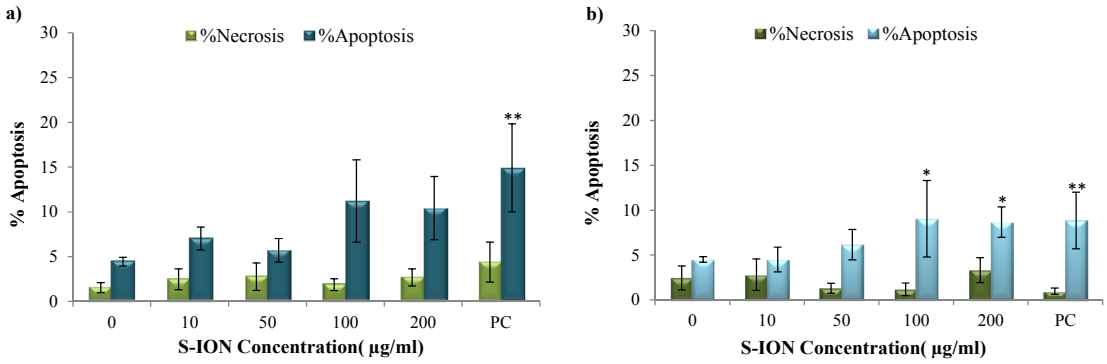

Figure 5.8. Apoptosis and necrosis induction by S-ION for 3h (a) and 24h (b) evaluated by annexinV/PI staining. PC: positive control. **P*<0.05, ***P*<0.01, significant difference with regard to the corresponding negative control.

Regarding cell death by necrosis (and/or late apoptosis), Namvar et al. (2014) obtained again results contrary to ours: time-dependent increase in the necrosis/late apoptosis rate in Jurkat cells treated with ION but, as mentioned above, toxicity of these nanoparticles (in terms of cell viability decrease) was much higher.

5.3.7. *Membrane integrity*

The potential alterations in the neuronal cell membrane integrity caused by S-ION exposure were measured by LDH activity in extracellular medium, since LDH is released when the cell membrane is damaged. Results obtained in this test are represented in Figure 5.9. No significant alteration in the percentage of LDH activity was observed at any concentration or treatment time tested.

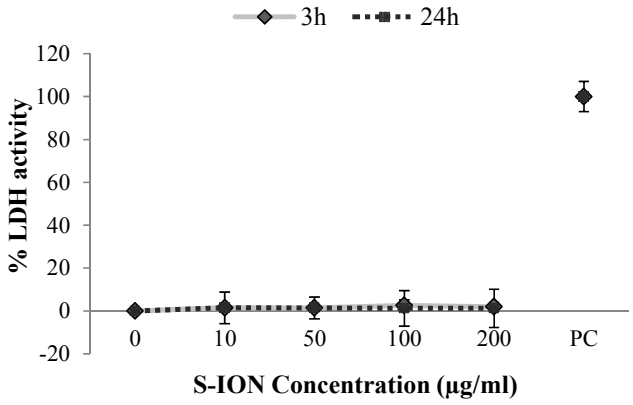

Figure 5.9. LDH leakage analysis after S-ION exposure. PC: positive control.

These negative results are essentially in agreement with most results obtained from cell cycle analysis, apoptosis or necrosis induction, and viability assays. Nevertheless, Malvindi et al. (2014) obtained positive LDH leakage after treatment of A549 and HeLa cells for 48 and 96h with 2.5nM S-ION (as already mentioned, equivalent to 30µg/ml of the current S-ION), according to their apoptosis assessment results and confirming the lower cytotoxicity of the S-ION.

5.3.8. *Genotoxicity*

For testing the potential of S-ION to induce damage on genetic material, we used a battery of genotoxicity tests, i.e., γH2AX assay, MN test, and comet assay.

As a rapid screening method for genotoxicity, we first analysed H2AX phosphorylation by FCM, an early cellular response to the induction of DSB. As it can be clearly seen in Figure 5.10, S-ION did not induce γH2AX at either of the conditions analysed. Yet, no other study employing γH2AX assay for testing genotoxicity caused by any type of ION could be found in the literature. In order to quantify chromosome alterations a relatively less specific approach, the MN test scored by FCM, was performed. The results of MN evaluation showed that no significant changes were produced in the MN ratio after treatment of the neuronal cells with S-ION (Figure 5.11). Comet assay results revealed that S-ION induced dose-dependent increases

of DNA damage in SH-SY5Y cells (r=0.948, $P<0.05$ for 3h treatment, and r=0.842, $P<0.05$ for 24h treatment) (Figure 5.12).

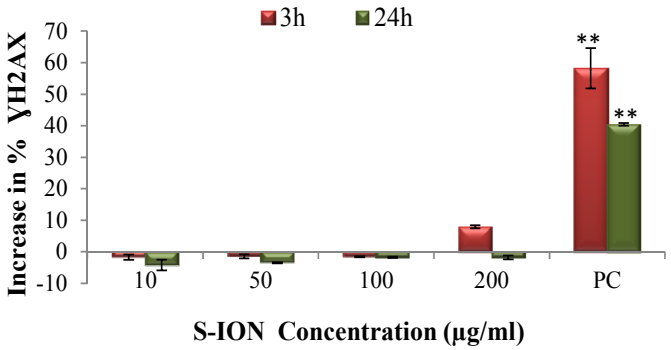

Figure 5.10. Results of γH2AX analysis on neuronal cells treated with S-ION. PC: positive control. $^{**}P<0.01$, significant difference with regard to the corresponding negative control.

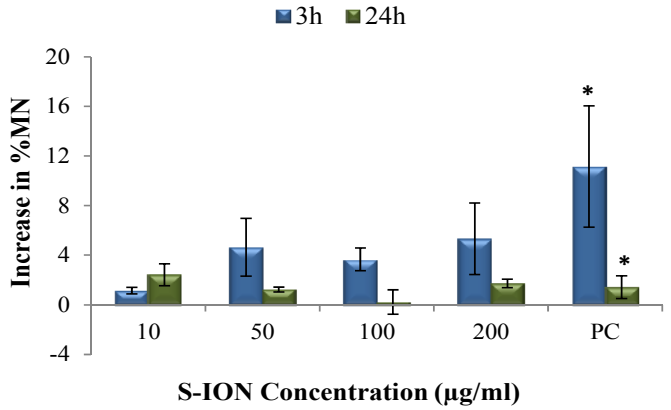

Figure 5.11. Results of MN evaluation in SH-SY5Y cells treated with S-ION. PC: positive control. $^{*}P<0.05$, significant difference with regard to the negative control.

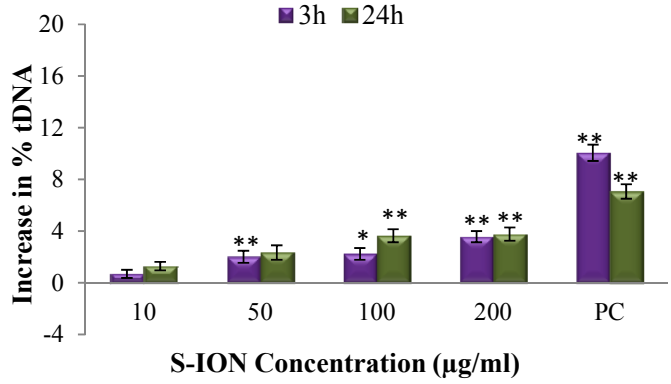

Figure 5.12. Results of comet assay in neuronal cells treated with S-ION. PC: positive control. $^{*}P<0.05$; $^{**}P<0.01$, significant difference with regard to the corresponding negative control.

The purpose of MN test is to identify chromosome aberrations, since MN may contain lagging chromosome fragments or whole chromosomes; therefore it detects both clastogenic and aneugenic events. After S-ION treatment no effects were observed in the neuronal cells in terms of MN formation. To our knowledge no studies have been reported on MN induction by S-ION in any type of cells so far, but passiveness of other types of ION on MN formation have been documented in cells from different origin both *in vitro* (Li et al., 2011; Shah et al., 2013; Singh et al., 2010; Zhang et al., 2012) and *in vivo* (Chen et al., 2012a; Li et al., 2011; Wu et al., 2010b).

The comet assay is one of the most frequently used methods for genotoxicity testing. Since it is simple, versatile, and able to detect different DNA lesions, it has been claimed to be the most promising assay to measure potential genotoxicity of nanomaterials (reviewed in Magdolenova et al., 2014). Hence, in this study, it was used for measuring primary DNA damage in SH-SY5Y cells caused by exposure to S-ION.

This dose- and time-dependent increase in the comet parameter after S-ION treatments is in agreement with the iron ion dissolution results, which showed important amounts of ions released from the NP into the cell culture medium. Although the human body contains relatively high concentrations of iron, the presence this metal at concentrations higher than physiological can lead to deleterious effects. Iron ions are able to interact with DNA in-between the bases, thereby unwinding the double-helix (Eichhorn and Shin, 1968) and causing SSB and oxidative base modification (Toyokuni and Sagripanti, 1999); this kind of damage, especially SSB, is detected by the standard alkaline comet assay but is not related to phosphorylation of H2AX or MN production. Therefore, this may help to explain the positive results obtained in the comet assay and the negative ones from H2AX assay and MN test.

These results provide evidence that a single genotoxicity assay is not sufficient to draw conclusions regarding the genotoxic potential of nanomaterials. It was already indicated that no single test can cover all the potential forms of DNA damage that might arise (Singh et al., 2009 ; Zhao and Castranova, 2011), so negative results obtained in one test do not guarantee that the ION assayed is free of genetic damage induction. According to the current results, the type of DNA damage induced by S-ION on neuronal cells is likely not related to DSB but mostly to more easily repairable DNA lesions (alkali labile sites and SSB), indicating recent damage (Azqueta and Collins, 2013).

Similar increases in comet assay parameters (tail length and tail DNA intensity) were shown by Malvindi et al. (2014) after incubation of A549 and HeLa cells with S-ION for 48h. In addition, comet assay evaluation of murine L-929 fibroblast cells treated with ION coated with (3-aminopropyl) trimethoxysilane (APTMS), tetraethyl-orthosilicate (TEOS)-APTMS, or citrate showed a concentration-dependent increase in tail content of DNA compared to control cells, indicating the presence of DNA damage (Hong et al., 2011). By using the same technique, Bhattacharya et al. (2009) had previously found DNA damage induction on human lung IMR-90

fibroblasts and human bronchial epithelial BEAS-2B cells treated with ION (Fe_2O_3). Moreover, no induction of chromosome aberrations (which require DSB production) was observed in human T lymphocytes treated with PAA-coated and non-coated ION (Couto et al., 2015), which further supports these results.

5.3.9. *Oxidative stress*

Among the different mechanisms that can cause NP toxicity in the body, it seems that the most toxicity from ION arise from the production of excess ROS (Nel et al., 2006; Shubayev et al., 2009; Soenen and De Cuyper, 2009; Unfried et al., 2007). High ROS levels can damage cells by producing lipid peroxidation, mitochondrial damage, DNA disruption, gene transcription modulation, and protein oxidation, which would eventually result in cell apoptosis/death (Stroh et al., 2004). Hence in this study, the oxidative stress produced by S-ION was evaluated by three different endpoints, namely DCFH assay, cellular GSH:GSSG determination, and OGG1-modified comet assay.

DCFH assay has been shown to be a useful tool for the quantitative measurement of NP-induced oxidative stress (Aranda et al., 2013). The logic behind this technique is basically that, in the presence of ROS, DCFH is rapidly oxidized to the highly fluorescent DCF, which is readily detectable. The dye is susceptible to reaction with a variety of ROS, including hydrogen peroxide, peroxyl radicals and peroxynitrite anions, to form DCF (LeBel et al., 1992).

Firstly, to assess the possibility that ION may generate ROS intrinsically and exclude their interference with dyes, we measured the production of ROS in cell free systems. As it can be seen from Figure 5.13, S-ION were unable to produce ROS in the absence of cells, which coincides with findings of similar previous studies (Bhatt and Tripathi, 2011; Guichard et al., 2012).

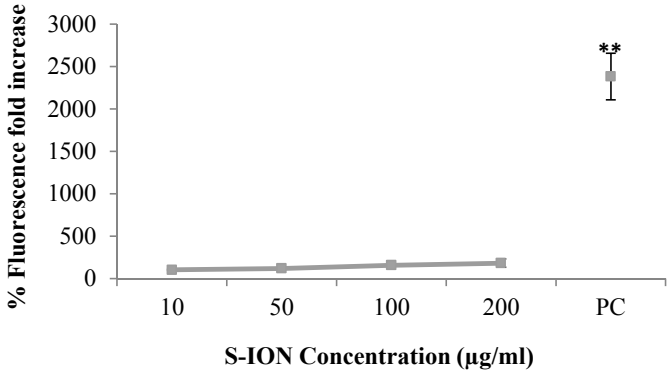

Figure 5.13. Results of the acellular DCFH assay with S-ION, expressed as %fluorescence fold increase. PC: positive control.

Since H_2O_2 cannot oxidize DCFH by itself, the enzyme HRP is added to catalyze generation of OH radicals. Therefore, HRP was added only when H_2O_2 was used (positive control). However, considerable inconsistency exist in the literature with regards to the addition of HRP to NP while measuring cellular ROS production, its concentration, and the sequence of events with regards to its use (when exactly HRP should be added to the reaction mixture). Addition of HRP to the wells containing NP and to the control increased fluorescence response of both NP treated cells and control cells by ~4-5 times (data not shown). Nevertheless, we have not found significant change in reactivity with regard to the control compared to the experiment without HRP, indicating that the observed increase was caused purely by oxidation of DCFH by HRP, which is known to occur (Rota et al., 1999). Therefore, there seems to be no added value for addition of HRP to the S-ION.

After excluding ROS production potential of S-ION in the absence of cells, it was decided to use a commercial kit, in order to improve the performance of cellular ROS assay to assess the capacity of S-ION to generate ROS in SH-SY5Y cell line. As it can be seen from Figure 5.14, significant increases in ROS generation were found in cells treated for 24h with S-ION at every concentration; whereas for 3h significant increases were only observed at 100 and 200µg/ml concentrations.

Glutathione serves as an endogenous antioxidant against free radicals and thus detoxifies the effect of external toxic materials. Cellular glutathione exists in reduced form (GSH) and oxidized form (GSSG), and their ratio controls various biochemical reactions and determines cellular activities (Hansen et al., 2009). Thus, this part of the research was focused on monitoring GSH: GSSG content in cells after S-ION exposure. Results obtained in this test are shown in Figure 5.15. It was observed that S-ION cause significant decrease in the GSH:GSSG ratio at almost every condition tested, indicative of oxidative stress generation, except for the lowest concentration at 3h treatment.

Lastly, to analyse the role of ROS production by S-ION in triggering and progression of oxidative DNA damage, OGG1 enzyme-modified comet assay was performed; results are shown in Figure 5.16. Neuronal cells exposed to S-ION revealed production of OGG1-sensitive sites at every condition tested, although difference with regard to the buffer was not significant for 3h treatments at low concentrations of S-ION (10 and 50µg/ml).

Taking all oxidative stress results together from these three assays, S-ION did not produce ROS in the acellular environment, but they showed ROS generation and DNA damaging potential at every concentration tested for 24h treatment, and only at the highest concentrations for 3h treatment, agreeing with the results of standard comet assay.

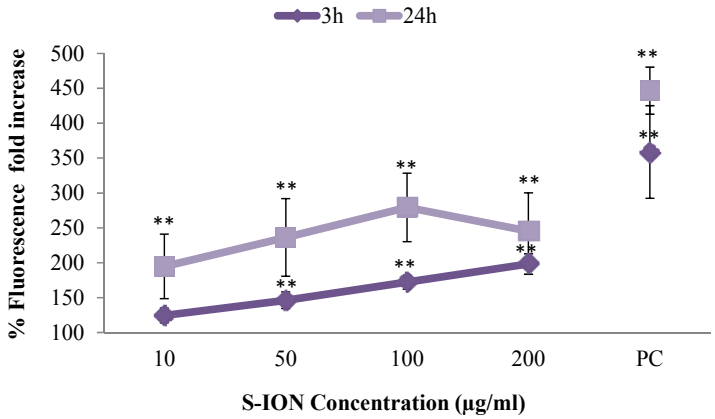

Figure 5.14. Results of the DCFH assay in neuronal cells treated with S-ION, expressed as % fold increase compared to control. PC: positive control. ***P*<0.01, significant difference with regard to the corresponding negative control.

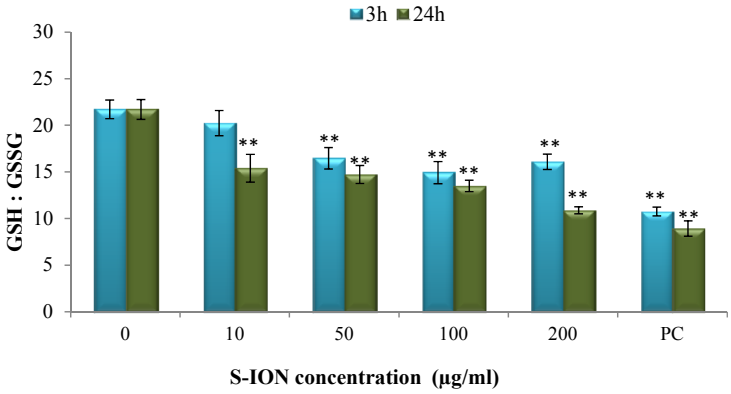

Figure 5.15. Ratio of reduced to oxidised glutathione in neuronal cells treated with S-ION. PC: positive control. ***P*<0.01, significant difference with regard to the corresponding negative control.

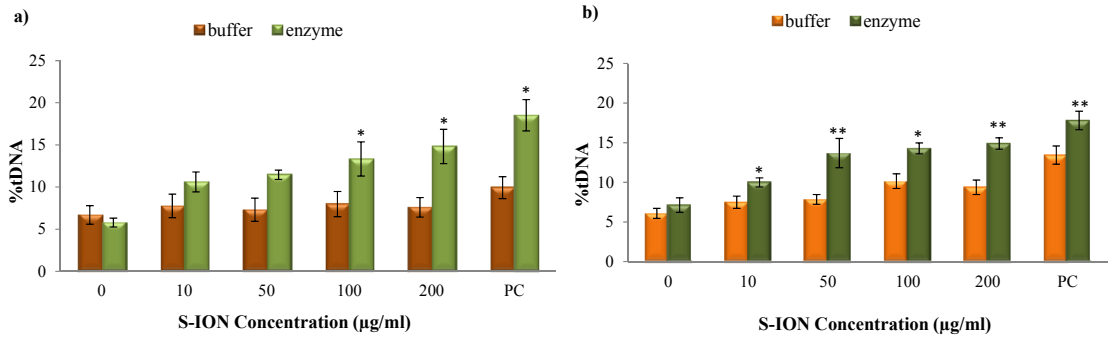

Figure 5.16. Results of OGG1-modified comet assay in neuronal cells treated with S-ION for 3h (a) and 24h (b). PC: positive control. **P*<0.05, ***P*<0.01, significant difference with regard to the corresponding buffer.

The generation of ROS has already been proposed as the underlying mechanism involved in the genotoxicity of metal oxide NP (Mesárošová et al., 2014). And several possible mechanisms that can play a role for ROS generation from ION are also well documented. ROS formation may occur due to iron ions released into the cytosol by lysosomal enzymatic degradation, that can participate in the Fenton reaction and produce hydroxyl (OH·) radicals (Valko et al., 2006), or to the catalytically active surfaces of particles (Klein et al., 2012).

The particle size and surface chemistry have been shown to have great importance in the ROS-mediated activity of ION (Hong et al., 2011; Hoskins et al., 2012). Bare ION might be significantly more toxic than coated ION because iron ions on the surface are more efficient inducers of ROS production (Voinov et al., 2011). However, data published so far are quite controversial. Bare ION were shown to induce ROS generation in human healthy and tumour cells (Choi et al., 2009; Hoskins et al., 2012; Karlsson et al., 2009; Mesárošová et al., 2014; Zhu et al., 2010), rat lung epithelial cells (Ramesh et al., 2012), and Chinese hamster ovary cells (Kawanishi et al., 2013), but not in Syrian hamster embryo cells (Guichard et al., 2012) or human lung adenocarcinoma epithelial A549 cells (Kain et al., 2012; Könczöl et al., 2011; Mesárošová et al., 2014).

The ION-mediated ROS generation was also found to be dependent on surface coating (Guichard et al., 2012; Könczöl et al., 2011; Magdolenova et al., 2012b; Sharma et al., 2014) and cell type (Guadagnini et al., 2013; Liu et al., 2011). Accordingly, increased ROS production, glutathione depletion, and inactivation of several antioxidant enzymes were detected in several human and mammalian cell lines treated with surface-modified ION. For instance, ROS generation was caused by sodium oleate-coated ION in monkey kidney Cos-1 cells (Magdolenova et al., 2012b), and by L-glutamic acid-coated ION (Fe_2O_3) in Chinese hamster lung cells (Zhang et al., 2012). Likewise, ROS production potential of ION coated with Tween 80 was observed in murine macrophage J774 cells (Naqvi et al., 2010).

In this current study with SH-SY5Y cells, ROS formation was found to be increased by S-ION exposure, resulting in decreased GSH and increased DNA damage, although surface coating is initially expected to function as a barrier and attenuate the potential toxic effects (Auffan et al., 2006). Yet, silica coating around the ION did not avoid the whole ROS formation capacity of ION. Kim et al. (2010b) reported that several silica particles smaller than 20nm increased ROS production dose-dependently in the SH-SY5Y human neural cell line, which may help explain these results. Besides, these positive results from S-ION are also consistent with another study showing a dose-dependent increase in ROS formation in SH-SY5Y cells treated with polyethyleneimine-coated ION (Hoskins et al., 2012).

5.3.10. *DNA repair competence assay*

Possible effects of S-ION on DNA repair processes were tested by DNA repair competence assay using H_2O_2 as challenging agent. H_2O_2 causes damage to DNA by generating hydroxyl-free radicals (OH·) (Jaruga and Dizdaroglu, 1996). These radicals attack DNA at the sugar residue of the DNA backbone, leading to SSB (Benhusein et al., 2010). Re-joining of SSB induced by H_2O_2 is a simple cellular process; thousands of breaks per cell can be repaired in a matter of half an hour in typical cultured mammalian cells (Azqueta and Collins, 2013).

In the current study, repair of approximately one-third of the DNA damage after H_2O_2 treatment occurred during a 30 min period (Figure 5.17), thus indicating this time as convenient for H_2O_2-induced DNA damage to be repaired in SH-SY5Y cells. Incubations with the S-ION were carried out at three different stages of the assay: before inducing DNA damage (pre-treatment or phase A, for 3 or 24h), during DNA damage induction (phase B), or during the repair period (phase C).

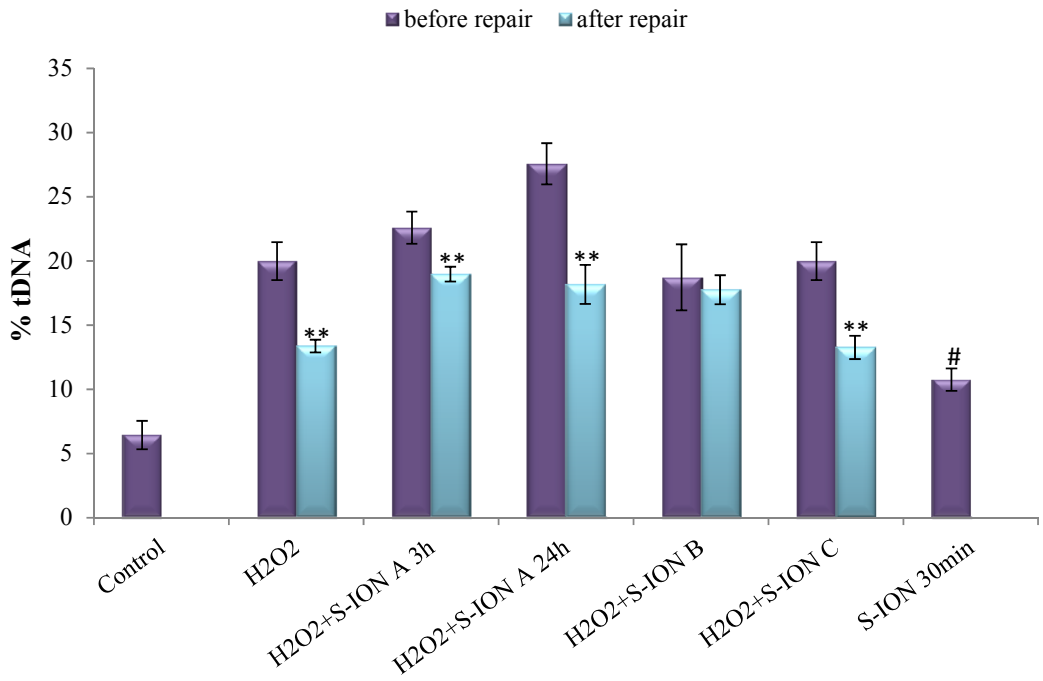

Figure 5.17. Effects of S-ION on repair of H_2O_2-induced DNA damage in neuronal cells. Incubation with S-ION was carried out either before H_2O_2 treatment (phase A), simultaneously (phase B), or during the repair period (phase C). **P*<0.05, ***P*<0.01, significant difference with regard to the same treatment before repair; $^{\#}P$<0.05, significant difference with regard to the control.

When cells were incubated with S-ION before damage induction by H_2O_2 (phase A, either 3 or 24h), %tDNA was significantly reduced implying the pre-incubation with S-ION did not affect the DNA repair process, which was more obvious at incubation for 24h than for 3h. When cells were left to repair the damage induced by H_2O_2 in the presence of S-ION for 30min

(phase C), the DNA damage after the repair process also decreased to the basal levels, although treatment of cells with S-ION for 30min showed a significant induction of damage to DNA. Thus S-ION did not influence the DNA repair machinery either in phase C. However, when cells were incubated with H_2O_2 and S-ION simultaneously (phase B), significant DNA repair was not observed, which would not entirely mean S-ION might be altering the repair process.

As shown before in Figure 5.4, a notable release of iron ions from the S-ION into the cell culture medium was observed. The deleterious effects of transition metal ions, such as iron, to DNA are greatly enhanced by the presence of oxygen and related species; thus, iron ions readily associate with DNA and, in the presence of hydrogen peroxide, a high ratio of DSB to SSB are generated (Lloyd and Phillips, 1999). Since the repair of DSB can take hours (Frankenberg-Schwager, 1989), the result obtained for phase B is probably related to the type of DNA damage induced, for which a 30min repair period is not long enough, more than to alterations in the repair process. To the best of our knowledge, this is the first study addressing the potential effects of ION on cellular repair systems. Therefore, further investigations are required to go into detail about all these findings.

5.4. CONCLUSIONS

In the present study the effects of S-ION on the human SH-SY5Y neuroblastoma cell line were investigated by means of a complete set of cytotoxicity and genotoxicity assays. Taking all results of this study together we can draw the following conclusions:

1. S-ION released iron ions to the cell culture medium in a dose- and time-dependent manner.
2. S-ION were effectively internalized by the neuronal cells but presented in general low cytotoxicity; although positive results were obtained for some experimental conditions, cell viability was higher than 80% in all cases.
3. S-ION exposure did not change neuronal cell membrane integrity, and only induced cell cycle alterations or apoptosis at the highest doses and longest time tested.
4. Treatment of neuronal cells with S-ION induced dose-dependent DNA damage which was not related to the production of DSB or chromosome loss (according to the results of H2AX assay and MN test).
5. Even though S-ION were not able to produce ROS in an acellular environment, ROS formation was found to be increased in the neuronal cells by S-ION exposure, resulting in decreased GSH and increased oxidative DNA damage.
6. According to DNA repair competence assay, DNA repair mechanisms were not affected by S-ION exposure when exposure was carried out before induction of DNA damage or

during the repair period. However, when exposure occurred simultaneously with H_2O_2, the 30 min period was not enough to repair the damage induced.

These results confirm that S-ION can be safely used at low doses as tracers for MRI of oncological tumours and as vehicles for therapeutic drug delivery. When S-ION are guided to regions of brain due to their magnetic properties, they can enhance redox-directed therapeutic effect by increasing ROS levels. Results obtained in this work highlight the need for screening the different possible interactions of NP with the living systems, especially with the nervous system components, in order to increase the knowledge on the effects at different levels and thus be able to guarantee manufacturers' and consumers' safety.

6. CONCLUDING REMARKS

Nanotechnology industry, focussing on the development and production of new nanoscale products for many fields of application, is rapidly growing. The emerging use of nanomaterials leads to their direct contact with the human being and their release to the environment, with still unknown consequences for occupational and environmental health. Metal oxide NP, are versatile platforms for very different uses, including healthcare products, biomedical applications and therapeutic intervention. Ti_2O-NP, ZnO-NP and ION are examples of such widely used engineered NP in the world consumer market.

Furthermore, in the past few decades, the incidence of primary brain tumours has been increasing at an alarming rate (Hu and Gao, 2010). Immense efforts have been focused on the chemotherapy of central nervous system (CNS) diseases. However, the existence of the blood–brain barrier (BBB), which limits the entry of many substances into the brain, makes it difficult to deliver drugs to lesions within the CNS. Thus, as NP made of different materials are mostly able to cross the BBB, nanocarriers appear to be a promising drug brain-targeting strategy (Kreuter, 2001). Besides, as NP can move inside the brain from the nasal cavity (Oberdörster et al., 2009), either intentionally instilled or coming from environmental exposures, they could accumulate within this organ to elicit further toxicity. Therefore, the neurotoxicity of NP should be carefully evaluated. In the present study, an attempt was made to evaluate the *in vitro* toxicity of Ti_2O-NP, ZnO-NP and S-ION on the human nervous system, and to elucidate the possible mechanisms underlying the neuronal cell response to these exposures. The human neuroblastoma cells (SH-SY5Y) were selected for assessing the NP toxicity, keeping in view the fact that those cells are frequently used in neurobiological, neurochemical and neurotoxicologial studies (Di Daniel et al., 2005; Hong et al., 2003) .

The results of this study demonstrated that all NP tested have some level of cytotoxic or genotoxic potential in *in vitro* system. But cytotoxicity inducing potential of metal oxide NP was found to be different for each NP. TiO_2-NP did not reduce the viability of neuronal cells and S-ION presented in general low cytotoxicity. ZnO-NP, however, induced significant concentration-dependent decreases in neuronal cell viability.

Their internalization potential by the neuronal cells was also found to be divergent. TiO_2-NP and S-ION were effectively internalized in a concentration and time-dependent manner; nevertheless, ZnO-NP were not taken up by the neuronal cells at any experimental condition assayed. Hence, it was also checked whether the observed decrease in viability by exposure to ZnO-NP could be due to the NP or to the Zinc(II)ions dissolved from them. Yet released Zinc(II)ions to the cell culture were insufficient to cause decrease in neuronal cell viability. Therefore, data also suggested that the NP dissolution does not play a significant role in ZnO-NP induced cytotoxicity.

Despite the differences in their crystalline structures, both TiO_2-NP tested induced dose-dependent cell cycle alterations and apoptosis by intrinsic pathway. Moreover, although

exposure to ZnO-NP did not alter neuronal cell membrane integrity, they caused important cell cycle alterations, including mitotic arrest and apoptosis induction by a mitochondria-independent pathway, whereas S-ION exposure did not change neuronal cell membrane integrity, and only induced cell cycle alterations or apoptosis at the highest doses and longest time tested.

Similar to cytotoxicity, genotoxicity inducing potential of metal oxide NP was found to be different for each NP. Genotoxicity assays with TiO_2-NP exposed neuronal cells revealed positive results in the comet assay and MN test, but negative results in γH2AX assay, suggesting that TiO_2-NP induce genotoxicity in neuronal cells not related to the production of DSB. ZnO-NP caused genotoxicity as measured by comet assay, MN test and γH2AX assay, depending on the exposure time. Besides, treatment of neuronal cells with S-ION showed positive results in the comet assay but negative results in γH2AX assay and MN test, indicating that they induce dose-dependent DNA damage which is not related to the production of DSB or chromosome loss. Additionally, possible effect of S-ION on DNA repair mechanisms was also checked; no influence was observed when exposure was carried out before induction of DNA damage or during the repair period. But when exposure occurred simultaneously with the DNA damage inducer (H_2O_2), the 30min incubation period was not enough to repair the damage induced.

Toxicity was found to be mediated by oxidative stress in ZnO-NP and S-ION exposed cells, as evidenced by decrease in the GSH:GSSG and increase in the oxidative DNA damage. On the other hand, TiO_2-NP did not induce such oxidation-related changes, suggesting that their effects are not associated with oxidative stress generation.

This work contributes to increase the knowledge on cytotoxic and genotoxic potential of metal oxide NP in general, and specifically on human neuronal cells. Results obtained highlight the need for screening the different possible interactions of NP with the living systems, in order to reveal their effects at different levels. These investigations are needed to develop the necessary safety precautions and exposure limits for people working with or producing materials containing these NP, and also for those who might be exposed to them when ENM are implemented in commercial, industrial and biomedical applications. Specifically, when these nanomaterials are designed for being in direct contact with the human being or even to be introduced in the human organism, it is of paramount importance to determine that they are safe enough; in other words, that the relationship benefit-to-risk is favourable and thus their enormous possibilities may be well-exploited with no or minimal health hazards.

7. REFERENCES

Adamcakova-Dodd, A., Stebounova, L.V., Kim, J.S., Vorrink, S.U., Ault, A.P., O'Shaughnessy, P.T., Grassian, V.H., and Thorne, P.S. (2014). Toxicity assessment of zinc oxide nanoparticles using sub-acute and sub-chronic murine inhalation models. Part. Fibre Toxicol. *11*, 15.

Adamson, A.W. (1990). Physical chemistry of surfaces (Wiley).

Adjei, I.M., Sharma, B., and Labhasetwar, V. (2014). Nanoparticles: cellular uptake and cytotoxicity. Adv. Exp. Med. Biol. *811*, 73–91.

Akhtar, M.J., Ahamed, M., Kumar, S., Khan, M.M., Ahmad, J., and Alrokayan, S.A. (2012). Zinc oxide nanoparticles selectively induce apoptosis in human cancer cells through reactive oxygen species. Int. J. Nanomedicine *7*, 845–857.

Alarifi, S., Ali, D., Alkahtani, S., Verma, A., Ahamed, M., Ahmed, M., and Alhadlaq, H.A. (2013). Induction of oxidative stress, DNA damage, and apoptosis in a malignant human skin melanoma cell line after exposure to zinc oxide nanoparticles. Int. J. Nanomedicine *8*, 983–993.

Alberts, B., Johnson, A., Lewis, J., Raff, M., Roberts, K., and Walter, P. (2002). An Overview of the Cell Cycle. In Molecular Biology of the Cell. 4th Edition, (Garland Science),.

Alkilany, A.M., and Murphy, C.J. (2010). Toxicity and cellular uptake of gold nanoparticles: what we have learned so far? J. Nanoparticle Res. *12*, 2313–2333.

Alwi, R., Telenkov, S., Mandelis, A., Leshuk, T., Gu, F., Oladepo, S., and Michaelian, K. (2012). Silica-coated super paramagnetic iron oxide nanoparticles (SPION) as biocompatible contrast agent in biomedical photoacoustics. Biomed. Opt. Express *3*, 2500–2509.

Ando, Y., and Kumar, M. (2010). A special issue on carbon nanotubes. There's plenty of room at the bottom... in the CNT basement strengthen the foundation before erecting the sky-tower. J. Nanosci. Nanotechnol. *10*, 3723–3725.

Aranda, A., Sequedo, L., Tolosa, L., Quintas, G., Burello, E., Castell, J.V., and Gombau, L. (2013). Dichloro-dihydro-fluorescein diacetate (DCFH-DA) assay: a quantitative method for oxidative stress assessment of nanoparticle-treated cells. Toxicol. Vitro Int. J. Publ. Assoc. BIBRA *27*, 954–963.

Armand, L., Dagouassat, M., Belade, E., Simon-Deckers, A., Le Gouvello, S., Tharabat, C., Duprez, C., Andujar, P., Pairon, J.-C., Boczkowski, J., et al. (2013). Titanium dioxide nanoparticles induce matrix metalloprotease 1 in human pulmonary fibroblasts partly via an interleukin-1β-dependent mechanism. Am. J. Respir. Cell Mol. Biol. *48*, 354–363.

Arruebo, M., Fernández-Pacheco, R., Ibarra, M.R., and Santamaría, J. (2007). Magnetic nanoparticles for drug delivery. Nano Today *2*, 22–32.

Arturo I Martinez, M.A.G.-L. (2009). Study Of The Properties Of Iron Oxide Nanostructures. In Research in Nanotechnology Developments, (Nova Science Publishers, Inc.),.

Asci, R., Vallefuoco, F., Andolfo, I., Bruno, M., De Falco, L., and Iolascon, A. (2013). Trasferrin receptor 2 gene regulation by microRNA 221 in SH-SY5Y cells treated with MPP^+ as Parkinson's disease cellular model. Neurosci. Res. *77*, 121–127.

AshaRani, P.V., Low Kah Mun, G., Hande, M.P., and Valiyaveettil, S. (2009). Cytotoxicity and Genotoxicity of Silver Nanoparticles in Human Cells. ACS Nano *3*, 279–290.

Au, C., Mutkus, L., Dobson, A., Riffle, J., Lalli, J., and Aschner, M. (2007). Effects of nanoparticles on the adhesion and cell viability on astrocytes. Biol. Trace Elem. Res. *120*, 248–256.

Au, K.-W., Liao, S.-Y., Lee, Y.-K., Lai, W.-H., Ng, K.-M., Chan, Y.-C., Yip, M.-C., Ho, C.-Y., Wu, E.X., Li, R.A., et al. (2009). Effects of iron oxide nanoparticles on cardiac differentiation of embryonic stem cells. Biochem. Biophys. Res. Commun. *379*, 898–903.

Auffan, M., Rose, J., Wiesner, M.R., and Bottero, J.-Y. (2009). Chemical stability of metallic nanoparticles: a parameter controlling their potential cellular toxicity in vitro. Environ. Pollut. Barking Essex 1987 *157*, 1127–1133.

Azqueta, A., and Collins, A.R. (2006). The Comet Assay: A Sensitive and Quantitative Method for Analysis of DNA Damage. In Encyclopedia of Analytical Chemistry, (John Wiley & Sons, Ltd),.

Azqueta, A., and Collins, A.R. (2013). The essential comet assay: a comprehensive guide to measuring DNA damage and repair. Arch. Toxicol. *87*, 949–968.

Baan, R., Straif, K., Grosse, Y., Secretan, B., El Ghissassi, F., Cogliano, V., and WHO International Agency for Research on Cancer Monograph Working Group (2006). Carcinogenicity of carbon black, titanium dioxide, and talc. Lancet Oncol. *7*, 295–296.

Baeza-Squiban, A., and Lanone, S. (2011). Exposure, Uptake, and Barriers. In Nanoethics and Nanotoxicology, P. Houdy, M. Lahmani, and F. Marano, eds. (Springer Berlin Heidelberg), pp. 37–61.

Barbara Rothen-Rutishauser, DagmarA Kuhn, Dimitri Vanhecke, Fabian Herzog, Alke Petri-Fink, and MartinJD Clift (2014). Cellular Uptake and Intracellular Trafficking. In Nanoparticles in the Lung, (CRC Press), pp. 147–166.

Beard, J.L. (2001). Iron Biology in Immune Function, Muscle Metabolism and Neuronal Functioning. J. Nutr. *131*, 568S – 580S.

Becker, K., Schroecksnadel, S., Geisler, S., Carriere, M., Gostner, J.M., Schennach, H., Herlin, N., and Fuchs, D. (2014). TiO(2) nanoparticles and bulk material stimulate human peripheral blood mononuclear cells. Food Chem. Toxicol. Int. J. Publ. Br. Ind. Biol. Res. Assoc. *65*, 63–69.

Begley, D.J. (1996). The blood-brain barrier: principles for targeting peptides and drugs to the central nervous system. J. Pharm. Pharmacol. *48*, 136–146.

Benhusein, G.M., Mutch, E., Aburawi, S., and Williams, F.M. (2010). Genotoxic effect induced by hydrogen peroxide in human hepatoma cells using comet assay. Libyan J. Med. *5*.

De Berardis, B., Civitelli, G., Condello, M., Lista, P., Pozzi, R., Arancia, G., and Meschini, S. (2010). Exposure to ZnO nanoparticles induces oxidative stress and cytotoxicity in human colon carcinoma cells. Toxicol. Appl. Pharmacol. *246*, 116–127.

Bhatt, I., and Tripathi, B.N. (2011). Interaction of engineered nanoparticles with various components of the environment and possible strategies for their risk assessment. Chemosphere *82*, 308–317.

Bhattacharya, K., Davoren, M., Boertz, J., Schins, R.P., Hoffmann, E., and Dopp, E. (2009). Titanium dioxide nanoparticles induce oxidative stress and DNA-adduct formation but not DNA-breakage in human lung cells. Part. Fibre Toxicol. *6*, 17.

Bilski, P., Belanger, A.G., and Chignell, C.F. (2002). Photosensitized oxidation of 2',7'-dichlorofluorescin: singlet oxygen does not contribute to the formation of fluorescent oxidation product 2',7'-dichlorofluorescein. Free Radic. Biol. Med. *33*, 938–946.

Binnig, G., and Rohrer, H. (1986). Scanning tunneling microscopy.

Blaunstein, R., and Linkov, I. (2010). Chapter 5 - Nanotechnology Risk Management: An Insurance Industry Perspective. In Nanotechnology Environmental Health and Safety, M. Hull, and D. Bowman, eds. (Boston: William Andrew Publishing), pp. 143–179.

Bonner, W.M., Redon, C.E., Dickey, J.S., Nakamura, A.J., Sedelnikova, O.A., Solier, S., and Pommier, Y. (2008). γH2AX and cancer. Nat. Rev. Cancer *8*, 957–967.

Borenfreund, E., and Puerner, J.A. (1985). Toxicity determined in vitro by morphological alterations and neutral red absorption. Toxicol. Lett. *24*, 119–124.

Borm, P.J.A., Robbins, D., Haubold, S., Kuhlbusch, T., Fissan, H., Donaldson, K., Schins, R., Stone, V., Kreyling, W., Lademann, J., et al. (2006). The potential risks of nanomaterials: a review carried out for ECETOC. Part. Fibre Toxicol. *3*, 11.

Botelho, M.C., Costa, C., Silva, S., Costa, S., Dhawan, A., Oliveira, P.A., and Teixeira, J.P. (2014). Effects of titanium dioxide nanoparticles in human gastric epithelial cells in vitro. Biomed. Pharmacother. Bioméd. Pharmacothérapie *68*, 59–64.

Botta, A., and Benameur, L. (2011). Nanoparticle Toxicity Mechanisms: Genotoxicity. In Nanoethics and Nanotoxicology, P. Houdy, M. Lahmani, and F. Marano, eds. (Springer Berlin Heidelberg), pp. 111–146.

Bourton, E.C., Plowman, P.N., Smith, D., Arlett, C.F., and Parris, C.N. (2011). Prolonged expression of the γ-H2AX DNA repair biomarker correlates with excess acute and chronic toxicity from radiotherapy treatment. Int. J. Cancer J. Int. Cancer *129*, 2928–2934.

Boyer, C., Whittaker, M.R., Bulmus, V., Liu, J., and Davis, T.P. (2010). The design and utility of polymer-stabilized iron-oxide nanoparticles for nanomedicine applications. NPG Asia Mater. *2*, 23–30.

Bréchignac, C., Houdy, P., and Lahmani, M. (2010). In Nanomaterials and Nanochemistry, (Berlin; New York: Springer),.

Brown, J.M., and Attardi, L.D. (2005). The role of apoptosis in cancer development and treatment response. Nat. Rev. Cancer *5*, 231–237.

Brown, D.M., Wilson, M.R., MacNee, W., Stone, V., and Donaldson, K. (2001). Size-dependent proinflammatory effects of ultrafine polystyrene particles: a role for surface area and oxidative stress in the enhanced activity of ultrafines. Toxicol. Appl. Pharmacol. *175*, 191–199.

Brunauer, S., Emmett, P.H., and Teller, E. (1938). Adsorption of Gases in Multimolecular Layers. J. Am. Chem. Soc. *60*, 309–319.

Brzozowska, K., Pinkawa, M., Eble, M.J., Müller, W.-U., Wojcik, A., Kriehuber, R., and Schmitz, S. (2012). In vivo versus in vitro individual radiosensitivity analysed in healthy donors and in prostate cancer patients with and without severe side effects after radiotherapy. Int. J. Radiat. Biol. *88*, 405–413.

BSI (2011). BSI PAS 71:2011. Vocabulary–Nanoparticles. Department of Trade and Industry and British Standards Institution, United Kingdom.

Buerki-Thurnherr, T., Xiao, L., Diener, L., Arslan, O., Hirsch, C., Maeder-Althaus, X., Grieder, K., Wampfler, B., Mathur, S., Wick, P., et al. (2012). In vitro mechanistic study towards a better understanding of ZnO nanoparticle toxicity. Nanotoxicology *7*, 402–416.

Butler, R.A., and Roesijadi, G. (2001). Disruption of Metallothionein Expression with Antisense Oligonucleotides Abolishes Protection Against Cadmium Cytotoxicity in Molluscan Hemocytes. Toxicol. Sci. *59*, 101–107.

Buzea, C., Pacheco, I.I., and Robbie, K. (2007). Nanomaterials and nanoparticles: sources and toxicity. Biointerphases *2*, MR17–MR71.

Cai, Y., Strømme, M., and Welch, K. (2013). Photocatalytic Antibacterial Effects Are Maintained on Resin-Based TiO2 Nanocomposites after Cessation of UV Irradiation. PLoS ONE *8*.

Catalán, J., Suhonen, S., Huk, A., and Dusinska, M. (2014). Analysis of Nanoparticle-Induced DNA Damage by the Comet Assay. In Genotoxicity and DNA Repair, (Springer New York), pp. 241–268.

CCOHS (2009). Titanium Dioxide Classified as Possibly Carcinogenic to Humans (Canadian Centre for Occupational Health and Safety).

Chan, L.L., Zhong, X., Qiu, J., Li, P.Y., and Lin, B. (2011). Cellometer vision as an alternative to flow cytometry for cell cycle analysis, mitochondrial potential, and immunophenotyping. Cytom. Part J. Int. Soc. Anal. Cytol. *79*, 507–517.

Chen, M., and von Mikecz, A. (2005). Formation of nucleoplasmic protein aggregates impairs nuclear function in response to SiO2 nanoparticles. Exp. Cell Res. *305*, 51–62.

Chen, D., Tang, Q., Li, X., Zhou, X., Zang, J., Xue, W., Xiang, J., and Guo, C. (2012a). Biocompatibility of magnetic Fe_3O_4 nanoparticles and their cytotoxic effect on MCF-7 cells. Int. J. Nanomedicine *7*, 4973–4982.

Chen, J., Dong, X., Zhao, J., and Tang, G. (2009). In vivo acute toxicity of titanium dioxide nanoparticles to mice after intraperitioneal injection. J. Appl. Toxicol. JAT *29*, 330–337.

Chen, T., Yan, J., and Li, Y. (2014a). Genotoxicity of titanium dioxide nanoparticles. J. Food Drug Anal. *22*, 95–104.

Chen, Z., Yin, J.-J., Zhou, Y.-T., Zhang, Y., Song, L., Song, M., Hu, S., and Gu, N. (2012b). Dual enzyme-like activities of iron oxide nanoparticles and their implication for diminishing cytotoxicity. ACS Nano *6*, 4001–4012.

Chen, Z., Wang, Y., Ba, T., Li, Y., Pu, J., Chen, T., Song, Y., Gu, Y., Qian, Q., Yang, J., et al. (2014b). Genotoxic evaluation of titanium dioxide nanoparticles in vivo and in vitro. Toxicol. Lett. *226*, 314–319.

Cheng, K.C., Cahill, D.S., Kasai, H., Nishimura, S., and Loeb, L.A. (1992). 8-Hydroxyguanine, an abundant form of oxidative DNA damage, causes G----T and A----C substitutions. J. Biol. Chem. *267*, 166–172.

Cheng, K.K., Chan, P.S., Fan, S., Kwan, S.M., Yeung, K.L., Wáng, Y.-X.J., Chow, A.H.L., Wu, E.X., and Baum, L. (2015). Curcumin-conjugated magnetic nanoparticles for detecting amyloid plaques in Alzheimer's disease mice using magnetic resonance imaging (MRI). Biomaterials *44*, 155–172.

Chiang, H.-M., Xia, Q., Zou, X., Wang, C., Wang, S., Miller, B.J., Howard, P.C., Yin, J.J., Beland, F.A., Yu, H., et al. (2012). Nanoscale ZnO induces cytotoxicity and DNA damage in human cell lines and rat primary neuronal cells. J. Nanosci. Nanotechnol. *12*, 2126–2135.

Cho, W.-S., Kang, B.-C., Lee, J.K., Jeong, J., Che, J.-H., and Seok, S.H. (2013). Comparative absorption, distribution, and excretion of titanium dioxide and zinc oxide nanoparticles after repeated oral administration. Part. Fibre Toxicol. *10*, 9.

Choi, S.-J., Oh, J.-M., and Choy, J.-H. (2009). Toxicological effects of inorganic nanoparticles on human lung cancer A549 cells. J. Inorg. Biochem. *103*, 463–471.

Clift, M.J.D., and Stone, V. (2012). Quantum Dots: An Insight and Perspective of Their Biological Interaction and How This Relates to Their Relevance for Clinical Use. Theranostics *2*, 668–680.

Coccini, T., Manzo, L., Bellotti, V., and De Simone, U. (2014). Assessment of Cellular Responses after Short- and Long-Term Exposure to Silver Nanoparticles in Human Neuroblastoma (SH-SY5Y) and Astrocytoma (D384) Cells. Sci. World J. *2014*, e259765.

Collins, A.R. (2009a). Investigating oxidative DNA damage and its repair using the comet assay. Mutat. Res. Mutat. Res. *681*, 24–32.

Collins, A.R. (2009b). The Use of Bacterial Repair Endonucleases in the Comet Assay. In Drug Safety Evaluation, pp. 137–147.

Collins, A.R. (2014). Measuring oxidative damage to DNA and its repair with the comet assay. Biochim. Biophys. Acta *1840*, 794–800.

Collins, A.R., El Yamani, N., Lorenzo, Y., Shaposhnikov, S., Brunborg, G., and Azqueta, A. (2014). Controlling variation in the comet assay. Front. Genet. *5*, 359.

Colognato, R., Park, M.V.D.Z., Wick, P., and De Jong, W.H. (2012). Chapter 1 - Interactions with the Human Body. In Adverse Effects of Engineered Nanomaterials, B.F.P.A. Shvedova, ed. (Boston: Academic Press), pp. 3–24.

Cooke, M.S., Evans, M.D., Dizdaroglu, M., and Lunec, J. (2003). Oxidative DNA damage: mechanisms, mutation, and disease. FASEB J. *17*, 1195–1214.

Corradi, S., Gonzalez, L., Thomassen, L.C.J., Bilaničová, D., Birkedal, R.K., Pojana, G., Marcomini, A., Jensen, K.A., Leyns, L., and Kirsch-Volders, M. (2012). Influence of serum on in situ proliferation and genotoxicity in A549 human lung cells exposed to nanomaterials. Mutat. Res. *745*, 21–27.

Couto, D., Sousa, R., Andrade, L., Leander, M., Lopez-Quintela, M.A., Rivas, J., Freitas, P., Lima, M., Porto, G., Porto, B., et al. (2015). Polyacrylic acid coated and non-coated iron oxide nanoparticles are not genotoxic to human T lymphocytes. Toxicol. Lett. *234*, 67–73.

Crosby, M.E. (2007). Cell Cycle: Principles of Control. Yale J. Biol. Med. *80*, 141–142.

Cui, Y., Chen, X., Zhou, Z., Lei, Y., Ma, M., Cao, R., Sun, T., Xu, J., Huo, M., Cao, R., et al. (2014). Prenatal exposure to nanoparticulate titanium dioxide enhances depressive-like behaviors in adult rats. Chemosphere *96*, 99–104.

Di Daniel, E., Mudge, A.W., and Maycox, P.R. (2005). Comparative analysis of the effects of four mood stabilizers in SH-SY5Y cells and in primary neurons. Bipolar Disord. *7*, 33–41.

Daniels, W.M.U., Hendricks, J., Salie, R., and van Rensburg, S.J. (2004). A mechanism for zinc toxicity in neuroblastoma cells. Metab. Brain Dis. *19*, 79–88.

Dar, A.M., Naseem, S., Gatoo, M.A., Arfat, M.Y., and Qasim, K. (2014). In Vivo Toxicity Of Nanoparticles: Modalities And Treatment. Eur. Chem. Bull. *3*, 992–1000.

Darzynkiewicz, Z., Crissman, H., and Jacobberger, J.W. (2004). Cytometry of the cell cycle: cycling through history. Cytom. Part J. Int. Soc. Anal. Cytol. *58*, 21–32.

Dawidczyk, C.M., Russell, L.M., and Searson, P.C. (2014). Nanomedicines for cancer therapy: state-of-the-art and limitations to pre-clinical studies that hinder future developments. Chem. Eng. *2*, 69.

Demir, E., Akça, H., Kaya, B., Burgucu, D., Tokgün, O., Turna, F., Aksakal, S., Vales, G., Creus, A., and Marcos, R. (2014a). Zinc oxide nanoparticles: genotoxicity, interactions with UV-light and cell-transforming potential. J. Hazard. Mater. *264*, 420–429.

Demir, E., Creus, A., and Marcos, R. (2014b). Genotoxicity and DNA repair processes of zinc oxide nanoparticles. J. Toxicol. Environ. Health A *77*, 1292–1303.

Demir, E., Akça, H., Turna, F., Aksakal, S., Burgucu, D., Kaya, B., Tokgün, O., Vales, G., Creus, A., and Marcos, R. (2015). Genotoxic and cell-transforming effects of titanium dioxide nanoparticles. Environ. Res. *136*, 300–308.

Deng, X., Luan, Q., Chen, W., Wang, Y., Wu, M., Zhang, H., and Jiao, Z. (2009). Nanosized zinc oxide particles induce neural stem cell apoptosis. Nanotechnology *20*, 115101.

Department for Environment, Food and Rural Affairs of the United Kingdom Government (2007). Characterising the Potential Risks posed by Engineered Nanoparticles - A Second UK Government Research Report.

Diebold, U. (2003). The surface science of titanium dioxide. Surf. Sci. Rep. *48*, 53–229.

Doak, S.H., Griffiths, S.M., Manshian, B., Singh, N., Williams, P.M., Brown, A.P., and Jenkins, G.J.S. (2009). Confounding experimental considerations in nanogenotoxicology. Mutagenesis *24*, 285–293.

Doak, S.H., Liu, Y., and Chen, C. (2012). Chapter 14 - Genotoxicity and Cancer. In Adverse Effects of Engineered Nanomaterials, B.F.P.A. Shvedova, ed. (Boston: Academic Press), pp. 243–261.

Dobrovolskaia, M.A., and McNeil, S.E. (2007). Immunological properties of engineered nanomaterials. Nat. Nanotechnol. *2*, 469–478.

Dobrzyńska, M.M., Gajowik, A., Radzikowska, J., Lankoff, A., Dušinská, M., and Kruszewski, M. (2014). Genotoxicity of silver and titanium dioxide nanoparticles in bone marrow cells of rats in vivo. Toxicology *315*, 86–91.

Donaldson, K., Poland, C.A., and Schins, R.P.F. (2010). Possible genotoxic mechanisms of nanoparticles: criteria for improved test strategies. Nanotoxicology *4*, 414–420.

Dousset, V., Ballarino, L., Delalande, C., Coussemacq, M., Canioni, P., Petry, K.G., and Caillé, J.M. (1999a). Comparison of ultrasmall particles of iron oxide (USPIO)-enhanced T2-weighted, conventional T2-weighted, and gadolinium-enhanced T1-weighted MR images in rats with experimental autoimmune encephalomyelitis. AJNR Am. J. Neuroradiol. *20*, 223–227.

Dousset, V., Delalande, C., Ballarino, L., Quesson, B., Seilhan, D., Coussemacq, M., Thiaudiére, E., Brochet, B., Canioni, P., and Caillé, J.M. (1999b). In vivo macrophage activity imaging in the central nervous system detected by magnetic resonance. Magn. Reson. Med. Off. J. Soc. Magn. Reson. Med. Soc. Magn. Reson. Med. *41*, 329–333.

Dousset, V., Brochet, B., Deloire, M.S.A., Lagoarde, L., Barroso, B., Caille, J.-M., and Petry, K.G. (2006). MR imaging of relapsing multiple sclerosis patients using ultra-small-particle iron oxide and compared with gadolinium. AJNR Am. J. Neuroradiol. *27*, 1000–1005.

Drexler, K.E. (1981). Molecular engineering: An approach to the development of general capabilities for molecular manipulation. Proc. Natl. Acad. Sci. U. S. A. *78*, 5275–5278.

Drexler, K.E. (1996). Engines of Creation (Fourth Estate).

Du, H., Zhu, X., Fan, C., Xu, S., Wang, Y., and Zhou, Y. (2012). Oxidative damage and OGG1 expression induced by a combined effect of titanium dioxide nanoparticles and lead acetate in human hepatocytes. Environ. Toxicol. *27*, 590–597.

Du, H., Wang, M., Wang, L., Dai, H., Wang, M., Hong, W., Nie, X., Wu, L., and Xu, A. (2015). Reproductive toxicity of endosulfan: Implication from germ cell apoptosis modulated by mitochondrial dysfunction and genotoxic response genes in Caenorhabditis elegans. Toxicol. Sci. Off. J. Soc. Toxicol.

Dusinska M., Fjellsbo L., Magdolenova Z., Ravnum S., Rinna A., and Rundén-Pran E. (2011). Safety of Nanoparticles in Medicine. In Nanomedicine in Health and Disease, (Science Publishers), pp. 203–228.

Earl Boysen, and Nancy C. Muir (2011). Nanotechnology For Dummies (Wiley).

Eichhorn, G.L., and Shin, Y.A. (1968). Interaction of metal ions with polynucleotides and related compounds. XII. The relative effect of various metal ions on DNA helicity. J. Am. Chem. Soc. *90*, 7323–7328.

Elder, A., Gelein, R., Silva, V., Feikert, T., Opanashuk, L., Carter, J., Potter, R., Maynard, A., Ito, Y., Finkelstein, J., et al. (2006). Translocation of inhaled ultrafine manganese oxide particles to the central nervous system. Environ. Health Perspect. *114*, 1172–1178.

Elgrabli, D., Beaudouin, R., Jbilou, N., Floriani, M., Pery, A., Rogerieux, F., and Lacroix, G. (2015). Biodistribution and Clearance of TiO2 Nanoparticles in Rats after Intravenous Injection. PloS One *10*, e0124490.

Elmore, S. (2007). Apoptosis: A Review of Programmed Cell Death. Toxicol. Pathol. *35*, 495–516.

El-Said, K., Ali, E., Kanehira, K., and Taniguchi, A. (2014). Molecular mechanism of DNA damage induced by titanium dioxide nanoparticles in toll-like receptor 3 or 4 expressing human hepatocarcinoma cell lines. J. Nanobiotechnology *12*, 48.

Eruslanov, E., and Kusmartsev, S. (2010). Identification of ROS using oxidized DCFDA and flow-cytometry. Methods Mol. Biol. Clifton NJ *594*, 57–72.

Estevanato, L., Cintra, D., Baldini, N., Portilho, F., Barbosa, L., Martins, O., Lacava, B., Miranda-Vilela, A.L., Tedesco, A.C., Báo, S., et al. (2011). Preliminary biocompatibility investigation of magnetic albumin nanosphere designed as a potential versatile drug delivery system. Int. J. Nanomedicine *6*, 1709–1717.

European Commission Joint Research Centre (2011). Engineered Nanoparticles: Review of Health and Environmental Safety (ENRHES).

Fairbairn, D.W., Olive, P.L., and O'Neill, K.L. (1995). The comet assay: a comprehensive review. Mutat. Res. *339*, 37–59.

Fang, Z.Z., Middlemas, S., Guo, J., and Fan, P. (2013). A new, energy-efficient chemical pathway for extracting Ti metal from Ti minerals. J. Am. Chem. Soc. *135*, 18248–18251.

Fazio, S., Guzmán, J., Colomer, M.T., Salomoni, A., and Moreno, R. (2008). Colloidal stability of nanosized titania aqueous suspensions. J. Eur. Ceram. Soc. *28*, 2171–2176.

FDA 2014 CFR - Code of Federal Regulations Title 21 accessed from http://www.accessdata.fda.gov/scripts/cdrh/cfdocs/cfCFR/CFRSearch.cfm?fr=73.575.

FDA 2015 FDA Established Pharmacologic Class (EPC) available from http://www.fda.gov/downloads/drugs/guidancecomplianceregulatoryinformation/lawsactsandrules/ucm428333.pdf.

Fenech, M., Kirsch-Volders, M., Natarajan, A.T., Surralles, J., Crott, J.W., Parry, J., Norppa, H., Eastmond, D.A., Tucker, J.D., and Thomas, P. (2011). Molecular mechanisms of micronucleus, nucleoplasmic bridge and nuclear bud formation in mammalian and human cells. Mutagenesis *26*, 125–132.

Fernandez-Capetillo, O., Chen, H.-T., Celeste, A., Ward, I., Romanienko, P.J., Morales, J.C., Naka, K., Xia, Z., Camerini-Otero, R.D., Motoyama, N., et al. (2002). DNA damage-induced G2-M checkpoint activation by histone H2AX and 53BP1. Nat. Cell Biol. *4*, 993–997.

Feynman, R.P. (1960). There's Plenty of Room at the Bottom. Eng. Sci. *23*, 22–36.

Filippi, C., Pryde, A., Cowan, P., Lee, T., Hayes, P., Donaldson, K., Plevris, J., and Stone, V. (2015). Toxicology of ZnO and TiO2 nanoparticles on hepatocytes: Impact on metabolism and bioenergetics. Nanotoxicology *9*, 126–134.

Fitzpatrick, J.A.J., Inouye, Y., Manley, S., and Moerner, W.E. (2014). From "There's Plenty of Room at the Bottom" to seeing what is actually there. Chemphyschem Eur. J. Chem. Phys. Phys. Chem. *15*, 547–549.

Floris, S., Blezer, E.L.A., Schreibelt, G., Döpp, E., van der Pol, S.M.A., Schadee-Eestermans, I.L., Nicolay, K., Dijkstra, C.D., and de Vries, H.E. (2004). Blood-brain barrier permeability and monocyte infiltration in experimental allergic encephalomyelitis: a quantitative MRI study. Brain J. Neurol. *127*, 616–627.

Forbe, T., García, M., and Gonzalez, E. (2011). Potencial risks of nanoparticles. Food Sci. Technol. Camp. *31*, 835–842.

Foucaud, L., Wilson, M.R., Brown, D.M., and Stone, V. (2007). Measurement of reactive species production by nanoparticles prepared in biologically relevant media. Toxicol. Lett. *174*, 1–9.

Fraker, P.J., King, L.E., Lill-Elghanian, D., and Telford, W.G. (1995). Quantification of apoptotic events in pure and heterogeneous populations of cells using the flow cytometer. Methods Cell Biol. *46*, 57–76.

Frankenberg-Schwager, M. (1989). Review of repair kinetics for DNA damage induced in eukaryotic cells in vitro by ionizing radiation. Radiother. Oncol. J. Eur. Soc. Ther. Radiol. Oncol. *14*, 307–320.

Fröhlich, E. (2013). Cellular targets and mechanisms in the cytotoxic action of non-biodegradable engineered nanoparticles. Curr. Drug Metab. *14*, 976–988.

Fubini B., Fenoglio I., and Tomatis M. (2007). Physicochemical Characteristics of Nanoparticles that Determine Potential Toxicity. In Nanotoxicology: Characterization, Dosing, and Health Effects, (Informa Healthcare), pp. 59–70.

Fukui, H., Iwahashi, H., Endoh, S., Nishio, K., Yoshida, Y., Hagihara, Y., and Horie, M. (2015). Ascorbic acid attenuates acute pulmonary oxidative stress and inflammation caused by zinc oxide nanoparticles. J. Occup. Health.

Galluzzi, L., Zamzami, N., de La Motte Rouge, T., Lemaire, C., Brenner, C., and Kroemer, G. (2007). Methods for the assessment of mitochondrial membrane permeabilization in apoptosis. Apoptosis Int. J. Program. Cell Death *12*, 803–813.

Gao, X., Wang, Y., Peng, S., Yue, B., Fan, C., Chen, W., and Li, X. (2015). Comparative toxicities of bismuth oxybromide and titanium dioxide exposure on human skin keratinocyte cells. Chemosphere *135*, 83–93.

Garza, K.M., Soto, K.F., and Murr, L.E. (2008). Cytotoxicity and reactive oxygen species generation from aggregated carbon and carbonaceous nanoparticulate materials. Int. J. Nanomedicine *3*, 83–94.

Gassman, N.R., Coskun, E., Stefanick, D.F., Horton, J.K., Jaruga, P., Dizdaroglu, M., and Wilson, S.H. (2015). Bisphenol A Promotes Cell Survival Following Oxidative DNA Damage in Mouse Fibroblasts. PloS One *10*, e0118819.

Geppert, M., Hohnholt, M., Gaetjen, L., Grunwald, I., Bäumer, M., and Dringen, R. (2009). Accumulation of iron oxide nanoparticles by cultured brain astrocytes. J. Biomed. Nanotechnol. *5*, 285–293.

Geppert, M., Hohnholt, M.C., Nürnberger, S., and Dringen, R. (2012). Ferritin up-regulation and transient ROS production in cultured brain astrocytes after loading with iron oxide nanoparticles. Acta Biomater. *8*, 3832–3839.

Gerloff, K., Albrecht, C., Boots, A.W., Förster, I., and Schins, R.P.F. (2009). Cytotoxicity and oxidative DNA damage by nanoparticles in human intestinal Caco-2 cells. Nanotoxicology *3*, 355–364.

Gheshlaghi, Z.N., Riazi, G.H., Ahmadian, S., Ghafari, M., and Mahinpour, R. (2008). Toxicity and interaction of titanium dioxide nanoparticles with microtubule protein. Acta Biochim. Biophys. Sin. *40*, 777–782.

Ghosh, M., Chakraborty, A., and Mukherjee, A. (2013). Cytotoxic, genotoxic and the hemolytic effect of titanium dioxide (TiO2) nanoparticles on human erythrocyte and lymphocyte cells in vitro. J. Appl. Toxicol. JAT *33*, 1097–1110.

Gilbert, B., Fakra, S.C., Xia, T., Pokhrel, S., Mädler, L., and Nel, A.E. (2012). The Fate of ZnO Nanoparticles Administered to Human Bronchial Epithelial Cells. ACS Nano *6*, 4921–4930.

Gitrowski, C., Al-Jubory, A.R., and Handy, R.D. (2014). Uptake of different crystal structures of TiO2 nanoparticles by Caco-2 intestinal cells. Toxicol. Lett. *226*, 264–276.

Golbamaki, N., Rasulev, B., Cassano, A., Robinson, R.L.M., Benfenati, E., Leszczynski, J., and Cronin, M.T.D. (2015). Genotoxicity of metal oxide nanomaterials: review of recent data and discussion of possible mechanisms. Nanoscale *7*, 2154–2198.

Goncalves, D.M., de Liz, R., and Girard, D. (2011). Activation of Neutrophils by Nanoparticles. ScientificWorldJournal *11*, 1877–1885.

Gopalan, R.C., Osman, I.F., Amani, A., De Matas, M., and Anderson, D. (2009). The effect of zinc oxide and titanium dioxide nanoparticles in the Comet assay with UVA photoactivation of human sperm and lymphocytes. Nanotoxicology *3*, 33–39.

Gottlieb, R.A. (2000). Mitochondria: execution central. FEBS Lett. *482*, 6–12.

Gould, P. (2006). Nanomagnetism shows in vivo potential. Nano Today *1*, 34–39.

Guadagnini, R., Halamoda Kenzaoui, B., Cartwright, L., Pojana, G., Magdolenova, Z., Bilanicova, D., Saunders, M., Juillerat, L., Marcomini, A., Huk, A., et al. (2013). Toxicity screenings of nanomaterials: challenges due to interference with assay processes and components of classic in vitro tests. Nanotoxicology.

Guan, R., Kang, T., Lu, F., Zhang, Z., Shen, H., and Liu, M. (2012). Cytotoxicity, oxidative stress, and genotoxicity in human hepatocyte and embryonic kidney cells exposed to ZnO nanoparticles. Nanoscale Res. Lett. *7*, 602.

Guichard, Y., Schmit, J., Darne, C., Gaté, L., Goutet, M., Rousset, D., Rastoix, O., Wrobel, R., Witschger, O., Martin, A., et al. (2012). Cytotoxicity and genotoxicity of nanosized and microsized titanium dioxide and iron oxide particles in Syrian hamster embryo cells. Ann. Occup. Hyg. *56*, 631–644.

Guo, D., Bi, H., Liu, B., Wu, Q., Wang, D., and Cui, Y. (2013a). Reactive oxygen species-induced cytotoxic effects of zinc oxide nanoparticles in rat retinal ganglion cells. Toxicol. Vitro Int. J. Publ. Assoc. BIBRA *27*, 731–738.

Guo, D., Bi, H., Wu, Q., Wang, D., and Cui, Y. (2013b). Zinc oxide nanoparticles induce rat retinal ganglion cell damage through bcl-2, caspase-9 and caspase-12 pathways. J. Nanosci. Nanotechnol. *13*, 3769–3777.

Gupta, A.K., and Gupta, M. (2005). Synthesis and surface engineering of iron oxide nanoparticles for biomedical applications. Biomaterials *26*, 3995–4021.

Al Gurabi, M.A., Ali, D., Alkahtani, S., and Alarifi, S. (2015). In vivo DNA damaging and apoptotic potential of silver nanoparticles in Swiss albino mice. OncoTargets Ther. *8*, 295–302.

Hackenberg, S., Scherzed, A., Gohla, A., Technau, A., Froelich, K., Ginzkey, C., Koehler, C., Burghartz, M., Hagen, R., and Kleinsasser, N. (2014). Nanoparticle-induced photocatalytic head and neck squamous cell carcinoma cell death is associated with autophagy. Nanomed. *9*, 21–33.

Hamzeh, M., and Sunahara, G.I. (2013). In vitro cytotoxicity and genotoxicity studies of titanium dioxide (TiO2) nanoparticles in Chinese hamster lung fibroblast cells. Toxicol. Vitro Int. J. Publ. Assoc. BIBRA *27*, 864–873.

Han, X., Gelein, R., Corson, N., Wade-Mercer, P., Jiang, J., Biswas, P., Finkelstein, J.N., Elder, A., and Oberdörster, G. (2011). Validation of an LDH assay for assessing nanoparticle toxicity. Toxicology *287*, 99–104.

Hanley, C., Thurber, A., Hanna, C., Punnoose, A., Zhang, J., and Wingett, D.G. (2009). The Influences of Cell Type and ZnO Nanoparticle Size on Immune Cell Cytotoxicity and Cytokine Induction. Nanoscale Res. Lett. *4*, 1409.

Hansen, R.E., Roth, D., and Winther, J.R. (2009). Quantifying the global cellular thiol-disulfide status. Proc. Natl. Acad. Sci. U. S. A. *106*, 422–427.

Hao, L., and Chen, L. (2012). Oxidative stress responses in different organs of carp (Cyprinus carpio) with exposure to ZnO nanoparticles. Ecotoxicol. Environ. Saf. *80*, 103–110.

Hart, G.W., and West, C.M. (2009). Nucleocytoplasmic Glycosylation. In Essentials of Glycobiology, A. Varki, R.D. Cummings, J.D. Esko, H.H. Freeze, P. Stanley, C.R. Bertozzi, G.W. Hart, and M.E. Etzler, eds. (Cold Spring Harbor (NY): Cold Spring Harbor Laboratory Press),.

Hengartner, M.O. (2000). The biochemistry of apoptosis. Nature *407*, 770–776.

Henry-Mowatt, J., Dive, C., Martinou, J.-C., and James, D. (2004). Role of mitochondrial membrane permeabilization in apoptosis and cancer. Oncogene *23*, 2850–2860.

Hernández, S., Hidalgo, D., Sacco, A., Chiodoni, A., Lamberti, A., Cauda, V., Tresso, E., and Saracco, G. (2015). Comparison of photocatalytic and transport properties of TiO2 and ZnO nanostructures for solar-driven water splitting. Phys. Chem. Chem. Phys. PCCP.

Hillegass, J.M., Shukla, A., Lathrop, S.A., MacPherson, M.B., Fukagawa, N.K., and Mossman, B.T. (2010). Assessing nanotoxicity in cells in vitro. Wiley Interdiscip. Rev. Nanomed. Nanobiotechnol. *2*, 219–231.

Hissin, P.J., and Hilf, R. (1976). A fluorometric method for determination of oxidized and reduced glutathione in tissues. Anal. Biochem. *74*, 214–226.

Hoet, P.H., Brüske-Hohlfeld, I., and Salata, O.V. (2004). Nanoparticles – known and unknown health risks. J. Nanobiotechnology *2*, 12.

Hohnholt, M.C., Geppert, M., Luther, E.M., Petters, C., Bulcke, F., and Dringen, R. (2013). Handling of iron oxide and silver nanoparticles by astrocytes. Neurochem. Res. *38*, 227–239.

Hola, K., Markova, Z., Zoppellaro, G., Tucek, J., and Zboril, R. (2015). Tailored functionalization of iron oxide nanoparticles for MRI, drug delivery, magnetic separation and immobilization of biosubstances. Biotechnol. Adv.

Hong, M.S., Hong, S.J., Barhoumi, R., Burghardt, R.C., Donnelly, K.C., Wild, J.R., Venkatraj, V., and Tiffany-Castiglioni, E. (2003). Neurotoxicity induced in differentiated SK-N-SH-SY5Y human neuroblastoma cells by organophosphorus compounds. Toxicol. Appl. Pharmacol. *186*, 110–118.

Hong, S.C., Lee, J.H., Lee, J., Kim, H.Y., Park, J.Y., Cho, J., Lee, J., and Han, D.-W. (2011). Subtle cytotoxicity and genotoxicity differences in superparamagnetic iron oxide nanoparticles coated with various functional groups. Int. J. Nanomedicine *6*, 3219–3231.

Horie, M., Nishio, K., Fujita, K., Endoh, S., Miyauchi, A., Saito, Y., Iwahashi, H., Yamamoto, K., Murayama, H., Nakano, H., et al. (2009). Protein adsorption of ultrafine metal oxide and its influence on cytotoxicity toward cultured cells. Chem. Res. Toxicol. *22*, 543–553.

Hoskins, C., Cuschieri, A., and Wang, L. (2012). The cytotoxicity of polycationic iron oxide nanoparticles: Common endpoint assays and alternative approaches for improved understanding of cellular response mechanism. J. Nanobiotechnology *10*, 15.

Hou, Y., Lai, M., Chen, X., Li, J., Hu, Y., Luo, Z., Ding, X., and Cai, K. (2014). Effects of mesoporous SiO2 , Fe3 O4 , and TiO2 nanoparticles on the biological functions of endothelial cells in vitro. J. Biomed. Mater. Res. A *102*, 1726–1736.

Hsiao, I.-L., and Huang, Y.-J. (2011). Effects of various physicochemical characteristics on the toxicities of ZnO and TiO2 nanoparticles toward human lung epithelial cells. Sci. Total Environ. *409*, 1219–1228.

Hu, Y.-L., and Gao, J.-Q. (2010). Potential neurotoxicity of nanoparticles. Int. J. Pharm. *394*, 115–121.

Hu, X., Cook, S., Wang, P., and Hwang, H. (2009). In vitro evaluation of cytotoxicity of engineered metal oxide nanoparticles. Sci. Total Environ. *407*, 3070–3072.

Huang, S., Li, C., Cheng, Z., Fan, Y., Yang, P., Zhang, C., Yang, K., and Lin, J. (2012). Magnetic Fe3O4@mesoporous silica composites for drug delivery and bioadsorption. J. Colloid Interface Sci. *376*, 312–321.

Huber, D.L. (2005). Synthesis, properties, and applications of iron nanoparticles. Small Weinh. Bergstr. Ger. *1*, 482–501.

Huerta-García, E., Pérez-Arizti, J.A., Márquez-Ramírez, S.G., Delgado-Buenrostro, N.L., Chirino, Y.I., Iglesias, G.G., and López-Marure, R. (2014). Titanium dioxide nanoparticles induce strong oxidative stress and mitochondrial damage in glial cells. Free Radic. Biol. Med. *73*, 84–94.

Huynh, K.A., and Chen, K.L. (2014). Disaggregation of heteroaggregates composed of multiwalled carbon nanotubes and hematite nanoparticles. Environ. Sci. Process. Impacts *16*, 1371–1378.

IARC (2010). Carbon black, titanium dioxide, and talc. IARC Monogr. Eval. Carcinog. Risks Hum. World Health Organ. Int. Agency Res. Cancer *93*, 1–413.

Ibuki, Y., and Toyooka, T. (2012). Nanoparticle uptake measured by flow cytometry. Methods Mol. Biol. Clifton NJ *926*, 157–166.

Institute of Medicine (US) Food Forum (2009). Nanotechnology in Food Products: Workshop Summary (Washington (DC): National Academies Press (US)).

ISO/TR27628 ISO: Workplace Atmospheres: Ultrafine, Nanoparticle and Nanostructured Aerosols – Inhalation Exposure Characterisation and Assessment. 34 p. (2007).

ISO/TS 27687 ISO: Nanotechnologies: Terminology and Definitions for Nano-Objects – Nanoparticle, Nanofibre and Nanoplate. 7 p. (2008).

Issa, B., Obaidat, I.M., Albiss, B.A., and Haik, Y. (2013). Magnetic Nanoparticles: Surface Effects and Properties Related to Biomedicine Applications. Int. J. Mol. Sci. *14*, 21266–21305.

Jacobsen, N.R., Pojana, G., White, P., Møller, P., Cohn, C.A., Korsholm, K.S., Vogel, U., Marcomini, A., Loft, S., and Wallin, H. (2008). Genotoxicity, cytotoxicity, and reactive oxygen species induced by single-walled carbon nanotubes and C(60) fullerenes in the FE1-Mutatrade markMouse lung epithelial cells. Environ. Mol. Mutagen. *49*, 476–487.

Janer, G., Mas del Molino, E., Fernández-Rosas, E., Fernández, A., and Vázquez-Campos, S. (2014). Cell uptake and oral absorption of titanium dioxide nanoparticles. Toxicol. Lett. *228*, 103–110.

Jaroszeski, M.J., and Radcliff, G. (1999). Fundamentals of flow cytometry. Mol. Biotechnol. *11*, 37–53.

Jaruga, P., and Dizdaroglu, M. (1996). Repair of products of oxidative DNA base damage in human cells. Nucleic Acids Res. *24*, 1389–1394.

Jeng, H.A., and Swanson, J. (2006). Toxicity of metal oxide nanoparticles in mammalian cells. J. Environ. Sci. Health Part A Tox. Hazard. Subst. Environ. Eng. *41*, 2699–2711.

Jiang, J., Oberdörster, G., and Biswas, P. (2008). Characterization of size, surface charge, and agglomeration state of nanoparticle dispersions for toxicological studies. J. Nanoparticle Res. *11*, 77–89.

Jiang, W., Mashayekhi, H., and Xing, B. (2009). Bacterial toxicity comparison between nano- and micro-scaled oxide particles. Environ. Pollut. *157*, 1619–1625.

Jin, C., Tang, Y., Yang, F.G., Li, X.L., Xu, S., Fan, X.Y., Huang, Y.Y., and Yang, Y.J. (2010). Cellular Toxicity of TiO2 Nanoparticles in Anatase and Rutile Crystal Phase. Biol. Trace Elem. Res. *141*, 3–15.

Jing, L., Xu, Z., Sun, X., Shang, J., and Cai, W. (2001). The surface properties and photocatalytic activities of ZnO ultrafine particles. Appl. Surf. Sci. *180*, 308–314.

De Jong, W.H., and Borm, P.J. (2008). Drug delivery and nanoparticles: Applications and hazards. Int. J. Nanomedicine *3*, 133–149.

Jud, C., Clift, M.J.D., Petri-Fink, A., and Rothen-Rutishauser, B. (2013). Nanomaterials and the human lung: what is known and what must be deciphered to realise their potential advantages? Swiss Med. Wkly. *143*, w13758.

Jugan, M.-L., Barillet, S., Simon-Deckers, A., Herlin-Boime, N., Sauvaigo, S., Douki, T., and Carriere, M. (2012). Titanium dioxide nanoparticles exhibit genotoxicity and impair DNA repair activity in A549 cells. Nanotoxicology *6*, 501–513.

Ju-Nam, Y., and Lead, J.R. (2008). Manufactured nanoparticles: An overview of their chemistry, interactions and potential environmental implications. Sci. Total Environ. *400*, 396–414.

Kaida, T., Kobayashi, K., Adachi, M., and Suzuki, F. (2004). Optical characteristics of titanium oxide interference film and the film laminated with oxides and their applications for cosmetics. J. Cosmet. Sci. *55*, 219–220.

Kain, J., Karlsson, H.L., and Möller, L. (2012). DNA damage induced by micro- and nanoparticles - interaction with FPG influences the detection of DNA oxidation in the comet assay. Mutagenesis *27*, 491–500.

Kang, M., Lim, C.-H., and Han, J.-H. (2013). Comparison of Toxicity and Deposition of Nano-Sized Carbon Black Aerosol Prepared With or Without Dispersing Sonication. Toxicol. Res. *29*, 121–127.

Kansara, K., Patel, P., Shah, D., Shukla, R.K., Singh, S., Kumar, A., and Dhawan, A. (2014). TiO2 nanoparticles induce DNA double strand breaks and cell cycle arrest in human alveolar cells. Environ. Mol. Mutagen.

Kao, Y.-Y., Cheng, T.-J., Yang, D.-M., Wang, C.-T., Chiung, Y.-M., and Liu, P.-S. (2012). Demonstration of an olfactory bulb-brain translocation pathway for ZnO nanoparticles in rodent cells in vitro and in vivo. J. Mol. Neurosci. MN *48*, 464–471.

Karagkiozaki, V., Logothetidis, S., and Vavoulidis, E. (2012). Nanomedicine Pillars and Monitoring Nano–biointeractions. In Nanomedicine and Nanobiotechnology, S. Logothetidis, ed. (Springer Berlin Heidelberg), pp. 27–56.

Karlsson, H.L. (2010). The comet assay in nanotoxicology research. Anal. Bioanal. Chem. *398*, 651–666.

Karlsson, H.L., Holgersson, Å., and Möller, L. (2008). Mechanisms Related to the Genotoxicity of Particles in the Subway and from Other Sources. Chem. Res. Toxicol. *21*, 726–731.

Karlsson, H.L., Gustafsson, J., Cronholm, P., and Möller, L. (2009). Size-dependent toxicity of metal oxide particles--a comparison between nano- and micrometer size. Toxicol. Lett. *188*, 112–118.

Karmakar, A., Zhang, Q., and Zhang, Y. (2014). Neurotoxicity of nanoscale materials. J. Food Drug Anal. *22*, 147–160.

Kaur, I.P., Kakkar, V., Deol, P.K., Yadav, M., Singh, M., and Sharma, I. (2014). Issues and concerns in nanotech product development and its commercialization. J. Control. Release Off. J. Control. Release Soc. *193*, 51–62.

Kawanishi, M., Ogo, S., Ikemoto, M., Totsuka, Y., Ishino, K., Wakabayashi, K., and Yagi, T. (2013). Genotoxicity and reactive oxygen species production induced by magnetite nanoparticles in mammalian cells. J. Toxicol. Sci. *38*, 503–511.

Kendig, D.M., and Tarloff, J.B. (2007). Inactivation of Lactate Dehydrogenase By Several Chemicals: Implications For In vitro Toxicology Studies. Toxicol. Vitro Int. J. Publ. Assoc. BIBRA *21*, 125–132.

Kenzaoui, B.H., Bernasconi, C.C., Hofmann, H., and Juillerat-Jeanneret, L. (2012). Evaluation of uptake and transport of ultrasmall superparamagnetic iron oxide nanoparticles by human brain-derived endothelial cells. Nanomed. *7*, 39–53.

Kermanizadeh, A., Gaiser, B.K., Hutchison, G.R., and Stone, V. (2012). An in vitro liver model - assessing oxidative stress and genotoxicity following exposure of hepatocytes to a panel of engineered nanomaterials. Part. Fibre Toxicol. *9*, 28.

Kerr, J.F., Wyllie, A.H., and Currie, A.R. (1972). Apoptosis: a basic biological phenomenon with wide-ranging implications in tissue kinetics. Br. J. Cancer *26*, 239–257.

Kettiger, H., Schipanski, A., Wick, P., and Huwyler, J. (2013). Engineered nanomaterial uptake and tissue distribution: from cell to organism. Int. J. Nanomedicine *8*, 3255–3269.

Khan, M., Naqvi, A.H., and Ahmad, M. (2015). Comparative study of the cytotoxic and genotoxic potentials of zinc oxide and titanium dioxide nanoparticles. Toxicol. Rep.

Kim, H.R., Kim, M.J., Lee, S.Y., Oh, S.M., and Chung, K.H. (2011). Genotoxic effects of silver nanoparticles stimulated by oxidative stress in human normal bronchial epithelial (BEAS-2B) cells. Mutat. Res. *726*, 129–135.

Kim, J.-E., Shin, J.-Y., and Cho, M.-H. (2012). Magnetic nanoparticles: an update of application for drug delivery and possible toxic effects. Arch. Toxicol. *86*, 685–700.

Kim, Y., Kong, S.D., Chen, L.-H., Pisanic II, T.R., Jin, S., and Shubayev, V.I. (2013). In vivo nanoneurotoxicity screening using oxidative stress and neuroinflammation paradigms. Nanomedicine Nanotechnol. Biol. Med. *9*, 1057–1066.

Kim, Y.H., Fazlollahi, F., Kennedy, I.M., Yacobi, N.R., Hamm-Alvarez, S.F., Borok, Z., Kim, K.-J., and Crandall, E.D. (2010a). Alveolar Epithelial Cell Injury Due to Zinc Oxide Nanoparticle Exposure. Am. J. Respir. Crit. Care Med. *182*, 1398–1409.

Kim, Y.-J., Yu, M., Park, H.-O., and Yang, S.I. (2010b). Comparative study of cytotoxicity, oxidative stress and genotoxicity induced by silica nanomaterials in human neuronal cell line. Mol. Cell. Toxicol. *6*, 336–343.

Klein, S., Sommer, A., Distel, L.V.R., Neuhuber, W., and Kryschi, C. (2012). Superparamagnetic iron oxide nanoparticles as radiosensitizer via enhanced reactive oxygen species formation. Biochem. Biophys. Res. Commun. *425*, 393–397.

Kleinschnitz, C., Schütz, A., Nölte, I., Horn, T., Frank, M., Solymosi, L., Stoll, G., and Bendszus, M. (2005). In vivo detection of developing vessel occlusion in photothrombotic ischemic brain lesions in the rat by iron particle enhanced MRI. J. Cereb. Blood Flow Metab. Off. J. Int. Soc. Cereb. Blood Flow Metab. *25*, 1548–1555.

Kolhatkar, A.G., Jamison, A.C., Litvinov, D., Willson, R.C., and Lee, T.R. (2013). Tuning the Magnetic Properties of Nanoparticles. Int. J. Mol. Sci. *14*, 15977–16009.

Koller, V.J., Auwärter, V., Grummt, T., Moosmann, B., Mišík, M., and Knasmüller, S. (2014). Investigation of the in vitro toxicological properties of the synthetic cannabimimetic drug CP-47,497-C8. Toxicol. Appl. Pharmacol. *277*, 164–171.

Kołodziejczak-Radzimska, A., and Jesionowski, T. (2014). Zinc Oxide—From Synthesis to Application: A Review. Materials *7*, 2833–2881.

Könczöl, M., Ebeling, S., Goldenberg, E., Treude, F., Gminski, R., Gieré, R., Grobéty, B., Rothen-Rutishauser, B., Merfort, I., and Mersch-Sundermann, V. (2011). Cytotoxicity and genotoxicity of size-fractionated iron oxide (magnetite) in A549 human lung epithelial cells: Role of ROS, JNK, and NF-κB. Chem. Res. Toxicol. *24*, 1460–1475.

Koppel, D.E. (1972). Analysis of Macromolecular Polydispersity in Intensity Correlation Spectroscopy: The Method of Cumulants. J. Chem. Phys. *57*, 4814–4820.

Kovalevich, J., and Langford, D. (2013). Considerations for the use of SH-SY5Y neuroblastoma cells in neurobiology. Methods Mol. Biol. Clifton NJ *1078*, 9–21.

Kreuter, J. (2001). Nanoparticulate systems for brain delivery of drugs. Adv. Drug Deliv. Rev. *47*, 65–81.

Kroemer, G., Galluzzi, L., and Brenner, C. (2007). Mitochondrial Membrane Permeabilization in Cell Death. Physiol. Rev. *87*, 99–163.

Kroll, A., Pillukat, M.H., Hahn, D., and Schnekenburger, J. (2012). Interference of engineered nanoparticles with in vitro toxicity assays. Arch. Toxicol. *86*, 1123–1136.

Kruszewski, M., Brzoska, K., Brunborg, G., Asare, N., Dobrzyńska, M., Dušinská, M., Fjellsbø, L.M., Georgantzopoulou, A., Gromadzka-Ostrowska, J., Gutleb, A.C., et al. (2011). Chapter Five - Toxicity of Silver Nanomaterials in Higher Eukaryotes. In Advances in Molecular Toxicology, J.C. Fishbein, ed. (Elsevier), pp. 179–218.

Kumar, A., and Dhawan, A. (2013). Genotoxic and carcinogenic potential of engineered nanoparticles: an update. Arch. Toxicol. *87*, 1883–1900.

Kumari, M., Rajak, S., Singh, S.P., Kumari, S.I., Kumar, P.U., Murty, U.S.N., Mahboob, M., Grover, P., and Rahman, M.F. (2012). Repeated oral dose toxicity of iron oxide nanoparticles: biochemical and histopathological alterations in different tissues of rats. J. Nanosci. Nanotechnol. *12*, 2149–2159.

Kung, M.-L., Hsieh, S.-L., Wu, C.-C., Chu, T.-H., Lin, Y.-C., Yeh, B.-W., and Hsieh, S. (2015). Enhanced reactive oxygen species overexpression by CuO nanoparticles in poorly differentiated hepatocellular carcinoma cells. Nanoscale *7*, 1820–1829.

Kunzmann, A., Andersson, B., Vogt, C., Feliu, N., Ye, F., Gabrielsson, S., Toprak, M.S., Buerki-Thurnherr, T., Laurent, S., Vahter, M., et al. (2011). Efficient internalization of silica-coated iron oxide nanoparticles of different sizes by primary human macrophages and dendritic cells. Toxicol. Appl. Pharmacol. *253*, 81–93.

Kuznetsov, A.V., Margreiter, R., Amberger, A., Saks, V., and Grimm, M. (2011). Changes in mitochondrial redox state, membrane potential and calcium precede mitochondrial dysfunction in doxorubicin-induced cell death. Biochim. Biophys. Acta BBA - Mol. Cell Res. *1813*, 1144–1152.

Kwon, D., Park, J., Park, J., Choi, S.Y., and Yoon, T.H. (2014a). Effects of surface-modifying ligands on the colloidal stability of ZnO nanoparticle dispersions in in vitro cytotoxicity test media. Int. J. Nanomedicine *9 Suppl 2*, 57–65.

Kwon, J.Y., Lee, S.Y., Koedrith, P., Lee, J.Y., Kim, K.-M., Oh, J.-M., Yang, S.I., Kim, M.-K., Lee, J.K., Jeong, J., et al. (2014b). Lack of genotoxic potential of ZnO nanoparticles in in vitro and in vivo tests. Mutat. Res. Toxicol. Environ. Mutagen. *761*, 1–9.

Laffon, B., Valdiglesias, V., Pásaro, E., and Méndez, J. (2010). The organic selenium compound selenomethionine modulates bleomycin-induced DNA damage and repair in human leukocytes. Biol. Trace Elem. Res. *133*, 12–19.

Lagopati, N., Tsilibary, E.-P., Falaras, P., Papazafiri, P., Pavlatou, E.A., Kotsopoulou, E., and Kitsiou, P. (2014). Effect of nanostructured TiO_2 crystal phase on photoinduced apoptosis of breast cancer epithelial cells. Int. J. Nanomedicine *9*, 3219–3230.

Lai, J.C.K., Lai, M.B., Jandhyam, S., Dukhande, V.V., Bhushan, A., Daniels, C.K., and Leung, S.W. (2008). Exposure to titanium dioxide and other metallic oxide nanoparticles induces cytotoxicity on human neural cells and fibroblasts. Int. J. Nanomedicine *3*, 533–545.

Laingam, S., Froscio, S.M., and Humpage, A.R. (2008). Flow-cytometric analysis of in vitro micronucleus formation: comparative studies with WIL2-NS human lymphoblastoid and L5178Y mouse lymphoma cell lines. Mutat. Res. *656*, 19–26.

Landgraf, L., Ernst, P., Schick, I., Köhler, O., Oehring, H., Tremel, W., and Hilger, I. (2014). Anti-oxidative effects and harmlessness of asymmetric $Au@Fe_3O_4$ Janus particles on human blood cells. Biomaterials *35*, 6986–6997.

Lanone, S., and Boczkowski, J. (2006). Biomedical applications and potential health risks of nanomaterials: molecular mechanisms. Curr. Mol. Med. *6*, 651–663.

Larumbe, S., Gómez-Polo, C., Pérez-Landazábal, J.I., and Pastor, J.M. (2012). Effect of a SiO2 coating on the magnetic properties of Fe3O4 nanoparticles. J. Phys. Condens. Matter Inst. Phys. J. *24*, 266007.

Laskar, A., Ghosh, M., Khattak, S.I., Li, W., and Yuan, X.-M. (2012). Degradation of superparamagnetic iron oxide nanoparticle-induced ferritin by lysosomal cathepsins and related immune response. Nanomed. *7*, 705–717.

Le Lay, S., Simard, G., Martinez, M.C., and Andriantsitohaina, R. (2014). Oxidative Stress and Metabolic Pathologies: From an Adipocentric Point of View. Oxid. Med. Cell. Longev. *2014*, e908539.

L'Azou, B., and Marano, F. (2011). Nanoparticle Toxicity Mechanisms: Oxidative Stress and Inflammation. In Nanoethics and Nanotoxicology, P. Houdy, M. Lahmani, and F. Marano, eds. (Springer Berlin Heidelberg), pp. 87–109.

LeBel, C.P., Ischiropoulos, H., and Bondy, S.C. (1992). Evaluation of the probe 2',7'-dichlorofluorescin as an indicator of reactive oxygen species formation and oxidative stress. Chem. Res. Toxicol. *5*, 227–231.

Lee, C.-M., Jeong, H.-J., Kim, D.W., Sohn, M.-H., and Lim, S.T. (2012). The effect of fluorination of zinc oxide nanoparticles on evaluation of their biodistribution after oral administration. Nanotechnology *23*, 205102.

Leist, M., and Jäättelä, M. (2001). Four deaths and a funeral: from caspases to alternative mechanisms. Nat. Rev. Mol. Cell Biol. *2*, 589–598.

Lévy, M., Lagarde, F., Maraloiu, V.-A., Blanchin, M.-G., Gendron, F., Wilhelm, C., and Gazeau, F. (2010). Degradability of superparamagnetic nanoparticles in a model of intracellular environment: follow-up of magnetic, structural and chemical properties. Nanotechnology *21*, 395103.

Li, J., Liu, X., Zhang, Y., Tian, F., Zhao, G., Yu, Q., Jiang, F., and Liu, Y. (2012a). Toxicity of nano zinc oxide to mitochondria. Toxicol. Res. *1*, 137–144.

Li, L., Mak, K.Y., Shi, J., Koon, H.K., Leung, C.H., Wong, C.M., Leung, C.W., Mak, C.S.K., Chan, N.M.M., Zhong, W., et al. (2012b). Comparative in vitro cytotoxicity study on uncoated magnetic nanoparticles: effects on cell viability, cell morphology, and cellular uptake. J. Nanosci. Nanotechnol. *12*, 9010–9017.

Li, Y., Liu, Zhong, Y., Zhang, D., Wang, Wang, An, Y., Lin, Gao, and Zhang (2011). Biocompatibility of Fe3O4@Au composite magnetic nanoparticles in vitro and in vivo. Int. J. Nanomedicine 2805.

Li, Y., Xu, S., Zhang, Q., Li, L., Lai, L., Zheng, T., Su, J., Yang, N., and Li, Y. (2014). Cytotoxicity study on SH‐SY5Y cells cultured at high glucose levels and treated with bupivacaine. Mol. Med. Rep. *9*, 515–520.

Lin, B., Li, X., Zhang, H., Lin, Z., Tian, L., Nie, C., Fang, Y., and Xi, Z. (2014). Comparison of in vitro toxicity of mainstream cigarette smoke particulate matter from nano- to micro-size. Food Chem. Toxicol. Int. J. Publ. Br. Ind. Biol. Res. Assoc. *64*, 353–360.

Lin, H., Rumaiz, A.K., Schulz, M., Wang, D., Rock, R., Huang, C.P., and Shah, S.I. (2008a). Photocatalytic activity of pulsed laser deposited TiO2 thin films. Mater. Sci. Eng. B *151*, 133–139.

Lin, W., Xu, Y., Huang, C.-C., Ma, Y., Shannon, K.B., Chen, D.-R., and Huang, Y.-W. (2008b). Toxicity of nano- and micro-sized ZnO particles in human lung epithelial cells. J. Nanoparticle Res. *11*, 25–39.

Liu, S., Xu, L., Zhang, T., Ren, G., and Yang, Z. (2010). Oxidative stress and apoptosis induced by nanosized titanium dioxide in PC12 cells. Toxicology *267*, 172–177.

Liu, Y., Chen, Z., and Wang, J. (2011). Systematic evaluation of biocompatibility of magnetic Fe3O 4 nanoparticles with six different mammalian cell lines. J. Nanoparticle Res. *13*, 199–212.

Liu, Z., Cai, W., He, L., Nakayama, N., Chen, K., Sun, X., Chen, X., and Dai, H. (2007). In vivo biodistribution and highly efficient tumour targeting of carbon nanotubes in mice. Nat. Nanotechnol. *2*, 47–52.

Lloyd, D.R., and Phillips, D.H. (1999). Oxidative DNA damage mediated by copper(II), iron(II) and nickel(II) fenton reactions: evidence for site-specific mechanisms in the formation of double-strand breaks, 8-hydroxydeoxyguanosine and putative intrastrand cross-links. Mutat. Res. *424*, 23–36.

Long, T.C., Saleh, N., Tilton, R.D., Lowry, G.V., and Veronesi, B. (2006). Titanium dioxide (P25) produces reactive oxygen species in immortalized brain microglia (BV2): implications for nanoparticle neurotoxicity. Environ. Sci. Technol. *40*, 4346–4352.

Long, T.C., Tajuba, J., Sama, P., Saleh, N., Swartz, C., Parker, J., Hester, S., Lowry, G.V., and Veronesi, B. (2007). Nanosize Titanium Dioxide Stimulates Reactive Oxygen Species in Brain Microglia and Damages Neurons in Vitro. Environ. Health Perspect. *115*, 1631–1637.

Lu, A.-H., Salabas, E.L., and Schüth, F. (2007). Magnetic Nanoparticles: Synthesis, Protection, Functionalization, and Application. Angew. Chem. Int. Ed. *46*, 1222–1244.

Luther, E.M., Petters, C., Bulcke, F., Kaltz, A., Thiel, K., Bickmeyer, U., and Dringen, R. (2013). Endocytotic uptake of iron oxide nanoparticles by cultured brain microglial cells. Acta Biomater. *9*, 8454–8465.

Ma, L., Liu, J., Li, N., Wang, J., Duan, Y., Yan, J., Liu, H., Wang, H., and Hong, F. (2010). Oxidative stress in the brain of mice caused by translocated nanoparticulate TiO2 delivered to the abdominal cavity. Biomaterials *31*, 99–105.

Ma, P., Luo, Q., Chen, J., Gan, Y., Du, J., Ding, S., Xi, Z., and Yang, X. (2012). Intraperitoneal injection of magnetic Fe_3O_4-nanoparticle induces hepatic and renal tissue injury via oxidative stress in mice. Int. J. Nanomedicine *7*, 4809–4818.

Maddirala, Y., Tobwala, S., and Ercal, N. (2015). N-acetylcysteineamide protects against manganese-induced toxicity in SH-SY5Y cell line. Brain Res.

Magdolenova, Z., Bilaničová, D., Pojana, G., Fjellsbø, L.M., Hudecova, A., Hasplova, K., Marcomini, A., and Dusinska, M. (2012a). Impact of agglomeration and different dispersions of titanium dioxide nanoparticles on the human related in vitro cytotoxicity and genotoxicity. J. Environ. Monit. JEM *14*, 455–464.

Magdolenova, Z., Lorenzo, Y., Collins, A., and Dusinska, M. (2012b). Can standard genotoxicity tests be applied to nanoparticles? J. Toxicol. Environ. Health A *75*, 800–806.

Magdolenova, Z., Collins, A., Kumar, A., Dhawan, A., Stone, V., and Dusinska, M. (2014). Mechanisms of genotoxicity. A review of *in vitro* and *in vivo* studies with engineered nanoparticles. Nanotoxicology *8*, 233–278.

Mahler, G.J., Esch, M.B., Tako, E., Southard, T.L., Archer, S.D., Glahn, R.P., and Shuler, M.L. (2012). Oral exposure to polystyrene nanoparticles affects iron absorption. Nat. Nanotechnol. *7*, 264–271.

Mahmoudi, M., Azadmanesh, K., Shokrgozar, M.A., Journeay, W.S., and Laurent, S. (2011). Effect of Nanoparticles on the Cell Life Cycle. Chem. Rev. *111*, 3407–3432.

Mahon, E., Hristov, D.R., and Dawson, K.A. (2012). Stabilising fluorescent silica nanoparticles against dissolution effects for biological studies. Chem. Commun. Camb. Engl. *48*, 7970–7972.

Majno, G., and Joris, I. (1995). Apoptosis, oncosis, and necrosis. An overview of cell death. Am. J. Pathol. *146*, 3–15.

Majuru, S., and Oyewumi, M.O. (2009). Nanotechnology in Drug Development and Life Cycle Management. In Nanotechnology in Drug Delivery, M.M. de Villiers, P. Aramwit, and G.S. Kwon, eds. (Springer New York), pp. 597–619.

Malvindi, M.A., De Matteis, V., Galeone, A., Brunetti, V., Anyfantis, G.C., Athanassiou, A., Cingolani, R., and Pompa, P.P. (2014). Toxicity assessment of silica coated iron oxide nanoparticles and biocompatibility improvement by surface engineering. PloS One *9*, e85835.

Manke, A., Wang, L., and Rojanasakul, Y. (2013). Mechanisms of Nanoparticle-Induced Oxidative Stress and Toxicity. BioMed Res. Int. *2013*, e942916.

Manninger, S.P., Muldoon, L.L., Nesbit, G., Murillo, T., Jacobs, P.M., and Neuwelt, E.A. (2005). An exploratory study of ferumoxtran-10 nanoparticles as a blood-brain barrier imaging agent targeting phagocytic cells in CNS inflammatory lesions. AJNR Am. J. Neuroradiol. *26*, 2290–2300.

Márquez-Ramírez, S.G., Delgado-Buenrostro, N.L., Chirino, Y.I., Iglesias, G.G., and López-Marure, R. (2012). Titanium dioxide nanoparticles inhibit proliferation and induce morphological changes and apoptosis in glial cells. Toxicology *302*, 146–156.

Martins, J., Barbosa, O., Bastos, M. de L., Carvalho, F., lix, Capela, J., and Paulo, O. (2013). Differential Effects of Methyl-4-Phenylpyridinium Ion, Rotenone, and Paraquat on Differentiated SH-SY5Y Cells. J. Toxicol. *2013*, e347312.

Martirosyan, A., and Schneider, Y.-J. (2014). Engineered nanomaterials in food: implications for food safety and consumer health. Int. J. Environ. Res. Public. Health *11*, 5720–5750.

Masserini, M. (2013). Nanoparticles for Brain Drug Delivery. Int. Sch. Res. Not. *2013*, e238428.

Matsuzaki, K., Harada, A., Takeiri, A., Tanaka, K., and Mishima, M. (2010). Whole cell-ELISA to measure the gammaH2AX response of six aneugens and eight DNA-damaging chemicals. Mutat. Res. *700*, 71–79.

Maynard, A.D., Aitken, R.J., Butz, T., Colvin, V., Donaldson, K., Oberdörster, G., Philbert, M.A., Ryan, J., Seaton, A., Stone, V., et al. (2006). Safe handling of nanotechnology. Nature *444*, 267–269.

Maynard, A.D., Warheit, D.B., and Philbert, M.A. (2010). The New Toxicology of Sophisticated Materials: Nanotoxicology and Beyond. Toxicol. Sci. kfq372.

Mc Carthy, D.J., Malhotra, M., O'Mahony, A.M., Cryan, J.F., and O'Driscoll, C.M. (2014). Nanoparticles and the Blood-Brain Barrier: Advancing from In-Vitro Models Towards Therapeutic Significance. Pharm. Res.

McDonald, I., Sloan, G.C., Zijlstra, A.A., Matsunaga, N., Matsuura, M., Kraemer, K.E., Bernard-Salas, J., and Markwick, A.J. (2010). Rusty Old Stars: A Source of the Missing Interstellar Iron? Astrophys. J. Lett. *717*, L92–L97.

Medina-Reyes, E.I., Bucio-López, L., Freyre-Fonseca, V., Sánchez-Pérez, Y., García-Cuéllar, C.M., Morales-Bárcenas, R., Pedraza-Chaverri, J., and Chirino, Y.I. (2015). Cell cycle synchronization reveals greater G2/M-phase accumulation of lung epithelial cells exposed to titanium dioxide nanoparticles. Environ. Sci. Pollut. Res. Int. *22*, 3976–3982.

Meena, R., Kumar, S., and Paulraj, R. (2015). Titanium oxide (TiO2) nanoparticles in induction of apoptosis and inflammatory response in brain. J. Nanoparticle Res. *17*, 1–14.

Mesárošová, M., Kozics, K., Bábelová, A., Regendová, E., Pastorek, M., Vnuková, D., Buliaková, B., Rázga, F., and Gábelová, A. (2014). The role of reactive oxygen species in the genotoxicity of surface-modified magnetite nanoparticles. Toxicol. Lett. *226*, 303–313.

Migliore, L., Uboldi, C., Di Bucchianico, S., and Coppedè, F. (2015). Nanomaterials and neurodegeneration. Environ. Mol. Mutagen. *56*, 149–170.

M. L. L. Freitas, L.P.S. (2002). A double-coated magnetite-based magnetic fluid evaluation by cytometry and genetic tests. J. Magn. Magn. Mater. - J MAGN MAGN MATER *252*, 396–398.

Mohammadipour, A., Fazel, A., Haghir, H., Motejaded, F., Rafatpanah, H., Zabihi, H., Hosseini, M., and Bideskan, A.E. (2014). Maternal exposure to titanium dioxide nanoparticles during pregnancy; impaired memory and decreased hippocampal cell proliferation in rat offspring. Environ. Toxicol. Pharmacol. *37*, 617–625.

Møller, P., Loft, S., Ersson, C., Koppen, G., Dusinska, M., and Collins, A. (2014). On the search for an intelligible comet assay descriptor. Front. Genet. *5*.

Montazer, M., and Seifollahzadeh, S. (2011). Enhanced self-cleaning, antibacterial and UV protection properties of nano TiO2 treated textile through enzymatic pretreatment. Photochem. Photobiol. *87*, 877–883.

Morgan, D.O. (2007). The Cell Cycle: Principles of Control (New Science Press in association with Oxford University Press: London).

Morgan, J.W., and Anders, E. (1980). Chemical composition of Earth, Venus, and Mercury. Proc. Natl. Acad. Sci. *77*, 6973–6977.

Morkoç, H., and Özgür, Ü. (2009). General Properties of ZnO. In Zinc Oxide, (Wiley-VCH Verlag GmbH & Co. KGaA), pp. 1–76.

Mosmann, T. (1983). Rapid colorimetric assay for cellular growth and survival: application to proliferation and cytotoxicity assays. J. Immunol. Methods *65*, 55–63.

M. Simkó, and Mats-Olof Mattsson (2014). Interactions Between Nanosized Materials and the Brain. Curr. Med. Chem. *21*, 4200–4214.

Mühlfeld, C., Gehr, P., and Rothen-Rutishauser, B. (2008). Translocation and cellular entering mechanisms of nanoparticles in the respiratory tract. Swiss Med. Wkly. *138*, 387–391.

Naahidi, S., Jafari, M., Edalat, F., Raymond, K., Khademhosseini, A., and Chen, P. (2013). Biocompatibility of engineered nanoparticles for drug delivery. J. Control. Release Off. J. Control. Release Soc. *166*, 182–194.

Nalika, N., and Parvez, S. (2015). Mitochondrial dysfunction in titanium dioxide nanoparticle-induced neurotoxicity. Toxicol. Mech. Methods 1–9.

Namvar, F., Rahman, H.S., Mohamad, R., Baharara, J., Mahdavi, M., Amini, E., Chartrand, M.S., and Yeap, S.K. (2014). Cytotoxic effect of magnetic iron oxide nanoparticles synthesized via seaweed aqueous extract. Int. J. Nanomedicine *9*, 2479–2488.

Nancy A Monteiro-Riviere, Alfred O Inman, and Jessica P Ryman-Rasmussen (2007). Dermal Effects of Nanomaterials. In Nanotoxicology: Characterization, Dosing, and Health Effects, (Informa Healthcare), pp. 317–338.

Naqvi, S., Samim, M., Abdin, M., Ahmed, F.J., Maitra, A., Prashant, C., and Dinda, A.K. (2010). Concentration-dependent toxicity of iron oxide nanoparticles mediated by increased oxidative stress. Int. J. Nanomedicine *5*, 983–989.

National Institute for Occupational Safety and Health (NIOSH) (2006). Approaches to Safe Nanotechnology .

Naya, M., Kobayashi, N., Ema, M., Kasamoto, S., Fukumuro, M., Takami, S., Nakajima, M., Hayashi, M., and Nakanishi, J. (2012). In vivo genotoxicity study of titanium dioxide

nanoparticles using comet assay following intratracheal instillation in rats. Regul. Toxicol. Pharmacol. RTP *62*, 1–6.

Nel, A., Xia, T., Mädler, L., and Li, N. (2006). Toxic potential of materials at the nanolevel. Science *311*, 622–627.

Nel, A.E., Mädler, L., Velegol, D., Xia, T., Hoek, E.M.V., Somasundaran, P., Klaessig, F., Castranova, V., and Thompson, M. (2009). Understanding biophysicochemical interactions at the nano–bio interface. Nat. Mater. *8*, 543–557.

Nemes, Z., Dietz, R., Lüth, J.B., Gomba, S., Hackenthal, E., and Gross, F. (1979). The pharmacological relevance of vital staining with neutral red. Experientia *35*, 1475–1476.

Neuwelt, E.A., Várallyay, P., Bagó, A.G., Muldoon, L.L., Nesbit, G., and Nixon, R. (2004). Imaging of iron oxide nanoparticles by MR and light microscopy in patients with malignant brain tumours. Neuropathol. Appl. Neurobiol. *30*, 456–471.

Nighoghossian, N., Wiart, M., Cakmak, S., Berthezène, Y., Derex, L., Cho, T.-H., Nemoz, C., Chapuis, F., Tisserand, G.-L., Pialat, J.-B., et al. (2007). Inflammatory response after ischemic stroke: a USPIO-enhanced MRI study in patients. Stroke J. Cereb. Circ. *38*, 303–307.

NIH (2014). Nanomaterials- National Institute of Environmental Health Sciences- available from http://www.niehs.nih.gov/health/topics/agents/sya-nano/.

Niska, K., Pyszka, K., Tukaj, C., Wozniak, M., Radomski, M.W., and Inkielewicz-Stepniak, I. (2015). Titanium dioxide nanoparticles enhance production of superoxide anion and alter the antioxidant system in human osteoblast cells. Int. J. Nanomedicine *10*, 1095–1107.

NNI (2007). The National Nanotechnology Initiative strategic plan. Science, Engineering and Technology Subcommittee; Committee on Technology, National Science and Technology Council.

Numano, T., Xu, J., Futakuchi, M., Fukamachi, K., Alexander, D.B., Furukawa, F., Kanno, J., Hirose, A., Tsuda, H., and Suzui, M. (2014). Comparative study of toxic effects of anatase and rutile type nanosized titanium dioxide particles in vivo and in vitro. Asian Pac. J. Cancer Prev. APJCP *15*, 929–935.

Nüsse, M., Beisker, W., Kramer, J., Miller, B.M., Schreiber, G.A., Viaggi, S., Weller, E.M., and Wessels, J.M. (1994). Chapter 9 Measurement of Micronuclei by Flow Cytometry. In Methods in Cell Biology, J.P.R. and H.A.C. Zbigniew Darzynkiewicz, ed. (Academic Press), pp. 149–158.

Oberdörster, G. (2001). Pulmonary effects of inhaled ultrafine particles. Int. Arch. Occup. Environ. Health *74*, 1–8.

Oberdörster, G. (2010). Safety assessment for nanotechnology and nanomedicine: concepts of nanotoxicology. J. Intern. Med. *267*, 89–105.

Oberdörster, G., Oberdörster, E., and Oberdörster, J. (2005). Nanotoxicology: an emerging discipline evolving from studies of ultrafine particles. Environ. Health Perspect. *113*, 823–839.

Oberdörster, G., Stone, V., and Donaldson, K. (2007). Toxicology of nanoparticles: A historical perspective. Nanotoxicology *1*, 2–25.

Oberdörster, G., Elder, A., and Rinderknecht, A. (2009). Nanoparticles and the Brain: Cause for Concern? In Journal of Nanoscience and Nanotechnology, pp. 4996–5007.

OECD (2014). Report of the OECD Expert Meeting On the Physical Chemical Properties of Manufactured Nanomaterials and Test Guidelines. Organisation for Economic Co-operation and Development. ENV/JM/MONO(2014)15.

Ohashi, T., Mizutani, A., Murakami, A., Kojo, S., Ishii, T., and Taketani, S. (2002). Rapid oxidation of dichlorodihydrofluorescin with heme and hemoproteins: formation of the fluorescein is independent of the generation of reactive oxygen species. FEBS Lett. *511*, 21–27.

Oliveira, P. (2012). The Elements Periodic Table Reference (PediaPress).

Olivieri, G., Hess, C., Savaskan, E., Ly, C., Meier, F., Baysang, G., Brockhaus, M., and Müller-Spahn, F. (2001). Melatonin protects SH-SY5Y neuroblastoma cells from cobalt-induced oxidative stress, neurotoxicity and increased beta-amyloid secretion. J. Pineal Res. *31*, 320–325.

Orazizadeh, M., Fakhredini, F., Mansouri, E., and Khorsandi, L. (2014). Effect of glycyrrhizic acid on titanium dioxide nanoparticles-induced hepatotoxicity in rats. Chem. Biol. Interact. *220*, 214–221.

Ortlieb M (2010). White Giant or White Dwarf?Particle Size Distribution Measurements of TiO2. GIT Lab J Eur *14*, 42–43.

Osman, I.F., Baumgartner, A., Cemeli, E., Fletcher, J.N., and Anderson, D. (2010). Genotoxicity and cytotoxicity of zinc oxide and titanium dioxide in HEp-2 cells. Nanomed. *5*, 1193–1203.

Osmond-McLeod, M.J., Osmond, R.I.W., Oytam, Y., McCall, M.J., Feltis, B., Mackay-Sim, A., Wood, S.A., and Cook, A.L. (2013). Surface coatings of ZnO nanoparticles mitigate differentially a host of transcriptional, protein and signalling responses in primary human olfactory cells. Part. Fibre Toxicol. *10*, 54.

Ostrovsky, S., Kazimirsky, G., Gedanken, A., and Brodie, C. (2009). Selective cytotoxic effect of ZnO nanoparticles on glioma cells. Nano Res. *2*, 882–890.

Oszlánczi, G., Papp, A., Szabó, A., Nagymajtényi, L., Sápi, A., Kónya, Z., Paulik, E., and Vezér, T. (2011). Nervous system effects in rats on subacute exposure by lead-containing nanoparticles via the airways. Inhal. Toxicol. *23*, 173–181.

Paino, I.M.M., and Zucolotto, V. (2014). Poly(vinyl alcohol)-coated silver nanoparticles: Activation of neutrophils and nanotoxicology effects in human hepatocarcinoma and mononuclear cells. Environ. Toxicol. Pharmacol. *39*, 614–621.

Pal, A.K., Bello, D., Budhlall, B., Rogers, E., and Milton, D.K. (2011). Screening for Oxidative Stress Elicited by Engineered Nanomaterials: Evaluation of Acellular DCFH Assay. Dose-Response *10*, 308–330.

Pandurangan, M., and Kim, D.H. (2015). In vitro toxicity of zinc oxide nanoparticles: a review. J. Nanoparticle Res. *17*, 1–8.

Pankhurst, Q.A., Connolly, J., Jones, S.K., and Dobson, J. (2003). Applications of magnetic nanoparticles in biomedicine. J. Phys. Appl. Phys. *36*, R167.

Pasupuleti, S., Alapati, S., Ganapathy, S., Anumolu, G., Pully, N.R., and Prakhya, B.M. (2012). Toxicity of zinc oxide nanoparticles through oral route. Toxicol. Ind. Health *28*, 675–686.

Paszek, E., Czyz, J., Woźnicka, O., Jakubiak, D., Wojnarowicz, J., Łojkowski, W., and Stepień, E. (2012). Zinc oxide nanoparticles impair the integrity of human umbilical vein endothelial cell monolayer in vitro. J. Biomed. Nanotechnol. *8*, 957–967.

Pavlica, S., Gaunitz, F., and Gebhardt, R. (2009). Comparative in vitro toxicity of seven zinc-salts towards neuronal PC12 cells. Toxicol. Vitro Int. J. Publ. Assoc. BIBRA *23*, 653–659.

Pedram, M.S.Z., Shamloo, A., GhafarZadeh, E., and Alasty, A. (2014). Modeling and simulation of crossing magnetic nanoparticles through Blood Brain Barrier (BBB). Conf. Proc. Annu. Int. Conf. IEEE Eng. Med. Biol. Soc. IEEE Eng. Med. Biol. Soc. Annu. Conf. *2014*, 5280–5283.

Periasamy, V.S., Athinarayanan, J., Al-Hadi, A.M., Juhaimi, F.A., and Alshatwi, A.A. (2014). Effects of Titanium Dioxide Nanoparticles Isolated from Confectionery Products on the Metabolic Stress Pathway in Human Lung Fibroblast Cells. Arch. Environ. Contam. Toxicol.

Periasamy, V.S., Athinarayanan, J., Al-Hadi, A.M., Juhaimi, F.A., Mahmoud, M.H., and Alshatwi, A.A. (2015). Identification of titanium dioxide nanoparticles in food products: Induce intracellular oxidative stress mediated by TNF and CYP1A genes in human lung fibroblast cells. Environ. Toxicol. Pharmacol. *39*, 176–186.

Perry, S.W., Norman, J.P., Barbieri, J., Brown, E.B., and Gelbard, H.A. (2011). Mitochondrial membrane potential probes and the proton gradient: a practical usage guide. BioTechniques *50*, 98–115.

Petersen, E.J., Reipa, V., Watson, S.S., Stanley, D.L., Rabb, S.A., and Nelson, B.C. (2014). DNA damaging potential of photoactivated p25 titanium dioxide nanoparticles. Chem. Res. Toxicol. *27*, 1877–1884.

Petković, J., Zegura, B., Stevanović, M., Drnovšek, N., Uskoković, D., Novak, S., and Filipič, M. (2011). DNA damage and alterations in expression of DNA damage responsive genes induced by TiO2 nanoparticles in human hepatoma HepG2 cells. Nanotoxicology *5*, 341–353.

Petrini, J.H.J., and Stracker, T.H. (2003). The cellular response to DNA double-strand breaks: defining the sensors and mediators. Trends Cell Biol. *13*, 458–462.

Pettmann, B., and Henderson, C.E. (1998). Neuronal cell death. Neuron *20*, 633–647.

Pisanic, T.R., 2nd, Blackwell, J.D., Shubayev, V.I., Fiñones, R.R., and Jin, S. (2007). Nanotoxicity of iron oxide nanoparticle internalization in growing neurons. Biomaterials *28*, 2572–2581.

Pitkethly, M.J. (2004). Nanomaterials – the driving force. Mater. Today *7*, 20–29.

Powers, K.W., Brown, S.C., Krishna, V.B., Wasdo, S.C., Moudgil, B.M., and Roberts, S.M. (2006). Research Strategies for Safety Evaluation of Nanomaterials. Part VI. Characterization of Nanoscale Particles for Toxicological Evaluation. Toxicol. Sci. *90*, 296–303.

Powers, K.W., Palazuelos, M., Moudgil, B.M., and Roberts, S.M. (2007). Characterization of the size, shape, and state of dispersion of nanoparticles for toxicological studies. Nanotoxicology *1*, 42–51.

Powers, K.W., Palazuelos, M., Brown, S.C., and Roberts, S.M. (2009). Characterization of Nanomaterials for Toxicological Evaluation. In Nanotoxicity, S.C. Sahu, and D.A. Casciano, eds. (John Wiley & Sons, Ltd), pp. 1–27.

Powers, K.W., Carpinone, P.L., and Siebein, K.N. (2012). Characterization of Nanomaterials for Toxicological Studies. In Nanotoxicity, pp. 13–32.

Prasad, R.Y., Chastain, P.D., Nikolaishvili-Feinberg, N., Smeester, L., Kaufmann, W.K., and Fry, R.C. (2013a). Titanium dioxide nanoparticles activate the ATM-Chk2 DNA damage response in human dermal fibroblasts. Nanotoxicology *7*, 1111–1119.

Prasad, R.Y., Wallace, K., Daniel, K.M., Tennant, A.H., Zucker, R.M., Strickland, J., Dreher, K., Kligerman, A.D., Blackman, C.F., and Demarini, D.M. (2013b). Effect of treatment media on the agglomeration of titanium dioxide nanoparticles: impact on genotoxicity, cellular interaction, and cell cycle. ACS Nano *7*, 1929–1942.

Prasad, R.Y., Simmons, S.O., Killius, M.G., Zucker, R.M., Kligerman, A.D., Blackman, C.F., Fry, R.C., and Demarini, D.M. (2014). Cellular interactions and biological responses to titanium dioxide nanoparticles in HepG2 and BEAS-2B cells: role of cell culture media. Environ. Mol. Mutagen. *55*, 336–342.

Premanathan, M., Karthikeyan, K., Jeyasubramanian, K., and Manivannan, G. (2011). Selective toxicity of ZnO nanoparticles toward Gram-positive bacteria and cancer cells by apoptosis through lipid peroxidation. Nanomedicine Nanotechnol. Biol. Med. *7*, 184–192.

Qiao, R., Jia, Q., Hüwel, S., Xia, R., Liu, T., Gao, F., Galla, H.-J., and Gao, M. (2012). Receptor-mediated delivery of magnetic nanoparticles across the blood-brain barrier. ACS Nano *6*, 3304–3310.

Radcliff, G., and Jaroszeski, M.J. (1998). Basics of flow cytometry. Methods Mol. Biol. Clifton NJ *91*, 1–24.

Ramasamy, M., Das, M., An, S.S.A., and Yi, D.K. (2014). Role of surface modification in zinc oxide nanoparticles and its toxicity assessment toward human dermal fibroblast cells. Int. J. Nanomedicine *9*, 3707–3718.

Ramesh, V., Ravichandran, P., Copeland, C.L., Gopikrishnan, R., Biradar, S., Goornavar, V., Ramesh, G.T., and Hall, J.C. (2012). Magnetite induces oxidative stress and apoptosis in lung epithelial cells. Mol. Cell. Biochem. *363*, 225–234.

Ranjit, K.T., and Klabunde, K.J. (2007). Nanotechnology: Fundamental Principles and Applications. In Kent and Riegel's Handbook of Industrial Chemistry and Biotechnology, J.A. Kent, ed. (Springer US), pp. 328–344.

Rausch, M., Hiestand, P., Baumann, D., Cannet, C., and Rudin, M. (2003). MRI-based monitoring of inflammation and tissue damage in acute and chronic relapsing EAE. Magn. Reson. Med. Off. J. Soc. Magn. Reson. Med. Soc. Magn. Reson. Med. *50*, 309–314.

Rausch, M., Hiestand, P., Foster, C.A., Baumann, D.R., Cannet, C., and Rudin, M. (2004). Predictability of FTY720 efficacy in experimental autoimmune encephalomyelitis by in vivo macrophage tracking: clinical implications for ultrasmall superparamagnetic iron oxide-enhanced magnetic resonance imaging. J. Magn. Reson. Imaging JMRI *20*, 16–24.

Redon, C.E., Nakamura, A.J., Gouliaeva, K., Rahman, A., Blakely, W.F., and Bonner, W.M. (2011). Q(γ-H2AX), an analysis method for partial-body radiation exposure using γ-H2AX in nonhuman primate lymphocytes. Radiat. Meas. *46*, 877–881.

Reed, R.B., Ladner, D.A., Higgins, C.P., Westerhoff, P., and Ranville, J.F. (2012). Solubility of nano-zinc oxide in environmentally and biologically important matrices. Environ. Toxicol. Chem. SETAC *31*, 93–99.

Repetto, G., del Peso, A., and Zurita, J.L. (2008). Neutral red uptake assay for the estimation of cell viability/cytotoxicity. Nat. Protoc. *3*, 1125–1131.

Rinna, A., Magdolenova, Z., Hudecova, A., Kruszewski, M., Refsnes, M., and Dusinska, M. (2015). Effect of silver nanoparticles on mitogen-activated protein kinases activation: role of reactive oxygen species and implication in DNA damage. Mutagenesis *30*, 59–66.

Rittikulsittichai, S., Singhana, B., Bryan, W.W., Sarangi, S., Jamison, A.C., Brazdeikis, A., and Lee, T.R. (2013). Preparation, characterization, and utilization of multi-functional magnetic-fluorescent composites for bio-imaging and magnetic hyperthermia therapy. RSC Adv. *3*, 7838–7849.

Rivera-Gil, P., Clift, M.J.D., Rutishauser, B.R., and Parak, W.J. (2012). Methods for understanding the interaction between nanoparticles and cells. Methods Mol. Biol. Clifton NJ *926*, 33–56.

Rivet, C.J., Yuan, Y., Borca-Tasciuc, D.-A., and Gilbert, R.J. (2012). Altering iron oxide nanoparticle surface properties induce cortical neuron cytotoxicity. Chem. Res. Toxicol. *25*, 153–161.

Rogakou, E.P., and Sekeri-Pataryas, K.E. (1999). Histone variants of H2A and H3 families are regulated during in vitro aging in the same manner as during differentiation. Exp. Gerontol. *34*, 741–754.

Rogakou, E.P., Pilch, D.R., Orr, A.H., Ivanova, V.S., and Bonner, W.M. (1998). DNA double-stranded breaks induce histone H2AX phosphorylation on serine 139. J. Biol. Chem. *273*, 5858–5868.

Roman, D., Locher, F., Suter, W., Cordier, A., and Bobadilla, M. (1998). Evaluation of a new procedure for the flow cytometric analysis of in vitro, chemically induced micronuclei in V79 cells. Environ. Mol. Mutagen. *32*, 387–396.

Rosemary M Gibson (2007). Understanding the Potential Neurotoxicology of Nanoparticles. In Nanotoxicology: Characterization, Dosing, and Health Effects, (Informa Healthcare), pp. 299–316.

Rosenberg, J.T., Sachi-Kocher, A., Davidson, M.W., and Grant, S.C. (2012). Intracellular SPIO labeling of microglia: high field considerations and limitations for MR microscopy. Contrast Media Mol. Imaging *7*, 121–129.

Rota, C., Fann, Y.C., and Mason, R.P. (1999). Phenoxyl Free Radical Formation during the Oxidation of the Fluorescent Dye 2′,7′-Dichlorofluorescein by Horseradish Peroxidase POSSIBLE CONSEQUENCES FOR OXIDATIVE STRESS MEASUREMENTS. J. Biol. Chem. *274*, 28161–28168.

Roy, R., Singh, S.K., Chauhan, L.K.S., Das, M., Tripathi, A., and Dwivedi, P.D. (2014). Zinc oxide nanoparticles induce apoptosis by enhancement of autophagy via PI3K/Akt/mTOR inhibition. Toxicol. Lett. *227*, 29–40.

Roy, R., Das, M., and Dwivedi, P.D. (2015). Toxicological mode of action of ZnO nanoparticles: Impact on immune cells. Mol. Immunol. *63*, 184–192.

Rubio, L., Annangi, B., Vila, L., Hernández, A., and Marcos, R. (2015). Antioxidant and anti-genotoxic properties of cerium oxide nanoparticles in a pulmonary-like cell system. Arch. Toxicol.

Sadeghiani, N., Barbosa, L.S., Silva, L.P., Azevedo, R.B., Morais, P.C., and Lacava, Z.G.M. (2005). Genotoxicity and inflammatory investigation in mice treated with magnetite nanoparticles surface coated with polyaspartic acid. J. Magn. Magn. Mater. *289*, 466–468.

Sahay, G., Alakhova, D.Y., and Kabanov, A.V. (2010). Endocytosis of Nanomedicines. J. Control. Release Off. J. Control. Release Soc. *145*, 182–195.

Sahu, S.C., and Casciano, D.A. (2009). Evaluation of Toxicity of Nanostructures in Biological Systems. In Nanotoxicity: From In Vivo and In Vitro Models to Health Risks, (John Wiley & Sons), pp. 115–158.

Sahu, D., Kannan, G.M., Vijayaraghavan, R., Anand, T., and Khanum, F. (2013). Nanosized zinc oxide induces toxicity in human lung cells. ISRN Toxicol. *2013*, 316075.

Sahu, D., Kannan, G.M., and Vijayaraghavan, R. (2014). Size-dependent effect of zinc oxide on toxicity and inflammatory potential of human monocytes. J. Toxicol. Environ. Health A *77*, 177–191.

Saleh, A., Schroeter, M., Jonkmanns, C., Hartung, H.-P., Mödder, U., and Jander, S. (2004). In vivo MRI of brain inflammation in human ischaemic stroke. Brain J. Neurol. *127*, 1670–1677.

Salem, W., Leitner, D.R., Zingl, F.G., Schratter, G., Prassl, R., Goessler, W., Reidl, J., and Schild, S. (2015). Antibacterial activity of silver and zinc nanoparticles against Vibrio cholerae and enterotoxic Escherichia coli. Int. J. Med. Microbiol. *305*, 85–95.

Salik Hussain, J.A.J.V. (2011). Interactions of nanomaterials with the immune system. Wiley Interdiscip. Rev. Nanomed. Nanobiotechnol. *4*, 169–183.

Sánchez-Flores, M., Pásaro, E., Bonassi, S., Laffon, B., and Valdiglesias, V. (2015). γH2AX Assay as DNA Damage Biomarker for Human Population Studies: Defining Experimental Conditions. Toxicol. Sci. Off. J. Soc. Toxicol. *144*, 406–413.

Sang, X., Fei, M., Sheng, L., Zhao, X., Yu, X., Hong, J., Ze, Y., Gui, S., Sun, Q., Ze, X., et al. (2014). Immunomodulatory effects in the spleen-injured mice following exposure to titanium dioxide nanoparticles. J. Biomed. Mater. Res. A *102*, 3562–3572.

Santamaria, A. (2012). Historical overview of nanotechnology and nanotoxicology. Methods Mol. Biol. Clifton NJ *926*, 1–12.

Santhosh, P.B., and Ulrih, N.P. (2013). Multifunctional superparamagnetic iron oxide nanoparticles: promising tools in cancer theranostics. Cancer Lett. *336*, 8–17.

Saptarshi, S.R., Feltis, B.N., Wright, P.F., and Lopata, A.L. (2015). Investigating the immunomodulatory nature of zinc oxide nanoparticles at sub-cytotoxic levels in vitro and after intranasal instillation in vivo. J. Nanobiotechnology *13*, 6.

Saquib, Q., Al-Khedhairy, A.A., Siddiqui, M.A., Abou-Tarboush, F.M., Azam, A., and Musarrat, J. (2012). Titanium dioxide nanoparticles induced cytotoxicity, oxidative stress and DNA damage in human amnion epithelial (WISH) cells. Toxicol. In Vitro *26*, 351–361.

Sarkar, A., Ghosh, M., and Sil, P.C. (2014a). Nanotoxicity: oxidative stress mediated toxicity of metal and metal oxide nanoparticles. J. Nanosci. Nanotechnol. *14*, 730–743.

Sarkar, J., Ghosh, M., Mukherjee, A., Chattopadhyay, D., and Acharya, K. (2014b). Biosynthesis and safety evaluation of ZnO nanoparticles. Bioprocess Biosyst. Eng. *37*, 165–171.

Sasidharan, A., Chandran, P., Menon, D., Raman, S., Nair, S., and Koyakutty, M. (2011). Rapid dissolution of ZnO nanocrystals in acidic cancer microenvironment leading to preferential apoptosis. Nanoscale *3*, 3657–3669.

Sayes, C.M., and Warheit, D.B. (2009). Characterization of nanomaterials for toxicity assessment. Wiley Interdiscip. Rev. Nanomed. Nanobiotechnol. *1*, 660–670.

Sayes, C.M., Wahi, R., Kurian, P.A., Liu, Y., West, J.L., Ausman, K.D., Warheit, D.B., and Colvin, V.L. (2006). Correlating nanoscale titania structure with toxicity: a cytotoxicity and inflammatory response study with human dermal fibroblasts and human lung epithelial cells. Toxicol. Sci. Off. J. Soc. Toxicol. *92*, 174–185.

Scarpato, R., Castagna, S., Aliotta, R., Azzarà, A., Ghetti, F., Filomeni, E., Giovannini, C., Pirillo, C., Testi, S., Lombardi, S., et al. (2013). Kinetics of nuclear phosphorylation (γ-H2AX) in human lymphocytes treated in vitro with UVB, bleomycin and mitomycin C. Mutagenesis *28*, 465–473.

Schäfer, R., Kehlbach, R., Wiskirchen, J., Bantleon, R., Pintaske, J., Brehm, B.R., Gerber, A., Wolburg, H., Claussen, C.D., and Northoff, H. (2007). Transferrin receptor upregulation: in vitro labeling of rat mesenchymal stem cells with superparamagnetic iron oxide. Radiology *244*, 514–523.

Schroeter, M., Saleh, A., Wiedermann, D., Hoehn, M., and Jander, S. (2004). Histochemical detection of ultrasmall superparamagnetic iron oxide (USPIO) contrast medium uptake in experimental brain ischemia. Magn. Reson. Med. Off. J. Soc. Magn. Reson. Med. Soc. Magn. Reson. Med. *52*, 403–406.

Seil, J.T., and Webster, T.J. (2008). Decreased astroglial cell adhesion and proliferation on zinc oxide nanoparticle polyurethane composites. Int. J. Nanomedicine *3*, 523–531.

Sekar, D., Falcioni, M.L., Barucca, G., and Falcioni, G. (2014). DNA damage and repair following In vitro exposure to two different forms of titanium dioxide nanoparticles on trout erythrocyte. Environ. Toxicol. *29*, 117–127.

Setyawati, M.I., Khoo, P.K.S., Eng, B.H., Xiong, S., Zhao, X., Das, G.K., Tan, T.T.-Y., Loo, J.S.C., Leong, D.T., and Ng, K.W. (2013). Cytotoxic and genotoxic characterization of titanium dioxide, gadolinium oxide, and poly(lactic-co-glycolic acid) nanoparticles in human fibroblasts. J. Biomed. Mater. Res. A *101*, 633–640.

Setyawati, M.I., Tay, C.Y., and Leong, D.T. (2015). Mechanistic Investigation of the Biological Effects of SiO2 , TiO2 , and ZnO Nanoparticles on Intestinal Cells. Small Weinh. Bergstr. Ger.

Shah, V., Taratula, O., Garbuzenko, O.B., Patil, M.L., Savla, R., Zhang, M., and Minko, T. (2013). Genotoxicity of different nanocarriers: possible modifications for the delivery of nucleic acids. Curr. Drug Discov. Technol. *10*, 8–15.

Shander, A., Cappellini, M.D., and Goodnough, L.T. (2009). Iron overload and toxicity: the hidden risk of multiple blood transfusions. Vox Sang. *97*, 185–197.

Shang, L., Nienhaus, K., and Nienhaus, G.U. (2014). Engineered nanoparticles interacting with cells: size matters. J. Nanobiotechnology *12*, 5.

Sharma, H.S., Hussain, S., Schlager, J., Ali, S.F., and Sharma, A. (2010). Influence of nanoparticles on blood-brain barrier permeability and brain edema formation in rats. Acta Neurochir. Suppl. *106*, 359–364.

Sharma, V., Shukla, R.K., Saxena, N., Parmar, D., Das, M., and Dhawan, A. (2009). DNA damaging potential of zinc oxide nanoparticles in human epidermal cells. Toxicol. Lett. *185*, 211–218.

Sharma, V., Anderson, D., and Dhawan, A. (2011). Zinc oxide nanoparticles induce oxidative stress and genotoxicity in human liver cells (HepG2). J. Biomed. Nanotechnol. *7*, 98–99.

Sharma, V., Anderson, D., and Dhawan, A. (2012). Zinc oxide nanoparticles induce oxidative DNA damage and ROS-triggered mitochondria mediated apoptosis in human liver cells (HepG2). Apoptosis Int. J. Program. Cell Death *17*, 852–870.

Sharma, V.K., Siskova, K.M., Zboril, R., and Gardea-Torresdey, J.L. (2014). Organic-coated silver nanoparticles in biological and environmental conditions: fate, stability and toxicity. Adv. Colloid Interface Sci. *204*, 15–34.

Sharma V. (2011). An Investigation Into The Mechanism Of Toxicity Of Zinc Oxide Nanoparticles. PhD dissertation. School of Life Sciences University of Bradford.

Shen, C., James, S.A., de Jonge, M.D., Turney, T.W., Wright, P.F.A., and Feltis, B.N. (2013). Relating cytotoxicity, zinc ions, and reactive oxygen in ZnO nanoparticle-exposed human immune cells. Toxicol. Sci. Off. J. Soc. Toxicol. *136*, 120–130.

Sheng, L., Ze, Y., Wang, L., Yu, X., Hong, J., Zhao, X., Ze, X., Liu, D., Xu, B., Zhu, Y., et al. (2015). Mechanisms of TiO2 nanoparticle-induced neuronal apoptosis in rat primary cultured hippocampal neurons. J. Biomed. Mater. Res. A *103*, 1141–1149.

Shi, H., Magaye, R., Castranova, V., and Zhao, J. (2013). Titanium dioxide nanoparticles: a review of current toxicological data. Part. Fibre Toxicol. *10*, 15.

Shim, K.H., Jeong, K.-H., Bae, S.O., Kang, M.O., Maeng, E.H., Choi, C.S., Kim, Y.-R., Hulme, J., Lee, E.K., Kim, M.-K., et al. (2014). Assessment of ZnO and SiO2 nanoparticle permeability through and toxicity to the blood-brain barrier using Evans blue and TEM. Int. J. Nanomedicine *9 Suppl 2*, 225–233.

Shrivastava, R., Raza, S., Yadav, A., Kushwaha, P., and Flora, S.J.S. (2014). Effects of sub-acute exposure to TiO2, ZnO and Al2O3 nanoparticles on oxidative stress and histological changes in mouse liver and brain. Drug Chem. Toxicol. *37*, 336–347.

Shubayev, V.I., Pisanic, T.R., 2nd, and Jin, S. (2009). Magnetic nanoparticles for theragnostics. Adv. Drug Deliv. Rev. *61*, 467–477.

Shukla, R.K., Sharma, V., Pandey, A.K., Singh, S., Sultana, S., and Dhawan, A. (2011). ROS-mediated genotoxicity induced by titanium dioxide nanoparticles in human epidermal cells. Toxicol. Vitro Int. J. Publ. Assoc. BIBRA *25*, 231–241.

Shukla, R.K., Kumar, A., Gurbani, D., Pandey, A.K., Singh, S., and Dhawan, A. (2013). TiO(2) nanoparticles induce oxidative DNA damage and apoptosis in human liver cells. Nanotoxicology *7*, 48–60.

Shukla, R.K., Kumar, A., Vallabani, N.V.S., Pandey, A.K., and Dhawan, A. (2014). Titanium dioxide nanoparticle-induced oxidative stress triggers DNA damage and hepatic injury in mice. Nanomed. *9*, 1423–1434.

Singh, B.P., Menchavez, R., Takai, C., Fuji, M., and Takahashi, M. (2005). Stability of dispersions of colloidal alumina particles in aqueous suspensions. J. Colloid Interface Sci. *291*, 181–186.

Singh, N., Manshian, B., Jenkins, G.J.S., Griffiths, S.M., Williams, P.M., Maffeis, T.G.G., Wright, C.J., and Doak, S.H. (2009). NanoGenotoxicology: the DNA damaging potential of engineered nanomaterials. Biomaterials *30*, 3891–3914.

Singh, N., Jenkins, G.J.S., Asadi, R., and Doak, S.H. (2010). Potential toxicity of superparamagnetic iron oxide nanoparticles (SPION). Nano Rev. *1*.

Singh, N., Jenkins, G.J.S., Nelson, B.C., Marquis, B.J., Maffeis, T.G.G., Brown, A.P., Williams, P.M., Wright, C.J., and Doak, S.H. (2012). The role of iron redox state in the genotoxicity of ultrafine superparamagnetic iron oxide nanoparticles. Biomaterials *33*, 163–170.

Singh, N.P., McCoy, M.T., Tice, R.R., and Schneider, E.L. (1988). A simple technique for quantitation of low levels of DNA damage in individual cells. Exp. Cell Res. *175*, 184–191.

Singh, S., Shi, T., Duffin, R., Albrecht, C., van Berlo, D., Höhr, D., Fubini, B., Martra, G., Fenoglio, I., Borm, P.J.A., et al. (2007). Endocytosis, oxidative stress and IL-8 expression in human lung epithelial cells upon treatment with fine and ultrafine TiO2: role of the specific surface area and of surface methylation of the particles. Toxicol. Appl. Pharmacol. *222*, 141–151.

Singh, S.K., Szulik, M.W., Ganguly, M., Khutsishvili, I., Stone, M.P., Marky, L.A., and Gold, B. (2011). Characterization of DNA with an 8-oxoguanine modification. Nucleic Acids Res. *39*, 6789–6801.

Singh, S.P., Rahman, M.F., Murty, U.S.N., Mahboob, M., and Grover, P. (2013). Comparative study of genotoxicity and tissue distribution of nano and micron sized iron oxide in rats after acute oral treatment. Toxicol. Appl. Pharmacol. *266*, 56–66.

Sioutas, C., Delfino, R.J., and Singh, M. (2005). Exposure Assessment for Atmospheric Ultrafine Particles (UFPs) and Implications in Epidemiologic Research. Environ. Health Perspect. *113*, 947–955.

S. Isfort, C., and Rochnia, M. (2009). Production and physico-chemical characterisation of nanoparticles. Toxicol. Lett. *186*, 148–151.

Sliwinska, A., Kwiatkowski, D., Czarny, P., Milczarek, J., Toma, M., Korycinska, A., Szemraj, J., and Sliwinski, T. (2015). Genotoxicity and cytotoxicity of ZnO and Al2O3 nanoparticles. Toxicol. Mech. Methods 1–8.

Smith, C.C., O'Donovan, M.R., and Martin, E.A. (2006). hOGG1 recognizes oxidative damage using the comet assay with greater specificity than FPG or ENDOIII. Mutagenesis *21*, 185–190.

Soenen, S.J.H., and De Cuyper, M. (2009). Assessing cytotoxicity of (iron oxide-based) nanoparticles: an overview of different methods exemplified with cationic magnetoliposomes. Contrast Media Mol. Imaging *4*, 207–219.

Soenen, S.J.H., Himmelreich, U., Nuytten, N., and De Cuyper, M. (2011). Cytotoxic effects of iron oxide nanoparticles and implications for safety in cell labelling. Biomaterials *32*, 195–205.

Song, Y., Guan, R., Lyu, F., Kang, T., Wu, Y., and Chen, X. (2014). In vitro cytotoxicity of silver nanoparticles and zinc oxide nanoparticles to human epithelial colorectal adenocarcinoma (Caco-2) cells. Mutat. Res. *769*, 113–118.

SOT (2005). Society of Toxicology (SOT).

Srivastava, R.K., Rahman, Q., Kashyap, M.P., Lohani, M., and Pant, A.B. (2011). Ameliorative Effects of Dimetylthiourea and N-Acetylcysteine on Nanoparticles Induced Cyto-Genotoxicity in Human Lung Cancer Cells-A549. PLoS ONE *6*.

Srivastava, R.K., Rahman, Q., Kashyap, M.P., Singh, A.K., Jain, G., Jahan, S., Lohani, M., Lantow, M., and Pant, A.B. (2013). Nano-titanium dioxide induces genotoxicity and apoptosis in human lung cancer cell line, A549. Hum. Exp. Toxicol. *32*, 153–166.

Stefano Zuin, Giulio Pojana, and Antonio Marcomini (2007). Effect-Oriented Physicochemical Characterization of Nanomaterials. In Nanotoxicology: Characterization, Dosing, and Health Effects, (Informa Healthcare), pp. 19–58.

Stone, V., Johnston, H., and Schins, R.P.F. (2009). Development of in vitro systems for nanotoxicology: methodological considerations. Crit. Rev. Toxicol. *39*, 613–626.

Stroh, A., Zimmer, C., Gutzeit, C., Jakstadt, M., Marschinke, F., Jung, T., Pilgrimm, H., and Grune, T. (2004). Iron oxide particles for molecular magnetic resonance imaging cause transient oxidative stress in rat macrophages. Free Radic. Biol. Med. *36*, 976–984.

Sutariya, V.B., and Pathak, Y. (2015). Biointeractions of Nanomaterials (CRC Press).

Suzuki, H., Toyooka, T., and Ibuki, Y. (2007). Simple and Easy Method to Evaluate Uptake Potential of Nanoparticles in Mammalian Cells Using a Flow Cytometric Light Scatter Analysis. Environ. Sci. Technol. *41*, 3018–3024.

Sweeney, S., Berhanu, D., Ruenraroengsak, P., Thorley, A.J., Valsami-Jones, E., and Tetley, T.D. (2014). Nano-titanium dioxide bioreactivity with human alveolar type-I-like epithelial cells: Investigating crystalline phase as a critical determinant. Nanotoxicology 1–11.

Syama, S., Sreekanth, P.J., Varma, H.K., and Mohanan, P.V. (2014). Zinc oxide nanoparticles induced oxidative stress in mouse bone marrow mesenchymal stem cells. Toxicol. Mech. Methods *24*, 644–653.

Takaki, K., Higuchi, Y., Hashii, M., Ogino, C., and Shimizu, N. (2014). Induction of apoptosis associated with chromosomal DNA fragmentation and caspase-3 activation in leukemia L1210 cells by TiO2 nanoparticles. J. Biosci. Bioeng. *117*, 129–133.

Tamás, M.J., and Martinoia, E. (2006). Molecular Biology of Metal Homeostasis and Detoxification: From Microbes to Man (Springer Science & Business Media).

Tanaka, T., Halicka, D., Traganos, F., and Darzynkiewicz, Z. (2009). Cytometric Analysis of DNA Damage: Phosphorylation of Histone H2AX as a Marker of DNA Double-Strand Breaks (DSBs). In Chromatin Protocols, S.P. Chellappan, ed. (Humana Press), pp. 161–168.

Tang, M., Russell, P.J., and Khatri, A. (2009). Magnetic Nanoparticles: Prospects in Cancer Imaging and Therapy. Discov. Med. *7*, 68–74.

Taniguchi, N. (1974). On the Basic Concept of "Nano-Technology." Bull. Jpn. Soc. Precis. Eng. 18–23.

Tavares, A.M., Louro, H., Antunes, S., Quarré, S., Simar, S., De Temmerman, P.-J., Verleysen, E., Mast, J., Jensen, K.A., Norppa, H., et al. (2014). Genotoxicity evaluation of nanosized titanium dioxide, synthetic amorphous silica and multi-walled carbon nanotubes in human lymphocytes. Toxicol. Vitro Int. J. Publ. Assoc. BIBRA *28*, 60–69.

Tedja, R., Lim, M., Amal, R., and Marquis, C. (2012). Effects of serum adsorption on cellular uptake profile and consequent impact of titanium dioxide nanoparticles on human lung cell lines. ACS Nano *6*, 4083–4093.

Thomsen, L.B., Linemann, T., Pondman, K.M., Lichota, J., Kim, K.S., Pieters, R.J., Visser, G.M., and Moos, T. (2013). Uptake and transport of superparamagnetic iron oxide nanoparticles through human brain capillary endothelial cells. ACS Chem. Neurosci. *4*, 1352–1360.

Tiano, L., Fedeli, D., Ballarini, P., Santoni, G., and Falcioni, G. (2001). Mitochondrial membrane potential in density-separated trout erythrocytes exposed to oxidative stress in vitro. Biochim. Biophys. Acta BBA - Bioenerg. *1505*, 226–237.

Tice, R.R., Agurell, E., Anderson, D., Burlinson, B., Hartmann, A., Kobayashi, H., Miyamae, Y., Rojas, E., Ryu, J.C., and Sasaki, Y.F. (2000). Single cell gel/comet assay: guidelines for in vitro and in vivo genetic toxicology testing. Environ. Mol. Mutagen. *35*, 206–221.

Tomankova, K., Horakova, J., Harvanova, M., Malina, L., Soukupova, J., Hradilova, S., Kejlova, K., Malohlava, J., Licman, L., Dvorakova, M., et al. (2015). Cytotoxicity, cell uptake and microscopic analysis of titanium dioxide and silver nanoparticles in vitro. Food Chem. Toxicol. Int. J. Publ. Br. Ind. Biol. Res. Assoc.

Tomasi, A., Özben, T., and Skulachev, V.P. (2003). Free Radicals, Nitric Oxide, and Inflammation: Molecular, Biochemical, and Clinical Aspects (IOS Press).

Toyokuni, S., and Sagripanti, J.L. (1999). Iron chelators modulate the production of DNA strand breaks and 8-hydroxy-2'-deoxyguanosine. Free Radic. Res. *31*, 123–128.

Toyooka, T., Amano, T., and Ibuki, Y. (2012). Titanium dioxide particles phosphorylate histone H2AX independent of ROS production. Mutat. Res. *742*, 84–91.

Trouiller, B., Reliene, R., Westbrook, A., Solaimani, P., and Schiestl, R.H. (2009). Titanium dioxide nanoparticles induce DNA damage and genetic instability in vivo in mice. Cancer Res. *69*, 8784–8789.

Tu, W.-Z., Li, B., Huang, B., Wang, Y., Liu, X.-D., Guan, H., Zhang, S.-M., Tang, Y., Rang, W.-Q., and Zhou, P.-K. (2013). γH2AX foci formation in the absence of DNA damage: mitotic H2AX phosphorylation is mediated by the DNA-PKcs/CHK2 pathway. FEBS Lett. *587*, 3437–3443.

Tuček, J., Kemp, K.C., Kim, K.S., and Zbořil, R. (2014). Iron-oxide-supported nanocarbon in lithium-ion batteries, medical, catalytic, and environmental applications. ACS Nano *8*, 7571–7612.

Tuomela, S., Autio, R., Buerki-Thurnherr, T., Arslan, O., Kunzmann, A., Andersson-Willman, B., Wick, P., Mathur, S., Scheynius, A., Krug, H.F., et al. (2013). Gene expression profiling of immune-competent human cells exposed to engineered zinc oxide or titanium dioxide nanoparticles. PloS One *8*, e68415.

Turney, T.W., Duriska, M.B., Jayaratne, V., Elbaz, A., O'Keefe, S.J., Hastings, A.S., Piva, T.J., Wright, P.F.A., and Feltis, B.N. (2012). Formation of zinc-containing nanoparticles from Zn^{2+} ions in cell culture media: implications for the nanotoxicology of ZnO. Chem. Res. Toxicol. *25*, 2057–2066.

Unfried, K., Albrecht, C., Klotz, L.-O., Von Mikecz, A., Grether-Beck, S., and Schins, R.P.F. (2007). Cellular responses to nanoparticles: Target structures and mechanisms. Nanotoxicology *1*, 52–71.

Ursini, C.L., Cavallo, D., Fresegna, A.M., Ciervo, A., Maiello, R., Tassone, P., Buresti, G., Casciardi, S., and Iavicoli, S. (2014). Evaluation of cytotoxic, genotoxic and inflammatory response in human alveolar and bronchial epithelial cells exposed to titanium dioxide nanoparticles. J. Appl. Toxicol. JAT *34*, 1209–1219.

Uttara, B., Singh, A.V., Zamboni, P., and Mahajan, R.. (2009). Oxidative Stress and Neurodegenerative Diseases: A Review of Upstream and Downstream Antioxidant Therapeutic Options. Curr. Neuropharmacol. *7*, 65–74.

Valdiglesias, V., Laffon, B., Pásaro, E., and Méndez, J. (2011a). Okadaic acid induces morphological changes, apoptosis and cell cycle alterations in different human cell types. J. Environ. Monit. *13*, 1831–1840.

Valdiglesias, V., Laffon, B., Pásaro, E., and Méndez, J. (2011b). Evaluation of Okadaic Acid-Induced Genotoxicity in Human Cells Using the Micronucleus Test and γH2AX Analysis. J. Toxicol. Environ. Health A *74*, 980–992.

Valdiglesias, V., Giunta, S., Fenech, M., Neri, M., and Bonassi, S. (2013). γH2AX as a marker of DNA double strand breaks and genomic instability in human population studies. Mutat. Res. Mutat. Res. *753*, 24–40.

Vales, G., Rubio, L., and Marcos, R. (2014). Long-term exposures to low doses of titanium dioxide nanoparticles induce cell transformation, but not genotoxic damage in BEAS-2B cells. Nanotoxicology 1–11.

Valko, M., Rhodes, C.J., Moncol, J., Izakovic, M., and Mazur, M. (2006). Free radicals, metals and antioxidants in oxidative stress-induced cancer. Chem. Biol. Interact. *160*, 1–40.

Vamanu, C.I., Cimpan, M.R., Høl, P.J., Sørnes, S., Lie, S.A., and Gjerdet, N.R. (2008). Induction of cell death by TiO2 nanoparticles: studies on a human monoblastoid cell line. Toxicol. Vitro Int. J. Publ. Assoc. BIBRA *22*, 1689–1696.

Vandebriel, R.J., and De Jong, W.H. (2012). A review of mammalian toxicity of ZnO nanoparticles. Nanotechnol. Sci. Appl. *5*, 61–71.

Vander Heiden, M.G., Plas, D.R., Rathmell, J.C., Fox, C.J., Harris, M.H., and Thompson, C.B. (2001). Growth factors can influence cell growth and survival through effects on glucose metabolism. Mol. Cell. Biol. *21*, 5899–5912.

Vaziri, N.D. (2013). Understanding iron: promoting its safe use in patients with chronic kidney failure treated by hemodialysis. Am. J. Kidney Dis. Off. J. Natl. Kidney Found. *61*, 992–1000.

Verma, A., and Stellacci, F. (2010). Effect of surface properties on nanoparticle-cell interactions. Small Weinh. Bergstr. Ger. *6*, 12–21.

Vesterdal, L.K., Danielsen, P.H., Folkmann, J.K., Jespersen, L.F., Aguilar-Pelaez, K., Roursgaard, M., Loft, S., and Møller, P. (2014). Accumulation of lipids and oxidatively damaged DNA in hepatocytes exposed to particles. Toxicol. Appl. Pharmacol. *274*, 350–360.

Di Virgilio, A.L., Reigosa, M., Arnal, P.M., and Fernández Lorenzo de Mele, M. (2010). Comparative study of the cytotoxic and genotoxic effects of titanium oxide and aluminium

oxide nanoparticles in Chinese hamster ovary (CHO-K1) cells. J. Hazard. Mater. *177*, 711–718.

Wahab, R., Kaushik, N.K., Verma, A.K., Mishra, A., Hwang, I.H., Yang, Y.-B., Shin, H.-S., and Kim, Y.-S. (2011). Fabrication and growth mechanism of ZnO nanostructures and their cytotoxic effect on human brain tumor U87, cervical cancer HeLa, and normal HEK cells. J. Biol. Inorg. Chem. JBIC Publ. Soc. Biol. Inorg. Chem. *16*, 431–442.

Wahab, R., Siddiqui, M.A., Saquib, Q., Dwivedi, S., Ahmad, J., Musarrat, J., Al-Khedhairy, A.A., and Shin, H.-S. (2014). ZnO nanoparticles induced oxidative stress and apoptosis in HepG2 and MCF-7 cancer cells and their antibacterial activity. Colloids Surf. B Biointerfaces *117*, 267–276.

Walkey C. (2012). The cellular response to nanomaterials depends on the environment. Nanowerk Spotlight.

Wan, R., Mo, Y., Zhang, X., Chien, S., Tollerud, D.J., and Zhang, Q. (2008). Matrix metalloproteinase-2 and -9 are induced differently by metal nanoparticles in human monocytes: The role of oxidative stress and protein tyrosine kinase activation. Toxicol. Appl. Pharmacol. *233*, 276–285.

Wan, R., Mo, Y., Feng, L., Chien, S., Tollerud, D.J., and Zhang, Q. (2012). DNA damage caused by metal nanoparticles: involvement of oxidative stress and activation of ATM. Chem. Res. Toxicol. *25*, 1402–1411.

Wang, Z.L. (2004). Zinc oxide nanostructures: growth, properties and applications. J. Phys. Condens. Matter *16*, R829.

Wang, B., Feng, W.Y., Wang, M., Shi, J.W., Zhang, F., Ouyang, H., Zhao, Y.L., Chai, Z.F., Huang, Y.Y., Xie, Y.N., et al. (2007). Transport of intranasally instilled fine Fe2O3 particles into the brain: micro-distribution, chemical states, and histopathological observation. Biol. Trace Elem. Res. *118*, 233–243.

Wang, G., Gong, Y., Anderson, J., Sun, D., Minuk, G., Roberts, M.S., and Burczynski, F.J. (2005). Antioxidative function of L-FABP in L-FABP stably transfected Chang liver cells. Hepatology *42*, 871–879.

Wang, J., Chen, C., Liu, Y., Jiao, F., Li, W., Lao, F., Li, Y., Li, B., Ge, C., Zhou, G., et al. (2008). Potential neurological lesion after nasal instillation of TiO2 nanoparticles in the anatase and rutile crystal phases. Toxicol. Lett. *183*, 72–80.

Wang, J., Sun, W., and Ali, S.F. (2009). Nanoparticles: Is Neurotoxicity a Concern? In Nanotoxicity, S.C. Sahu, and D.A. Casciano, eds. (John Wiley & Sons, Ltd), pp. 171–182.

Wang, J., Deng, X., Zhang, F., Chen, D., and Ding, W. (2014a). ZnO nanoparticle-induced oxidative stress triggers apoptosis by activating JNK signaling pathway in cultured primary astrocytes. Nanoscale Res. Lett. *9*, 117.

Wang, L., Wang, L., Ding, W., and Zhang, F. (2010). Acute toxicity of ferric oxide and zinc oxide nanoparticles in rats. J. Nanosci. Nanotechnol. *10*, 8617–8624.

Wang, S., Hunter, L.A., Arslan, Z., Wilkerson, M.G., and Wickliffe, J.K. (2011a). Chronic exposure to nanosized, anatase titanium dioxide is not cyto- or genotoxic to Chinese hamster ovary cells. Environ. Mol. Mutagen. *52*, 614–622.

Wang, Y., Wang, B., Zhu, M.-T., Li, M., Wang, H.-J., Wang, M., Ouyang, H., Chai, Z.-F., Feng, W.-Y., and Zhao, Y.-L. (2011b). Microglial activation, recruitment and phagocytosis as linked phenomena in ferric oxide nanoparticle exposure. Toxicol. Lett. *205*, 26–37.

Wang, Y., Cui, H., Zhou, J., Li, F., Wang, J., Chen, M., and Liu, Q. (2014b). Cytotoxicity, DNA damage, and apoptosis induced by titanium dioxide nanoparticles in human non-small cell lung cancer A549 cells. Environ. Sci. Pollut. Res. Int.

Watters, G.P., Smart, D.J., Harvey, J.S., and Austin, C.A. (2009). H2AX phosphorylation as a genotoxicity endpoint. Mutat. Res. Toxicol. Environ. Mutagen. *679*, 50–58.

Weir, A., Westerhoff, P., Fabricius, L., Hristovski, K., and von Goetz, N. (2012). Titanium Dioxide Nanoparticles in Food and Personal Care Products. Environ. Sci. Technol. *46*, 2242–2250.

Wibke Busch (2010). Toxicity of engineered nanoparticles towards vertebrate cells in vitro. PhD Dissertation. The Helmholtz Centre for Environmental Research - UFZ.

Wilhelmi, V., Fischer, U., Weighardt, H., Schulze-Osthoff, K., Nickel, C., Stahlmecke, B., Kuhlbusch, T.A.J., Scherbart, A.M., Esser, C., Schins, R.P.F., et al. (2013). Zinc oxide

nanoparticles induce necrosis and apoptosis in macrophages in a p47phox- and Nrf2-independent manner. PloS One *8*, e65704.

Williams, V.M., Filippova, M., Soto, U., and Duerksen-Hughes, P.J. (2011). HPV-DNA integration and carcinogenesis: putative roles for inflammation and oxidative stress. Future Virol. *6*, 45–57.

Winckler, J. (1976). [Vital staining of lysosomes and other cell organelles of the rat with neutral red (a summary)]. Acta Histochem. Suppl. *16*, 15–22.

Winkler, J. (2003). Titanium dioxide (Hannover: Vincentz Network).

Witschger, O. (2011). Monitoring Nanoaerosols and Occupational Exposure. In Nanoethics and Nanotoxicology, P. Houdy, M. Lahmani, and F. Marano, eds. (Springer Berlin Heidelberg), pp. 163–199.

Wolf, R., Matz, H., Orion, E., and Lipozencić, J. (2003). Sunscreens--the ultimate cosmetic. Acta Dermatovenerol. Croat. ADC *11*, 158–162.

Wong, S.W.Y., Leung, P.T.Y., Djurisić, A.B., and Leung, K.M.Y. (2010). Toxicities of nano zinc oxide to five marine organisms: influences of aggregate size and ion solubility. Anal. Bioanal. Chem. *396*, 609–618.

Woodruff, R.S., Li, Y., Yan, J., Bishop, M., Jones, M.Y., Watanabe, F., Biris, A.S., Rice, P., Zhou, T., and Chen, T. (2012). Genotoxicity evaluation of titanium dioxide nanoparticles using the Ames test and Comet assay. J. Appl. Toxicol. JAT *32*, 934–943.

Wu, J., and Sun, J. (2011). Investigation on mechanism of growth arrest induced by iron oxide nanoparticles in PC12 cells. J. Nanosci. Nanotechnol. *11*, 11079–11083.

Wu, H., Yin, J.-J., Wamer, W.G., Zeng, M., and Lo, Y.M. (2014). Reactive oxygen species-related activities of nano-iron metal and nano-iron oxides. J. Food Drug Anal. *22*, 86–94.

Wu, J., Liu, W., Xue, C., Zhou, S., Lan, F., Bi, L., Xu, H., Yang, X., and Zeng, F.-D. (2009). Toxicity and penetration of TiO2 nanoparticles in hairless mice and porcine skin after subchronic dermal exposure. Toxicol. Lett. *191*, 1–8.

Wu, J., Sun, J., and Xue, Y. (2010a). Involvement of JNK and P53 activation in G2/M cell cycle arrest and apoptosis induced by titanium dioxide nanoparticles in neuron cells. Toxicol. Lett. *199*, 269–276.

Wu, W., He, Q., and Jiang, C. (2008). Magnetic iron oxide nanoparticles: synthesis and surface functionalization strategies. Nanoscale Res. Lett. *3*, 397–415.

Wu, W., Chen, B., Cheng, J., Wang, J., Xu, W., Liu, L., Xia, G., Wei, H., Wang, X., Yang, M., et al. (2010b). Biocompatibility of Fe3O4/DNR magnetic nanoparticles in the treatment of hematologic malignancies. Int. J. Nanomedicine *5*, 1079–1084.

Xia, T., Hamilton, R.F., Bonner, J.C., Crandall, E.D., Elder, A., Fazlollahi, F., Girtsman, T.A., Kim, K., Mitra, S., Ntim, S.A., et al. (2013). Interlaboratory evaluation of in vitro cytotoxicity and inflammatory responses to engineered nanomaterials: the NIEHS Nano GO Consortium. Environ. Health Perspect. *121*, 683–690.

Xiang, J.-J., Tang, J.-Q., Zhu, S.-G., Nie, X.-M., Lu, H.-B., Shen, S.-R., Li, X.-L., Tang, K., Zhou, M., and Li, G.-Y. (2003). IONP-PLL: a novel non-viral vector for efficient gene delivery. J. Gene Med. *5*, 803–817.

Xiao, N., Gu, W., Wang, H., Deng, Y., Shi, X., and Ye, L. (2014). T1-T2 dual-modal MRI of brain gliomas using PEGylated Gd-doped iron oxide nanoparticles. J. Colloid Interface Sci. *417*, 159–165.

Xie, H., Mason, M.M., and Wise, J.P. (2011). Genotoxicity of metal nanoparticles. Rev. Environ. Health *26*, 251–268.

Xie, Y., Wang, Y., Zhang, T., Ren, G., and Yang, Z. (2012). Effects of nanoparticle zinc oxide on spatial cognition and synaptic plasticity in mice with depressive-like behaviors. J. Biomed. Sci. *19*, 14.

Xiong, S., George, S., Yu, H., Damoiseaux, R., France, B., Ng, K.W., and Loo, J.S.-C. (2013). Size influences the cytotoxicity of poly (lactic-co-glycolic acid) (PLGA) and titanium dioxide (TiO(2)) nanoparticles. Arch. Toxicol. *87*, 1075–1086.

Xu, M., Li, J., Hanagata, N., Su, H., Chen, H., and Fujita, D. (2013). Challenge to assess the toxic contribution of metal cation released from nanomaterials for nanotoxicology--the case of ZnO nanoparticles. Nanoscale *5*, 4763–4769.

Xue, C., Wu, J., Lan, F., Liu, W., Yang, X., Zeng, F., and Xu, H. (2010). Nano titanium dioxide induces the generation of ROS and potential damage in HaCaT cells under UVA irradiation. J. Nanosci. Nanotechnol. *10*, 8500–8507.

Xue, Y., Wu, J., and Sun, J. (2012). Four types of inorganic nanoparticles stimulate the inflammatory reaction in brain microglia and damage neurons in vitro. Toxicol. Lett. *214*, 91–98.

Yang, Han, Tian, Zhang, and Ren (2011a). Nano-zinc oxide damages spatial cognition capability via over-enhanced long-term potentiation in hippocamus of Wistar rats. Int. J. Nanomedicine 1453.

Yang, C.-Y., Hsiao, J.-K., Tai, M.-F., Chen, S.-T., Cheng, H.-Y., Wang, J.-L., and Liu, H.-M. (2011b). Direct labeling of hMSC with SPIO: the long-term influence on toxicity, chondrogenic differentiation capacity, and intracellular distribution. Mol. Imaging Biol. MIB Off. Publ. Acad. Mol. Imaging *13*, 443–451.

Yang, T.J., Haimovitz-Friedman, A., and Verheij, M. (2012). Anticancer therapy and apoptosis imaging. Exp. Oncol. *34*, 269–276.

Yang, X., Shao, H., Liu, W., Gu, W., Shu, X., Mo, Y., Chen, X., Zhang, Q., and Jiang, M. (2015). Endoplasmic reticulum stress and oxidative stress are involved in ZnO nanoparticle-induced hepatotoxicity. Toxicol. Lett. *234*, 40–49.

Yemisci, M., Caban, S., Gursoy-Ozdemir, Y., Lule, S., Novoa-Carballal, R., Riguera, R., Fernandez-Megia, E., Andrieux, K., Couvreur, P., Capan, Y., et al. (2014). Systemically administered brain-targeted nanoparticles transport peptides across the blood-brain barrier and provide neuroprotection. J. Cereb. Blood Flow Metab. Off. J. Int. Soc. Cereb. Blood Flow Metab.

Yi, D.K., Lee, S.S., Papaefthymiou, G.C., and Ying, J.Y. (2006). Nanoparticle Architectures Templated by SiO2/Fe2O3 Nanocomposites. Chem. Mater. *18*, 614–619.

Yin, Y., Lin, Q., Sun, H., Chen, D., Wu, Q., Chen, X., and Li, S. (2012). Cytotoxic effects of ZnO hierarchical architectures on RSC96 Schwann cells. Nanoscale Res. Lett. *7*, 439.

Yoshioka, Y., Higashisaka, K., Tsunoda, S., and Tsutsumi, Y. (2014). The Absorption, Distribution, Metabolism, and Excretion Profile of Nanoparticles. In Engineered Cell Manipulation for Biomedical Application, M. Akashi, T. Akagi, and M. Matsusaki, eds. (Springer Japan), pp. 259–271.

Yousef, J.M., and Mohamed, A.M. (2015). Prophylactic role of B vitamins against bulk and zinc oxide nano-particles toxicity induced oxidative DNA damage and apoptosis in rat livers. Pak. J. Pharm. Sci. *28*, 175–184.

Ze, Y., Zheng, L., Zhao, X., Gui, S., Sang, X., Su, J., Guan, N., Zhu, L., Sheng, L., Hu, R., et al. (2013). Molecular mechanism of titanium dioxide nanoparticles-induced oxidative injury in the brain of mice. Chemosphere *92*, 1183–1189.

Ze, Y., Sheng, L., Zhao, X., Hong, J., Ze, X., Yu, X., Pan, X., Lin, A., Zhao, Y., Zhang, C., et al. (2014a). TiO2 Nanoparticles Induced Hippocampal Neuroinflammation in Mice. PLoS ONE *9*, e92230.

Ze, Y., Sheng, L., Zhao, X., Ze, X., Wang, X., Zhou, Q., Liu, J., Yuan, Y., Gui, S., Sang, X., et al. (2014b). Neurotoxic characteristics of spatial recognition damage of the hippocampus in mice following subchronic peroral exposure to TiO2 nanoparticles. J. Hazard. Mater. *264*, 219–229.

Zhang, C., Zhai, S., Wu, L., Bai, Y., Jia, J., Zhang, Y., Zhang, B., and Yan, B. (2015). Induction of Size-Dependent Breakdown of Blood-Milk Barrier in Lactating Mice by TiO2 Nanoparticles. PloS One *10*, e0122591.

Zhang, L., Bai, R., Li, B., Ge, C., Du, J., Liu, Y., Le Guyader, L., Zhao, Y., Wu, Y., He, S., et al. (2011). Rutile TiO_2 particles exert size and surface coating dependent retention and lesions on the murine brain. Toxicol. Lett. *207*, 73–81.

Zhang, T., Qian, L., Tang, M., Xue, Y., Kong, L., Zhang, S., and Pu, Y. (2012). Evaluation on cytotoxicity and genotoxicity of the L-glutamic acid coated iron oxide nanoparticles. J. Nanosci. Nanotechnol. *12*, 2866–2873.

Zhao, J., and Castranova, V. (2011). Toxicology of nanomaterials used in nanomedicine. J. Toxicol. Environ. Health B Crit. Rev. *14*, 593–632.

Zhao, J., Xu, L., Zhang, T., Ren, G., and Yang, Z. (2009). Influences of nanoparticle zinc oxide on acutely isolated rat hippocampal CA3 pyramidal neurons. Neurotoxicology *30*, 220–230.

Zhu, M.-T., Wang, Y., Feng, W.-Y., Wang, B., Wang, M., Ouyang, H., and Chai, Z.-F. (2010). Oxidative stress and apoptosis induced by iron oxide nanoparticles in cultured human umbilical endothelial cells. J. Nanosci. Nanotechnol. *10*, 8584–8590.

Zimmer, C., Weissleder, R., Poss, K., Bogdanova, A., Wright, S.C., and Enochs, W.S. (1995). MR imaging of phagocytosis in experimental gliomas. Radiology *197*, 533–538.

Zucker, R.M., and Daniel, K.M. (2012). Detection of TiO2 nanoparticles in cells by flow cytometry. Methods Mol. Biol. Clifton NJ *906*, 497–509.

Zucker, R.M., Daniel, K.M., Massaro, E.J., Karafas, S.J., Degn, L.L., and Boyes, W.K. (2013). Detection of silver nanoparticles in cells by flow cytometry using light scatter and far-red fluorescence. Cytom. Part J. Int. Soc. Anal. Cytol.

Zupanc, J., Valant, J., Dobnikar, A., Kralj-Iglic, V., Iglic, A., and Drobne, D. (2009). Interactions of nanoparticles with lipid vesicles: A population based computer aided image analysis approach. In Annual International Conference of the IEEE Engineering in Medicine and Biology Society, 2009. EMBC 2009, pp. 1400–1403.

Cover image source: www.mistbreaker.com

UNIVERSIDADE DA CORUÑA